ChemRxiv™

doi.org/10.26434/chemrxiv.11383659.v1

Bioorthogonal Tetrazine Carbamate Cleavage by Highly Reactive Trans-Cyclooctene

Arthur van Onzen, Ron M. Versteegen, Freek J. M. Hoeben, Ivo A.W. Filot, Raffaella Rossin, tong zhu, Jeremy Wu, Peter J. Hudson, Henk M. Janssen, Wolter ten Hoeve, Marc Robillard

Submitted date: 17/12/2019 • Posted date: 20/12/2019

Licence: CC BY-NC-ND 4.0

Citation information: van Onzen, Arthur; Versteegen, Ron M.; Hoeben, Freek J. M.; Filot, Ivo A.W.; Rossin, Raffaella; zhu, tong; et al. (2019): Bioorthogonal Tetrazine Carbamate Cleavage by Highly Reactive Trans-Cyclooctene. ChemRxiv. Preprint. https://doi.org/10.26434/chemrxiv.11383659.v1

The high reaction rate of the 'click-to-release' reaction between allylic substituted trans-cyclooctene and tetrazine has enabled exceptional control over chemical and biological processes. Here we report the development of a new bioorthogonal cleavage reaction based on trans-cyclooctene and tetrazine with up to 3 orders of magnitude higher reactivity compared to the parent reaction, and 4 to 6 orders higher than other cleavage reactions. In this new pyridazine elimination mechanism, wherein the roles a reversed, a trans-cyclooctene activator reacts with a tetrazine that is substituted with a methylene-linked carbamate, leading to an 1,4-elimination of the carbamate and liberation of an amine. Through a series of mechanistic studies, we identified the 2,5-dihydropyridazine tautomer as the releasing species and found factors that govern its formation and subsequent fragmentation. The bioorthogonal utility was demonstrated by the selective cleavage of a tetrazine-linked antibody-drug conjugate by trans-cyclooctenes, affording efficient drug liberation in plasma and cell culture. Finally, the parent and the new reaction were compared at low concentration, showing that the use of a highly reactive trans-cyclooctene as activator leads to a complete reaction with antibody-drug conjugate in seconds vs. hours for the parent system. We believe that this new reaction may allow markedly reduced click-to-release reagent doses in vitro and in vivo and could expand the application scope to conditions wherein the trans-cyclooctene has limited stability.

File list (2)

20191217_Click-to-Release from Tetrazine.pdf (1.66 MiB) view on ChemRxiv • download file

20191217_Click-to-Release from Tetrazine_SI.pdf (12.72 MiB) view on ChemRxiv • download file

Bioorthogonal Tetrazine Carbamate Cleavage by Highly Reactive *Trans*-Cyclooctene

Arthur H.A.M van Onzen[1], Ron M. Versteegen[2], Freek J.M. Hoeben[2], Ivo A.W. Filot[3], Raffaella Rossin[1], Tong Zhu[4], Jeremy Wu[5], Peter J. Hudson[5], Henk M. Janssen[2], Wolter ten Hoeve[6], Marc S. Robillard[1,*]

1 Tagworks Pharmaceuticals, Geert Grooteplein Zuid 10, 6525 GA Nijmegen, The Netherlands.
2 SyMO-Chem B.V., Den Dolech 2, 5612 AZ Eindhoven, The Netherlands.
3 Laboratory of Inorganic Materials Chemistry, Schuit Institute of Catalysis, Eindhoven University of Technology, P.O. Box 513, 5600 MB Eindhoven, The Netherlands
4 Levena Biopharma, 4955 Directors Place, Suite 300, San Diego, CA 92121, USA.
5 Avipep Pty Ltd, 343 Royal Parade, Parkville, VIC 3052, Australia.
6 Syncom B.V., Kadijk 3, 9747 AT Groningen, The Netherlands.

* Corresponding author. Email: marc.robillard@tagworkspharma.com

Abstract

The high reaction rate of the 'click-to-release' reaction between allylic substituted *trans*-cyclooctene and tetrazine has enabled exceptional control over chemical and biological processes. Here we report the development of a new bioorthogonal cleavage reaction based on *trans*-cyclooctene and tetrazine with up to 3 orders of magnitude higher reactivity compared to the parent reaction, and 4 to 6 orders higher than other cleavage reactions. In this new pyridazine elimination mechanism, wherein the roles a reversed, a *trans*-cyclooctene activator reacts with a tetrazine that is substituted with a methylene-linked carbamate, leading to an 1,4-elimination of the carbamate and liberation of an amine. Through a series of mechanistic studies, we identified the 2,5-dihydropyridazine tautomer as the releasing species and found factors that govern its formation and subsequent fragmentation. The bioorthogonal utility was demonstrated by the selective cleavage of a tetrazine-linked antibody-drug conjugate by *trans*-cyclooctenes, affording efficient drug liberation in plasma and cell culture. Finally, the parent and the new reaction were compared at low concentration, showing that the use of a highly reactive *trans*-cyclooctene as activator leads to a complete reaction with antibody-drug conjugate in seconds *vs*. hours for the parent system. We believe that this new reaction may allow markedly reduced click-to-release reagent doses *in vitro* and *in vivo* and could expand the application scope to conditions wherein the *trans*-cyclooctene has limited stability.

Keywords:

Bioorthogonal • Cleavage • Click Chemistry • IEDDA • Pyridazine Elimination • 1,4-elimination • Tetrazine *Trans*-Cyclooctene

Introduction

Bioorthogonal cleavage reactions have emerged as powerful strategies to control the release or activation of small molecules and biomolecules in chemical and biological settings.[1–3] Most organic cleavage reactions were derived from their click conjugation counterparts and include the reactions between tetrazines and vinyl ethers,[4–6] vinylboronic acids,[7] 3-isocyanopropyls,[8] cyclooctynes[9] and benzonorbornadienes,[10] the iminosydnone cyclooctyne reaction,[11,12] the azide-to-amine reduction by *trans*-cyclooctene (TCO),[13,14] in addition to the use of the Staudinger reaction[15,16] and ligation.[17] We reported that the fastest bioorthogonal conjugation reaction, the inverse-electron-demand Diels-Alder (IEDDA) between TCO and tetrazine derivatives,[18] widely used for selective and efficient bioconjugations *in vitro* and *in vivo*,[19,20] could be transformed into a bioorthogonal cleavage reaction.[21] In this IEDDA pyridazine elimination reaction, termed 'click-to-release' (Scheme 1A), a carbamate-linked payload is installed on the allylic position of TCO. Following reaction of the TCO-carbamate with a tetrazine, the resulting 1,4-dihydropyridazine intermediate rapidly eliminates the amine-containing payload and CO_2.

The high reactivity and selectivity of the IEDDA pyridazine elimination reaction has led to its widespread application, such as in *in vivo* cleavage or unmasking of TCO-containing antibody-drug conjugates (ADCs),[22,23] prodrugs,[24,25] proteins,[26,27] and peptide antigens,[28] by the administration of a tetrazine activator. In addition, this click-to-release approach has been used in a range of diverse *in vitro* applications, such as uncaging of fluorogenic compounds[29,30] and enzyme substrates,[31] cell-specific proteome labelling,[32] oligonucleotide delivery into cells,[33] and purification of solid phase synthesized oligonucleotides.[34]

Nevertheless, a further increase of the click-to-release reaction rate would be beneficial for a number of applications. For example, complete *in vivo* activation of a target-localized protein or ADC requires the intravenous administration of a large excess of tetrazine activator. A higher click reaction rate may allow a lower dose of the activator, which would facilitate clinical translation and may open up other prodrug approaches. Likewise, a higher reactivity would enable *in vitro* assays that use low concentrations. Here, the TCO is a limiting factor, as it has a reduced reactivity due to the allylic-positioned payload and as it needs to remain stable for hours or days when used as a linker or mask. The latter precludes increasing the reactivity by designing more strained TCO derivatives as these will likely become too unstable.[35] Furthermore, TCOs in general and highly strained TCOs in particular do not combine well with high thiol concentrations, low pH or UV light, which may affect their application scope in, for example, *in vitro* assays or chemistry.

We therefore set out to develop a new click-to-release strategy, still based on the robust IEDDA reaction between TCO and tetrazine and the unique and versatile properties of the dihydropyridazine intermediates, but now with the TCO being the activator and the tetrazine the linker. In such a system, wherein the roles are reversed, the TCO does not require the allylic substitution, and its reactivity can be boosted further as the stability requirements for the activator are less stringent than for the linker, which typically has to withstand harsher conditions and/or remain intact for a longer time. Another advantage of such a system would be that relatively simple, even commercially available, TCOs could be used. IEDDA reactions give 4,5-dihydropyridazines (DHPs), which usually rapidly tautomerize to 1,4- and 2,5-dihydropyridazines.[36,37] We envisioned that the dihydropyridazine IEDDA intermediates, of which the 1,4-dihydropyridazine leads to an electron cascade elimination of a carbamate from the part originating from the allylic position on the TCO,[21,31] may also be enlisted for an electron cascade elimination of a carbamate from the part originating from the tetrazine. Specifically, we hypothesized that a reaction of a TCO with a tetrazine substituted with a methylene-linked carbamate and subsequent tautomerization of the 4,5-dihydropyrididazine (**4,5-DHP**) to the 1,4- and 2,5- dihydropyridazines (**1,4-DHP** and **2,5-DHP**) would lead to an 1,4-elimination of the

carbamate from either **1,4-DHP** or **2,5-DHP**, or both, liberating the amine, CO_2 and pyridazine **P2** (Scheme 1B).[38]

Here we show that the dihydropyridazine product from the reaction between *trans*-cyclooctene and tetrazine can indeed be enlisted to induce an 1,4-elimination of a methylene-linked carbamate on the tetrazine. Through a series of mechanistic studies we found that **4,5-DHP** preferentially tautomerizes to **2,5-DHP** and that, fortuitously, **2,5-DHP** is the releasing species. Depending on the TCO used the reactivity increased 6- and 800-fold compared to the parent pyridazine elimination reaction, and affording release yields of 67 to 93 %. The bioorthogonality of the system was demonstrated in the context of an antibody-drug conjugate comprising the new tetrazine linker, which could be efficiently reacted and cleaved in biological conditions.

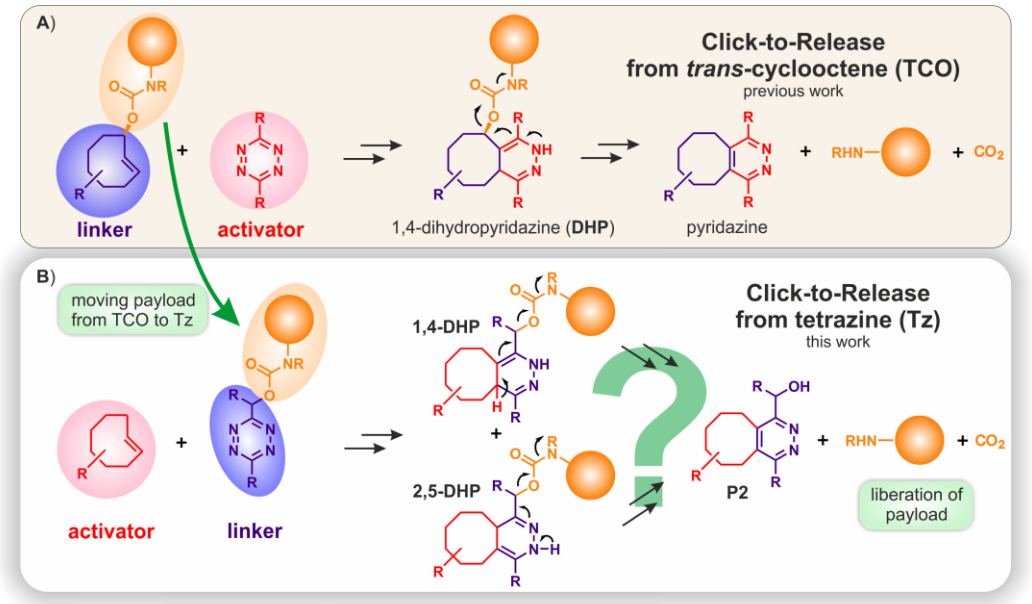

Scheme 1. A) Established click-to-release reaction with *trans*-cyclooctene as the tetrazine-cleavable linker. B) Envisioned click-to-release reaction with tetrazine as the *trans*-cyclooctene-cleavable linker.

Results and Discussion

We commenced with the preparation of a range of model 1,2,4,5-tetrazines with methylene carbamate derivatives on the 3-position, or both the 3- and 6- positions, comprising benzylic or aromatic amines with and without alkyl substituents on the amine and the methylene bridge (Figure 1A). These compounds were then screened for stability and TCO **12**-triggered carbamate cleavage in 20 % acetonitrile (ACN) / phosphate buffered saline (PBS) at 37 °C (Figure 1B,C).

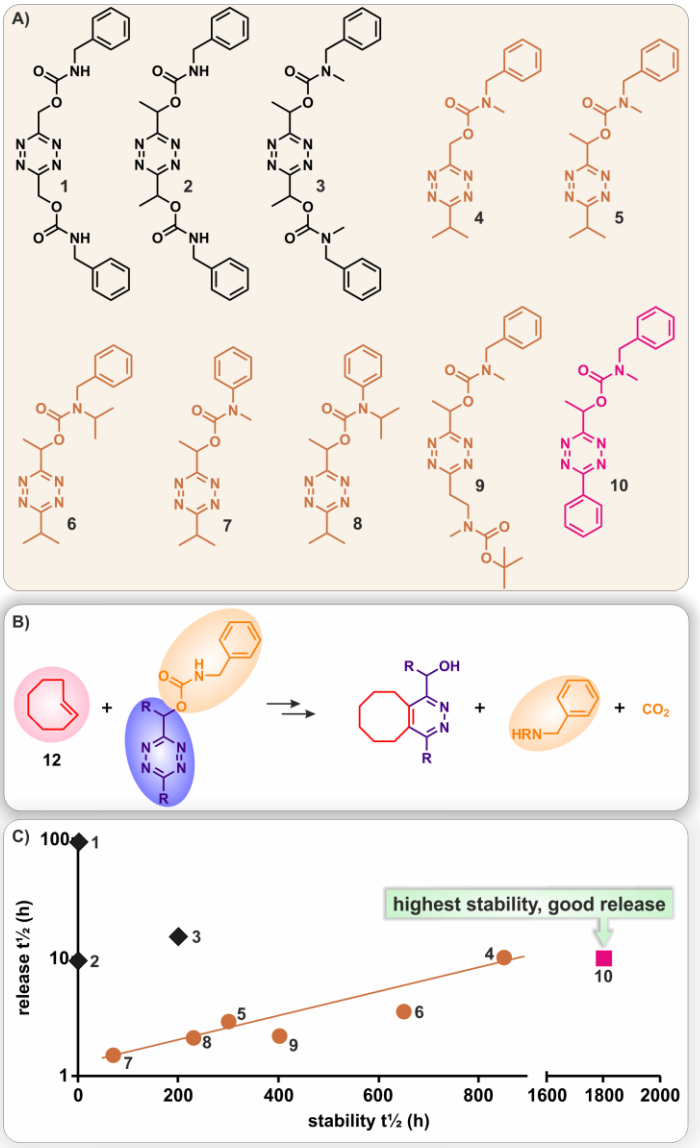

Figure 1. Stability and release study of several model tetrazine linkers. A) Structures of the evaluated model tetrazine carbamates. B) Reaction between TCO **12** and model tetrazines. C) Plot of tetrazine stability half-life *vs.* TCO **12**-triggered release half-life, in 20 % ACN/PBS, 37°C; stability determined by monitoring UV-Vis absorption at 520 nm; release measured by rapid formation of IEDDA adduct and monitoring its decrease upon carbamate elimination with LC-MS.

To our delight, already among the first three prepared compounds, symmetrical tetrazines **1**-**3**, we observed good TCO-triggered cleavage and reasonable stability for **3**. While compounds **1** and **2** showed release as well, they were highly unstable, indicating a destabilizing effect from the primary carbamate NH on the tetrazine. Based on these results, we designed non-symmetrical model compounds **4**-**10** that could form the basis of a click-cleavable linker. Perusal of Figure 1C shows triggered cleavage half-lives between 1.5 h and 10 h and a correlation between release rate and stability half-lives. Installing a methyl substituent on the methylene appears to facilitate the cleavage (**5** *vs.* **4**, and **2** *vs.* **1**). This is in line with structure activity relationships established for the widely used self-immolative *para*-aminobenzyloxycarbonyl linker wherein a methyl substituent on the methylene bridge leads to more efficient liberation due to stabilization of the increasing positive charge upon release of the carbamate.[39,40] Furthermore, benzylamine-derived tetrazine carbamates were more stable than aniline-derived carbamates (**5** *vs.* **7**, **6** *vs.* **8**) and both carbamate types could be stabilized further by replacing the N-methyl by the bulkier N-isopropyl substituent (**6** *vs.* **5**, **8** *vs.* **7**). However, comparing **5** with **9** suggests that the increased steric bulk of a branched *vs.* linear alkyl substituent on the 6-position of the tetrazine does not further improve the stability.

On the contrary, the analogous tetrazine **10** with a phenyl substituent showed a 6-fold higher stability. While this was accompanied by a slower release than the isopropyl analog **5**, we believed the enhanced stability was more important for most applications, and we continued our investigations with this tetrazine motif.

To further study the release, we prepared **11** (Figure 2A), the dimethylamine analog of **10**, and started by monitoring its TCO-triggered cleavage in a range of ACN/PBS ratios with liquid chromatography–mass spectrometry (LC-MS). To facilitate analysis, reaction mixture aliquots were rapidly oxidized to give stable mixtures of (aromatic) pyridazines **P1** and **P2** (Figure 2A), the ratio of which affording the release yield. The structure of **P2** was confirmed by reference compound synthesis (see Supporting Information), indicating that 1,4-elimination of the carbamate is followed by hydration of the exocyclic double bond of the elimination product (**EP**, Figure 2A, 2D). While the IEDDA cycloaddition between **11** and **12** was instantaneous in all mixtures, the ensuing dimethylamine elimination from the dihydropyridazine intermediate showed a strong correlation with the water content (Figure 2B). Reaction in 25 % ACN/PBS afforded dimethylamine liberation with a half-life of 20h, but in 50 % ACN/PBS, the release slowed down to a 54h half-life and, interestingly, no cleavage was observed in 100 % ACN. This trend, together with the 10h release half-life observed in 20 % ACN for the product of **10** and **12** (Figure 1C), indicated that the release half-life in fully aqueous conditions was likely to be less than 3h.

Subsequently, the reaction between **11** and **12** was studied in $CDCl_3$ with ^1H NMR, UV-Vis and IR, showing instantaneous formation of the initial 4,5-dihydropyridazine product (**4,5-DHP**) with λ-max of 279 nm as a mixture of two diastereomers (83 *vs.* 17 %), arising from the stereocenter on the methylene (Figure 2E, F, Supporting Information Section S3.2). In these conditions, **4,5-DHP** did not tautomerize further and did not release dimethylamine. Addition of 0.1 v/v% formic acid resulted in complete tautomerization[31,41] within 3h to give a mixture in a 73/27 ratio of the 2,5- and 1,4-dihydropyridazines (**2,5-DHP** and **1,4-DHP**), each present as two diastereomers, as demonstrated by the loss of peaks at 7.9 and 3.2 ppm and the appearance of 4 new sets of peaks between 6.0 and 5.4 ppm and 3.8 and 3.1 ppm (Figure 2E; see Figure S6 for 2D NMR characterization). This tautomerization was accompanied by the appearance of an IR resonance at 3340 cm^{-1} for the N-H moiety (Figure S9), and the appearance of a UV absorbance at 340 nm in addition to the band at 280 nm (Figure 2F). To understand this, the UV spectra of the three tautomers were simulated using time-dependent density functional theory (TDDFT) in conjunction with implicit solvent effects employing the COSMO model with parameters for water, leading to a predicted λ-max of 276, 290/307 and 346 nm for respectively the 4,5-, 2,5 and the 1,4-tautomer, matching the trend in the previous observations (Figure 3). Extending the incubation in acidic conditions to 184h resulted in conversion of **2,5-DHP** into **1,4-DHP**, affording a 26/74 mixture and a concomitant increase of the 340/280 nm absorbance ratio, as predicted (Figure 2E, F). Also some oxidation to the aromatic pyridazine (**P1**) occurred, similar to the previously reported pyridazine elimination reaction.[21,31] Even though all three tautomers could be formed in $CDCl_3$, no release was observed, which is possibly due to the need to stabilize the charges on the carbamate and methylene that develop upon release.[39,40] Alternatively, proton-assisted mechanisms wherein water acts as the proton carrier can be a critical pathway in the cleavage mechanism.

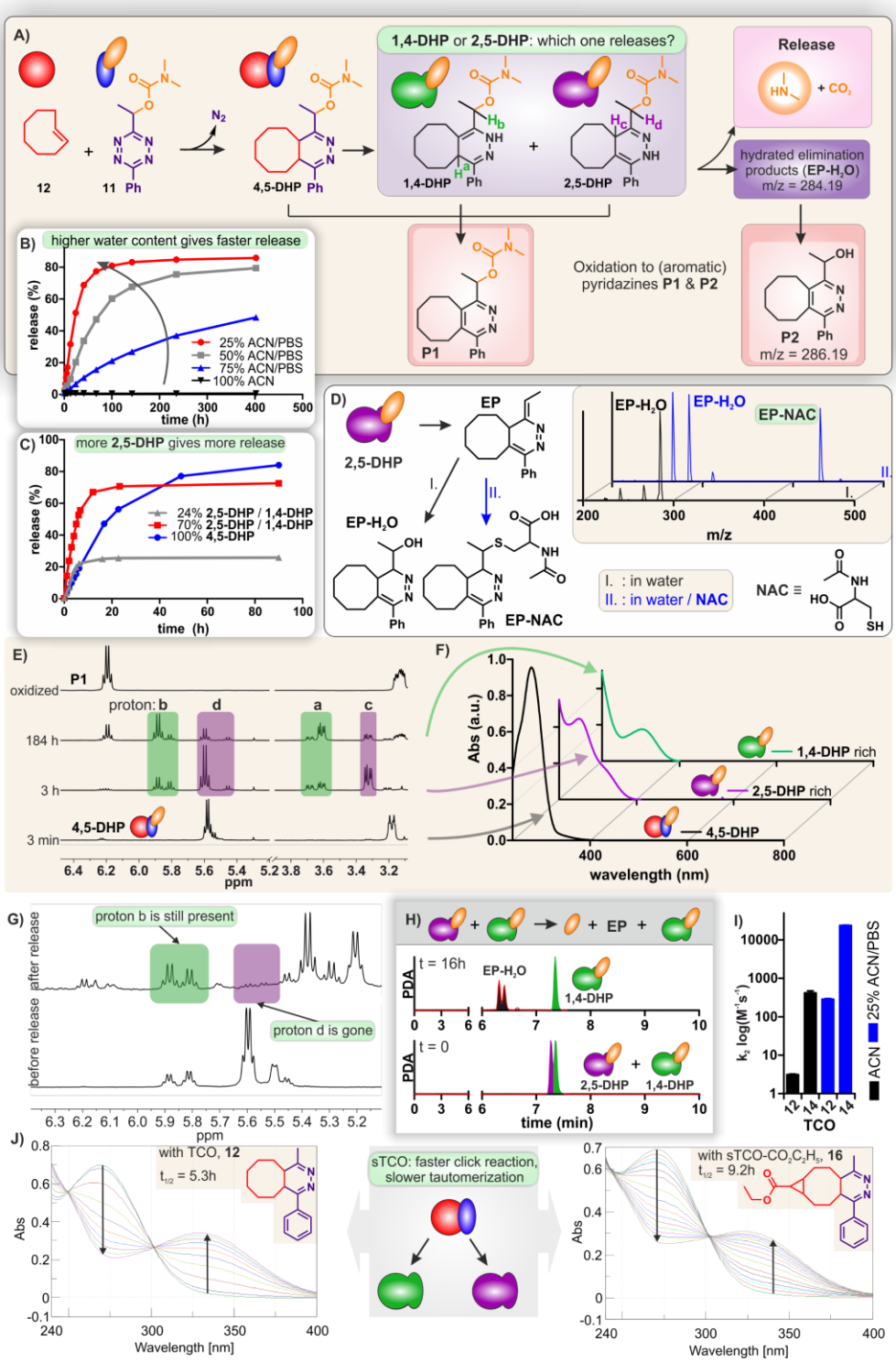

Figure 2. Mechanistic studies. A) Reaction of TCO **12** with model tetrazine **11**, affording **4,5-DHP** and then **1,4-DHP** and **2,5-DHP**, of which one liberates dimethylamine, in conjunction with hydrated elimination product (**EP-H₂O**), and oxidized pyridazines **P1** and **P2**. B) Release reaction between **11** and **12** in ACN/PBS mixtures at 37°C, quantified with LC-MS after sample oxidation to **P1**/**P2**. C) Release reaction between **11** and **12**, starting from different tautomer compositions in 25% ACN/PBS at 37°C, quantified with LC-MS after sample oxidation to **P1**/**P2**. D) Putative structure of the elimination product (**EP**), formed upon release from **2,5-DHP**, and its (I) reaction with water and (II) trapping by N-acetyl cysteine (**NAC**), as demonstrated by LC-MS. E) ^{1}H NMR of reaction of **11** with **12** in $CDCl_3$. F) UV of NMR samples of E) diluted in ACN. G) ^{1}H NMR of reaction product of **11** with **12** in $CDCl_3$ that was incubated in 25 % ACN/PBS for 3 days (top) compared to a non-incubated sample (bottom). H) PDA trace of reaction product of **11** with **12** (70/30 mixture of **2,5-/1,4-DHP**) in 25% ACN/PBS at 37°C, monitored with LC-MS of non-oxidized samples. I) Second order rate constants of the reaction of tetrazine **11** with TCOs **12** and **14** in ACN and 25% ACN/PBS at 20°C. J) UV of tautomerization of the **4,5-DHP** product from the reaction between 3-methyl-6-phenyl-tetrazine and, resp. TCO **12** and sTCO ethyl ester **16** in 25% ACN/PBS at 20°C.

The ability to control the tautomerization in chloroform was subsequently applied to identify the releasing tautomer by comparing the release profiles when starting from **4,5-DHP**, or a composition rich in respectively **2,5-DHP** or **1,4-DHP**. This was achieved by starting the reaction between **11** and **12** in $CDCl_3$ and by controlling the tautomer formation as shown above. Samples with the desired tautomer were concentrated and then dissolved in 25 % ACN/PBS, incubated at 37°C, followed by oxidation of aliquots and evaluation of the **P1/P2** ratio with LC-MS (Figure 2C). Starting from **4,5-DHP** led to a steady release of eventually 85 % with a half-life of the maximum cleavage yield of 14h, similar to when the release was started directly in 25 % ACN/PBS (Figure 2B). Interestingly, starting from a 70/30 mixture of **2,5-/1,4-DHP** afforded a much faster liberation, with a half-life of the maximum cleavage yield of 3h, leading to a maximum cleavage of 71 %. On the contrary, starting from a 24/76 mixture of **2,5-/1,4-DHP** led to a reduced maximum release yield of only 26 %. The strong correlation between the **2,5-DHP** percentage and release yield as well as the marked release rate increase when starting from **2,5-DHP** clearly indicates this is the releasing species. To confirm this, we set out to identify the non-releasing tautomer by incubating tetrazine **11** and TCO **12** in 25 % ACN/PBS at 37°C for 3 days. Given the release rate observed in these conditions (see Figure 2B) it follows that the releasing tautomer(s) would have to be consumed at that time. Indeed, subsequent lyophilization and NMR in $CDCl_3$ clearly showed that **1,4-DHP** was still present, together with some oxidized **P1**, but the signals belonging to the **2,5-DHP** had disappeared, confirming this is the releasing species (Figure 2G). In line with this and the established UV signatures of the tautomers, LC-MS of non-oxidized aliquots from of the 70/30 mixture of **2,5-/1,4-DHP** in 25 % ACN/PBS, showed the two tautomers as adjacent peaks with respectively a λ-max of 278 and 327 nm, with the 278 nm peak disappearing in time, in conjunction with the formation of hydrated elimination product (**EP-H_2O**) (Figure 2H and D). To confirm that the formation of **EP-H2O** and the corresponding **P2** is the result of 1,4-elimination followed by addition of water to the exocyclic double bond of **EP**, instead of hydrolysis of the carbamate bond of **2,5-DHP**, **11** and **12** were incubated in 25 % ACN/PBS containing the N-acetyl cysteine (NAC) to trap **EP**. As expected, LC-MS of the reaction mixture clearly showed the formation of the cysteine adduct **EP-NAC** in addition to **EP-H2O** (Figure 2D). The foregoing demonstrates that in aqueous conditions the **4,5-DHP** predominantly tautomerizes to the **2,5-DHP** and to a minor extent to the **1,4-DHP**, of which **2,5-DHP** then liberates the carbamate. Furthermore, the formation of **EP-H_2O**, **EP-NAC** and **P2** indicates that this release occurs via the envisioned 1,4-elimination.

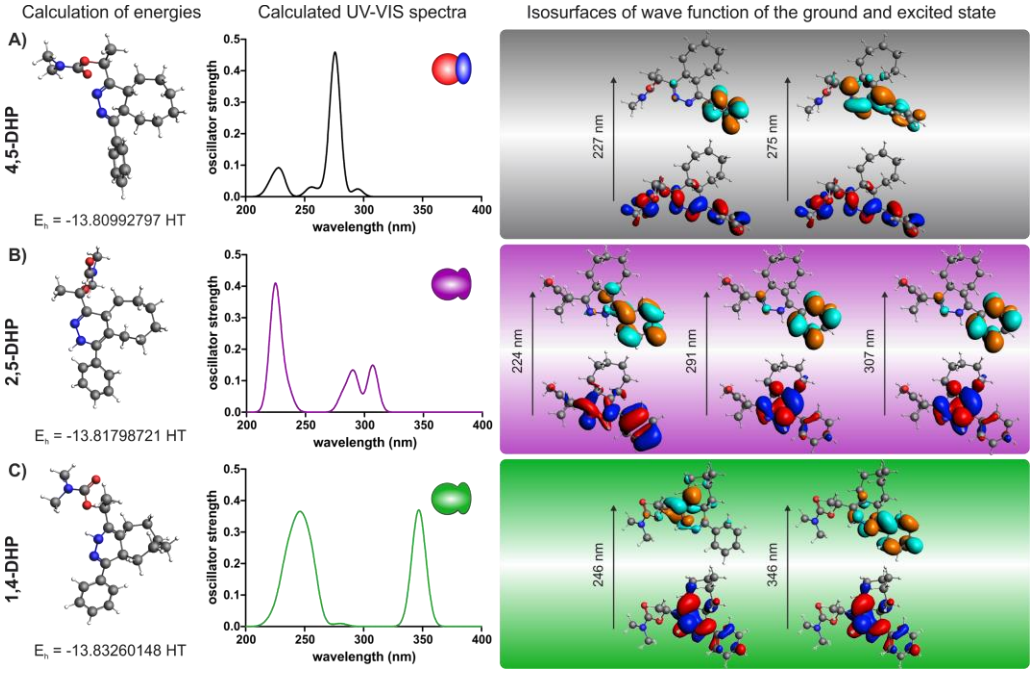

Figure 3. Simulated UV-VIS spectra of A) **4,5-DHP**; B) **2,5-DHP** and C) **1,4-DHP**. The isosurfaces of the ground and excited state corresponding to the transitions with the highest oscillator strength are shown on the right. (ground state: red and blue; excited state: teal and orange). Bonding energies of the ground states are given using water as implicit solvent.

To further support the mechanistic findings we calculated the minimal energies of **4,5-DHP**, **2,5-DHP** and **1,4-DHP** (Figure 3) and several other possible tautomers of the reaction product of **11** and **12**, including the 1,2-dihydropyridazine and its exocyclic analog (Table S1). Using a B3LYP exchange-correlation functional and water as an implicit solvent, the **2,5-DHP** and **1,4-DHP** were indeed shown to have the lowest energy, with the **1,4-DHP** being slightly lower. Calculations in vacuum showed essentially the same result, but with a slightly smaller energetic difference between the two tautomers (Table S1). These values, combined with the NMR study (Figure 2E), suggest that upon **4,5-DHP** tautomerization **2,5-DHP** is kinetically favoured and can slowly convert to the thermodynamically favoured **1,4-DHP**. The high release yield in 25 % ACN/PBS indicates that this 2,5- to 1,4-tautomerization does not readily occur in neutral aqueous conditions.

Having identified the releasing tautomer, we evaluated the potential reactivity advantage of this system. Click reaction of **11** with **12** in ACN afforded a k_2=3.14 +/- 0.10 M^{-1} s^{-1} at 20°C, which is already 6-fold faster than the parent reaction of allylic substituted TCO with 3,6-bisalkyl-tetrazine.[21] Conformationally strained TCO (sTCO) based on a *cis*-fusion of a cyclopropyl to the TCO ring represents the most reactive TCO that still has good utility in bioorthogonal conjugations.[42] Reaction of **11** with this much more reactive sTCO-acid **14** was found to have a very high k_2= 420 ± 49 $M^{-1}s^{-1}$, 800-fold higher than the parent click-to-release reaction (Figure 2I).[21] As expected, in 25 % ACN/PBS these rates increased further to 287 ± 10 M^{-1} s^{-1} for **12** and to the very high rate of 23800 ± 400 M^{-1} s^{-1} for **14**.

To demonstrate the proof of principle of this novel click-to-release reaction in a biological environment, we developed an antibody-drug conjugate (ADC) comprising the drug monomethyl auristatin E (MMAE) linked via the tetrazine to a pegylated CC49 diabody that targets tumor associated glycoprotein 72 (TAG72).[23] Based on model compound **11** we prepared tetrazine linker **18** via a modified Pinner synthesis (Figure 4A) followed by PNP carbonate formation and introduction of the MMAE. After Boc-deprotection, tetrazine-MMAE **21** was conjugated to PEG derivative **22**, affording maleimide-functionalized Tz-MMAE linker **23**. Linker-drug **23** was then site-specifically conjugated to four engineered cysteine residues in the CC49 diabody providing **tz-ADC** with a drug-to-antibody ratio (DAR) of 4 (61 kDa, Figure 4B). **Tz-ADC** exhibited excellent stock stability (PBS, 4°C) as no tetrazine degradation or spontaneous drug liberation was observed in 1 year (Figure S22). In addition to TCO **12** and sTCO-acid **14** we also prepared the DOTA chelate-conjugated analogs **13** and **15**, for increased hydrophilicity and to be able to monitor their reaction with **tz-ADC** by labeling the chelate with a radiometal (Figure 4D). The four TCOs were subsequently examined for their ability to liberate MMAE from the **tz-ADC** (Figure 4C,E-G). For all TCOs, mass spectrometry of the diabody in PBS showed efficient conversion of the ADC (30691 Da for the scFv monomer, each monomer linked to 2 MMAE) to the IEDDA product, followed by formation of species that had eliminated 1 or 2 MMAE moieties. Whereas TCO **12** and its DOTA analog **13** afforded a MMAE release yield of 93 %, the sTCO motif had a lower maximal cleavage yield of ca. 67 % (Figure 4F). Similar results were obtained in mouse plasma, while only low levels of free MMAE were found when the ADC was incubated without a TCO (Figure 4G). We hypothesized that the lower release from sTCO may be caused by a slower tautomerization of the **4,5-DHP** derivative, which may allow for more oxidative deactivation to **P1**. Indeed, when we used UV to evaluate the tautomerization of the **4,5-DHP** product from the reaction between 3-methyl-6-phenyl-tetrazine and, respectively TCO **12** and sTCO ethyl ester **16** in 25 % ACN/PBS, we found a markedly slower tautomerization for the sTCO (Figure 2J). Despite the lower overall release from sTCO-derived **2,5-DHP**, the remarkable reactivity increase offered by these TCOs provides a compelling argument for their use when the application is relatively demanding (e.g. at low concentrations). Furthermore, the cleavage yield is on par with the release observed for the widely used 3-pyrimidyl-6-methyl-tetrazine based activators[29,30] and TCO-linked ADC (data not shown).

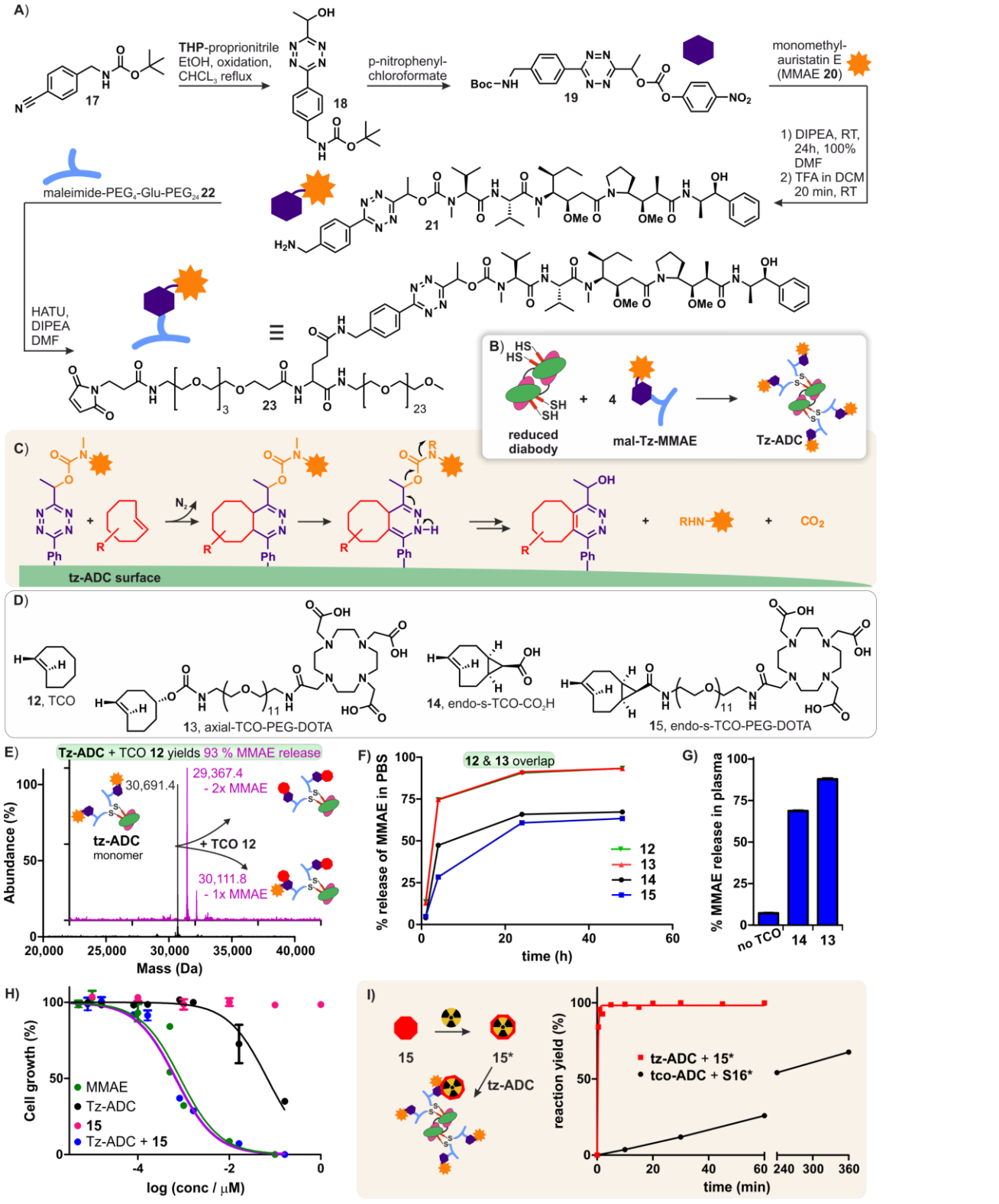

Figure 4. Evaluation of a TCO-cleavable antibody-drug conjugate. A) Synthesis of maleimide-PEG-tetrazine-MMAE **23**. B) Conjugation of **23** to diabody affording **tz-ADC**. C) TCO-triggered cleavage of MMAE from **tz-ADC**. D) Structures of TCO derivates used for release studies. E) Protein MS of **tz-ADC** (black) and of TCO **13**-activated **tz-ADC** (magenta) after 24h in PBS. F) TCO-triggered release of MMAE from **tz-ADC** in PBS. G) TCO-triggered release of MMAE from **tz-ADC** in mouse plasma after 24h quantified by LC-MS of liberated MMAE. H) Cell proliferation assay on TAG72-positive LS174T human colon carcinoma cells treated with **tz-ADC** alone or in combination with activator **15**, **15** alone or free MMAE; data are the mean with s.e.m (n=3); I) Schematic representation of radiolabelling of TCO **15** with 111-indium, resulting in **15***, which was reacted with **tz-ADC** in PBS at 37°C at 0.15 equivalents with respect to the diabody (0.6 μM); similarly **tco-ADC** (0.6 μM) was reacted with 0.36 equivalents of radiolabelled tetrazine **S16**.

ADCs allow the safe and effective use of highly potent drugs like MMAE, which are too toxic to be used as free drugs. After ADC targeting of the cancer cell, these drugs typically need to be cleaved from their antibody linker to exert their therapeutic effect. As a proof of principle of the TCO-cleavable **tz-ADC** we evaluated the cytotoxicity of **tz-ADC** and TCO **15** alone and in combination in a human colorectal cancer cell culture. TCO **15** alone was not toxic while **tz-ADC** alone only exhibited a relatively moderate activity (Figure 4H). However, when a fixed dose of 3.3 µM of TCO **15** was combined with the **tz-ADC,** the cytotoxicity increased 100-fold, affording an EC50 value of 0.67 nM, matching the toxicity of the parent drug MMAE, clearly underlining the efficacy of this new cleavage system. Finally, to demonstrate the reactivity advance offered by click-to-release from tetrazine *vs.* click-to-release from TCO, we compared the click reaction between a previously reported TCO-linked MMAE diabody ADC (**tco-ADC**)[23] and ^{177}Lu-labelled DOTA-tetrazine activator (**S16**) with the reaction of **tz-ADC** with ^{111}In-labelled DOTA-sTCO **15** in PBS at 37°C at a very low concentration of 0.6 µM in nearly equimolar conditions. Figure 4I shows the striking difference between the two systems, with the conjugation of **15** complete within 1 minute, while the conjugation of the tetrazine activator had a 3h half-life.

Conclusion

We have developed a new and highly reactive bioorthogonal elimination reaction that enables traceless release of an amine-containing payload from a tetrazine following reaction with a *trans*-cyclooctene. This was achieved by switching the roles of the tetrazine and TCO in the parent IEDDA pyridazine elimination, now permitting the use of highly reactive sTCO derivatives as activators, boosting the reactivity 3 orders of magnitude compared to the parent click-to-release reaction, and 4 to 6 orders of magnitude compared to the other known cleavage reactions.[4-17] Even the non-conformationally strained TCOs already gives 6-fold higher reactivity than the parent reaction combined with near quantitative release yields. Through mechanistic studies we demonstrated that the releasing tautomer is the 2,5-dihydropyridazine, which fortuitously is the favoured IEDDA product, and we found that the formation rate of this species is dependent on the type of TCO being used. By trapping the elimination product, we could show that the release occurs via the hypothesized 1,4-elimination. Furthermore, the strong dependence on water indicates a direct role for water in the electron cascade elimination mechanism. The new click-cleavable linker was subsequently applied in an ADC, which exhibited TCO-triggered drug cleavage half-lives down to 2h in fully aqueous conditions and showed good controlled release in biological conditions in plasma and in cell culture. Activation of the ADC led to effective cancer cell killing with the same potency as the free drug. Furthermore, a head-to-head comparison of the click reaction of TCO-linked ADC with radiolabelled tetrazine and tetrazine-linked ADC with radiolabelled TCO at very low concentration, underlined the pronounced advance offered by the highly reactive TCO-triggered dihydropyridazine elimination, for example for cases when the activator cannot be used in large excess.

These results hold promise for *in vivo* drug release and unmasking applications, potentially allowing substantially reduced activator doses. We also envision the use of this reaction in chemical biology, life-science assays, and material chemistry, enabling the controlled (dis)assembly of molecules, proteins, cells, or biomaterials at low concentration or in conditions that are incompatible with the TCO. For example, contrary to TCOs, tetrazines are typically stable at low pH. While the click-to-release from TCO offers faster release kinetics, we expect that the versatile click-to-release from tetrazine harbours ample opportunity for further improvements in cleavage rate and yield. Finally, the presented release chemistry can be performed with commercially available TCOs and uses tetrazine linkers and masks that are easier to prepare than TCO linkers, making highly reactive click-to-release chemistry available to a larger research community.

Acknowledgements

We thank Kim Bonger (Radboud University, Nijmegen) for critical reading of the manuscript. We gratefully acknowledge the support of the European Regional Development Fund (EFRO), Operation Program Oost, for Project "Proeftuin Nanomedicine".

References

1. Li, J. & Chen, P. R. Development and application of bond cleavage reactions in bioorthogonal chemistry. *Nat. Chem. Biol.* **12**, 129–137 (2016).
2. Tu, J., Xu, M. & Franzini, R. M. Dissociative Bioorthogonal Reactions. *ChemBioChem* **20**, 1615–1627 (2019).
3. Sabatino, V., Rebelein, J. G. & Ward, T. R. “Close-to-Release”: Spontaneous Bioorthogonal Uncaging Resulting from Ring-Closing Metathesis. *J. Am. Chem. Soc.* **141**, 17048–17052 (2019).
4. Jiménez-Moreno, E. *et al.* Vinyl Ether/Tetrazine Pair for the Traceless Release of Alcohols in Cells. *Angew. Chem. Int. Ed.* **56**, 243–247 (2017).
5. Neumann, K. *et al.* Tetrazine-Responsive Self-immolative Linkers. *ChemBioChem* **18**, 91–95 (2017).
6. Wu, H., Alexander, S. C., Jin, S. & Devaraj, N. K. A Bioorthogonal Near-Infrared Fluorogenic Probe for mRNA Detection. *J. Am. Chem. Soc.* **138**, 11429–11432 (2016).
7. Lelieveldt, L. P. W. M., Eising, S., Wijen, A. & Bonger, K. M. Vinylboronic acid-caged prodrug activation using click-to-release tetrazine ligation. *Org. Biomol. Chem.* **17**, 8816–8821 (2019).
8. Tu, J., Xu, M., Parvez, S., Peterson, R. T. & Franzini, R. M. Bioorthogonal Removal of 3-Isocyanopropyl Groups Enables the Controlled Release of Fluorophores and Drugs in Vivo. *J. Am. Chem. Soc.* **140**, 8410–8414 (2018).
9. Zheng, Y. *et al.* Enrichment-triggered Prodrug Activation Demonstrated through Mitochondria-targeted Delivery of Doxorubicin and Carbon Monoxide. *Nat. Chem.* **10**, 787–794 (2018).
10. Xu, M., Galindo-Murillo, R., Cheatham, T. E. & Franzini, R. M. Dissociative reactions of benzonorbornadienes with tetrazines: scope of leaving groups and mechanistic insights. *Org. Biomol. Chem.* **15**, 9855–9865 (2017).
11. Bernard, S. *et al.* Bioorthogonal Click and Release Reaction of Iminosydnones with Cycloalkynes. *Angew. Chem. Int. Ed Engl.* **56**, 15612–15616 (2017).
12. Riomet, M. *et al.* Design and Synthesis of Iminosydnones for Fast Click and Release Reactions with Cycloalkynes. *Chem. Eur. J.* **24**, 8535–8541 (2018).
13. Matikonda, S. S. *et al.* Bioorthogonal prodrug activation driven by a strain-promoted 1,3-dipolar cycloaddition. *Chem. Sci.* **6**, 1212–1218 (2015).
14. Matikonda, S. S. *et al.* Mechanistic Evaluation of Bioorthogonal Decaging with trans-Cyclooctene: The Effect of Fluorine Substituents on Aryl Azide Reactivity and Decaging from the 1,2,3-Triazoline. *Bioconjug. Chem.* **29**, 324–334 (2018).
15. Luo, J., Liu, Q., Morihiro, K. & Deiters, A. Small Molecule Control of Protein Function through Staudinger Reduction. *Nat. Chem.* **8**, 1027–1034 (2016).
16. van Brakel, R., Vulders, R. C. M., Bokdam, R. J., Grüll, H. & Robillard, M. S. A doxorubicin prodrug activated by the staudinger reaction. *Bioconjug. Chem.* **19**, 714–718 (2008).
17. Azoulay, M., Tuffin, G., Sallem, W. & Florent, J.-C. A new drug-release method using the Staudinger ligation. *Bioorg. Med. Chem. Lett.* **16**, 3147–3149 (2006).

18. Blackman, M. L., Royzen, M. & Fox, J. M. Tetrazine Ligation: Fast Bioconjugation Based on Inverse-Electron-Demand Diels−Alder Reactivity. *J. Am. Chem. Soc.* **130**, 13518–13519 (2008).

19. Oliveira, B. L., Guo, Z. & Bernardes, G. J. L. Inverse electron demand Diels–Alder reactions in chemical biology. *Chem. Soc. Rev.* **46**, 4895–4950 (2017).

20. Rossin, R. *et al.* In Vivo Chemistry for Pretargeted Tumor Imaging in Live Mice. *Angew. Chem. Int. Ed.* **49**, 3375–3378 (2010).

21. Versteegen, R. M., Rossin, R., ten Hoeve, W., Janssen, H. M. & Robillard, M. S. Click to Release: Instantaneous Doxorubicin Elimination upon Tetrazine Ligation. *Angew. Chem. Int. Ed.* **52**, 14112–14116 (2013).

22. Rossin, R. *et al.* Triggered Drug Release from an Antibody–Drug Conjugate Using Fast "Click-to-Release" Chemistry in Mice. *Bioconjug. Chem.* **27**, 1697–1706 (2016).

23. Rossin, R. *et al.* Chemically triggered drug release from an antibody-drug conjugate leads to potent antitumour activity in mice. *Nat. Commun.* **9**, 1484 (2018).

24. Czuban, M. *et al.* Bio-Orthogonal Chemistry and Reloadable Biomaterial Enable Local Activation of Antibiotic Prodrugs and Enhance Treatments against Staphylococcus aureus Infections. *ACS Cent. Sci.* **4**, 1624–1632 (2018).

25. Yao, Q. *et al.* Synergistic enzymatic and bioorthogonal reactions for selective prodrug activation in living systems. *Nat. Commun.* **9**, 5032 (2018).

26. Li, J., Jia, S. & Chen, P. R. Diels-Alder reaction-triggered bioorthogonal protein decaging in living cells. *Nat. Chem. Biol.* **10**, 1003–1005 (2014).

27. Zhang, G. *et al.* Bioorthogonal Chemical Activation of Kinases in Living Systems. *ACS Cent. Sci.* **2**, 325–331 (2016).

28. van der Gracht, A. M. F. *et al.* Chemical Control over T-Cell Activation in Vivo Using Deprotection of trans-Cyclooctene-Modified Epitopes. *ACS Chem. Biol.* **13**, 1569–1576 (2018).

29. Fan, X. *et al.* Optimized Tetrazine Derivatives for Rapid Bioorthogonal Decaging in Living Cells. *Angew. Chem. Int. Ed.* **55**, 14046–14050 (2016).

30. Sarris, A. J. C. *et al.* Fast and pH-Independent Elimination of trans-Cyclooctene by Using Aminoethyl-Functionalized Tetrazines. *Chem. Eur. J.* **24**, 18075–18081 (2018).

31. Versteegen, R. M. *et al.* Click-to-Release from trans-Cyclooctenes: Mechanistic Insights and Expansion of Scope from Established Carbamate to Remarkable Ether Cleavage. *Angew. Chem. Int. Ed.* **57**, 10494–10499 (2018).

32. Du, S. *et al.* Cell type-selective imaging and profiling of newly synthesized proteomes by using puromycin analogues. *Chem. Commun.* **53**, 8443–8446 (2017).

33. Khan, I., Seebald, L. M., Robertson, N. M., Yigit, M. V. & Royzen, M. Controlled in-cell activation of RNA therapeutics using bond-cleaving bio-orthogonal chemistry. *Chem. Sci.* **8**, 5705–5712 (2017).

34. Agustin, E. *et al.* A fast click–slow release strategy towards the HPLC-free synthesis of RNA. *Chem. Commun.* **52**, 1405–1408 (2016).

35. Rossin, R. *et al.* Highly Reactive trans-Cyclooctene Tags with Improved Stability for Diels–Alder Chemistry in Living Systems. *Bioconjug. Chem.* **24**, 1210–1217 (2013).

36. Stanovnik, B., Tišler, M., Katritxky, A. R. & Denisko, O. V. The Tautomerism of Heterocycles. Six-Membered Heterocycles: Part 1, Annular Tautomerism. in *Advances in Heterocyclic Chemistry* (ed. Katritzky, A. R.) vol. 81 253–303 (Academic Press, 2001).

37. Sauer, J. *et al.* 1,2,4,5-Tetrazine: Synthesis and Reactivity in [4+2] Cycloadditions. *Eur. J. Org. Chem.* **1998**, 2885–2896 (1998).

38. Upon completion of this manuscript, Tu *et al.* reported the efficient removal of tetrazylmethyl by isonitriles compared to other dienophiles. Tu, J. *et al.* Isonitrile-responsive and bioorthogonally removable tetrazine protecting groups. *Chem. Sci.* (2020) doi:10.1039/C9SC04649F

39. Alouane, A., Labruère, R., Le Saux, T., Schmidt, F. & Jullien, L. Self-Immolative Spacers: Kinetic Aspects, Structure–Property Relationships, and Applications. *Angew. Chem. Int. Ed.* **54**, 7492–7509 (2015).

40. Hay, M. P., Sykes, B. M., Denny, W. A. & O'Connor, C. J. Substituent effects on the kinetics of reductively-initiated fragmentation of nitrobenzyl carbamates designed as triggers for bioreductive prodrugs. *J. Chem. Soc. Perkin 1* 2759–2770 (1999).

41. Carlson, J. C. T., Mikula, H. & Weissleder, R. Unraveling Tetrazine-Triggered Bioorthogonal Elimination Enables Chemical Tools for Ultrafast Release and Universal Cleavage. *J. Am. Chem. Soc.* **140**, 3603–3612 (2018).

42. Taylor, M. T., Blackman, M. L., Dmitrenko, O. & Fox, J. M. Design and Synthesis of Highly Reactive Dienophiles for the Tetrazine–trans-Cyclooctene Ligation. *J. Am. Chem. Soc.* **133**, 9646–9649 (2011).

20191217_Click-to-Release from Tetrazine.pdf (1.66 MiB) view on ChemRxiv • download file

Supplementary Information

Bioorthogonal Tetrazine Carbamate Cleavage by Highly Reactive *Trans*-Cyclooctene

van Onzen *et al.*

Content

S1: Supplementary Methods

1.1 Materials

All reagents, chemicals, materials and solvents were obtained from commercial sources, and were used as received: Biosolve, Merck and Cambridge Isotope Laboratories for (deuterated) solvents, and Aldrich, Acros, ABCR, Merck, Fluka, and Fluorochem for chemicals, materials and reagents, also including nitrile starting compounds that have not been described. All solvents were of AR quality. Tablets for the preparation of phosphate buffered saline solution (PBS) were purchased from Calbiochem. Water was distilled and deionized (18 MΩcm) by means of a milli-Q water filtration system (Millipore). Monomethyl auristatin E (MMAE) and d8-MMAE were purchased from Selleck Chemicals and MedChem Express, respectively. Dry CH_2Cl_2, THF and DMF were dispensed from a MBRAUN MB-SPS-800 system. *t*-Butyl (32-amino-3,6,9,12,15,18,21,24,27,30-decaoxadotriacontyl)carbamate **S10** was obtained from PurePEG. MAL-dPEG®$_4$-Glu(TFP ester)-NH-m-dPEG®$_{24}$ was obtained from Quanta Biodesign limited. 3-Methyl-6-phenyl-1,2,4,5-tetrazine was prepared according to a literature procedure.[1] *rel*-(1*R*,4*E*,p*S*)-Cyclooct-4-enol was purchased from Kerafast. (1*R*,8*S*,9*s*,*E*)-Bicyclo[6.1.0]non-4-ene-9-carboxylic acid **14** and (1*R*,8*S*,9*s*,*E*)-2,5-Dioxopyrrolidin-1-yl bicyclo[6.1.0]non-4-ene-9-carboxylate **S13** were prepared according to a literature procedure.[2] (*E*)-cyclooctene **12** was prepared according to a literature procedure.[3] Sodium [^{125}I]iodide and [^{177}Lu]lutetium chloride solutions were purchased from PerkinElmer. [^{111}In]Indium chloride solution was purchased from Curium. The Bolton-Hunter reagent (*N*-succinimidyl-3-[4-hydroxyphenyl]propionate, SHPP) and Zeba desalting spin columns (7 and 40 kDa MW cut-off, 0.5 mL) were purchased from Pierce Protein Research (Thermo Fisher Scientific). Amicon Ultra centrifugal filter units (10 kDa MW cut-off) and PD-10 desalting columns were purchased from Merck and GE Healthcare Life Science, respectively. Mouse serum was purchased from Innovative Research.

1.2 General Methods

Moisture or oxygen-sensitive reactions were performed under an Ar atmosphere. In the synthetic procedures, equivalents (eq) are molar equivalents. Concentrations of reactants used in the synthetic procedures generally range from about 0.05 to about 3 M, and are typically and mostly in between 0.1 M and 1.0 M. Analytical thin layer chromatography was performed on Kieselgel F-254 precoated silica plates. Column chromatography was carried out on Screening Devices B.V. flash silica gel (40-63 μm mesh) or normal silica gel (60-200 μm mesh). ^{1}H-NMR and ^{13}C-NMR spectra were recorded on a Bruker Avance III HD (400 MHz for ^{1}H-NMR and 100 MHz for ^{13}C-NMR), a Varian Mercury (400 MHz for ^{1}H-NMR and 100 MHz for ^{13}C-NMR) spectrometer or a Varian Unity Inova 500 MHz spectrometer (500 MHz for ^{1}H-NMR) spectrometer at 298 K. Chemical shifts are reported in ppm downfield from TMS at room temperature. Abbreviations used for splitting patterns are s = singlet, d = doublet, t = triplet, q = quartet, qn = quintet, sept = septet, m = multiplet and br = broad. UV-Vis spectroscopy was performed on a Jasco V-650 spectrometer equipped with a Jasco CTU-100 circulating thermostat unit. Stopped-flow UV-Vis measurements were performed with a BioLogic stopped-flow setup consisting of a SFM-400/S stopped-flow module with Berger Ball mixer, a MOS-500 spectrometer with Xe/Hg light source, an ALX 250 Arc Lamp Power Supply, a SAS PMT-450 photomultiplier tube, a BioLogic TC 100 cuvet (optical path length 10 mm), a MPS-60 microprocessor unit and a Julabo F-12 temperature controller. BioKine 32 software was used to operate the stopped-flow setup and analyze the results. GC-MS was recorded using a Shimadzu GCMS-QP2010 plus on a Phenomenex Zebron ZB-5MS column, employing helium as carrier gas and using a temperature program from 50°C or 80°C to 300°C (heating rate 25 °C/min.). IR spectra were recorded on

a Perkin Elmer 1600 FT-IR (UATR) or a Shimadzu IRAffinity-1 (UATR). HPLC-PDA/MS was performed using a Shimadzu LC-10 AD VP series HPLC coupled to a diode array detector (Finnigan Surveyor PDA Plus detector, Thermo Electron Corporation) and an Ion-Trap (LCQ Fleet, Thermo Scientific). HPLC-analyses were performed using a Alltech Alltima HP C_{18} 3µ column using an injection volume of 1-4 µL, a flow rate of 0.2 mL min^{-1} and typically a gradient (5 % to 100 % in 10 min, held at 100 % for a further 3 min) of ACN in water (both containing 0.1 % formic acid) at 35 °C. Preparative RP-HPLC (ACN / water with 0.1 % formic acid) was performed using a Shimadzu SCL-10A VP coupled to two Shimadzu LC-8A pumps and a Shimadzu SPD-10AV VP UV-Vis detector on a Phenomenex Gemini 5µ C_{18} 110A column. Quantitative HPLC-SIM-MS was performed on a Shimadzu Nexera-I LC-2040C system.

Size exclusion chromatography (SEC) was performed on an Akta system equipped with a Superdex 200 column. Protein HPLC-QTOF-MS analysis was performed on a Waters Acquity UPLC system equipped with a Sample Manager and a Xevo G2 Quadrupole Time of Flight (QTOF) detector, applying Zspray lockspray ionisation. Mass Lynx v4.1 software was used. Radio-HPLC was performed on an Agilent 1100 system, equipped with a Gabi radioactive detector (Raytest). The samples were loaded on an Alltima C_{18} column (4.6 × 150mm, 5µ), which was eluted at 1 mL/min with a linear gradient of water (A) and ACN (B) containing 0.1 v/v% TFA (4 min at 20% B followed by an increase to 70% B in 11 min). Radio-ITLC was performed on ITLC-SG strips (Varian Inc.) eluted with 200 mM EDTA in saline solution (^{111}In- and ^{177}Lu-labeling) or a 1:1 mixture of methanol/ethyl acetate (^{125}I-labeling). In these conditions the radiolabeled products remain at the base while unbound ^{111}In/^{177}Lu and [^{125}I]I-SHPP migrates with an R_f of 0.7-0.9. SDS polyacrylamide gel electrophoresis (SDS-PAGE) was performed on a Mini-PROTEAN Tetra Cell system using 4-15 % precast Mini-PROTEAN TGX gels and Precision Plus Protein All Blue Prestained protein standards (Bio-Rad Laboratories). The radioactivity distribution on TLC plates and SDS-PAGE gels was monitored with a Typhoon FLA 7000 phosphor imager (GE Healthcare Life Science) using the AIDA software.

1.3 Stability of tetrazines

The assessment of tetrazine stability was performed in 20 % ACN in PBS at 37 °C in triplicate. Tetrazine solutions in DMSO (25 mM, 10 µL) were diluted with ACN (0.60 mL) and PBS (2.40 mL), filtered, and incubated at 37 °C. The decrease of the absorption band at 520 nm (specific for the tetrazine moiety) was monitored using UV spectroscopy. The rate of hydrolysis and half-life time was derived by fitting a monoexponential decay through these data.

1.4 Reaction kinetics between tetrazines and *trans*-cyclooctenes

The second-order rate constant of the IEDDA reaction between tetrazine **11** and TCOs **12** and **14** in ACN and between tetrazine **11** and TCOs **12** in 25% ACN/PBS at 20°C was determined in triplicate by UV-Vis spectrometry under second-order conditions. A cuvette was filled with a solution of **11** (3 mL 0.167 mM in 25% ACN/PBS, 0.50 µmol), and equilibrated at 20 °C. Next, a solution of **12** (5.0 µL 100 mM in DMSO, 0.50 µmol) was added. The absorption at 526 nm (specific for the tetrazine moiety) was measured every second in a time course experiment. From the decay of this absorption, the conversion *x* was calculated. The second-order rate constant k_2 was determined from the slope of the curve of a plot of 1/c-1/c0 versus time.

The second-order rate constant of the IEDDA reaction between tetrazine **11** and sTCO **14** in 25% ACN/PBS at 20°C was determined (N=4) by stopped-flow UV-Vis spectrometry under pseudo first-order conditions.

Solutions of **11** (0.50 mM in 25% ACN/PBS) and **14** (4.39 mM in in 25% ACN/PBS) were mixed with 25% ACN/PBS in a volume ratio of 1:1:8, resulting in a concentration of 0.050 mM and 0.439 mM, respectively. The absorption at 270 nm was measured every 10 ms, and from the decay of this absorption, the pseudo first-order rate constant k_1' was determined by a nonlinear Simplex regression analysis of the data points using BioKine software. The second-order rate constant k_2 was calculated: $k_2 = k_1' / c_{,TCO}$.

1.5 Tautomerization and release reactions of tetrazine derivatives with trans-cyclooctenes

Release from model tetrazines

A solution of the tetrazines (10 µL 25 mM in DMSO) was diluted with ACN (200 µL), and PBS (800 µL). Next, a solution of TCO **12** (10 µL 50 mM in DMSO) was added, and the pink solution was homogenized, and left at room temperature until it became colorless (typically 10 – 20 min). Then a sample was analyzed by HPLC-MS/PDA, and subsequently incubated at 37°C. At specific time points, the sample was again analyzed by HPLC-MS/PDA (Supplementary Fig. S1), and the tautomerization of and release from the IEDDA adducts was monitored at a wavelength of 308 nm, which is the isosbestic point of the tautomerization reaction. From these spectral changes, the release yield was determined.

Correlation between water content and release

A 100 mM stock solution was prepared of tetrazine **11** (22.75 mg, 83.2 µmol) in ACN (0.833 mL) and a 200 mM stock solution of TCO **12** (26.98 mg, 233 µmol) in ACN (1.165 mL). Reaction mixtures with a specific water content were prepared in triplicate by diluting the tetrazine stock solution (25 µL, 2.5 µmol) with a specific volume of ACN (212.5 – 1000 µL) and PBS (787.5 – 0 µL) to obtain a total volume of 1025 µL. Subsequently the TCO solution was added (25 µL. 5.0 µmol), and the mixture was homogenized and incubated at 37°C. The progress of the release reaction was analyzed at specific time points using HPLC-MS/PDA. To facilitate analysis, aliquots were oxidized to afford stable mixtures. Therefore, an aliquot of 100 µL of the mixture was taken and diluted with ACN (175 – 100 µL), water (625 – 700 µL), and an aqueous solution of sodium nitrite (100 µL 50 mM) to obtain 1 mL of the sample solution containing 20 v/v% ACN. Oxidation of the sample solution started upon addition of formic acid (10 µL), and was instantaneous. The progress of the release reaction was determined from the ratio of **P1** and **P2** , which were quantified by HPLC-MS/PDA at a wavelength of 235 nm (Supplementary Fig. S2).

Release from a specific tautomer

^{1}H-NMR spectroscopy was used to analyze the composition of a mixture of tautomers of the IEDDA adducts from tetrazine **11** and TCO **12** in $CDCl_3$ (see section 1.6) . To study the release from a specific tautomer, at a selected time point an aliquot of 100 µL of the NMR solution was evaporated to dryness and redissolved in ACN (0.75 mL) and PBS (2.25 mL). Subsequently, this reaction mixture was incubated at 37 °C. The progress of the release reaction was sampled at specific time points, by taking an aliquot of 100 µL of the mixture and diluting this with ACN (175 µL), water (625 µL), and an aqueous solution of sodium nitrite (100 µL 50 mM). Oxidation of the sample solution was started upon addition of formic acid (10 µL), and

was instantaneous. The progress of the release reaction was determined from the ratio of **P1** and **P2**, which were analyzed by HPLC-MS/PDA.

Trapping of elimination product (EP) with *N*-acetyl-L-cysteine (NAC)

A solution of tetrazine **11** in DMSO (10 µL 25 mM, 0.25 µmol) was diluted with ACN (200 µL). Next, a solution of *N*-acetyl-L-cysteine in PBS (800 µL 20 mM; 16 µmol) was added, followed by a solution of TCO **12** in DMSO (10 µL 50 mM; 0.50 µmol). The mixture was subsequently incubated at 37°C for 40 h and then analyzed by HPLC-MS/PDA to prove the formation of **EP-NAC**. HPLC-MS/PDA: *m/z* Calc. for $C_{23}H_{31}N_3O_3S$ 429.21; Obs. $[M+H]^+$ 430.25.

Rate of tautomerization of the 4,5-tautomer of IEDDA adduct of 3-phenyl-6-methyl-1,2,4,5-tetrazine with either trans-cyclooctene or ethyl (E)-bicyclo[6.1.0]non-4-ene-9-carboxylate

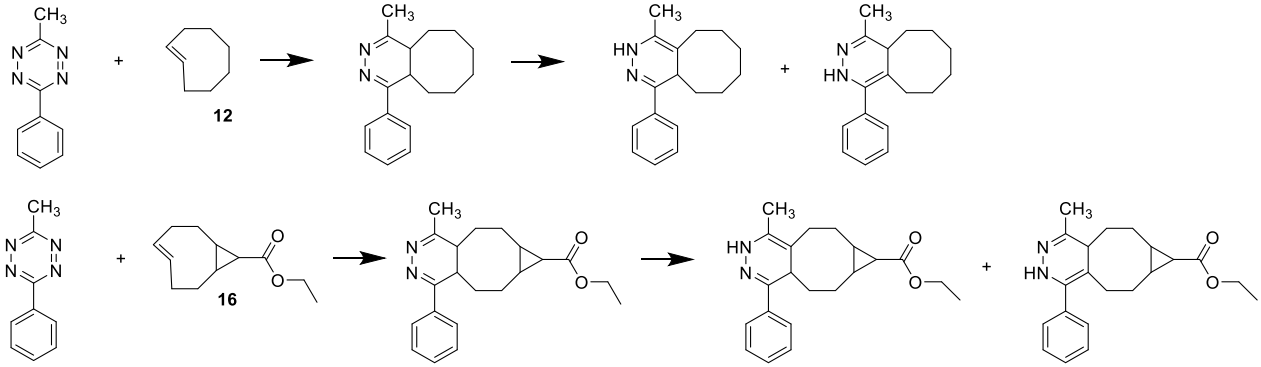

A 3 mL UV cuvette was kept at 20°C, and filled with ACN (100 µL), a solution of 3-phenyl-6-methyl-1,2,4,5-tetrazine (10 µL 25 mM in DMSO, 0.25 µmol), and a solution of *trans*-cyclooctene **12** or ethyl (*E*)-bicyclo[6.1.0]non-4-ene-9-carboxylate **16** (10 µL 100 mM in DMSO, 1.00 µmol). After the pink color disappeared (approx. 1 min), the mixture was diluted with ACN (0.65 mL) and PBS (2.25 mL). The tautomerization was monitored by UV-Vis spectroscopy at regular intervals, and the rate of tautomerization was determined from the decay of the absorption at 272 nm, which is typical for the 4,5-tautomer. A half-life of 5.3 h was determined for **12** and 9.2 h for **16**.

1.6 NMR studies

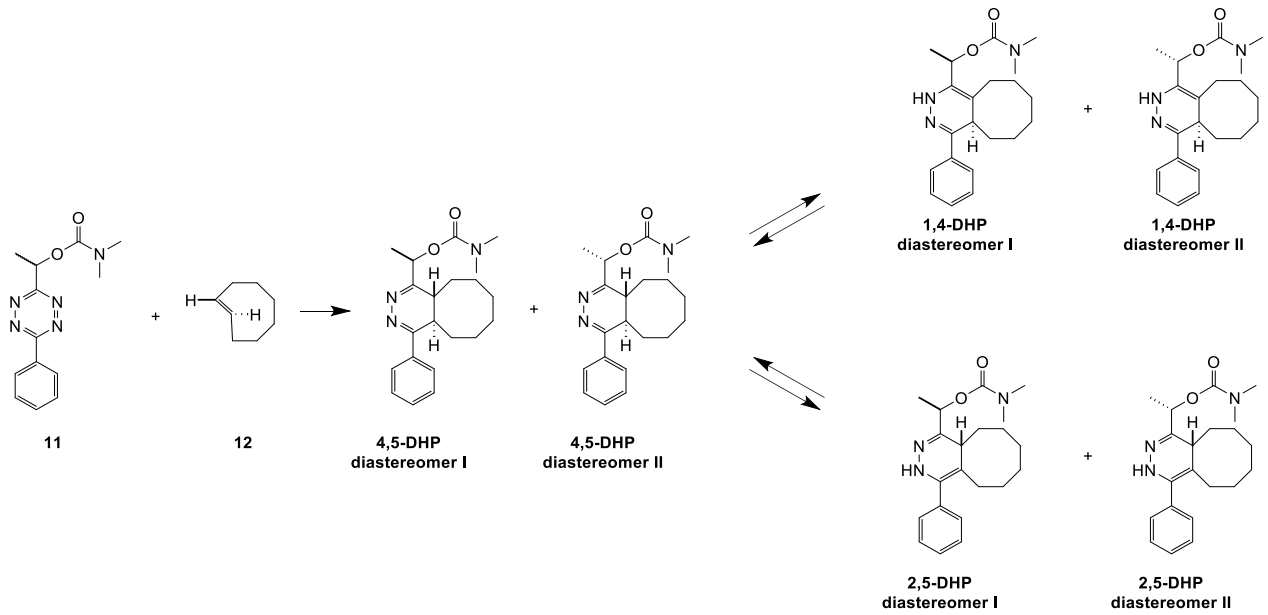

NMR evaluation of IEDDA reaction and acid induced tautomerization

The IEDDA reaction and subsequent tautomerization of **11** and *trans*-cyclooctene **12** was monitored by ^{1}H-NMR. TCO **12** (16.9 mg, 154 µmol) was dissolved in $CDCl_3$ (600 µL) and tetrazine **11** (38.2 mg, 140 µmol) was added. The pink mixture became colorless within seconds, and some gas bubbles were observed. The solution was transferred into an NMR tube, and the reaction was monitored at specific timepoints with consecutive ^{1}H-NMR spectra. The relative amounts of the different species were obtained by integration of the relevant peaks, and were plotted as a function of time. At selected time points, the mixture was further analyzed by FTIR, UV (1 drop $CDCl_3$ solution in 3 mL ACN), and NOESY NMR. Characterization of the mixture revealed the initial formation of the 4,5-tautomer, which was stable in these conditions. To induce the tautomerization of the 4,5- to the 2,5- and 1,4-tautomer, formic acid (0.5 µL) was added to the NMR solution. After 3 h, the 4,5-tautomer had completely disappeared, resulting in a mixture of 2,5- and 1,4-DHP in a ratio of 73/27 . When the NMR solution was allowed to stand for a longer time, the ratio between 2,5- and 1,4-DHP changed in favor of the 1,4-DHP. After 184 h, a ratio of 26/74 was obtained.

NMR characterization of the non-releasing tautomer

TCO **12** (6.6 mg, 60 µmol) was dissolved in ACN (8 mL), and potassium phosphate buffer (30 mL 20 mM, pH=7.4) was added, followed by tetrazine **11** (14.9 mg, 54.6 µmol) in ACN (2 mL). The pink mixture became colorless within seconds. The solution was stirred at 37°C under an inert atmosphere for 3 days. After lyophilization, the organics were dissolved in $CDCl_3$ (2 mL) and this solution was washed with aqueous sodium bicarbonate (1 mL 0.5 M), and dried over sodium sulfate. The $CDCl_3$ solution was characterized by NMR, showing the disappearance of the peaks corresponding to the 2,5-tautomer, while the peaks of the 1,4-tautomer were still present.

NMR characterization of product P1

TCO **12** (6.6 mg, 60 µmol) was dissolved in ACN (8 mL), and potassium phosphate buffer (30 mL 20 mM, pH=7.4) was added, followed by tetrazine **11** (14.9 mg, 54.6 µmol) in ACN (2 mL). The pink mixture became colorless within seconds. Then, it was cooled to 0°C, and subsequently sodium nitrite (18.8 mg, 273 µmol) and formic acid (0.4 mL) were added to oxidize the intermediates. The mixture was stirred for 15 min at room temperature and then lyophilized. The organics were dissolved in chloroform (10 mL), washed with aqueous sodium bicarbonate (5 mL), dried over sodium sulfate, and evaporated to dryness, to yield 13 mg of an off-white solid containing mainly **P1**. Characterization of the product proved its identical structure compared to reference compound **P1** (Section S2).

NMR characterization of product P2

TCO **12** (6.6 mg, 60 µmol) was dissolved in ACN (8 mL), and potassium phosphate buffer (30 mL 20 mM, pH=7.4) was added, followed by tetrazine **11** (14.9 mg, 54.6 µmol) in ACN (2 mL). The pink mixture became colorless within seconds. The solution was stirred at 37°C under an inert atmosphere for 3 days. Then, it was cooled to 0°C, and subsequently sodium nitrite (18.8 mg, 273 µmol) and formic acid (0.4 mL) were added to oxidize the intermediates. The mixture was stirred for 15 min at room temperature and then lyophilized. The organics were dissolved in chloroform (10 mL), washed with aqueous sodium bicarbonate (5 mL), dried over sodium sulfate, and evaporated to dryness, to yield 13 mg of an off-white solid containing mainly **P2**. Characterization of the product proved its identical structure compared to reference compound **P2** (Section S2).

1.7 Computational Modelling

The Amsterdam Density Functional (ADF) program was employed for performing DFT and TDDFT calculations on the structures presented in the scheme below.[4]

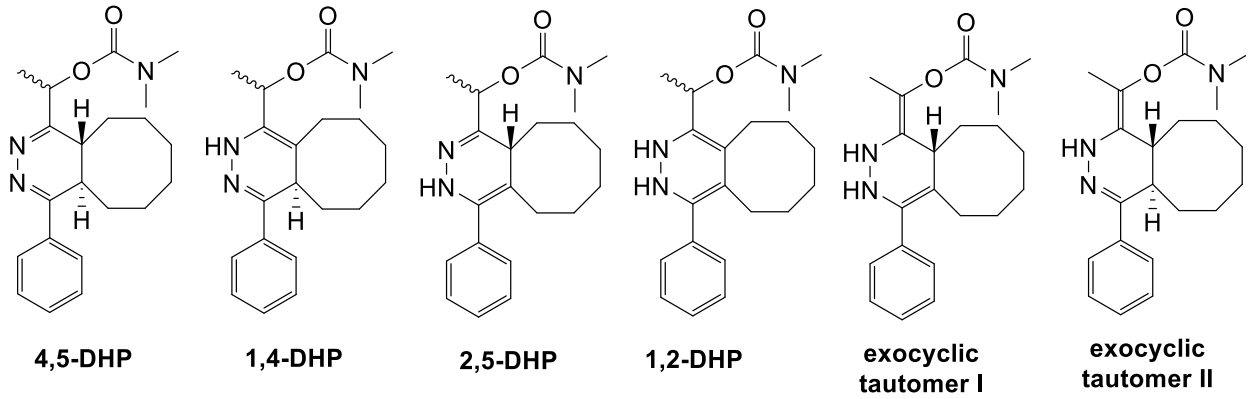

The B3LYP exchange-correlation functional in conjunction with a triple-ζ (TZP) Slater-type basis set was used in all calculations.[5–8] Implicit solvation effects on the geometry and optical spectra were considered by employing the COSMO model with parameters for water.[9] Optical absorption was convoluted with a Gaussian width of 14 nm.

1.8 Synthesis and characterization of tz-ADC

The anti-TAG72 diabody AVP04-58 (MW 51088 Da) was provided by Avipep Ltd. AVP04-58 was prepared as previously described[10] without the C-terminal His_6 tag, and differs from the parent anti-TAG72 diabody AVP04-07 by the substitution of cysteine residues into positions L8 and L11 in the VL domain, thus affording two additional cysteine residues per scFv monomer (4 cysteines per diabody). These 4 cysteine residues were used for site-specific conjugation of maleimide-Tz-MMAE **23** yielding **tz-ADC**.

Diabody functionalization was achieved via maleimide chemistry as described previously,[11] by reduction of the disulfide bonds with dithiothreitol (DTT) followed by diabody reaction with **23**. Briefly, a ca. 2 mg/mL diabody solution in degassed 100 mM phosphate buffer pH 6.8 containing 2 mM EDTA (EDTA-PB) was combined with freshly dissolved 100 mM DTT in EDTA-PB (6 mM final DTT concentration) and incubated at room temperature for 1 h. The reduced diabody was then loaded on a PD-10 column and eluted from the column with EDTA-PB, and immediately afterwards combined with a solution of **23** (7.5 eq. per SH) in DMSO (ca. 15 v/v% DMSO in the final mixture) and incubated overnight at 4°C. Subsequently the ADC was purified by gel filtration on a AKTA system equipped with a Superdex 75 26/60 prep-grade column which was eluted with EDTA-PB at 2.5 mL/min. The purified fractions were combined and mixed with 5% DMSO. The solution was then concentrated using Amicon Ultra-15 centrifugal filters and the ADC concentration was measured by NanoDrop. The ADC was then analysed by SDS-PAGE (Supplementary Fig. S19) and ESI-TOF MS (Supplementary Fig. S20/S21) confirming the identity of the conjugate with drug-to-antibody ratio (DAR) of 4 in the presence of only trace amounts of aggregates.

1.9 Analyses of tz-ADC - TCO reaction and MMAE release

Stock stability

The stability of the **tz-ADC** stock solution at 4°C was monitored by QTOF-MS analysis. An aliquot of the stock solution (10 µL 2 µg/µL in 5% DMSO/EDTA-PBS) was diluted with PBS (90 µL), and analyzed with HPLC-QTOF-MS (supplementary Fig. S22). This procedure was repeated over the course of 1 year. No degradation of the diabody conjugates was observed in this time frame Supplementary Fig. S22/S23.

Reaction tz-ADC with TCOs and release of MMAE

A stock solution of **tz-ADC** (127 µL 2.36 mg/mL in 5% DMSO/EDTA-PB) was diluted with PBS (3 mL). This solution was analyzed by protein MS analysis. Subsequently, an aliquot of this solution (100 µL) was reacted with a TCO derivative (2 µL 25 mM in DMSO). After 1 h, this mixture was analyzed by protein MS analysis, and then it was incubated at 37°C followed by protein MS analysis at 4 h, 24 h, and 48 h, measuring the formation diabody reaction products and the elimination of MMAE. The MS spectra after 48h incubation with TCO **12**-**15** are presented in Supplementary Fig. S24 – S27 respectively.

Reaction between tz-ADC and 111-indium labeled 15

The reaction between **tz-ADC** and [111-In]**15** was performed in PBS at 37°C. The **tz-ADC** concentration was $5.548*10^{-7}$ M and the concentration of labelled activator **15** was $8.592*10^{-8}$ M. At various times between 30 s and 1 h, aliquots of the reaction mixture were taken and quenched with a large excess of a TCO derivative. After 30 min incubation at room temperature, these aliquots were analysed by SDS-PAGE and

phosphor imager. The reaction between **tco-ADC** ($5.867*10^{-7}$ M) and [177Lu]Lu-labelled tetrazine (**S16**, $2.119*10^{-7}$ M)[11] was performed in a similar way.[11]

1.10 Radiolabeling of 13 and 15

Axial-TCO-PEG-DOTA 13 and s-TCO-PEG-DOTA 15 radiolabelling and analysis

Ca 15 MBq of indium-111 was added to ca 25 µL of 0.2 M NH_4OAc pH 6.0 buffer and 2 nmol **13** or **15** was added. Non radioactive indium (0.95 eq) was also added to the labeling mixture of **15**. The solutions were incubated at 60°C for 10 min and subsequently 50 nmol of DTPA was added to challenge unbound indium. Radio-ITLC and HPLC confirmed a purity of > 94 % for **13**. **15** Was loaded on a sep-pak tC18 light cartridge and rinsed with water and 20 % EtOH / water. Next, **15** was eluted from the sep-pak with EtOH, followed by blowing of the EtOH and dissolving labeled **15**. Radio-ITLC and HPLC confirmed a purity of > 93 %

1.11 Cell culture and proliferation assay

Cell culture

The human colon cancer LS174T cell line used in this study was obtained from ATCC and was maintained at 37°C in a humidified atmosphere with 5% CO2. The cell line was cultured in RPMI-1640 medium (Gibco) supplemented with 2 mM glutamine (Gibco) and 10% heat inactivated fetal calf serum (Sigma-Aldrich).

Cell proliferation assay

The LS174T cells were plated in 96-well plates (Nunc) at a 5000 cells/well density 24 h prior to the experiment. Activator **15** (9.81 mM in DMSO), **tz-ADC** (1.48 mg/mL in EDTA-PB containing 5% DMSO) and MMAE (63 µM in DMSO) were serially diluted in pre-warmed culture medium immediately before the experiment and added to the wells (200 µL final volume per well). The **tz-ADC** was either added alone or followed by 3 µM activator (5 eq. with respect to the highest tetrazine concentration). After 72 h incubation at 37°C, cell proliferation was assessed by an MTT assay. Briefly, methylthiazolyldiphenyltetrazolium bromide (MTT) was dissolved in PBS at a 5 mg/mL concentration, filtered through a 0.22 µm filter and 30 µL solution was added to each well. After 120 min incubation at 37°C the medium was gently aspirated. The formed formazan crystals were dissolved in 200 µL DMSO and the absorbance at 560 nm was measured with a plate reader (Infinite 200 PRO, TECAN Technologies). The proliferation assay was performed in triplicate. EC_{50} values were derived from normalized cell growth curves generated with GraphPad Prism 5.01.

1.12 MMAE quantification

MMAE release in vitro

In a 1.5 mL vial, the following was combined: 480 µL mouse serum, 80 µL PBS, 130 µL **tz-ADC** (0.1 µg/µL in PBS) and 110 µL d8-MMAE solution ($1.0x10^{-2}$ µg/µL). Next, aliquots of 20 µL were prepared to which 4 µL of a TCO solution (0.25 mM in PBS) was added and the solution was incubated at 37°C. At the

desired timepoint, 72 µL of cold ACN was added to the aliquot and the mixture was vortexed, stored at 4°C for 30 min. and centrifuged. 30 µL of supernatant was taken and combined with 70 uL of 1 % formic acid (aq) solution for LC-MS analysis *vide infra*.

S2: Synthesis

2.1 General Synthetic Procedures

General procedure A – Tetrazine (TZ) synthesis

The nitrile (or combination of two different nitriles) and zinc triflate (0.05 eq to the total nitrile content) were combined. When this did not yield a clear solution this was achieved by shortly heating the mixture at 60 °C or by the addition of a minimum amount of EtOH. When a clear solution was obtained hydrazine monohydrate (5 eq to the total nitrile content) was added at once and the mixture was stirred at 60 °C for typically 16 h. The volatiles were removed *in vacuo*, the crude mixture containing dihydrotetrazine precursor ([2H]-TZ) was re-dissolved in THF / AcOH (1:1) and this solution was cooled on an ice-bath. $NaNO_2$ (5 eq to the total nitrile content) in water (5 to 10 mL per gram $NaNO_2$) was added dropwise (CAUTION: toxic fumes!). After stirring at room temperature for 10 min (or until a clear solution was achieved as a consequence of a delayed reaction due to a limited solubility of a reactant), water was added and the solution was extracted with $CHCl_3$ until an aqueous layer was obtained that lacked the typical TZ pink (sometimes red or purple) coloration. The organic layer was dried with Na_2SO_4 and the volatiles were removed *in vacuo*. Traces of AcOH were removed by flushing with $CHCl_3$, or by performing an additional sat. $NaHCO_3$ wash.

General procedure B – THP deprotection

The synthesis of THP-protected TZs was directly followed by THP-deprotection since, as a consequence of the acidic conditions, the THP group was largely removed during the oxidation process from [2H]-TZ to TZ. (Partly) THP-protected TZ was dissolved in $CHCl_3$ / EtOH 2:1 and concentrated HCl was added (1 drop). The mixture was stirred at room temperature until TLC analysis indicated full conversion (generally around 1 h). The volatiles were removed *in vacuo* and the resulting product was flushed twice with $CHCl_3$. Note: if present, this procedure will generally remove around 5 % of *N*-*t*-Boc-protecting groups.

General procedure C – Isocyanate coupling to TZ-alcohol

The TZ-alcohol was dissolved in dry THF. When necessary gentle heating was applied to dissolve all starting compound. Dibutyltindilaurate (catalyst, 0.1 eq per alcohol) and isocyanate (2 eq per alcohol) were added, the mixture was stirred at 40 °C for 1 h and the solvent was removed *in vacuo*.

General procedure D – TZ-alcohol activation and coupling to secondary amine to produce TZ-carbamate

Examples for primary alcohols: The primary TZ-alcohol and *N*,*N*-diisopropylethylamine (1.5 eq) were dissolved in CH_2Cl_2 and *p*-nitrophenylchloroformate (1.5 eq) was added as a solid. Upon addition, TLC analysis showed full conversion and the secondary amine was added (3 eq). An instantaneous color change as well as TLC analysis indicated full conversion. $CHCl_3$ was added and the organic layer was sequentially washed with 0.1 M HCl, sat. $NaHCO_3$ (until a colorless aqueous layer was obtained) and brine, dried with Na_2SO_4, filtrated and the filtrate was concentrated *in vacuo*.

Examples for secondary alcohols: The secondary TZ-alcohol and 4-dimethylaminopyridine (1.5 eq) were dissolved in CH_2Cl_2 and *p*-nitrophenylchloroformate (1.5 eq) was added as a solution in CH_2Cl_2 at once (minimizing the formation of symmetrical TZ carbonate). Upon addition, TLC analysis showed full conversion and the secondary amine was added (4 eq). A color change occurred gradually and the mixture was stirred at room temperature until TLC analysis indicated full conversion. $CHCl_3$ was added and the organic layer was sequentially washed with 0.1 M HCl, sat. $NaHCO_3$ (until a colorless aqueous layer was obtained) and brine, dried with Na_2SO_4, filtrated and the filtrate was concentrated *in vacuo*.

General procedure E – Lactonitrile activation and coupling to secondary amine to produce carbamate

Lactonitrile (racemate) was dissolved in a 1.9 M toluene solution of phosgene (2 eq) followed by the dropwise addition of *N*,*N*-diisopropylethylamine (1 eq). After stirring at room temperature for 1 h the solid was removed by filtration and the filtrate was concentrated *in vacuo*. The resulting oil was re-dissolved in $CHCl_3$ and the solution was washed with 0.1 M HCl (2x) and brine, dried using Na_2SO_4, filtrated and the filtrate was evaporated to dryness. This yielded α-cyanoethyl chloroformate as a yellow oil which was used immediately without further purification. The secondary amine (2 eq) was dissolved in toluene and, on an ice bath, a solution of the chloroformate (1 eq) in toluene was added dropwise. The mixture was stirred at room temperature for 16 h after which the white solid was removed by filtration. The solution containing the desired nitrile was evaporated to dryness and flushed with $CHCl_3$ (2x).

2.2 Purification

The general procedures for the synthesis of the desired TZs and intermediates typically yield a product that is not (completely) pure. The specific purification method is indicated for each compound separately. Whenever purification implied column chromatography, eluent conditions were based on the outcome of TLC analyses. Indicated percentages (%) of eluent used in column chromatography are v/v %.

2.3 Synthetic Procedures

Compounds S1, S2, 1, 2

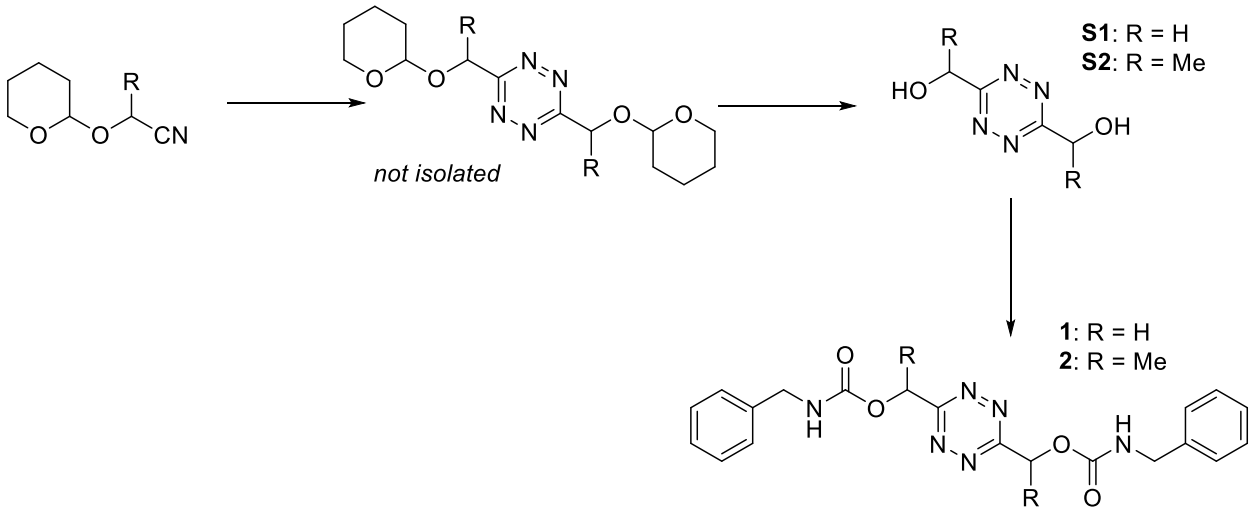

The following compounds **S1** and **S2** have been prepared according to general procedures A and B.

(1,2,4,5-Tetrazine-3,6-diyl)dimethanol (S1): This compound was prepared from 2-((tetrahydro-2*H*-pyran-2-yl)oxy)ACN.[12] Column chromatography (flash SiO_2, 6 % MeOH in $CHCl_3$) yielded pure **S1** (49 mg, 0.34 mmol, 38 % over two steps) as a pink solid. ^{1}H-NMR (CD_3OD): δ = 5.17 (s, 4H, CH_2). ^{13}C-NMR (CD_3OD): δ = 170.5, 63.5. HPLC-MS/PDA: *m/z* Calc. for $C_4H_6N_4O_2$ 142.05; Obs. $[M+H]^+$ 143.00, λ_{max} = 269 and 515 nm. FT-IR (ATR): υ (cm^{-1}) = 3393, 2920, 2518, 1463, 1443, 1401, 1363, 1308, 1226, 1102, 1075, 976, 918, 743, 639.

1,1'-(1,2,4,5-Tetrazine-3,6-diyl)diethanol (S2): This compound was prepared from 2-((tetrahydro-2*H*-pyran-2-yl)oxy)propionitrile.[2] Column chromatography (flash SiO_2, 50 % EtOAc in $CHCl_3$) yielded pure **S2** (16 mg, 91 µmol, 56 % over two steps) as a pink solid. ^{1}H-NMR ($CDCl_3$): δ = 5.48 (q, J = 6.7 Hz, 2H, C*H*), 3.45 (br, 2H, O*H*), 1.80 (d, J = 6.7 Hz, 6H, CH_3). ^{13}C-NMR (CD_3OD): δ = 173.0, 69.5, 22.3. GC-MS: *m/z* Calc. for $C_6H_{10}N_4O_2$ 170.08; Obs. $[M]^+$ 170. FT-IR (ATR): υ (cm^{-1}) = 3328, 2984, 2910, 2855, 1742, 1443, 1392, 1375, 1352, 1296, 1257, 1123, 1103, 1086, 1067, 1031, 901, 796, 730, 659, 612.

The following compounds **1** and **2** have been prepared according to general procedure C using benzyl isocyanate.

(1,2,4,5-Tetrazine-3,6-diyl)bis(methylene) bis(benzylcarbamate) (1): This compound was prepared from **S1**. Recrystallization from $CHCl_3$ (8 mL) yielded pure **1** (51 mg, 0.12 mmol, 85 %) as a pink solid. ^{1}H-NMR (DMSO-d6): δ = 8.16 (t, J = 6.1 Hz, 2H, N*H*), 7.35–7.21 (m, 10H, Ar*H*), 5.65 (s, 4H, OCH_2), 4.22 (d, J = 6.1 Hz, 4H, ArCH_2). ^{13}C-NMR (DMSO-d6): δ = 166.9, 155.9, 139.4, 128.3, 127.0, 126.9, 63.0, 43.9. HPLC-MS/PDA: *m/z* Calc. for $C_{20}H_{20}N_6O_4$ 408.15; Obs. $[M+H]^+$ 409.17, $[M+Na]^+$ 431.33, $[2M+H]^+$ 817.08, $[2M+Na]^+$ 838.92, λ_{max} = 267 and 520 nm. FT-IR (ATR): υ (cm^{-1}) = 3316, 3085, 3032, 1692, 1553, 1493, 1453, 1433, 1411, 1371, 1293, 1272, 1256, 1202, 1157, 1145, 1080, 1056, 1037, 1017, 914, 903, 879, 821, 779, 753, 731, 694, 661, 623, 612.

(1,2,4,5-Tetrazine-3,6-diyl)bis(ethane-1,1-diyl) bis(benzylcarbamate) (2): This compound was prepared from **S2**. Column chromatography (flash SiO_2, 20 % EtOAc in $CHCl_3$) and precipitation, induced

by adding heptane (3 mL) to a stirred solution in $CHCl_3$ (3 mL) at 55 °C, followed by cooling down, filtration, washing with pentane and drying of the solid *in vacuo* yielded pure **2** (29 mg, 66 µmol, 73 %) as a pink solid. ^{1}H-NMR (DMSO-d6): δ = 8.12 (t, J = 5.2 Hz, 2H, N*H*), 7.31 (t, J = 7.4 Hz, 4H, Ar*H*), 7.23 (m, 6H, Ar*H*), 6.13 (2 q, J = 6.5 Hz, 2H, C*H*), 4.17 (d, J = 6.1 Hz, 4H, ArCH_2), 1.71 (d, J = 6.8 Hz, 6H, CH_3). ^{13}C-NMR (DMSO-d6): δ = 169.7, 155.6, 139.4, 128.3, 127.0, 126.9, 126.8, 70.1, 43.8, 19.6. HPLC-MS/PDA: *m/z* Calc. for $C_{22}H_{24}N_6O_4$ 436.19; Obs. $[M+H]^+$ 437.08, $[2M+H]^+$ 872.92, $[2M+Na]^+$ 894.75, λ_{max} = 267 and 524 nm. FT-IR (ATR): υ (cm^{-1}) = 3312, 3031, 2996, 2940, 1695, 1533, 1498, 1455, 1396, 1373, 1352, 1317, 1298, 1252, 1144, 1091, 1078, 1051, 1028, 944, 896, 777, 751, 699, 662.

Compounds S3, S4, S5

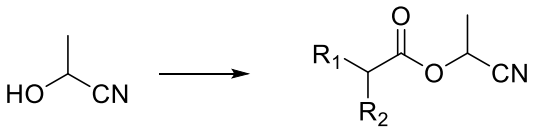

code	R_1	R_2
S3	Benzyl	Me
S4	Benzyl	*i*Pr
S5	Ph	*i*Pr

The following compounds **S3**, **S4**, and **S5** have been prepared according to general procedure E. All NMR spectra (except for **S5**) indicate the presence of two carbamate rotamers.

1-Cyanoethyl benzyl(methyl)carbamate (S3): This compound was prepared from *N*-benzylmethylamine. Column chromatography (flash SiO_2) using an elution gradient of pentane / $CHCl_3$ 1:1 to $CHCl_3$ yielded pure **S3** (0.20 g, 0.92 mmol, 56 % over two steps) as a colorless oil. ^{1}H-NMR ($CDCl_3$): δ = 7.39–7.17 (m, 5H, Ar*H*), 5.46 (q, J = 6.9 Hz, 1H, C*H*), 4.48 (m, 2H, CH_2), 2.92 and 2.86 (2 s, 3H, NCH_3), 1.69–1.62 (2 d, J = 6.9 Hz, 3H, CHCH_3). ^{13}C-NMR ($CDCl_3$): δ = 154.5, 154.0, 136.6, 136.5, 128.8, 128.7, 127.9, 127.7, 127.3, 118.3, 118.1, 58.7, 52.9, 52.4, 34.7, 33.6, 19.24, 19.18. GC-MS: *m/z* Calc. for $C_{12}H_{14}N_2O_2$ 218.11; Obs. $[M]^+$ 218. FT-IR (ATR): υ (cm^{-1}) = 2941, 1707, 1657, 1452, 1427, 1402, 1362, 1308, 1288, 1267, 1229, 1215, 1196, 1130, 1099, 1080, 1055, 1022, 1003, 968, 920, 845, 814, 762, 735, 700, 662, 615.

1-Cyanoethyl benzyl(isopropyl)carbamate (S4): This compound was prepared from *N*-isopropylbenzylamine. Column chromatography (flash SiO_2) using an elution gradient of pentane / $CHCl_3$ 1:1 to $CHCl_3$ yielded pure **S4** (0.61 g, 2.5 mmol, 58 % over two steps) as a colorless oil. ^{1}H-NMR ($CDCl_3$): δ = 7.36–7.17 (m, 5H, Ar*H*), 5.51 and 5.42 (2 br, 1H, C*H*CH$_3$), 4.44 (2 br, 2H, CH_2), 4.34 and 4.11 (2 br, 1H, NC*H*), 1.68 and 1.50 (2 br d, 3H, CHCH_3), 1.15 (d, J = 5.5 Hz, 6H, CH(CH_3)$_2$). ^{13}C-NMR ($CDCl_3$): δ = 154.7, 153.7, 138.7, 128.5, 127.3, 127.2, 126.6, 118.2, 58.5, 58.2, 49.2, 49.0, 47.7, 46.5, 21.1, 20.4, 19.2, 19.0. GC-MS: *m/z* Calc. for $C_{14}H_{18}N_2O_2$ 246.14; Obs. $[M]^+$ 246. FT-IR (ATR): υ (cm^{-1}) = 2976, 2940, 1701, 1497, 1454, 1416, 1369, 1335, 1319, 1285, 1263, 1252, 1207, 1182, 1167, 1148, 1130, 1099, 1065, 1028, 1003, 955, 920, 872, 845, 818, 797, 764, 731, 700, 669.

1-Cyanoethyl isopropyl(phenyl)carbamate (S5): This compound was prepared from *N*-isopropylaniline. Column chromatography (flash SiO_2) using an elution gradient of heptane / $CHCl_3$ 1:1 via $CHCl_3$ to 2 % EtOAc in $CHCl_3$ yielded pure **S5** (1.15 g, 5.0 mmol, 61 % over two steps) as a colorless solid. ^{1}H-NMR ($CDCl_3$): δ = 7.37 (m, 3H, Ar*H*), 7.09 (d, J = 6.9 Hz, 2H, Ar*H*), 5.39 (br, 1H, C*H*CH$_3$), 4.56 (br, 1H, NC*H*), 1.46 (br, 3H, CHCH_3), 1.13 (d, J = 6.8 Hz, 6H, CH(CH_3)$_2$). ^{13}C-NMR ($CDCl_3$): δ = 153.2, 137.2, 129.6, 128.9, 127.9, 118.2, 58.3, 49.9, 21.2, 19.0. GC-MS: *m/z* Calc. for $C_{13}H_{16}N_2O_2$ 232.12; Obs. $[M]^+$ 232.

FT-IR (ATR): υ (cm^{-1}) = 2978, 2941, 2876, 1707, 1595, 1497, 1452, 1400, 1383, 1354, 1323, 1288, 1254, 1179, 1132, 1098, 1072, 1028, 1005, 974, 916, 816, 789, 758, 700, 677.

Compound 3

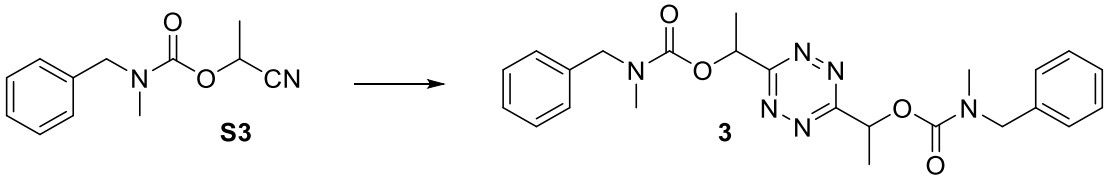

The following compound **3** has been prepared according to general procedure A. EtOH was used as reaction solvent in the preparation of the [2H]-TZ precursor. The NMR spectra indicate the presence of two carbamate rotamers.

(1,2,4,5-Tetrazine-3,6-diyl)bis(ethane-1,1-diyl) bis(benzyl(methyl)carbamate) (3): This compound was prepared from **S3**. Column chromatography (flash SiO_2) using an elution gradient of 5 % to 15 % EtOAc in $CHCl_3$ yielded pure **3** (50 mg, 0.11 mmol, 23 %) as a pink oil. ^{1}H-NMR ($CDCl_3$): δ = 7.39–7.21 (m, 10H, Ar*H*), 6.32 (m, 2H, C*H*), 4.72–4.38 (m, 4H, CH_2), 2.97 and 2.88 (2 s, 6H, NCH_3), 1.84 (2 d, J = 6.9 Hz, 6H, CHCH_3). ^{13}C-NMR ($CDCl_3$): δ = 170.2, 156.0, 155.4, 137.2, 137.1, 128.7, 127.8, 127.7, 127.6, 71.3, 52.8, 52.7, 34.4, 33.9, 20.1. HPLC-MS/PDA: *m/z* Calc. for $C_{24}H_{28}N_6O_4$ 464.22; Obs. $[M+H]^+$ 465.25, $[M+Na]^+$ 487.33, $[2M+H]^+$ 928.75, $[2M+Na]^+$ 951.08, λ_{max} = 265 and 524 nm. FT-IR (ATR): υ (cm^{-1}) = 2934, 1699, 1452, 1427, 1400, 1377, 1364, 1288, 1269, 1227, 1215, 1196, 1136, 1092, 1078, 1047, 1013, 966, 895, 851, 818, 766, 735, 700, 665, 608.

Compounds 5, 6, 8, 9

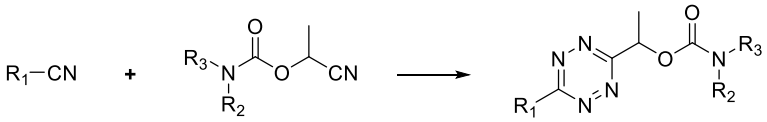

Code	R_1	R_2	R_3
5	*i*Pr	Me	Benzyl
6	*i*Pr	*i*Pr	Benzyl
8	*i*Pr	*i*Pr	Ph
9	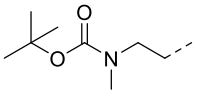	Me	Benzyl

The following compounds **5**, **6**, **8** and **9** have been prepared according to general procedure A. EtOH was used as reaction solvent in the preparation of the [2H]-TZ precursor. All NMR spectra indicate the presence of two carbamate rotamers.

1-(6-Isopropyl-1,2,4,5-tetrazin-3-yl)ethyl benzyl(methyl)carbamate (5): This compound was prepared from isobutyronitrile and **S3** that were reacted in a 10:1 molar ratio. Column chromatography (flash SiO_2) using an elution gradient of 0 % to 4 % EtOAc in $CHCl_3$ and, in a second chromatography step, 1 % to 4 % acetone in heptane yielded pure **5** (22 mg, 70 µmol, 7 %) as a pink oil. ^{1}H-NMR ($CDCl_3$): δ = 7.39–7.23 (m, 5H, Ar*H*), 6.27 (2 q, J = 6.9 Hz, 1H, C*H*CH_3), 4.71–4.37 (m, 2H, CH_2), 3.66 (sept, J = 7.0 Hz, 1H, C*H*$(CH_3)_2$), 2.97 and 2.87 (2 s, 3H, NCH_3), 1.83 (2 d, J = 6.9 Hz, 3H, CHCH_3), 1.54 (d, J = 7.0 Hz,

6H, CH(CH_3)$_2$). ^{13}C-NMR ($CDCl_3$): δ = 174.8, 169.4, 169.3, 156.1, 155.5, 137.3, 137.2, 128.8, 127.9, 127.7, 127.6, 71.4, 52.8, 52.7, 34.5, 34.4, 33.9, 21.4, 20.2, 20.1. HPLC-MS/PDA: *m/z* Calc. for $C_{16}H_{21}N_5O_2$ 315.17; Obs. $[M+H]^+$ 316.25, $[M+Na]^+$ 338.17, $[2M+Na]^+$ 653.00, λ_{max} = 269 and 530 nm. FT-IR (ATR): υ (cm^{-1}) = 2974, 2932, 2876, 1705, 1472, 1452, 1427, 1398, 1383, 1290, 1231, 1198, 1140, 1094, 1076, 1045, 1015, 966, 897, 851, 766, 731, 700.

1-(6-Isopropyl-1,2,4,5-tetrazin-3-yl)ethyl benzyl(isopropyl)carbamate (6): This compound was prepared from isobutyronitrile and **S4** that were reacted in a 8:1 molar ratio. Column chromatography (flash SiO_2) using an elution gradient of 0 % to 3 % EtOAc in $CHCl_3$ and, in a second chromatography step, 1 % to 2 % acetone in heptane yielded pure **6** (22 mg, 64 µmol, 18 %) as a pink oil. ^{1}H-NMR ($CDCl_3$): δ = 7.37–7.16 (br m, 5H, Ar*H*), 6.24 (br, 1H, C*H*CH_3), 4.64–4.23 (br m, 3H, CH_2, NC*H*), 3.65 (sept, *J* = 6.9 Hz, 1H, CC*H*(CH_3)$_2$), 1.86 and 1.70 (2 br, 3H, CHCH_3), 1.54 (d, *J* = 6.9 Hz, 6H, CCH(CH_3)$_2$), 1.19 and 1.13 (2 br, 6H, NCH(CH_3)$_2$). ^{13}C-NMR ($CDCl_3$): δ = 174.7, 169.5, 169.3, 156.2, 155.3, 139.5, 139.2, 128.5, 127.2, 127.00, 126.95, 71.3, 71.1, 48.9, 48.8, 47.4, 46.7, 34.5, 21.4, 21.3, 20.6, 20.3, 20.0. HPLC-MS/PDA: *m/z* Calc. for $C_{18}H_{25}N_5O_2$ 343.20; Obs. $[M+H]^+$ 344.17, $[M+Na]^+$ 366.08, $[2M+Na]^+$ 709.00, λ_{max} = 269 and 531 nm. FT-IR (ATR): υ (cm^{-1}) = 2974, 2934, 2876, 1697, 1497, 1452, 1416, 1400, 1369, 1341, 1288, 1254, 1209, 1188, 1167, 1155, 1101, 1070, 1018, 955, 899, 806, 770, 727, 700.

1-(6-Isopropyl-1,2,4,5-tetrazin-3-yl)ethyl isopropyl(phenyl)carbamate (8): This compound was prepared from isobutyronitrile and **S5** that were reacted in a 10:1 molar ratio. Column chromatography (flash SiO_2) using an elution gradient of 0 % to 3 % EtOAc in $CHCl_3$ and, in a second chromatography step, 1 % to 2 % acetone in heptane yielded pure **8** (44 mg, 0.13 mmol, 20 %) as a pink oil. ^{1}H-NMR ($CDCl_3$): δ = 7.40–7.18 (m, 5H, Ar*H*), 6.17 (br, 1H, C*H*CH_3), 4.56 (br, 1H, NC*H*), 3.65 (sept, *J* = 7.0 Hz, 1H, CC*H*(CH_3)$_2$), 1.63 (br, 3H, CHCH_3), 1.53 (d, *J* = 7.0 Hz, 6H, CCH(CH_3)$_2$), 1.17 and 1.13 (2 br d, *J* = 5.4 Hz, 6H, NCH(CH_3)$_2$). ^{13}C-NMR ($CDCl_3$): δ = 174.6, 169.4, 154.8, 138.1, 129.9, 128.7, 127.6, 71.2, 49.6, 34.5, 21.5 (br), 21.4, 21.3, 19.9 (br). HPLC-MS/PDA: *m/z* Calc. for $C_{17}H_{23}N_5O_2$ 329.19; Obs. $[M+H]^+$ 330.08, $[M+Na]^+$ 352.17, $[2M+Na]^+$ 681.00, λ_{max} = 270 and 533 nm. FT-IR (ATR): υ (cm^{-1}) = 2974, 2934, 2876, 1701, 1595, 1497, 1474, 1450, 1398, 1381, 1364, 1342, 1325, 1294, 1260, 1180, 1155, 1130, 1096, 1074, 1028, 1015, 974, 899, 799, 758, 700, 677.

1-(6-(2-((t-Butoxycarbonyl)(methyl)amino)ethyl)-1,2,4,5-tetrazin-3-yl)ethyl benzyl(methyl)carbamate (9): This compound was prepared from *t*-butyl *N*-(2-cyanoethyl)-*N*-methylcarbamate and **S3** that were reacted in a 1:1 molar ratio. Column chromatography (flash SiO_2) using an elution gradient of 5 % to 40 % EtOAc in $CHCl_3$ and, in a second chromatography step, 5 % to 10 % acetone in heptane yielded pure **9** (16 mg, 37 µmol, 3 %) as a pink oil. ^{1}H-NMR ($CDCl_3$): δ = 7.39–7.22 (m, 5H, Ar*H*), 6.26 (br, 1H, C*H*), 4.68–4.38 (m, 2H, ArCH_2), 3.82 (br, 2H, NCH_2CH_2), 3.54 (t, *J* = 6.8 Hz, 2H, NCH_2CH_2), 2.96 and 2.85 (2 s, 3H, $ArCH_2NCH_3$), 2.92 (s, 3H, $CH_2CH_2NCH_3$), 1.82 (br, 3H, CHCH_3), 1.35 (s, 9H, C(CH_3)$_3$). ^{13}C-NMR ($CDCl_3$): δ = 169.2, 156.0, 155.5, 137.2, 128.8, 127.9, 127.7, 127.6, 80.0 (br), 71.4, 52.8, 52.7, 47.8, 34.9 (br), 34.5 (br), 34.4, 33.9, 33.6 (br), 29.8, 28.4, 20.1. HPLC-MS/PDA: *m/z* Calc. for $C_{21}H_{30}N_6O_4$ 430.23; Obs. $[M-t\text{boc}+2H]^+$ 331.33, $[M+Na]^+$ 453.33, $[2M+Na]^+$ 882.92, λ_{max} = 260 and 530 nm. FT-IR (ATR): υ (cm^{-1}) = 2970, 2928, 2870, 1694, 1479, 1452, 1427, 1393, 1366, 1348, 1287, 1260, 1234, 1221, 1196, 1159, 1136, 1092, 1049, 1016, 966, 934, 891, 858, 802, 768, 733, 700, 667.

Compounds S6, S7, S8, 18

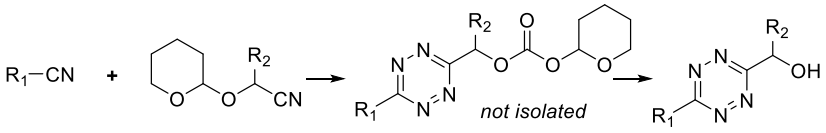

Code	R_1	R_2
S6	*i*Pr	H
S7	*i*Pr	Me
S8	Ph	Me
18	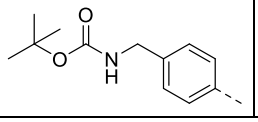	Me

The following compounds **S6**, **S7**, **S8** and **18** have been prepared according to general procedures A and B.

(6-Isopropyl-1,2,4,5-tetrazin-3-yl)methanol (S6): This compound was prepared from isobutyronitrile and 2-[(tetrahydro-2*H*-pyran-2-yl)oxy]ACN[1] that were reacted in a 2:1 molar ratio. Column chromatography (flash SiO_2) using an elution gradient of 0 % to 30 % EtOAc in $CHCl_3$ yielded pure **S6** (37 mg, 0.24 mmol, 15 % over two steps) as a pink oil. ^{1}H-NMR ($CDCl_3$): δ = 5.28 (s, 2H, CH_2), 3.70 (sept, J = 7.0 Hz, 1H, C*H*), 3.12 (br, 1H, O*H*), 1.54 (d, J = 7.0 Hz, 6H, CH_3). ^{13}C-NMR ($CDCl_3$): δ = 175.3, 167.8, 62.8, 34.5, 21.4. HPLC-MS/PDA: *m/z* Calc. for $C_6H_{10}N_4O$ 154.09; Obs. $[M+H]^+$ 154.92, λ_{max} = 273 and 519 nm. FT-IR (ATR): υ (cm^{-1}) = 3202, 2972, 2932, 2874, 1692, 1657, 1520, 1470, 1462, 1385, 1366, 1343, 1300, 1260, 1190, 1152, 1092, 1070, 1030, 978, 968, 930, 905, 847, 797, 731, 687, 648, 631.

1-(6-Isopropyl-1,2,4,5-tetrazin-3-yl)ethanol (S7): This compound was prepared from isobutyronitrile and 2-[(tetrahydro-2*H*-pyran-2-yl)oxy]propionitrile[2] that were reacted in a 1:1 molar ratio. Column chromatography (flash SiO_2) using an elution gradient of 0 % to 16 % EtOAc in $CHCl_3$ yielded pure **S7** (48 mg, 0.29 mmol, 17 % over two steps) as a pink solid. ^{1}H-NMR ($CDCl_3$): δ = 5.43 (qn, J = 6.6 Hz, 1H, C*H*O), 3.69 (sept, J = 7.0 Hz, 1H, C*H*(CH_3)$_2$), 3.40 (d, J = 6.4 Hz, 1H, O*H*), 1.78 (d, J = 6.7 Hz, 3H, OCHCH_3), 1.55 (d, J = 7.0 Hz, 6H, CH(CH_3)$_2$). ^{13}C-NMR ($CDCl_3$): δ = 175.0, 170.6, 68.6, 34.5, 22.8, 21.4. HPLC-MS/PDA: *m/z* Calc. for $C_7H_{12}N_4O$ 168.10; Obs. $[M+H]^+$ 169.00, λ_{max} = 271 and 521 nm. FT-IR (ATR): υ (cm^{-1}) = 3362, 2974, 2934, 2876, 1659, 1474, 1460, 1450, 1395, 1366, 1341, 1292, 1258, 1219, 1192, 1155, 1107, 1069, 1024, 966, 899, 820, 802, 714, 640, 629, 602.

1-(6-Phenyl-1,2,4,5-tetrazin-3-yl)ethanol (S8): This compound was prepared from benzonitrile and 2-[(tetrahydro-2*H*-pyran-2-yl)oxy]propionitrile[2] that were reacted in a 4:1 molar ratio. EtOH was used as a solvent. Directly after oxidation and work-up the volatiles were removed *in vacuo* and the mixture was stirred at 50 °C in $CHCl_3$ for 5 min. After cooling to room temperature, most of the relatively insoluble diphenyltetrazine byproduct was removed by filtration. Column chromatography (flash SiO_2) using an elution gradient of 0 % to 10 % EtOAc in $CHCl_3$ yielded pure **S8** (95 mg, 0.47 mmol, 30 % over two steps) as a pink solid. ^{1}H-NMR ($CDCl_3$): δ = 8.62 (m, 2H, Ar*H*), 7.69–7.58 (m, 3H, Ar*H*), 5.49 (qn, J = 6.7 Hz, 1H, C*H*), 3.39 (d, J = 6.4 Hz, 1H, O*H*), 1.82 (d, J = 6.7 Hz, 3H, CH_3). ^{13}C-NMR ($CDCl_3$): δ = 170.4, 165.4, 133.1, 131.6, 129.5, 128.3, 68.7, 22.9. HPLC-MS/PDA: *m/z* Calc. for $C_{10}H_{10}N_4O$ 202.09; Obs. $[M+H]^+$ 203.00, λ_{max} = 259 and 527 nm. FT-IR (ATR): υ (cm^{-1}) = 3391, 2980, 2932, 1599, 1443, 1391, 1368, 1348, 1315, 1248, 1179, 1113, 1088, 1074, 1049, 1026, 1001, 903, 837, 764, 718, 691, 604.

t-Butyl 4-(6-(1-hydroxyethyl)-1,2,4,5-tetrazin-3-yl)benzylcarbamate (18): This compound was prepared from *t*-butyl *N*-(4-cyanobenzyl)carbamate **17** and 2-[(tetrahydro-2*H*-pyran-2-yl)oxy]propionitrile[13] that were reacted in a 2:1 molar ratio. EtOH was used as a solvent. Directly after oxidation and work-up the volatiles were removed *in vacuo* and the mixture was stirred at reflux in $CHCl_3$

for 5 min. After cooling to room temperature, most of the relatively insoluble diphenyltetrazine derivative byproduct was removed by filtration. Column chromatography (flash SiO_2, compound adsorbed onto silica from $CHCl_3$ / MeOH) using an elution gradient of 0 % to 30 % EtOAc in $CHCl_3$ was followed by precipitation, induced by adding heptane (2 mL) to a stirred solution in $CHCl_3$ (0.5 mL). Filtration, washing with pentane and drying of the solid *in vacuo* yielded pure **18** (50 mg, 0.15 mmol, 12 % over two steps) as a pink solid. ^{1}H-NMR ($CDCl_3$): δ = 8.56 (d, J = 8.3 Hz, 2H, Ar*H*), 7.51 (d, J = 8.2 Hz, 2H, Ar*H*), 5.48 (q, J = 6.7 Hz, 1H, C*H*), 5.04 (br t, 1H, N*H*), 4.45 (d, J = 5.6 Hz, 2H, ArCH_2), 3.50 (br, 1H, O*H*), 1.82 (d, J = 6.7 Hz, 3H, CHCH_3), 1.49 (s, 9H, C(CH_3)$_3$). HPLC-MS/PDA: *m/z* Calc. for $C_{16}H_{21}N_5O_3$ 331.16; Obs. [M-*t*boc+2H]$^+$ 232.00, [M-*t*butyl+2H]$^+$ 275.92, λ_{max} = 263 and 530 nm.

Compounds 4, 7, S9, 10, 11, 19

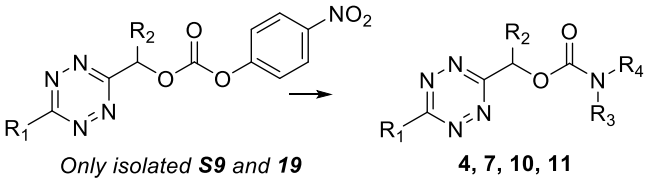

Code	R_1	R_2	R_3	R_4
4	*i*Pr	H	Me	Benzyl
7	*i*Pr	Me	Me	Ph
S9	Ph	Me	-	-
10	Ph	Me	Me	Benzyl
11	Ph	Me	Me	Me
19	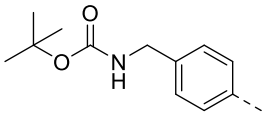	Me	-	-

The following compounds **4**, **7**, **S9**, **10**, **11** and **19** have been prepared according to general procedure D. For **S9** and **11** the synthetic procedure was modified and it is described completely. The NMR spectra for **4**, **10** and **11** indicate the presence of two carbamate rotamers.

(6-Isopropyl-1,2,4,5-tetrazin-3-yl)methyl benzyl(methyl)carbamate (4): This compound was prepared from **S6** and *N*-benzylmethylamine. Column chromatography (flash SiO_2) using an elution gradient of 0 % to 4 % EtOAc in $CHCl_3$ yielded pure **4** (15 mg, 50 µmol, 77 %) as a pink oil. ^{1}H-NMR ($CDCl_3$): δ = 7.39–7.26 (m, 5H, Ar*H*), 5.76 (s, 2H, CH_2O), 4.60 and 4.53 (2 s, 2H, ArCH_2), 3.68 (sept, J = 6.9 Hz, 1H, C*H*), 2.96 and 2.93 (2 s, 3H, NCH_3), 1.54 (d, J = 6.9 Hz, 6H, CH(CH_3)$_2$). ^{13}C-NMR ($CDCl_3$): δ = 175.1, 166.0, 156.2, 155.7, 137.1, 128.8, 127.9, 127.7, 127.6, 64.1, 53.0, 52.7, 34.7, 34.5, 34.0, 21.4. HPLC-MS/PDA: *m/z* Calc. for $C_{15}H_{19}N_5O_2$ 301.15; Obs. [M+H]$^+$ 301.92, λ_{max} = 269 and 527 nm. FT-IR (ATR): υ (cm^{-1}) = 2972, 2930, 2874, 1707, 1472, 1452, 1433, 1402, 1358, 1308, 1285, 1271, 1225, 1198, 1138, 1088, 1069, 1030, 991, 953, 903, 829, 808, 766, 733, 700, 621.

1-(6-Isopropyl-1,2,4,5-tetrazin-3-yl)ethyl methyl(phenyl)carbamate (7): This compound was prepared from **S7** and *N*-methylaniline. Column chromatography (flash SiO_2) using an elution gradient of 0 % to 4 % EtOAc in $CHCl_3$ and, in a second chromatography step (normal SiO_2), elution with 5 % acetone in heptane yielded pure **7** (9.0 mg, 30 µmol, 49 %) as a pink oil. ^{1}H-NMR ($CDCl_3$): δ = 7.35 (d, J = 4.9 Hz, 4H, Ar*H*), 7.22 (m, 1H, Ar*H*), 6.23 (q, J = 6.8 Hz, 1H, C*H*O), 3.66 (sept, J = 7.0 Hz, 1H, C*H*(CH$_3$)$_2$), 3.36 (br, 3H, NCH_3), 1.76 (br, 3H, OCHCH_3), 1.54 (d, J = 7.0 Hz, 6H, CH(CH_3)$_2$). ^{13}C-NMR ($CDCl_3$): δ = 174.8, 169.3, 154.9, 143.1, 129.0, 126.4, 125.9 (br), 71.6, 34.5, 29.8, 21.43, 21.39, 20.0 (br). HPLC-MS/PDA: *m/z* Calc. for $C_{15}H_{19}N_5O_2$ 301.15; Obs. [M+H]$^+$ 301.92, λ_{max} = 234, 269 and 529 nm. FT-IR (ATR): υ (cm^{-1}) =

2955, 2922, 2853, 1707, 1597, 1497, 1462, 1375, 1342, 1296, 1275, 1260, 1152, 1078, 1022, 972, 897, 799, 764, 719, 696, 665.

4-Nitrophenyl (1-(6-phenyl-1,2,4,5-tetrazin-3-yl)ethyl) carbonate (S9): **S8** (101 mg, 0.50 mmol) was dissolved in CH_2Cl_2 (6 mL) and pyridine (1 mL) was added. Under Ar, the solution was cooled to 0 °C and 4-nitrophenyl chloroformate (96 mg, 0.48 mmol, 0.96 eq) was added. The mixture was allowed to warm to room temperature while stirring overnight. Subsequently, it was evaporated to dryness, redissolved in $CHCl_3$ (10 mL) and washed with respectively 1 M citric acid (2 × 10 mL), 1 M NaOH (2 × 5 mL) and water (5 mL). The organic layer was dried over Na_2SO_4, filtrated and evaporated to dryness. The crude product was purified using column chromatography (flash SiO_2, 10 % EtOAc in heptane) yielding pure **S9** as a pink solid (94 mg, 0.26 mmol, 51 %). ^{1}H-NMR ($CDCl_3$) δ = 8.75–8.54 (m, 2H, Ar*H*), 8.29 (d, *J* = 9.2 Hz, 2H, Ar*H*), 7.79–7.54 (m, 3H, Ar*H*), 7.44 (d, *J* = 9.2 Hz, 2H, Ar*H*), 6.37 (q, *J* = 6.8 Hz, 1H, C*H*), 2.02 (d, *J* = 6.9 Hz, 3H, CH_3). ^{13}C-NMR ($CDCl_3$) δ = 167.2, 165.3, 155.3, 152.0, 145.6, 133.3, 131.2, 129.4, 128.4, 125.4, 121.8, 74.8, 19.4. HPLC-MS/PDA: *m/z* Calc. for $C_{17}H_{13}N_5O_5$ 376.09; no MS signal observed, λ_{max} = 263 and 530 nm.

1-(6-Phenyl-1,2,4,5-tetrazin-3-yl)ethyl benzyl(methyl)carbamate (10): This compound was prepared from **S8** and *N*-benzylmethylamine. Column chromatography (flash SiO_2) using an elution gradient of 0 % to 2 % EtOAc in $CHCl_3$ and, in a second chromatography step (normal SiO_2), elution with 4 % acetone in heptane yielded pure **10** (6.0 mg, 17 µmol, 16 %) as a pink oil. ^{1}H-NMR ($CDCl_3$): δ = 8.62 (d, *J* = 7.1 Hz, 2H, Ar*H*), 7.67–7.57 (m, 3H, Ar*H*), 7.39–7.24 (m, 5H, Ar*H*), 6.31 (2 q, *J* = 6.9 Hz, 1H, C*H*), 4.72–4.38 (m, 2H, ArCH_2), 2.99 and 2.88 (2 s, 3H, NCH_3), 1.88 (2 d, *J* = 7.1 Hz, 3H, CHCH_3). ^{13}C-NMR ($CDCl_3$): δ = 169.3, 169.2, 165.0, 156.1, 155.5, 137.2, 137.1, 132.9, 131.8, 129.4, 128.7, 128.3, 127.9, 127.7, 127.6, 71.5, 52.8, 52.7, 34.4, 33.9, 20.2, 20.1. HPLC-MS/PDA: *m/z* Calc. for $C_{19}H_{19}N_5O_2$ 349.15; Obs. $[M+H]^+$ 350.00, λ_{max} = 260 and 531 nm. FT-IR (ATR): υ (cm^{-1}) = 3065, 2986, 2924, 2855, 1701, 1601, 1443, 1396, 1375, 1348, 1314, 1288, 1269, 1229, 1217, 1198, 1179, 1138, 1094, 1024, 1011, 966, 903, 851, 764, 731, 691.

1-(6-Phenyl-1,2,4,5-tetrazin-3-yl)ethyl dimethylcarbamate (11): **S9** (56 mg, 0.152 mmol) was dissolved in THF (4 mL) and *N*,*N*-diisopropylethylamine (53 µL, 0.30 mmol, 2 eq) and dimethylamine (114 µL of a 2 M solution in THF, 0.23 mmol, 1.5 eq) were added. The solution was stirred at room temperature for 1 h, concentrated and redissolved in diethyl ether (6 mL). This solution was washed with respectively 1 M citric acid (2 × 3 mL), 1 M NaOH (2 × 3 mL) and water (3 mL). The organic layer was dried over Na_2SO_4, filtrated and evaporated to dryness. The crude product was purified using column chromatography (flash SiO_2, 4 % EtOAc in $CHCl_3$) yielding pure **11** as a pink oil (41 mg, 0.15 mmol, 99 %). ^{1}H-NMR ($CDCl_3$) δ = 8.65–8.57 (m, 2H, Ar*H*), 7.68–7.55 (m, 3H, Ar*H*), 6.23 (q, *J* = 6.9 Hz, 1H, C*H*), 3.05 (s, 3H, NCH_3), 2.92 (s, 3H, NCH_3), 1.87 (d, *J* = 6.9 Hz, 3H, CHCH_3). ^{13}C-NMR ($CDCl_3$) δ = 169.2, 164.8, 155.6, 132.8, 131.6, 129.2, 128.1, 71.1, 36.5, 36.1, 30.3, 20.0. HPLC-MS/PDA: *m/z* Calc. for $C_{13}H_{15}N_5O_2$ 273.12; Obs. $[M+H]^+$ 274.08, λ_{max} = 262 and 527 nm.

t-Butyl 4-(6-(1-(((4-nitrophenoxy)carbonyl)oxy)ethyl)-1,2,4,5-tetrazin-3-yl)benzylcarbamate (19): This compound was prepared from **18**. Upon addition of *p*-nitrophenylchloroformate TLC analysis showed full conversion and $CHCl_3$ (50 mL) was added. The organic phase was washed with 0.1 M HCl, sat. $NaHCO_3$ (5×, until the aqueous phase is colorless) and brine (all 20 mL). After drying with Na_2SO_4 and filtration, the solvents were removed *in vacuo*. Column chromatography (normal SiO_2) using an elution gradient of 5 % EtOAc in $CHCl_3$ yielded pure **19** (847 mg, 1.7 mmol, 79 %) as a pink solid. ^{1}H-NMR ($CDCl_3$): δ = 8.60 (d, *J* = 8.4 Hz, 2H, Ar*H*), 8.28 (d, *J* = 9.2 Hz, 2H, Ar*H*), 7.53 (d, *J* = 8.3 Hz, 2H, Ar*H*), 7.44 (d, *J* = 9.3 Hz, 2H, Ar*H*), 6.36 (q, *J* = 6.8 Hz, 1H, C*H*), 4.99 (br, 1H, N*H*), 4.45 (d, *J* = 5.6 Hz, 2H,

CH_2), 2.02 (d, J = 6.9 Hz, 3H, CHCH_3), 1.49 (s, 9H, C(CH_3)$_3$). ^{13}C-NMR ($CDCl_3$): δ = 167.3, 165.2, 156.1, 155.4, 152.1, 145.7, 145.0, 130.3, 128.8, 128.3, 125.5, 121.9, 80.0, 74.9, 44.5, 28.5, 19.5. HPLC-MS/PDA: *m/z* Calc. for $C_{23}H_{24}N_6O_7$ 496.17; Obs. [M-*t*boc+2H]$^+$ 397.08, [M-*t*butyl+2H]$^+$ 440.83, λ_{max} = 271 and 530 nm. FT-IR (ATR): υ (cm^{-1}) = 3429, 3362, 2978, 2936, 1767, 1705, 1612, 1593, 1524, 1493, 1443, 1416, 1396, 1364, 1346, 1312, 1248, 1215, 1163, 1130, 1096, 1076, 1049, 1013, 1001, 962, 935, 908, 860, 812, 799, 775, 731, 700, 673, 662, 646, 627.

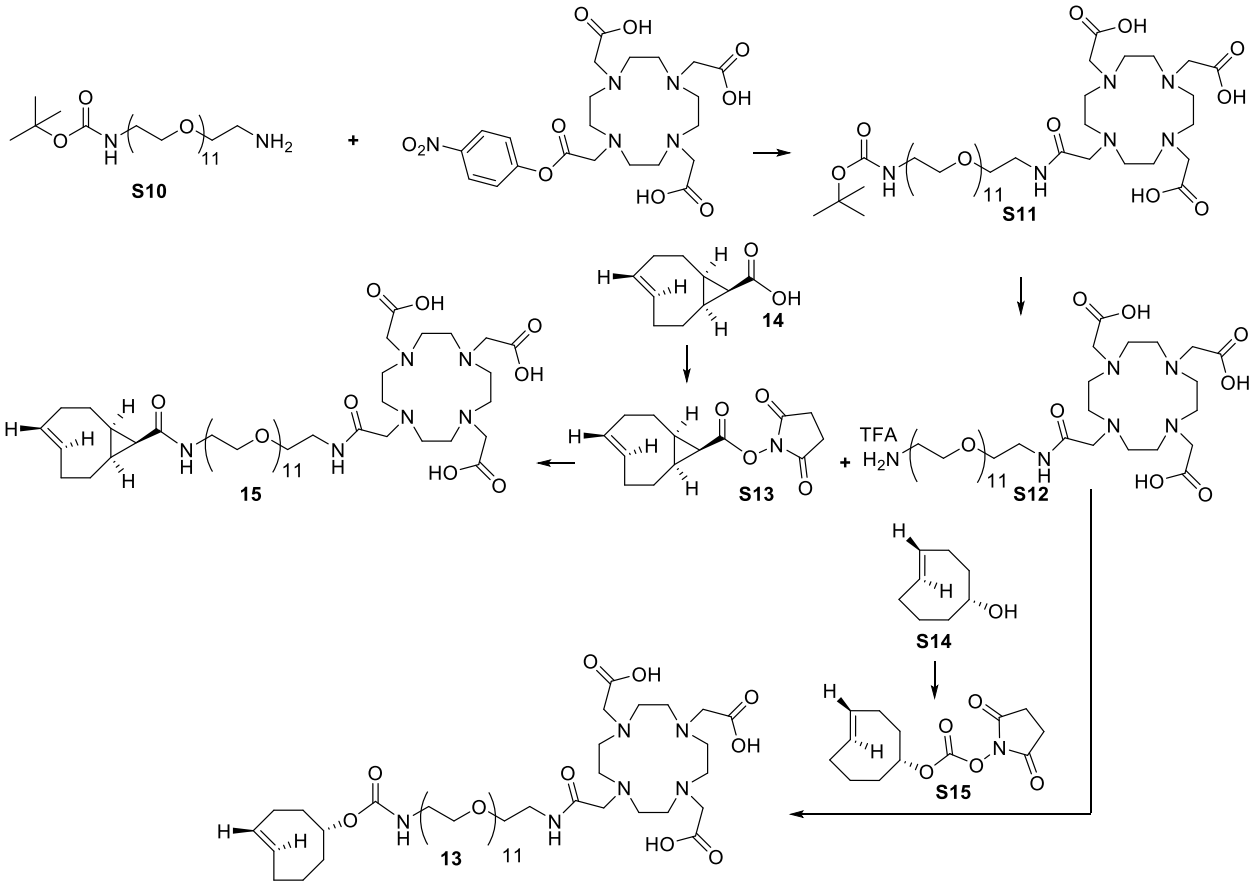

2,2',2''-(10-(2,2-Dimethyl-4,42-dioxo-3,8,11,14,17,20,23,26,29,32,35,38-dodecaoxa-5,41-diazatritetracontan-43-yl)-1,4,7,10-tetraazacyclododecane-1,4,7-triyl)triacetic acid (S11): *t*-Butyl (32-amino-3,6,9,12,15,18,21,24,27,30-decaoxadotriacontyl)carbamate **S10** (103 mg, 0.16 mmol) and *N*,*N*-diisopropylethylamine (140 µL, 0.80 mmol, 5 eq) were dissolved in dry DMF (1 mL). 1,4,7,10-Tetraazacyclododecane-1,4,7,10-tetraacetic acid mono(4-nitrophenyl) ester[14] (120 mg, 0.16 mmol, 1 eq) was added as a solid and the mixture was stirred at room temperature for 2 h. The reaction mixture was added dropwise to a stirring solution of diethyl ether (35 mL), centrifuged (5 min at 4000 rpm) and decanted. The resulting solid was washed with diethyl ether (20 mL) after which centrifugation and decantation were repeated. Drying of the solid *in vacuo* yielded pure **S11** (165 mg, 0.16 mmol, 100 %) as a white solid. ESI-MS: *m/z* Calc. for $C_{45}H_{86}N_6O_{20}$ 1030.59; Obs. [M+2H]$^{2+}$ 516.33, [M+H]$^+$ 1031.67, [M+Na]$^+$ 1053.50.

2,2',2''-(10-(38-Amino-2-oxo-6,9,12,15,18,21,24,27,30,33,36-undecaoxa-3-azaoctatriacontyl)-1,4,7,10-tetraazacyclododecane-1,4,7-triyl)triacetic acid, TFA salt (S12): Compound **S11** (165 mg, 0.16 mmol) was dissolved in DMF / TFA 1:2 (1.5 mL) and the solution was stirred at room temperature

for 2 h. The reaction mixture was added dropwise to a stirring solution of diisopropylether (35 mL), centrifuged (5 min at 4000 rpm) and decanted. Precipitation (1.5 mL ACN → 35 mL diethyl ether), centrifugation and decantation were repeated and drying of the solid *in vacuo* and lyophilization yielded pure **S12** (167 mg, 0.16 mmol, 100 %) as a white solid. ESI-MS: *m/z* Calc. for $C_{42}H_{79}F_3N_6O_{20}$ 1044.53; Obs. $[M\text{-}TFA+2H]^{2+}$ 466.58, $[M\text{-}TFA+H]^{+}$ 931.58.

***rel*-(1*R*,4*E*,p*S*)-Cyclooct-4-enyl 2,5-dioxopyrrolidin-1-yl carbonate (S15)**

rel-(1*R*,4*E*,p*S*)-Cyclooct-4-enol **S14** (26 mg, 0.21 mmol) was suspended in dry ACN (1 mL) and triethylamine (120 µL, 0.85 mmol, 4 eq) and *N*,*N*'-disuccinimidyl carbonate (137 mg, 0.52 mmol, 2.5 eq) were added. The suspension slowly cleared and the solution was stirred at room temperature for 69 h, with intermittent addition of *N*,*N*'-disuccinimidyl carbonate (137 mg, 0.52 mmol, 2.5 eq after 19 h and the same amount after 43 h) and triethylamine (120 µL, 0.85 mmol, 4 eq after 43 h). The suspension was filtered and the white solid was washed with $CHCl_3$ (2 × 1 mL). The filtrate was evaporated to dryness and the resulting brown oil was purified with column chromatography (flash SiO_2) using an elution gradient of 20 % to 30 % EtOAc in heptane. This yielded pure **S15** as a colorless oil (32 mg, 0.12 mmol, 58 %). ^{1}H-NMR ($CDCl_3$) δ = 5.76–5.62 (m, 1H, C*H*=CH), 5.62–5.48 (m, 1H, CH=C*H*), 4.98 (dd, *J* = 10.4, 5.0 Hz, 1H, OC*H*), 2.84 (s, 4H, C(O)CH_2CH_2), 2.57–2.27 (m, 4H), 2.21–2.13 (m, 1H), 1.97–1.81 (m, 2H), 1.79–1.55 (m, 2H), 1.41–1.27 (m, 1H).

-2,2',2''-(10-(1-(*rel*-(1*R*,4*E*,p*S*)-Cyclooct-4-en-1-yloxy)-1,39-dioxo-5,8,11,14,17,20,23,2,29,32,35-undecaoxa-2,38-diazatetracontan-40-yl)-1,4,7,10-tetraazacyclododecane-1,4,7-triyl)triacetic acid (13)

Compound **S12** (88 mg, 84 µmol) and *N*,*N*-diisopropylethylamine (120 µL, 0.68 mmol, 8 eq) were dissolved in DMF (1 mL). **S15** (32 mg, 0.12 mmol, 1.4 eq) was added and the mixture was stirred at room temperature in the dark for 1 h. The reaction mixture was added dropwise to a stirring solution of diethylether (30 mL), centrifuged (5 min at 4000 rpm) and decanted. The resulting solid was washed with diethylether (20 mL) after which centrifugation and decantation were repeated. The solid was dried *in vacuo* and lyophilized followed by purification with preparative RP-HPLC using an elution gradient of 28 % to 30 % ACN in H_2O (both containing 0.1 % formic acid). After lyophilization in the dark this yielded pure TCO-derivative **13** (49 mg, 45 µmol, 54 %; axial isomer) as a white solid. ESI-MS: *m/z* Calc. for $C_{49}H_{90}N_6O_{20}$ 1082.62; Obs. $[M+2H]^{2+}$ 542.33, $[M+H]^{+}$ 1083.92, $[M+Na]^{+}$ 1105.75.

2,2',2''-(10-(1-((1R,8S,9s,E)-Bicyclo[6.1.0]non-4-en-9-yl)-1,39-dioxo-5,8,11,14,17,20,23,26,29,32,35-undecaoxa-2,38-diazatetracontan-40-yl)-1,4,7,10-tetraazacyclododecane-1,4,7-triyl)triacetic acid (15): Compound **S12** (38 mg, 36 µmol) and *N*,*N*-diisopropylethylamine (51 µL, 0.29 mmol, 8 eq) were dissolved in DMF (400 µL). (1R,8S,9s,E)-2,5-Dioxopyrrolidin-1-yl bicyclo[6.1.0]non-4-ene-9-carboxylate **S13** (10.4 mg, 40 µmol, 1.1 eq) was added and the mixture was stirred at room temperature for 30 min. In three portions, additional (1R,8S,9s,E)-2,5-Dioxopyrrolidin-1-yl bicyclo[6.1.0]non-4-ene-9-carboxylate (total 13.2 mg, 50 µmol, 1.4 eq) was added with intermittent stirring at room temperature for 30 min and a conversion check using LC-MS. After (1R,8S,9s,E)-2,5-Dioxopyrrolidin-1-yl bicyclo[6.1.0]non-4-ene-9-carboxylate had been consumed the reaction mixture was added dropwise to a stirring solution of diethyl ether (25 mL), centrifuged (5 min at 4000 rpm) and decanted. The resulting solid was washed with diethyl ether (20 mL) after which centrifugation and decantation were repeated. The solid was dissolved in DMF (1 mL) and the precipitation procedure including ether wash was repeated once. The obtained solid was dried *in vacuo* yielding pure **15** (39 mg, 36 µmol, 100 %) as a white solid, which should be stored at -80 °C in order to avoid degradation by epoxidation. ESI-MS: *m/z* Calc. for $C_{50}H_{90}N_6O_{19}$ 1078.63; Obs. $[M+2H]^{2+}$ 540.58, $[M+H]^{+}$ 1079.92, $[M+Na]^{+}$ 1102.00. ^{1}H-NMR (CD_3OD) δ = 5.89–5.71 (m, 1H), 5.30–5.11 (m, 1H), 3.84–3.09 (m, 72H), 2.40–2.16 (m, 2H), 2.09–1.67 (m, 6H), 1.64–1.44 (m, 1H), 1.15–0.85 (m, 2H).

Synthesis of reference compound for P1

Formation in $CDCl_3$: Tetrazine **11** (6.45 mg, 23.6 µmol) was dissolved in $CDCl_3$ (600 µL) and TCO **12** (2.74 mg, 24.9 µmol) was added. The pink mixture became colorless within minutes, and was stirred for an additional 8 days at 20°C under an atmosphere of air, which resulted in complete oxidation. Then, the mixture was evaporated to dryness to yield **P1** as a beige oil (8.3 mg, 100 %). ^{1}H-NMR($CDCl_3$): δ = 7.47 (m, 5H), 6.20 (q, J = 6.6 Hz, 1H), 3.12 (m, 1H), 2.98 (s, 3H), 2.89 (s + m, 4H), 2.76 (m, 2H), 1.94 (m, 1H), 1.76 (d, J = 6.6 Hz, 3H), 1.66 (m, 2H), 1.6 – 1.2 (br. m, 5 H) ppm. ^{13}C-NMR ($CDCl_3$) δ = 161.26, 158.71, 156.20, 139.00, 138.66, 138.27, 129.14, 128.34, 128.13, 68.98, 36.41, 36.15, 30.61, 29.82, 27.28, 26.06, 25.96, 25.45, 20.45 ppm. HPLC-MS/PDA: *m/z* Calc. for $C_{21}H_{27}N_3O_2$ 353.21; Obs. $[M+H]^+$ 354.33, λ_{max} = 236 nm.

Synthesis of reference compound for P2

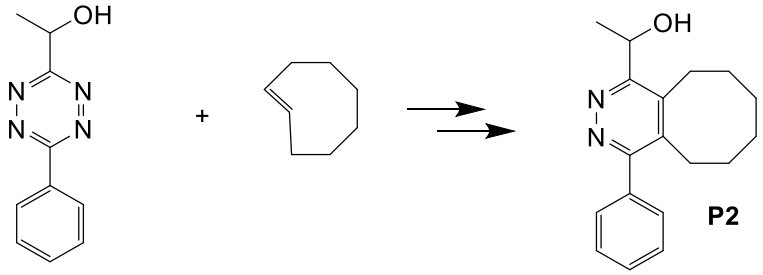

Tetrazine **S8** (27.2 mg, 134 µmol) was dissolved in ACN (3 mL), and potassium phosphate buffer (15 mL 20 mM, pH=7.4) was added, followed by TCO **12** (16.3 mg, 148 µmol) in ACN (2 mL). The pink mixture became colorless within seconds. Then, it was cooled to 0°C, and subsequently sodium nitrite (46.2 mg, 670 µmol) and formic acid (0.3 mL) were added to oxidize the intermediates. The mixture was stirred for 10 min at room temperature and then lyophilized. The organics were dissolved in chloroform (1.5 mL), washed with aqueous sodium carbonate (1 mL 1 M), dried over sodium sulfate, and evaporated to dryness, to yield **P2** as an off-white solid (30 mg, 79%). ^{1}H-NMR($CDCl_3$): δ = 7.59 – 7.36 (m, 5H), 5.20 (d, J = 6.4 Hz, 1H), 4.65 (br.s, 1 H), 2.87 (m, 4H), 1.8 (m, 3H), 1.60 (d, J = 6.4 Hz, 3H), 1.56 – 1.02 (m, 5H) ppm. ^{13}C-NMR ($CDCl_3$) δ = 161.76, 160.90, 139.52, 137.90, 137.50, 128.99, 128.53, 128.27, 65.99, 30.32, 29.76, 26.99, 26.02, 25.75, 25.45, 25.38 ppm. HPLC-MS/PDA: *m/z* Calc. for $C_{18}H_{22}N_2O$ 282.17; Obs. $[M+H]^+$ 283.33, λ_{max} = 236 nm.

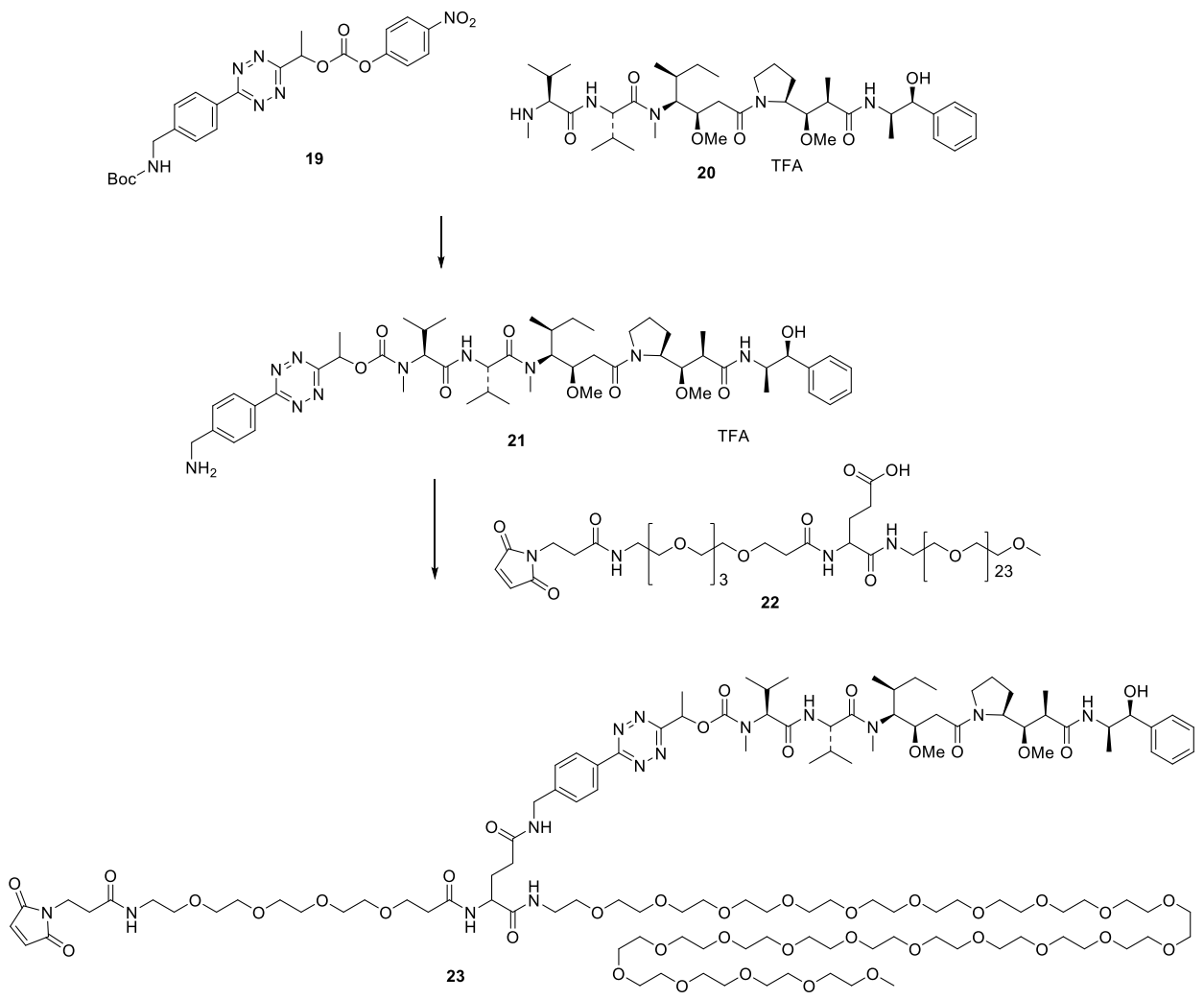

Synthesis of compound 21

To a solution of compound **19** (388 mg, 0.78 mmol) and MMAE **20** (650 mg, 0.78 mmol) in anhydrous DMF (5 mL) was added DIEA (0.275 mL) and the mixture was stirred at room temperature for 24 h. LC/MS analysis indicated completion of the reaction. The reaction mixture was diluted with EtOAc (150 mL) and washed successively with water (2 x 50 mL) and brine (50 mL). The organic layer was dried over Na_2SO_4 and concentrated to dryness under reduced pressure. The resulting red syrup was treated with TFA/DCM (1/4, v/v, 15 mL) at room temperature. After 20 min, the reaction mixture was concentrated under reduced pressure and the residue was purified directly by reverse phase preparative HPLC to give compound **21** as a red solid after lyophilization (407 mg, 0.37 mmol). MS m/z : 976.0 $(M+H)^+$. $)^+$. ^{1}H NMR ($CDCl_3$): δ = 8.60 (d, 2H), 8.54 (d, 2H), 7.74-7.68 (m, 1H), 7.66 (d, 1H), 7.34-7.15 (m, 5H), 6.95 (m), 6.62-6.45 (m), 6.31-6.02 (m), 4.88-4.78 (m), 4.68-4.42 (m), 4.40-3.78 (m), 3.56-3.22 (m), 3.18 (s), 3.12 (s), 3.04(d), 3.01(s), 2.97(d), 2.93 (br s), 2.85 (s), 2.48 -1.55 (m), 1.32-1.24 (m), 1.21 (d), 1.17 (t), -1.12 (m), 1.06-0.72 (m), 0.65 (d) ppm. ^{13}C NMR ($CDCl_3$): δ = 175.17, 173.01, 170.64, 169.68, 169.49, 169.36, 168.71, 164.58, 164.50, 164.44, 156.85, 155.27, 140.67, 140.25, 138.35, 138.07, 132.39, 130.16, 130.09, 130.03, 129.00, 128.81, 128.30, 127.76, 126.79, 126.68, 82.15, 79.14, 75.54, 72.01, 65.18, 61.46, 61.38, 60.35, 60.12, 58.06, 54.93, 50.68, 50.47, 48.27, 48.13, 45.74, 45.56, 43.49, 38.25, 37.79, 33.09, 31.06, 30.02, 29.76, 26.30, 26.13, 25.96, 25.11, 25.04, 24.87, 20.30, 20.14, 19.82, 19.59, 19.42, 19.08, 18.81, 18.73, 17.77, 15.95, 15.46, 15.14, 10.97, 10.92 ppm.

Prep HPLC conditions for compound **21**: **c**olumn: Gemini NX 5µ, C18, 110 Å, 150 x 50 mm; mobile phase: ACN / water (0.1% TFA); gradient: 20 min, from 10 to 60 % of ACN at 50 mL/min; elution time: 17-18 min.

Synthesis of compound 23

To a solution of compound **21** (388, 0.35 mmol) in anhydrous DMF (6 mL) was added MAL-dPEG®$_4$-Glu(TFP ester)-NH-m-dPEG®$_{24}$, compound **22** (580 mg, 0.35 mmol), followed by HATU (135 mg, 0.35 mmol) and DIPEA (0.25 mL, 1.4 mmol). The reaction was stirred at room temperature for 10 mins. LC/MS analysis indicated that most of compound **21** was consumed. The reaction mixture was purified by reverse phase preparative HPLC to give compound **23** as a red gum after lyophilization (487 mg, 0.19 mmol). MS m/z : 1287.0 ($M+2H^+$)/2. ^{1}H NMR ($CDCl_3$): δ = 8.56-8.48 (m), 7.52-7.38 (m), 7.36-7.18 (m), 7.14-7.06 (m), 6.68-6.64 (m), 6.59-6.45 (m), 6.38-6.20 (m), 4.94-4.86 (m), 4.77-4.43 (m), 4.35-3.98 (m), 3.95-3.72(m), 3.7-3.45 (m), 3.44-3.40 (m), 3.38 (s), 3.36 (s), 3.30 (d), 3.28 (s), 3.26 (d), 3.24 (s), 3.10 (d), 3.05 (d), 3.02 (d), 2.98 (br s), 2.95-2.92 (m), 2.86 (d), 2.84 (s), 2.52-2.34 (m), 2.20-1.76 (m), 1.40-1.26 (m), 1.25-1.18 (m), 1.06-0.76 (m), 0.70-0.66 (m) ppm. ^{13}C NMR ($CDCl_3$): δ = 173.37, 172.05, 171.71, 170.74, 170.55, 156.70, 144.03, 141.44, 134.39, 130.82, 128.77, 128.64, 128.52, 128.25, 127.49, 126.49, 82.21, 75.93, 72.10, 70.71, 70.65, 70.63, 70.49, 70.34, 70.26, 69.97, 69.72, 67.43, 65.49, 61.06, 60.20, 59.17, 58.14, 54.13, 52.69, 51.62, 48.03, 45.04, 43.45, 39.62, 39.48, 37.09, 34.70, 34.59, 33.51, 32.53, 29.93, 29.29, 26.44, 25.90, 25.14, 25.07, 20.14, 19.48, 18.70, 16.13, 14.49, 14.13, 11.07 ppm.

Prep HPLC conditions for compound **23**: **c**olumn: Gemini NX 5µ, C18, 110 Å, 150 x 50 mm; mobile phase: ACN / H_2O (0.1% TFA); gradient: 20 min, from 10 to 70 % of ACN at 50 mL/min; elution time: 19-20 min.

S3: Supplementary Figures and Tables

S3.1 Tautomerization and release reaction of tetrazine derivatives with TCOs

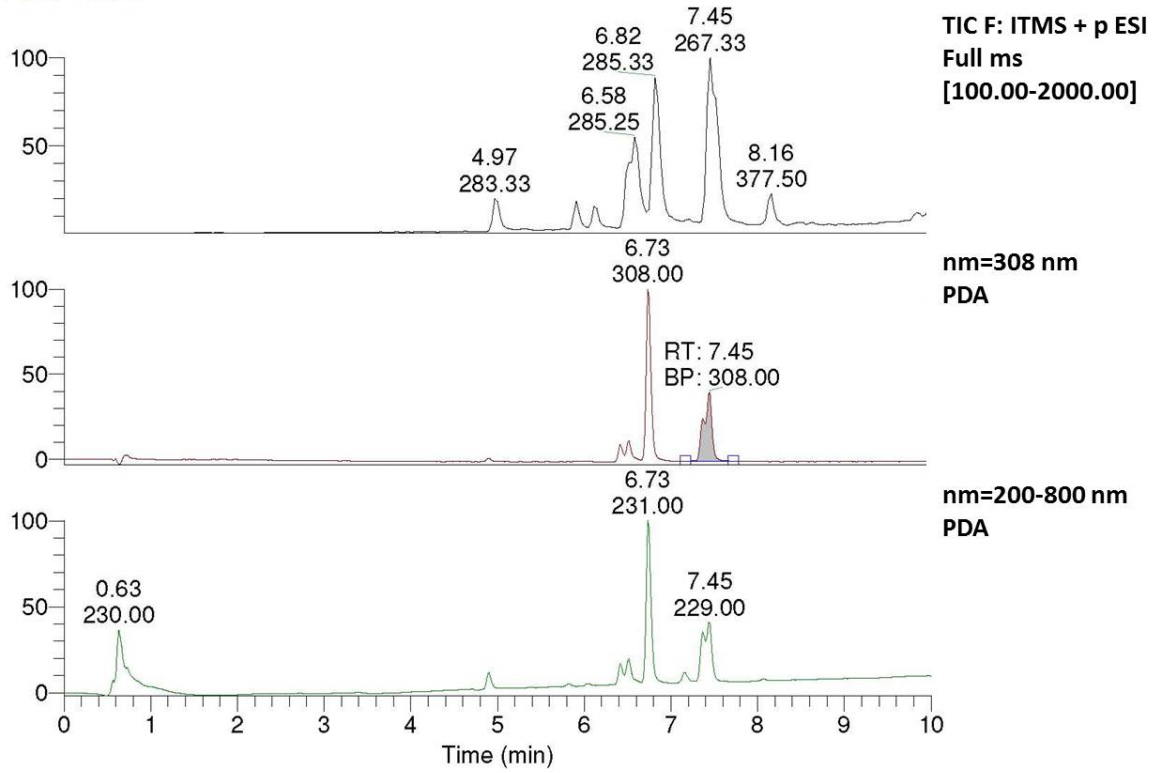

Supplementary Figure S1: typical HPLC-MS/PDA chromatogram of the release reaction of **11** and TCO after incubation at 37°C for 40 h. Quantification of the amount of IEDDA adduct was performed by integration at λ=308 nm of the corresponding peak.

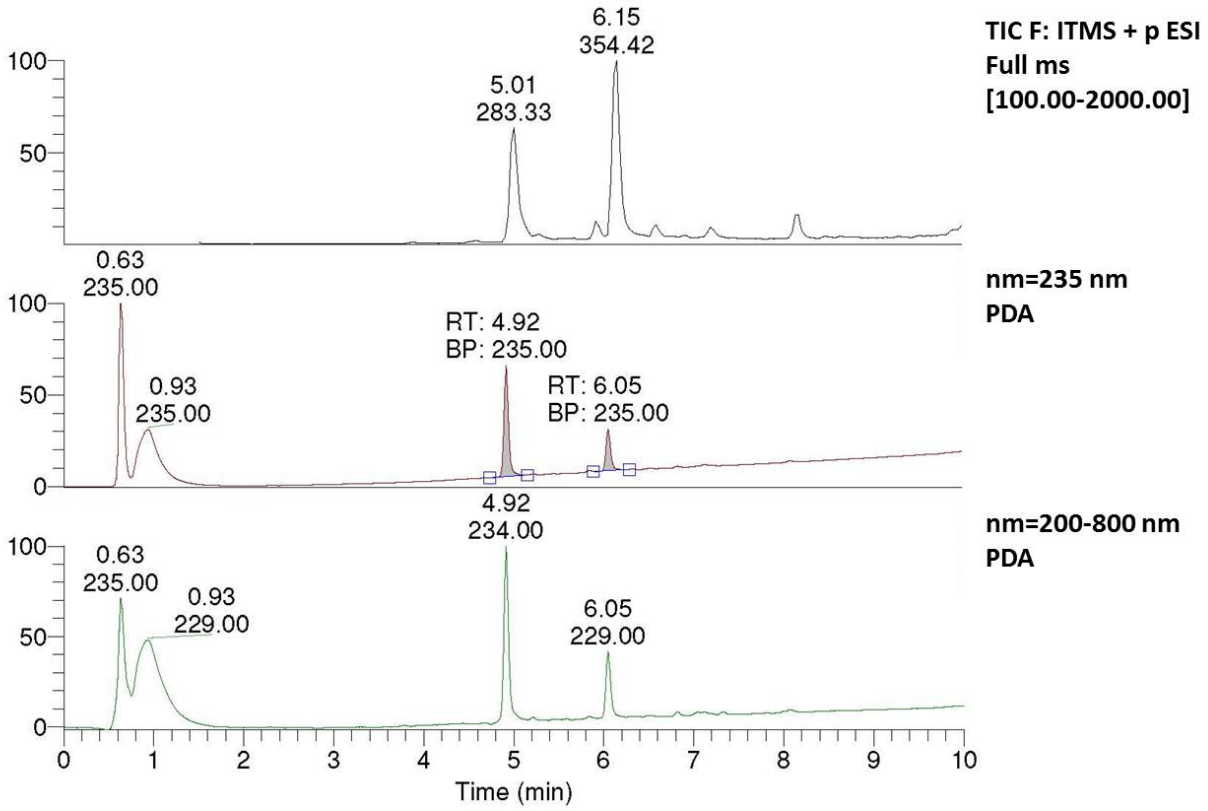

Supplementary Figure S2: typical HPLC-MS/PDA chromatogram of the release reaction of **11** and TCO after incubation at 37°C for 40 h. Prior to analysis, the sample was oxidized by addition of sodium nitrite and formic acid. Quantification was performed by integration at λ=235 nm of the peaks corresponding to **P1** and **P2**, at 6.05 and 4.92 min, respectively.

S3.2 Characterization of tautomers formed upon reaction of TCO 12 with tetrazine 11

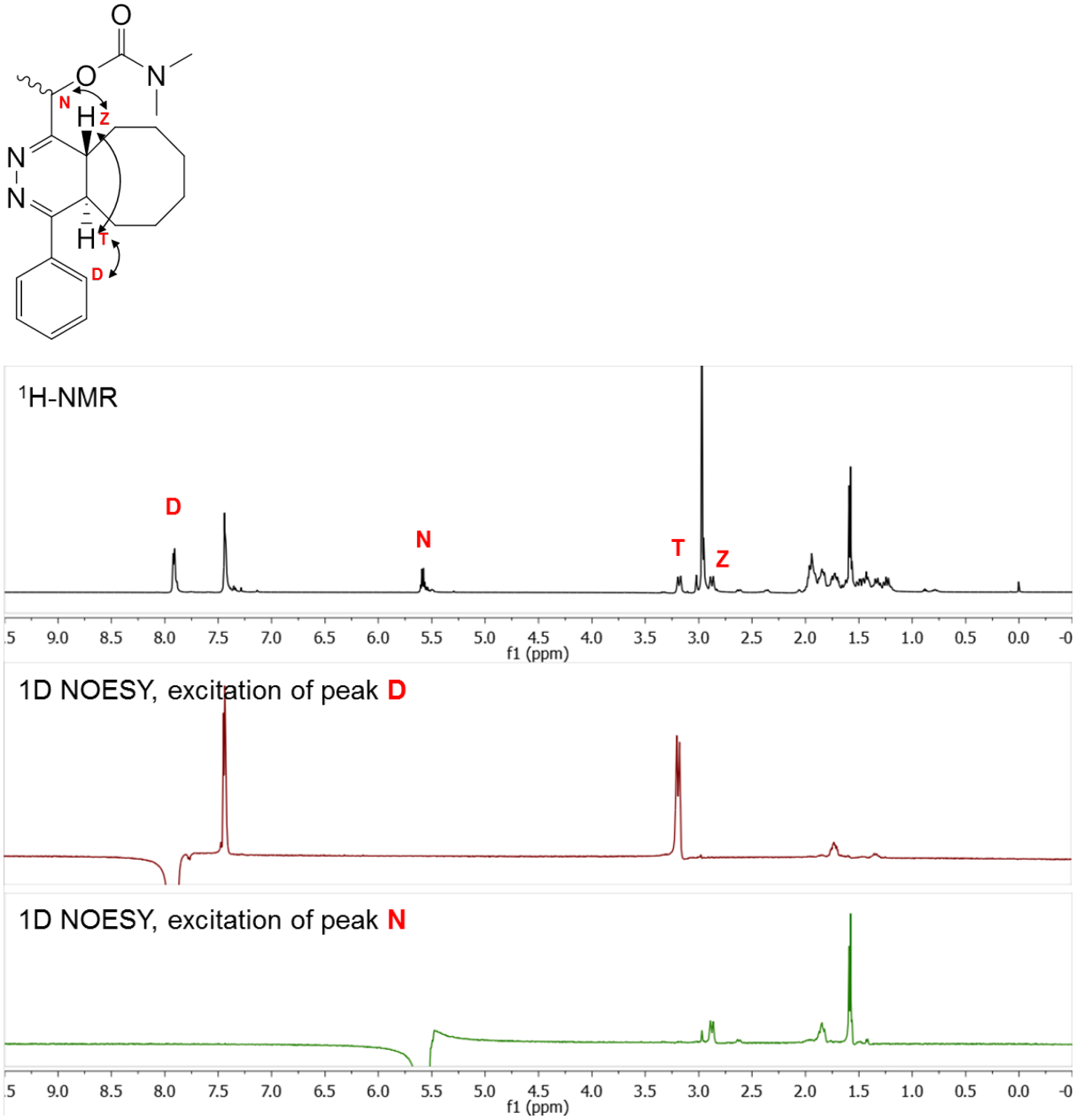

Supplementary Figure S3: ^{1}H-NMR and 1D-NOESY spectra of the initially formed **4,5-DHP**

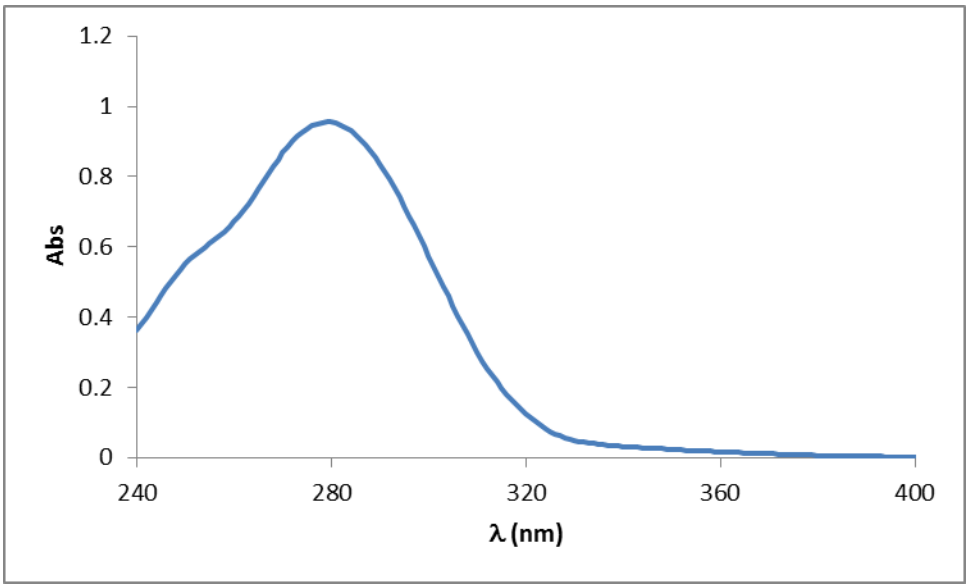

Supplementary Figure S4: UV-VIS spectrum of the initially formed **4,5-DHP**

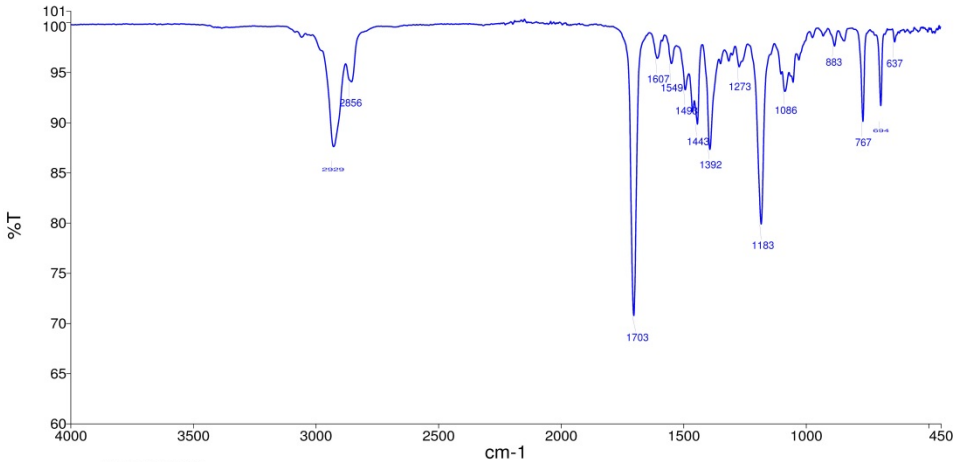

Supplementary Figure S5: FTIR spectrum of the initially formed **4,5-DHP**

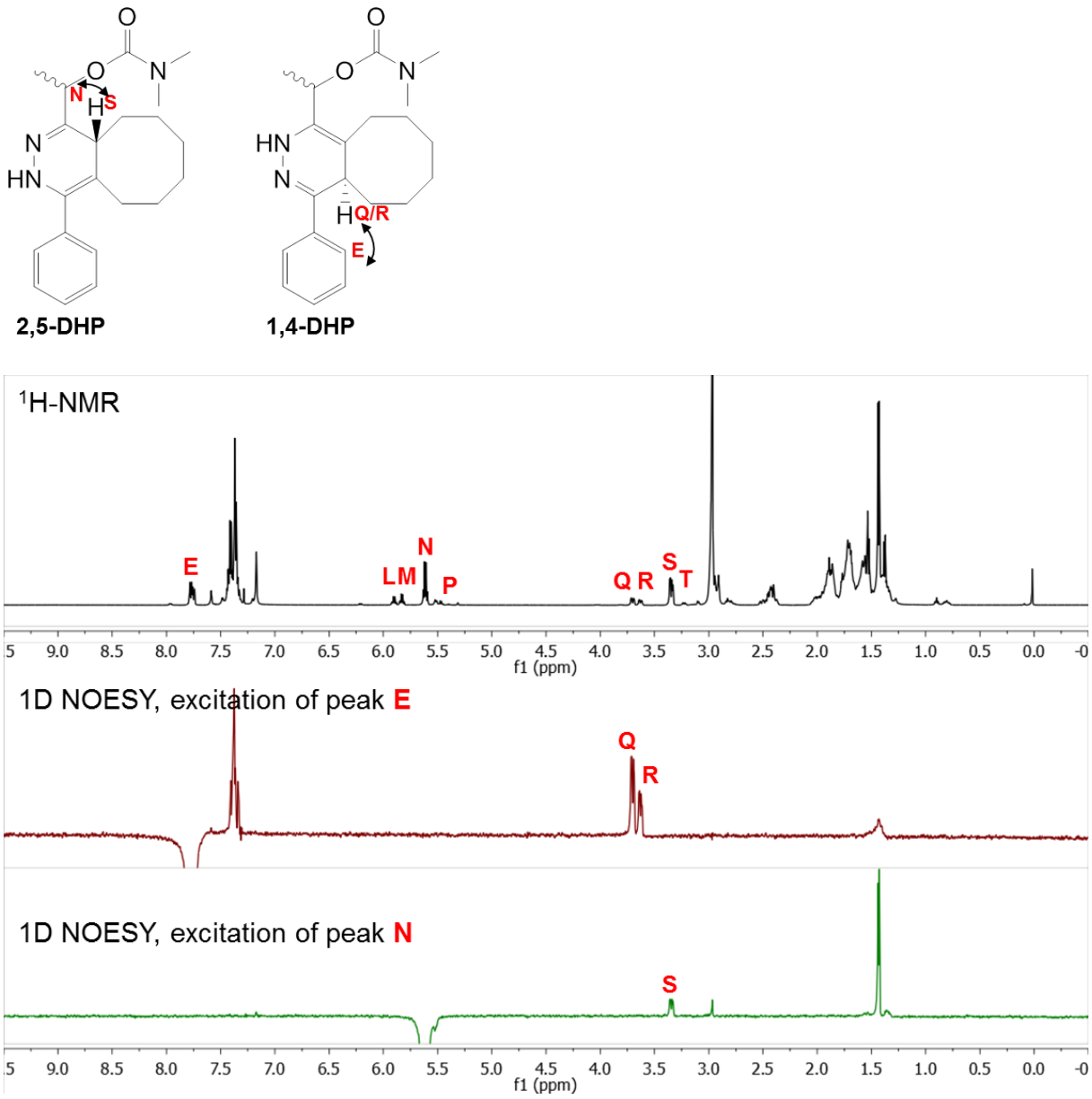

Supplementary Figure S6: ^{1}H-NMR and 1D-NOESY spectra of **2,5-** and **1,4-DHP**, ratio of 73 %/ 27 %

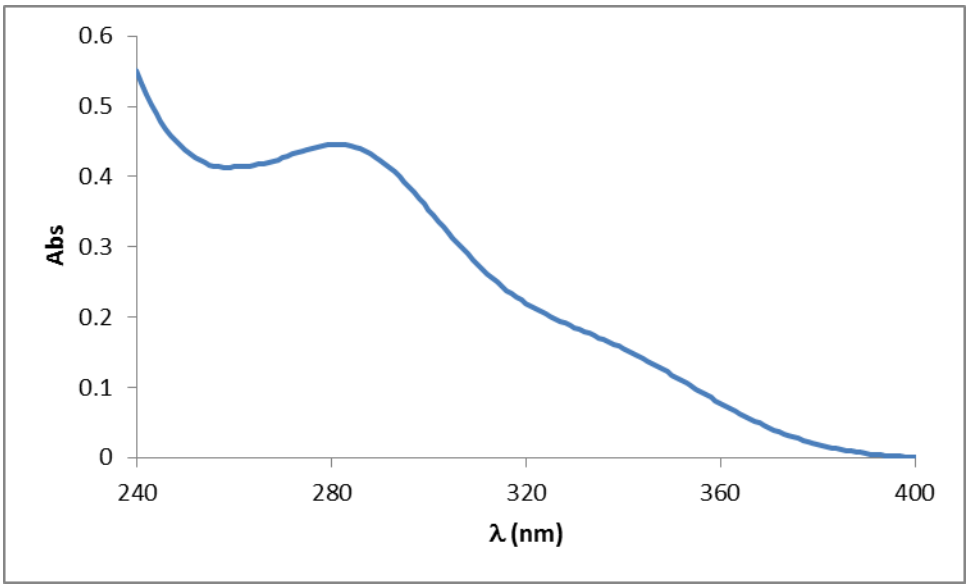

Supplementary Figure S7: UV-VIS spectrum of mixture of **2,5-** and **1,4-DHP**, ratio of 73 %/ 27 %

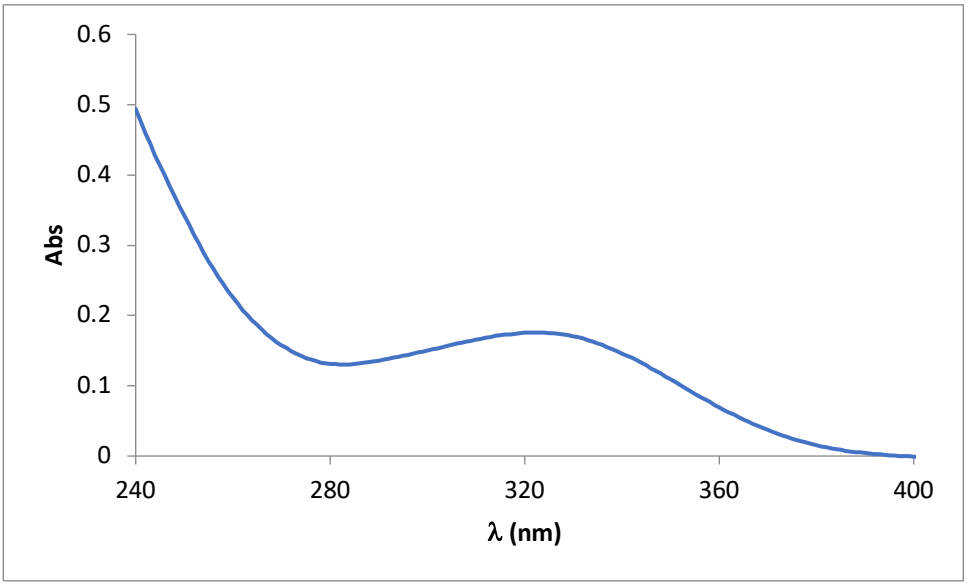

Supplementary Figure S8: UV-VIS spectrum of mixture of **2,5-** and **1,4-DHP**, ratio of 26 %/ 74 %

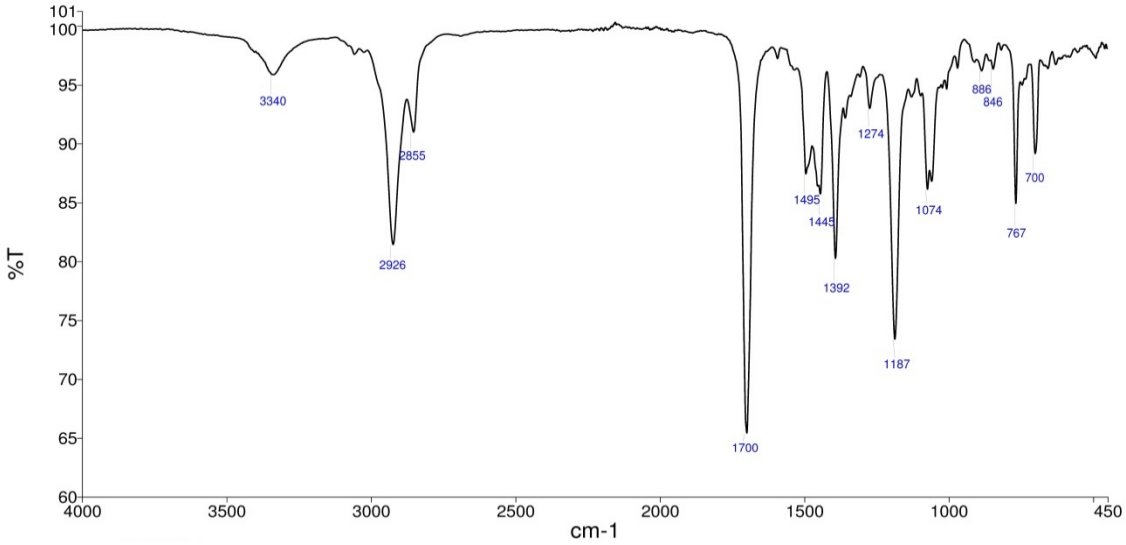

Supplementary Figure S9: FTIR spectrum of mixture of **2,5-** and **1,4-DHP**-ratio of 73%/27%.

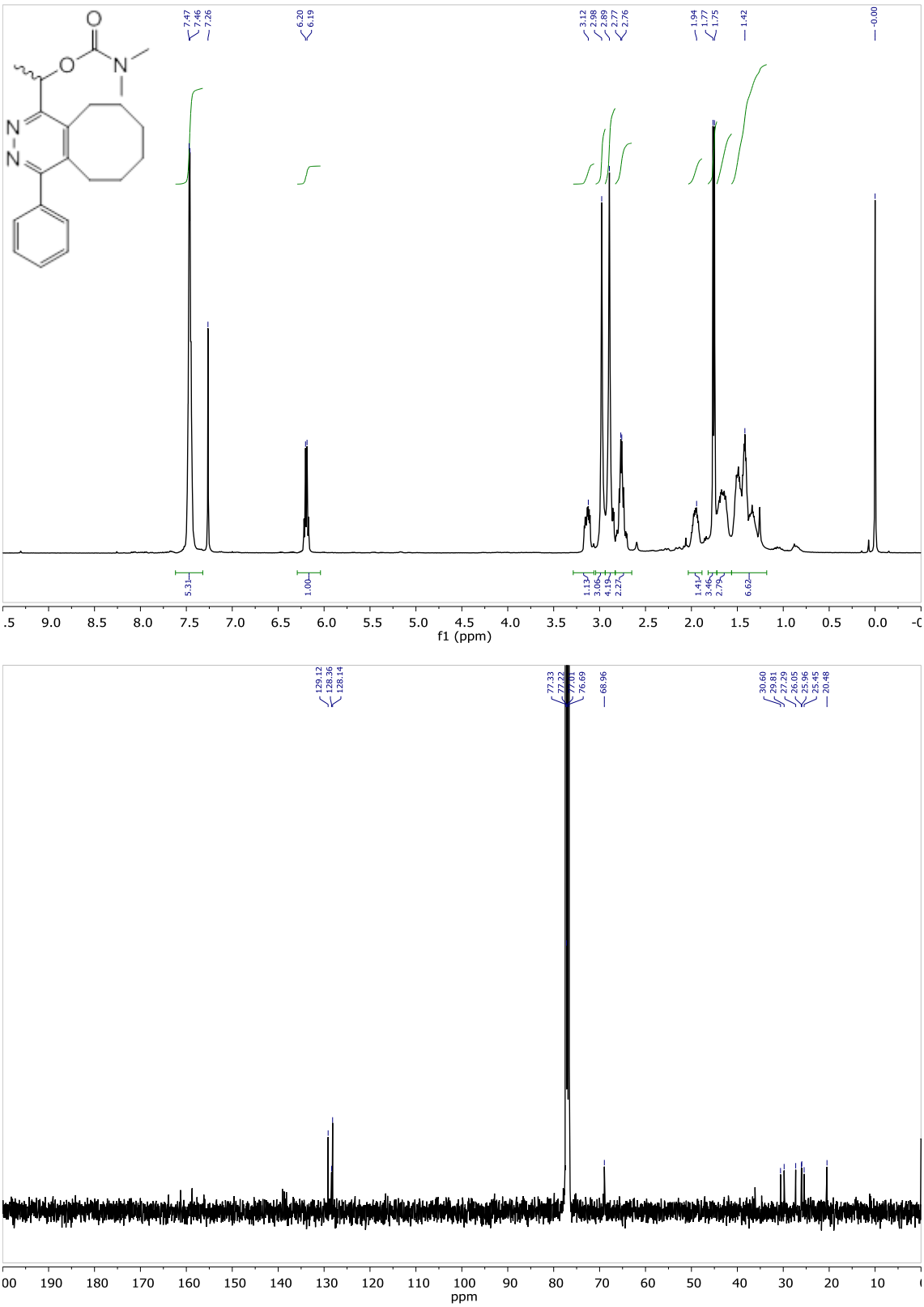

Supplementary Figure S10: ^{1}H- and ^{13}C-NMR ($CDCl_3$) spectrum of 1-(4-phenyl-5,6,7,8,9,10-hexahydrocycloocta[d]pyridazin-1-yl)ethyl dimethylcarbamate (**P1**)

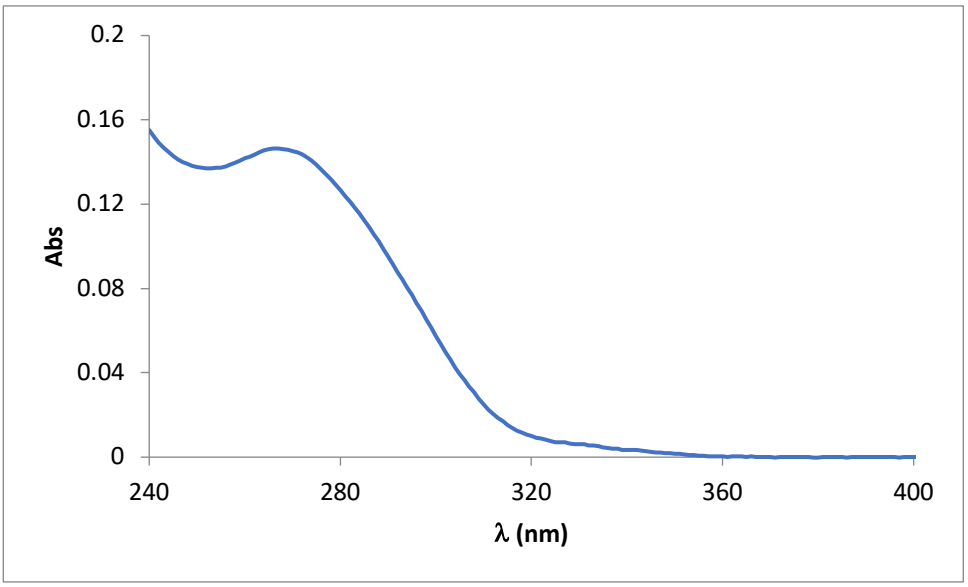

Supplementary Figure S11: UV-VIS spectrum of 1-(4-phenyl-5,6,7,8,9,10-hexahydrocycloocta[d]pyridazin-1-yl)ethyl dimethylcarbamate (**P1**)

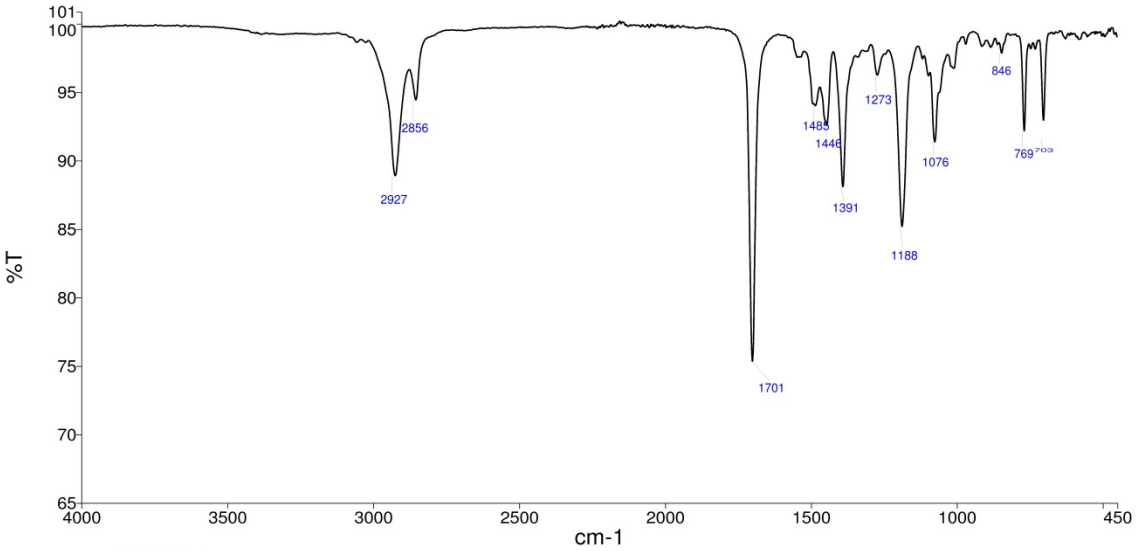

Supplementary Figure S12: FTIR spectrum of 1-(4-phenyl-5,6,7,8,9,10-hexahydrocycloocta[d]pyridazin-1-yl)ethyl dimethylcarbamate (**P1**)

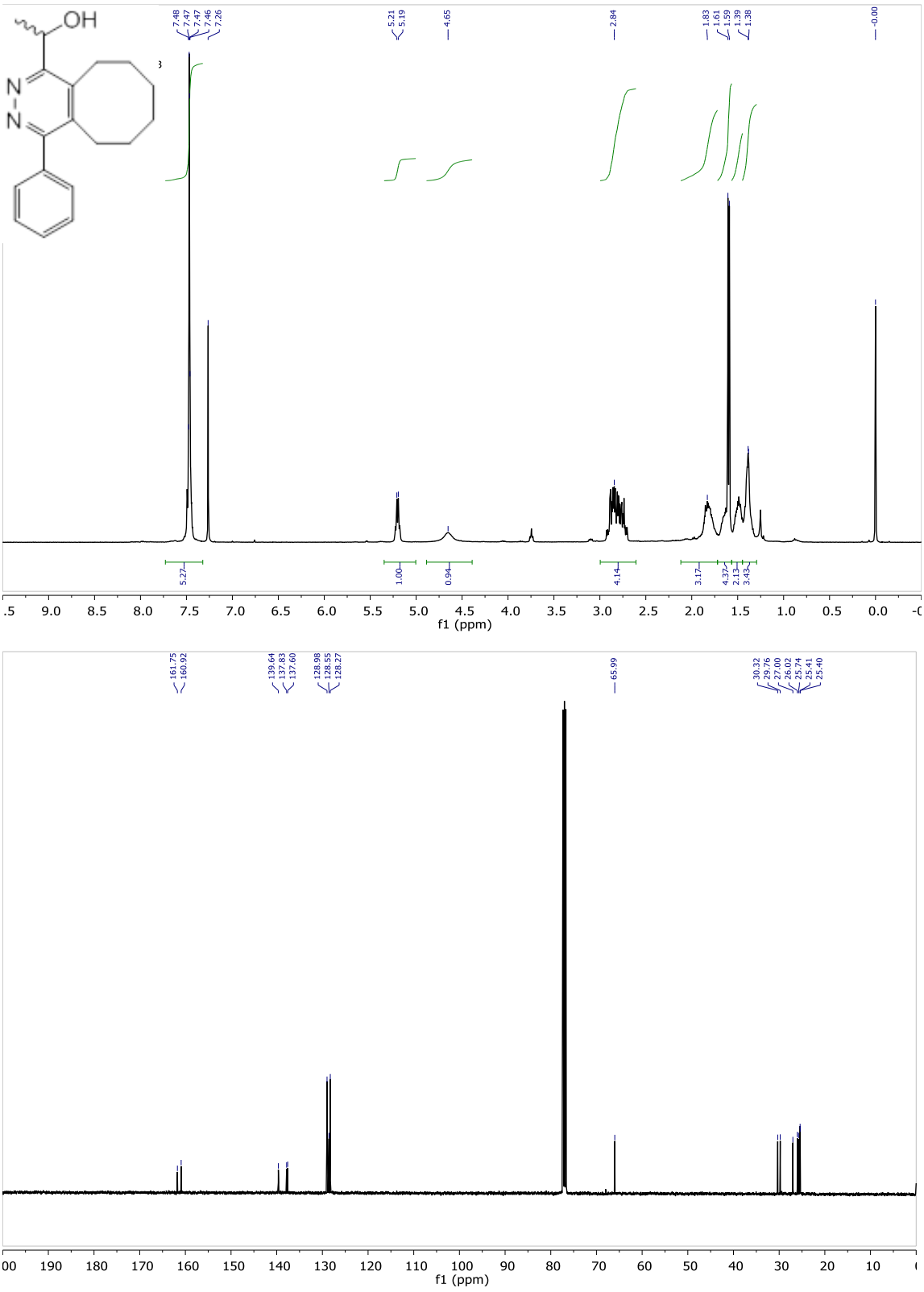

Supplementary Figure S13: ^{1}H- and ^{13}C-NMR spectra ($CDCl_3$) of 1-(4-phenyl-5,6,7,8,9,10-hexahydrocycloocta[d]pyridazin-1-yl)ethan-1-ol (**P2**)

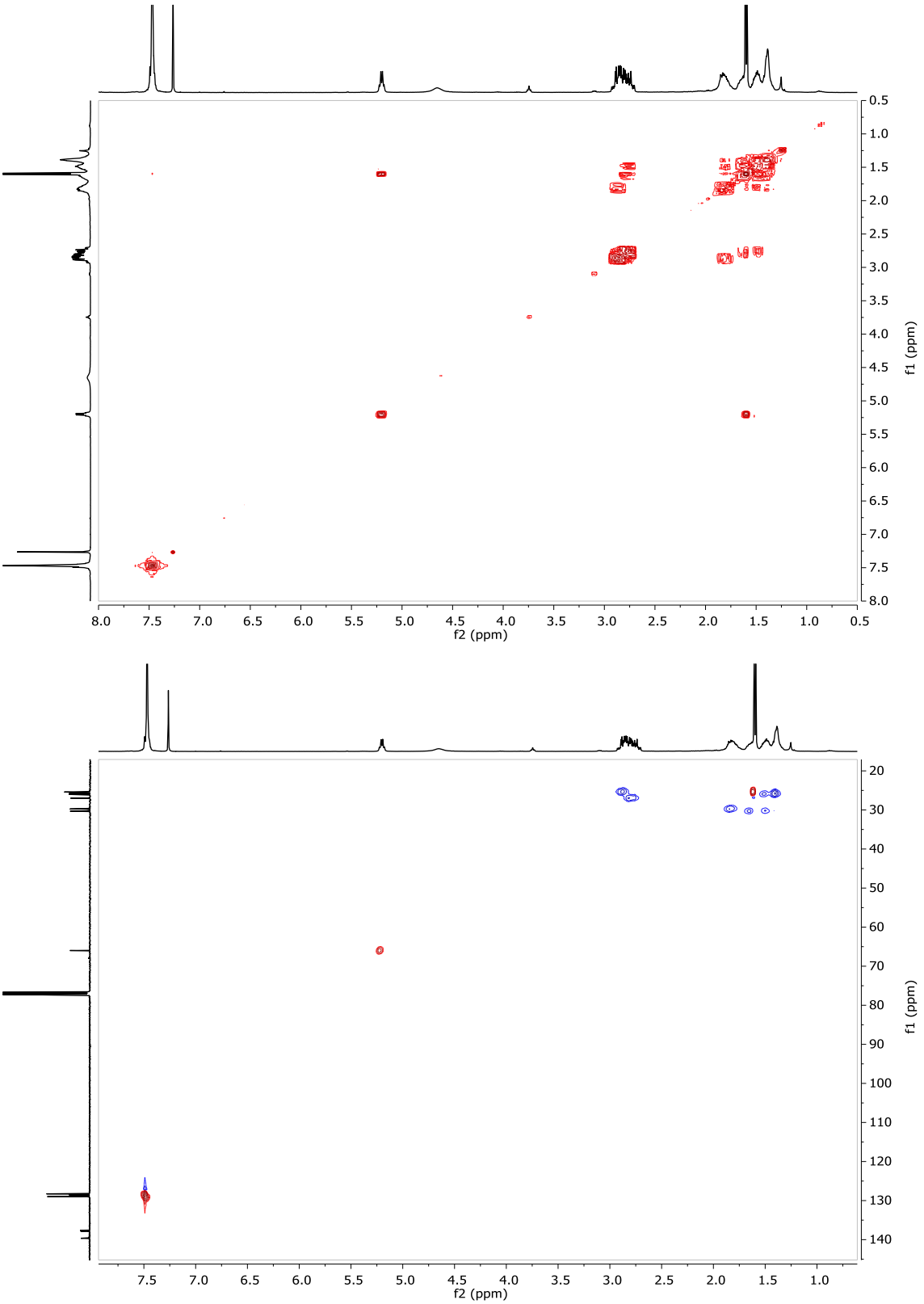

Supplementary Figure S14: COSY and HSQC spectra ($CDCl_3$) of 1-(4-phenyl-5,6,7,8,9,10-hexahydrocycloocta[d]pyridazin-1-yl)ethan-1-ol (**P2**)

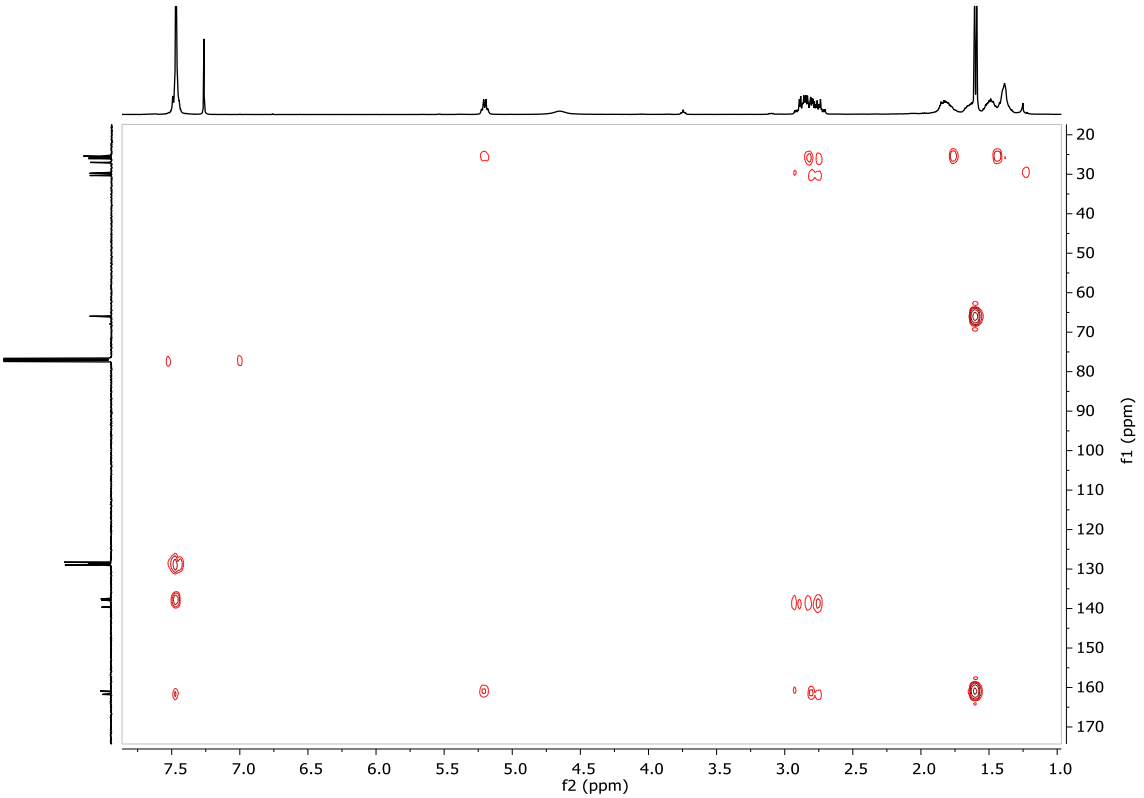

Supplementary Figure S15: HMBC spectrum ($CDCl_3$) of 1-(4-phenyl-5,6,7,8,9,10-hexahydrocycloocta[d]pyridazin-1-yl)ethan-1-ol (**P2**)

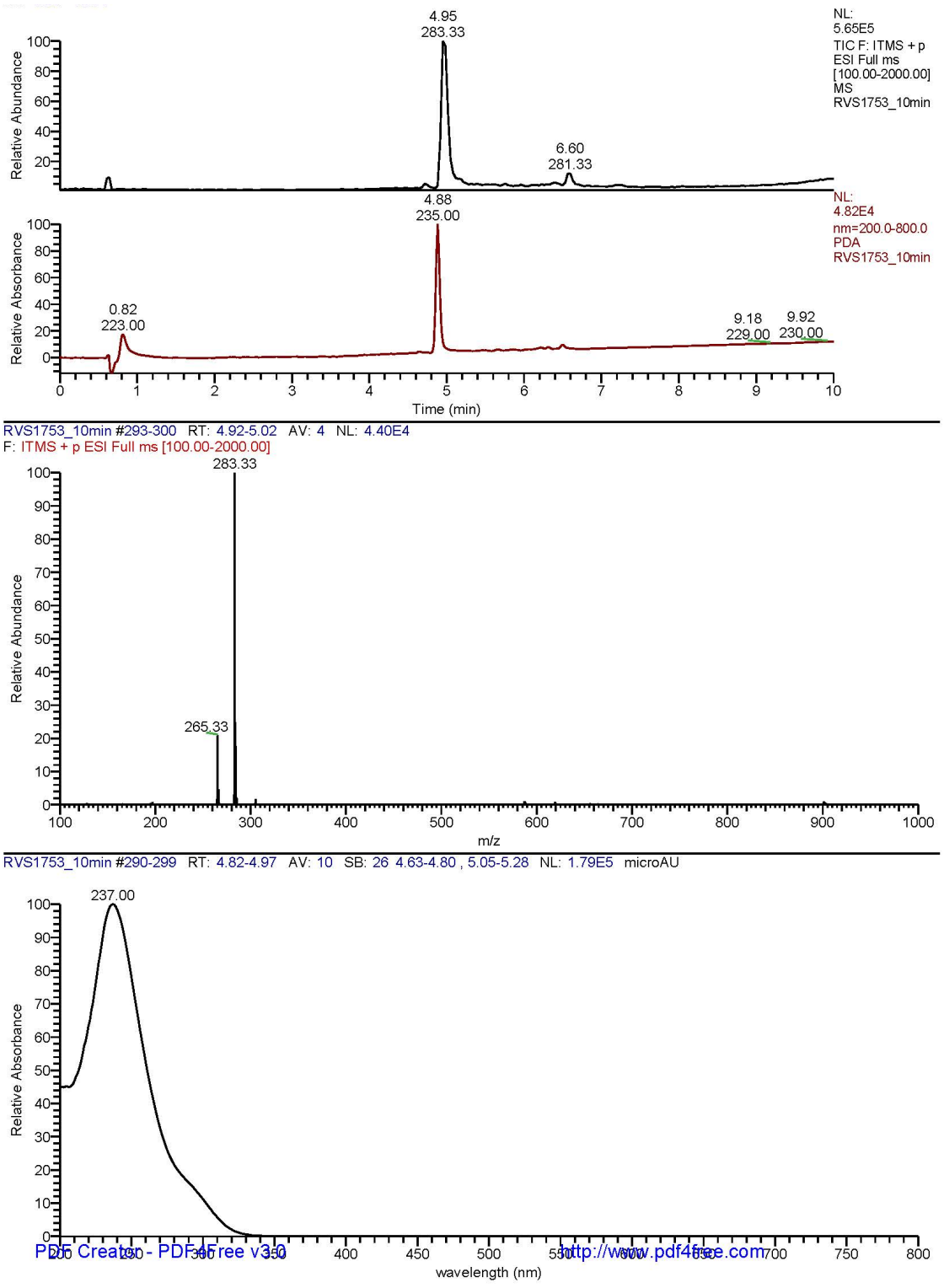

Supplementary Figure S16: HPLC-MS/PDA analysis of 1-(4-phenyl-5,6,7,8,9,10-hexahydrocycloocta[d]pyridazin-1-yl)ethan-1-ol (**P2**)

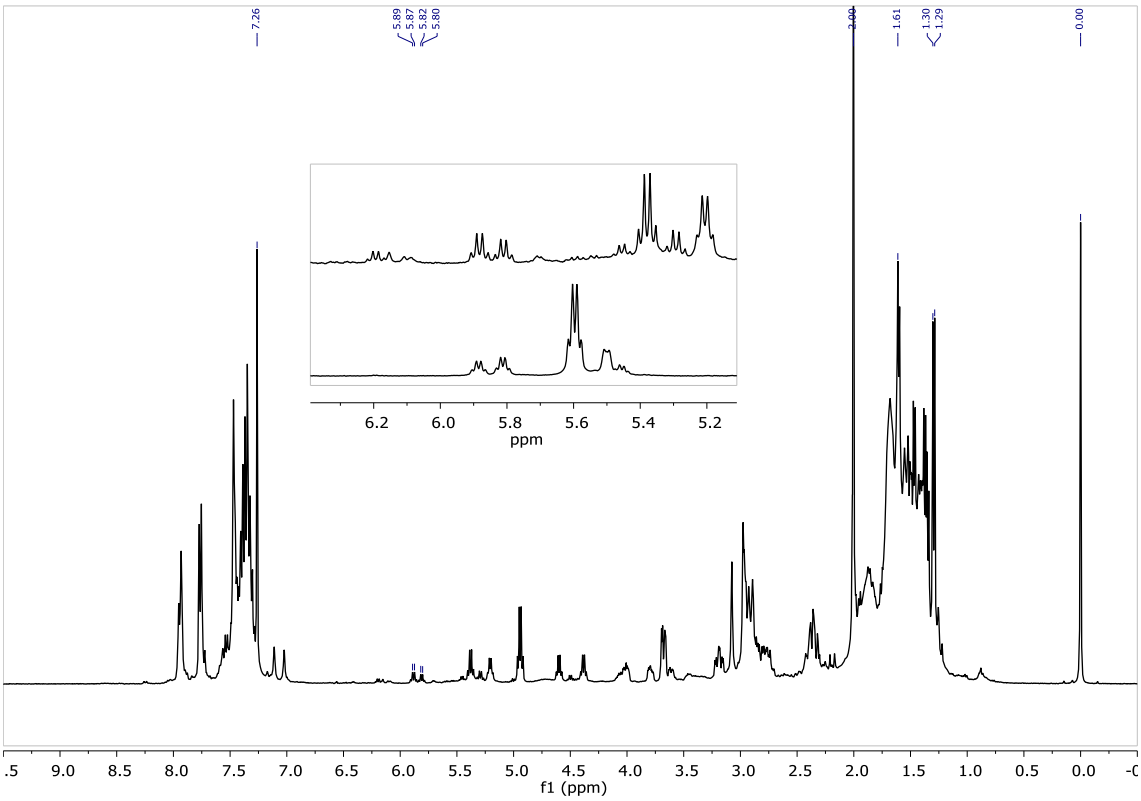

Supplementary Figure S17: ^{1}H-NMR analysis of the product mixture of **11** and **12** after 3 days at 37°C in 25 % ACN/PBS and after subsequent reconstitution in $CDCl_3$, containing the non-releasing tautomer. Insert: comparison of the product mixture (top) with the mixture of tautomers obtained after tautomerization in $CDCl_3$ (bottom), demonstrating the disappearance of the peaks at 5.60 and 5.50 ppm corresponding to the 2,5-tautomer, and the persistence of the peaks at 5.88 and 5.81 ppm corresponding to the 1,4-tautomer.

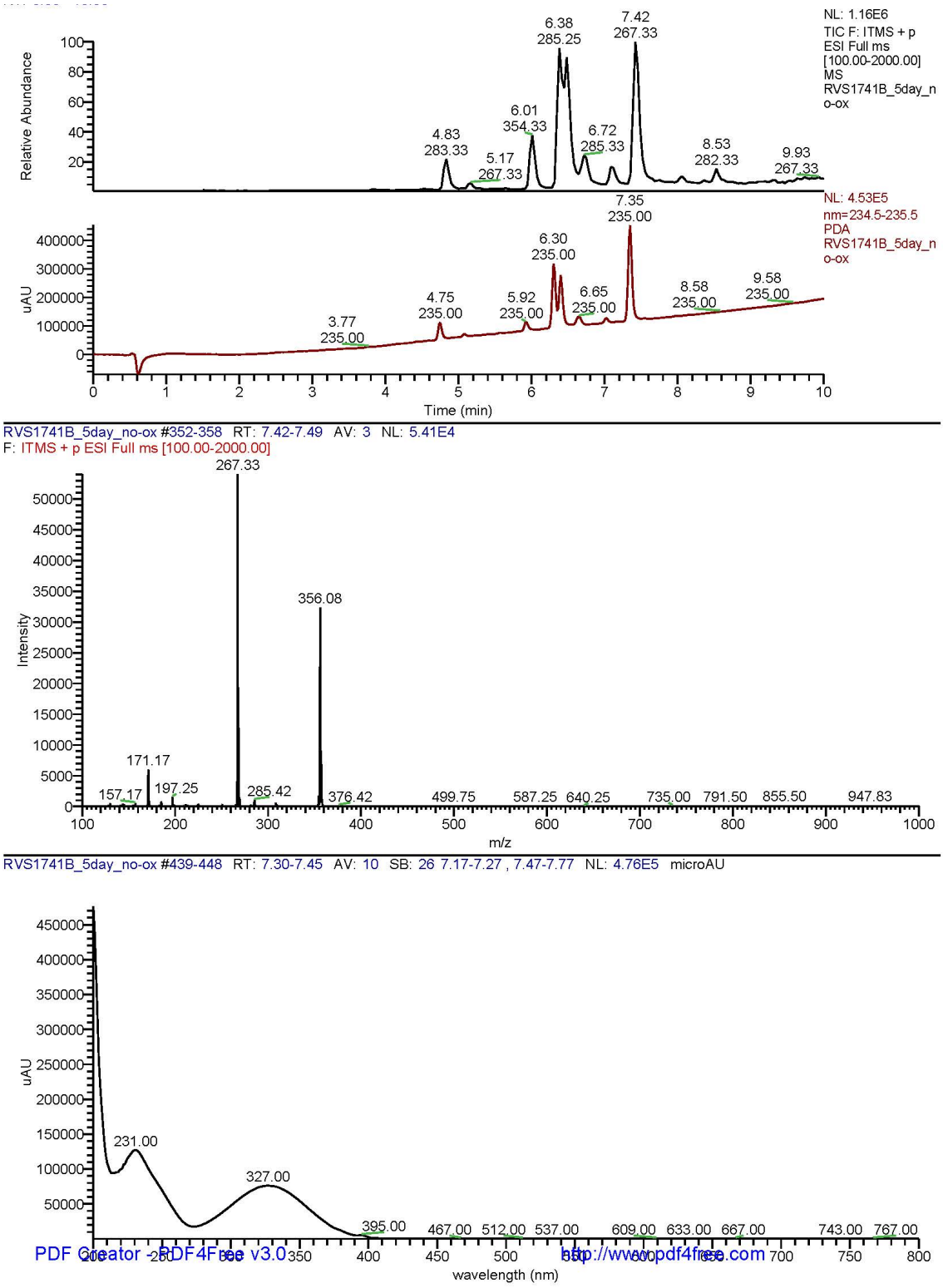

Supplementary Figure S18: HPLC-MS/PDA analysis of the product mixture after 3 days at 37°C in 25 % ACN/PBS, containing the non-releasing tautomer at 7.4 min with λmax = 327 nm.

S3.3 Calculated Ground energies of tautomers

Supplementary Table S1: Electronic ground-state energies of the DHP tautomers.

	Vacuum [HT]	**Implicit water solvent [HT]**
1,4-DHP	-13.81967109	-13.83260148
2,5-DHP	-13.80527692	-13.81798721
4,5-DHP	-13.79166621	-13.80992797
1,2-DHP	*Not calculated*	-13.80404850
Exocyclic tautomer I	*Not calculated*	-13.76706520
Exocyclic tautomer II	*Not calculated*	-13.80447984

Supplementary Table S2: Geometries (XYZ coordinates) of calculated tautomers

1,4-DHP

1 N	-0.357653	1.014967	1.338594
2 C	0.570209	1.644105	0.694629
3 N	-1.415667	1.768552	1.786061
4 C	0.542165	3.159528	0.582363
5 C	-1.828277	2.895339	1.048213
6 C	-0.902042	3.571185	0.345062
7 H	2.986069	2.529914	-0.243324
8 C	-1.190879	4.627382	-0.691688
9 C	-3.294283	3.223311	1.126091
10 C	1.171796	3.790465	1.864822
11 H	-2.156049	1.166023	2.114707
12 C	-3.828413	3.353600	2.549315
13 O	-4.022292	2.153790	0.430344
14 C	-5.150455	2.529287	-0.235686
15 O	-5.550402	3.693344	-0.272905
16 N	-5.771674	1.482406	-0.829829
17 C	-5.202661	0.137138	-0.898897
18 C	-6.922025	1.735624	-1.692794
19 C	0.779772	5.238935	2.175094
20 C	-0.746823	6.078806	-0.402834
21 C	0.769979	6.296694	-0.231050
22 C	1.278905	6.331639	1.221825
23 H	1.310768	5.540154	-0.806234
24 C	1.686980	0.844252	0.136069
25 C	1.594874	-0.556286	0.041713
26 C	2.649790	-1.310136	-0.455850
27 C	3.825211	-0.687180	-0.881234
28 C	3.928035	0.698671	-0.803863
29 C	2.871192	1.456071	-0.301979
30 H	0.683856	-1.046314	0.358615
31 H	2.554364	-2.387918	-0.519006
32 H	4.646700	-1.276383	-1.271331
33 H	4.833303	1.196975	-1.130406
34 H	-2.256022	4.641217	-0.926622
35 H	-0.688581	4.311675	-1.614751
36 H	-3.482263	4.146973	0.590554
37 H	2.260458	3.706855	1.792540
38 H	0.872521	3.179775	2.720330
39 H	-3.278769	4.132628	3.079489
40 H	-3.731374	2.421477	3.107177
41 H	-4.881913	3.631084	2.521236
42 H	2.374347	6.326571	1.208686
43 H	0.986922	7.293924	1.655859
44 H	-4.498920	-0.020484	-0.090170
45 H	-4.693709	-0.021621	-1.854464
46 H	-6.011254	-0.588856	-0.813032
47 H	-6.632366	1.698792	-2.747396
48 H	-7.335572	2.713608	-1.471977
49 H	-7.679425	0.972141	-1.513999
50 H	1.165192	5.470742	3.172563
51 H	-0.308741	5.298603	2.259424
52 H	-1.282199	6.460385	0.472003
53 H	-1.092798	6.675174	-1.251317
54 H	1.040051	7.252844	-0.687757
55 H	1.126745	3.462808	-0.284687

2.5-DHP

1 N	-0.337365	0.985731	2.184397
2 C	0.507883	1.558795	1.201615
3 N	-1.704660	1.101816	2.015471
4 C	0.117100	2.709689	0.624664
5 C	-2.122606	2.198210	1.500293
6 C	-1.146719	3.349931	1.212722
7 H	0.649788	-1.029904	0.407897
8 C	-1.766822	4.523245	0.424519
9 C	-3.622539	2.325711	1.309442
10 C	0.897030	3.399493	-0.460713
11 H	-0.886310	3.743977	2.210340
12 C	-4.458082	1.231139	1.952341
13 O	-3.855437	2.323577	-0.137562
14 C	-4.875101	3.105308	-0.595242
15 O	-5.563685	3.809948	0.144228
16 N	-5.028277	3.019111	-1.937069
17 C	-6.077833	3.787569	-2.597497
18 C	-4.221440	2.170122	-2.810560
19 C	1.677068	4.636401	0.071219
20 C	-1.056446	5.901887	0.480977
21 C	-0.171280	6.272497	-0.728340
22 C	1.332592	5.967004	-0.604532
23 H	-0.577575	5.778155	-1.615803
24 C	1.731918	0.769401	0.901727
25 C	3.008616	1.332315	1.025535
26 C	4.148027	0.579391	0.750565
27 C	4.031277	-0.751463	0.353980
28 C	2.766360	-1.327285	0.238438
29 C	1.628261	-0.574922	0.514249
30 H	3.109712	2.360440	1.349016
31 H	5.127531	1.031448	0.854329
32 H	4.918022	-1.336293	0.139442
33 H	2.664791	-2.360639	-0.071887
34 H	-2.764368	4.680436	0.832104
35 H	-1.916533	4.234081	-0.618241
36 H	-3.953062	3.291709	1.687318
37 H	0.216845	3.708091	-1.257135
38 H	1.589191	2.692874	-0.917062
39 H	-4.313512	1.233689	3.032819
40 H	-4.188165	0.248950	1.567856
41 H	-5.511129	1.421628	1.744788
42 H	1.774743	6.000396	-1.605669
43 H	1.814744	6.766724	-0.033170
44 H	-6.597660	4.396758	-1.866424
45 H	-6.789714	3.113524	-3.080186
46 H	-5.638952	4.432887	-3.361797
47 H	-4.861043	1.437175	-3.308416
48 H	-3.461460	1.650568	-2.240486
49 H	-3.740067	2.783564	-3.575766
50 H	2.750222	4.456380	-0.030545
51 H	1.496511	4.729969	1.144306
52 H	-0.491000	5.996280	1.413522
53 H	-1.846932	6.653080	0.543121
54 H	-0.272654	7.343580	-0.923509
55 H	-0.102113	0.036190	2.437569

4,5-DHP

1 N	-0.796572	0.925904	0.855876
2 C	0.155614	1.630779	0.349089
3 N	-2.103377	1.457328	0.846717
4 C	-0.084200	3.070907	-0.095108
5 C	-2.257191	2.726923	0.924141
6 C	-1.054191	3.661777	0.963983
7 H	1.708003	1.236829	-1.867245
8 C	-1.366987	5.168850	0.835068
9 C	-3.686026	3.244520	1.000474
10 C	1.175874	3.915979	-0.339913
11 H	-0.604353	3.506284	1.954065
12 C	-4.129048	3.451566	2.445485
13 O	-4.623830	2.317487	0.413667
14 C	-4.649460	2.289287	-0.950333
15 O	-3.961640	3.037420	-1.644388
16 N	-5.505385	1.355052	-1.425555
17 C	-5.783996	1.306702	-2.857687
18 C	-6.387695	0.563068	-0.570130
19 C	1.951692	4.323777	0.930114
20 C	-0.457725	6.160209	1.604108
21 C	0.819136	6.667792	0.908306
22 C	2.101936	5.841785	1.105460
23 H	0.608401	6.786966	-0.158759
24 C	1.484991	0.961183	0.261444
25 C	2.065283	0.409099	1.409101
26 C	3.295078	-0.239836	1.336742
27 C	3.953247	-0.358726	0.113670
28 C	3.375061	0.175006	-1.036829
29 C	2.151997	0.837149	-0.963542
30 H	1.554519	0.499040	2.359831
31 H	3.738726	-0.651622	2.235750
32 H	4.909312	-0.865784	0.056950
33 H	3.874640	0.076386	-1.993384
34 H	-2.367217	5.337654	1.230114
35 H	-1.416206	5.453465	-0.220382
36 H	-0.633513	3.023018	-1.046495
37 H	0.858690	4.807312	-0.881066
38 H	1.830175	3.383214	-1.027904
39 H	-3.451178	4.135245	2.956691
40 H	-4.127055	2.501630	2.980754
41 H	-5.132051	3.877608	2.469927
42 H	2.856471	6.217172	0.406126
43 H	2.497181	6.031279	2.108418
44 H	-5.027047	1.869331	-3.393534
45 H	-6.768194	1.732674	-3.073600
46 H	-5.771993	0.269314	-3.193839
47 H	-7.370431	1.034561	-0.474947
48 H	-5.953452	0.442749	0.415809
49 H	-6.517974	-0.419926	-1.022601
50 H	2.945480	3.871161	0.921144
51 H	1.459541	3.918933	1.816724
52 H	-0.214201	5.742489	2.587072
53 H	-1.079277	7.036821	1.804002
54 H	1.027128	7.677307	1.274063
55 H	-3.754912	4.176581	0.445768

1,2-DHP				Exocyclic tautomer I				Exocyclic tautomer II			
1	N	11.475774	7.615150	9.605824	1	N	0.263822	1.462836	2.987657	1	N	-0.546608	1.025805	-0.494938
2	C	12.454084	8.495405	9.074849	2	C	0.499374	1.625531	1.695834	2	C	0.491533	1.715674	-0.183570
3	N	10.123999	7.883101	9.273908	3	N	-0.347887	2.282552	3.832239	3	N	-1.687049	1.776552	-0.833653
4	C	12.087481	9.739762	8.660372	4	C	0.075388	2.840323	0.956073	4	C	0.434124	3.231977	-0.278963
5	C	9.777389	9.278543	9.302493	5	C	-2.282369	2.373723	1.419850	5	C	-2.015999	2.839218	0.052875
6	C	10.721003	10.198441	8.999686	6	C	-1.220912	3.199152	0.810006	6	C	-0.858145	3.750046	0.419224
7	H	13.092549	5.997841	8.302577	7	H	0.352748	0.916110	-0.886939	7	H	2.877386	1.528853	-1.519309
8	C	10.488110	11.689050	9.041933	8	C	-1.634113	4.465388	0.073720	8	C	-1.124451	5.251609	0.109732
9	C	8.337866	9.549861	9.649212	9	C	-3.440562	1.979369	0.885598	9	C	-3.260048	2.952220	0.538211
10	C	12.998279	10.602025	7.798815	10	C	1.220818	3.673424	0.411452	10	C	1.707646	3.995778	0.137611
11	H	11.572679	7.444985	10.603678	11	H	0.578241	0.566923	3.357829	11	H	-2.457952	1.128837	-0.930643
12	C	7.862414	8.907716	10.943612	12	C	-4.451149	1.106459	1.561153	12	C	-3.791692	3.941976	1.523286
13	O	7.504284	8.985002	8.565438	13	O	-3.701703	2.232390	-0.478803	13	O	-4.178954	1.928328	0.188193
14	C	6.988646	9.864347	7.663636	14	C	-4.800446	3.000435	-0.783911	14	C	-5.227197	2.282764	-0.631806
15	O	6.994495	11.085618	7.826274	15	O	-5.390488	3.667613	0.061962	15	O	-5.291491	3.376831	-1.183168
16	N	6.471948	9.237235	6.578412	16	N	-5.110346	2.946511	-2.095874	16	N	-6.140142	1.292206	-0.734728
17	C	5.706019	10.003942	5.600495	17	C	-6.178463	3.791514	-2.621192	17	C	-7.237658	1.429411	-1.688748
18	C	6.423707	7.782842	6.437949	18	C	-4.405410	2.129532	-3.082058	18	C	-5.976448	-0.029753	-0.129009
19	C	13.774663	11.808425	8.408915	19	C	1.628763	4.791294	1.415690	19	C	1.854889	4.286773	1.646888
20	C	11.341858	12.395857	10.127174	20	C	-1.234108	5.825014	0.721457	20	C	-0.705922	6.261930	1.197741
21	C	12.212525	13.539691	9.598114	21	C	0.051388	6.481194	0.175004	21	C	0.775080	6.674723	1.261431
22	C	13.076821	13.182141	8.374314	22	C	1.367631	6.228404	0.933318	22	C	1.759082	5.778663	2.034638
23	H	11.582667	14.397006	9.339106	23	H	0.168767	6.184051	-0.871236	23	H	1.135625	6.830914	0.240060
24	C	13.809356	7.894179	9.019950	24	C	1.287006	0.576980	1.022625	24	C	1.708548	0.937331	0.194490
25	C	14.953909	8.600374	9.419682	25	C	2.248932	-0.199283	1.697427	25	C	1.699809	0.154068	1.353602
26	C	16.212358	8.006387	9.379920	26	C	2.952675	-1.199773	1.034625	26	C	2.817212	-0.598119	1.711990
27	C	16.354621	6.690115	8.943767	27	C	2.733376	-1.438470	-0.321576	27	C	3.956620	-0.581331	0.910559
28	C	15.224911	5.969462	8.556899	28	C	1.799425	-0.663476	-1.009110	28	C	3.971993	0.188764	-0.252258
29	C	13.966537	6.561578	8.602405	29	C	1.085131	0.328938	-0.346519	29	C	2.858027	0.945802	-0.606273
30	H	14.855864	9.613301	9.784611	30	H	2.479382	-0.005081	2.739046	30	H	0.814770	0.138679	1.978146
31	H	17.081238	8.570095	9.699492	31	H	3.689993	-1.780903	1.576376	31	H	2.795970	-1.196324	2.615394
32	H	17.334485	6.228047	8.912860	32	H	3.291147	-2.210789	-0.837881	32	H	4.826490	-1.165554	1.187369
33	H	15.324502	4.944498	8.218619	33	H	1.621561	-0.836480	-2.064136	33	H	4.850639	0.197982	-0.886619
34	H	9.434423	11.912420	9.184899	34	H	-2.716941	4.454584	-0.011785	34	H	-2.193421	5.376205	-0.057042
35	H	10.738173	12.095839	8.059493	35	H	-1.248421	4.444014	-0.950261	35	H	-0.646288	5.518153	-0.837663
36	H	8.143304	10.614732	9.670199	36	H	-0.354841	1.781080	4.719516	36	H	0.275458	3.419425	-1.350860
37	H	12.416039	10.979136	6.951240	37	H	0.952345	4.111000	-0.551240	37	H	1.721884	4.933988	-0.416862
38	H	13.741497	9.932710	7.366159	38	H	2.075146	3.023259	0.222698	38	H	2.574554	3.443455	-0.218919
39	H	8.444979	9.298667	11.779367	39	H	-4.140241	0.892129	2.582388	39	H	-2.991539	4.505049	1.997536
40	H	7.987126	7.826264	10.912275	40	H	-4.556206	0.161648	1.020311	40	H	-4.337682	3.408958	2.306046
41	H	6.811207	9.144727	11.113561	41	H	-5.431345	1.585355	1.585845	41	H	-4.484504	4.647671	1.058464
42	H	12.478179	13.244876	7.460521	42	H	2.188709	6.545368	0.282018	42	H	2.749427	6.231461	1.920290
43	H	13.841244	13.957462	8.272816	43	H	1.408343	6.885446	1.807791	43	H	1.524748	5.839621	3.102390
44	H	5.846038	11.063871	5.781803	44	H	-6.592051	4.395259	-1.821117	44	H	-7.309083	2.460829	-2.015833
45	H	4.641222	9.763653	5.671814	45	H	-6.966640	3.170917	-3.053048	45	H	-8.171691	1.135065	-1.208973
46	H	6.051070	9.759259	4.594730	46	H	-5.782394	4.444348	-3.402334	46	H	-7.072925	0.785445	-2.557264
47	H	5.475337	7.380244	6.806223	47	H	-5.135362	1.559494	-3.659680	47	H	-6.958612	-0.398500	0.165994
48	H	7.239981	7.321281	6.982028	48	H	-3.725751	1.443238	-2.592314	48	H	-5.343378	0.029198	0.748860
49	H	6.516918	7.535097	5.380490	49	H	-3.842867	2.767265	-3.768402	49	H	-5.539739	-0.735583	-0.841257
50	H	14.693243	11.894839	7.822894	50	H	2.690318	4.698989	1.658753	50	H	2.820163	3.913572	1.996106
51	H	14.092121	11.580403	9.429513	51	H	1.091099	4.623533	2.350511	51	H	1.112441	3.718684	2.209916
52	H	11.988064	11.657421	10.606325	52	H	-1.182194	5.719321	1.808539	52	H	-1.032846	5.899138	2.179110
53	H	10.688521	12.775102	10.916919	53	H	-2.059693	6.513900	0.526998	53	H	-1.282338	7.172592	1.011086
54	H	12.864853	13.874301	10.411244	54	H	-0.096844	7.564647	0.150286	54	H	0.823994	7.659988	1.735203
55	H	9.940608	7.474593	8.360080	55	H	-2.092208	2.035271	2.435521	55	H	-0.721718	3.654926	1.498651

S3.4 ADC characterization and stability

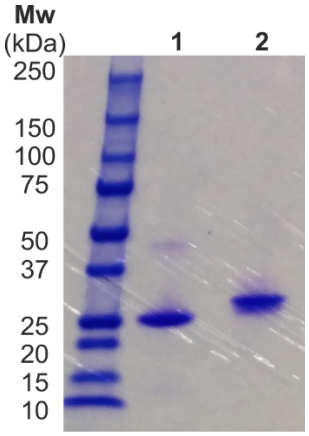

Supplementary Figure S19. SDS-PAGE analysis (protein stain) of (1) AVP04-58 monomer, (2) **tz-ADC**.

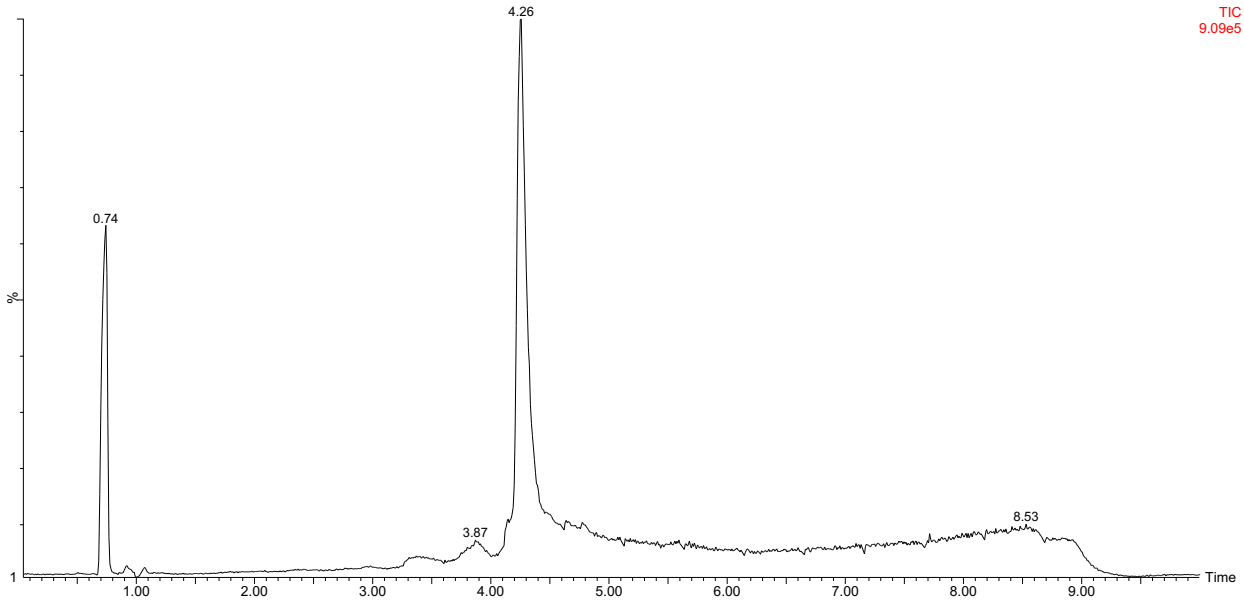

Supplementary Figure S20: LC-trace of LC-MS analysis of **tz-ADC.**

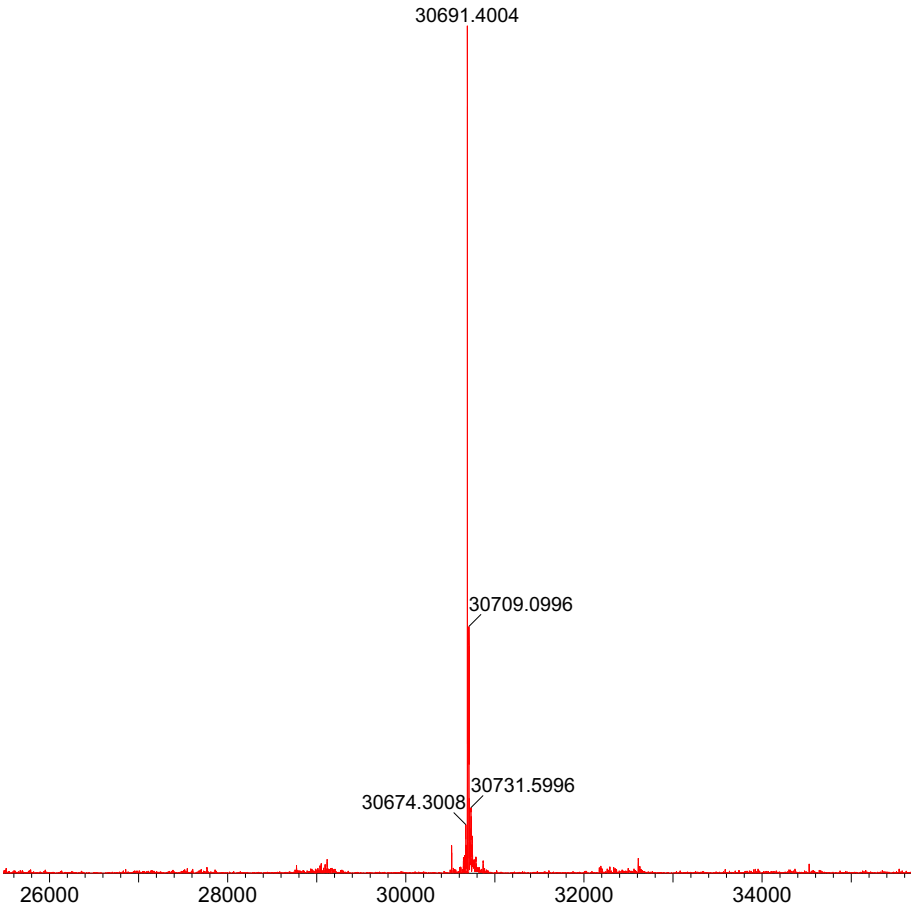

Supplementary Figure S21: Deconvoluted MS spectrum of LC-trace in Supplementary Fig. S20 analysed between 3.4 and 5 minutes. $M_{expected}$ = 30691 Da, $M_{observed}$ = 30691 Da, confirming a DAR of 2 per monomer.

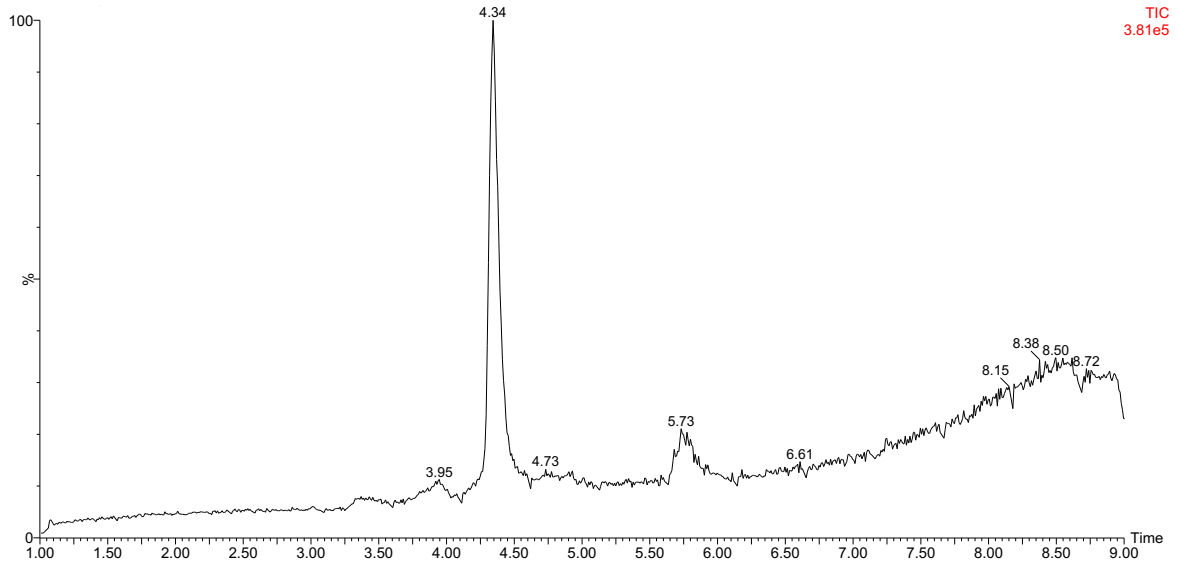

Supplementary Figure S22: LC-trace of LC-MS analysis of **tz-ADC** after in year in 5% DMSO/EDTA-PB at 4°C**.**

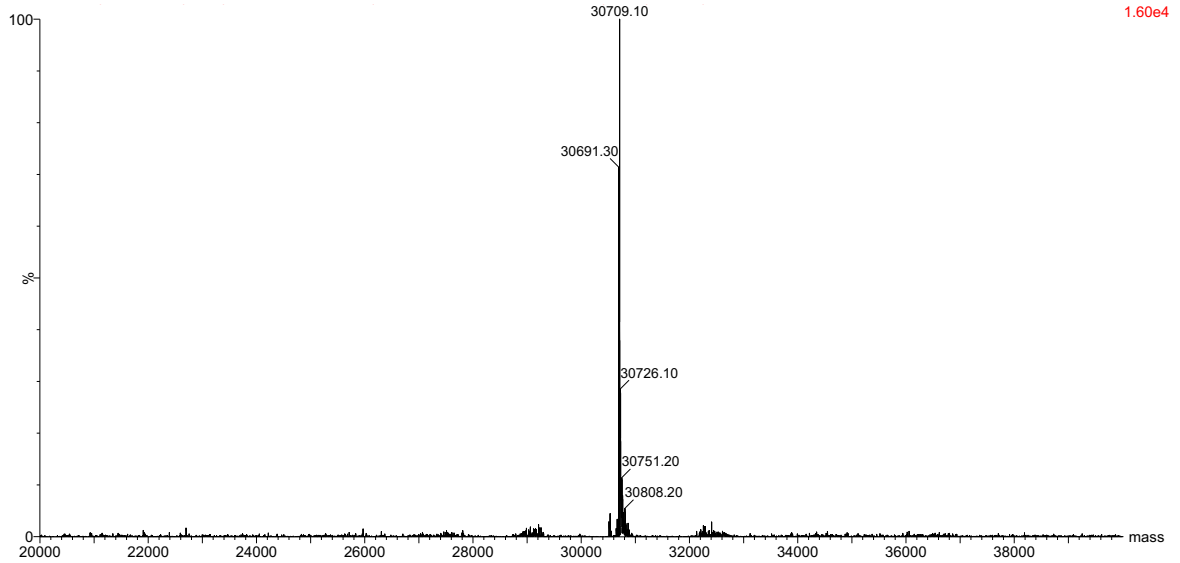

Supplementary Figure S23: Deconvoluted MS spectrum of LC-trace in Supplementary Fig. S22 analysed between 3.4 and 5 minutes. $M_{expected}$ = 30691 Da, $M_{observed}$ = 30691 Da and 30709 ($+H_2O$), confirming a DAR of 2 per monomer.

S3.5 MMAE release from ADC by TCOs

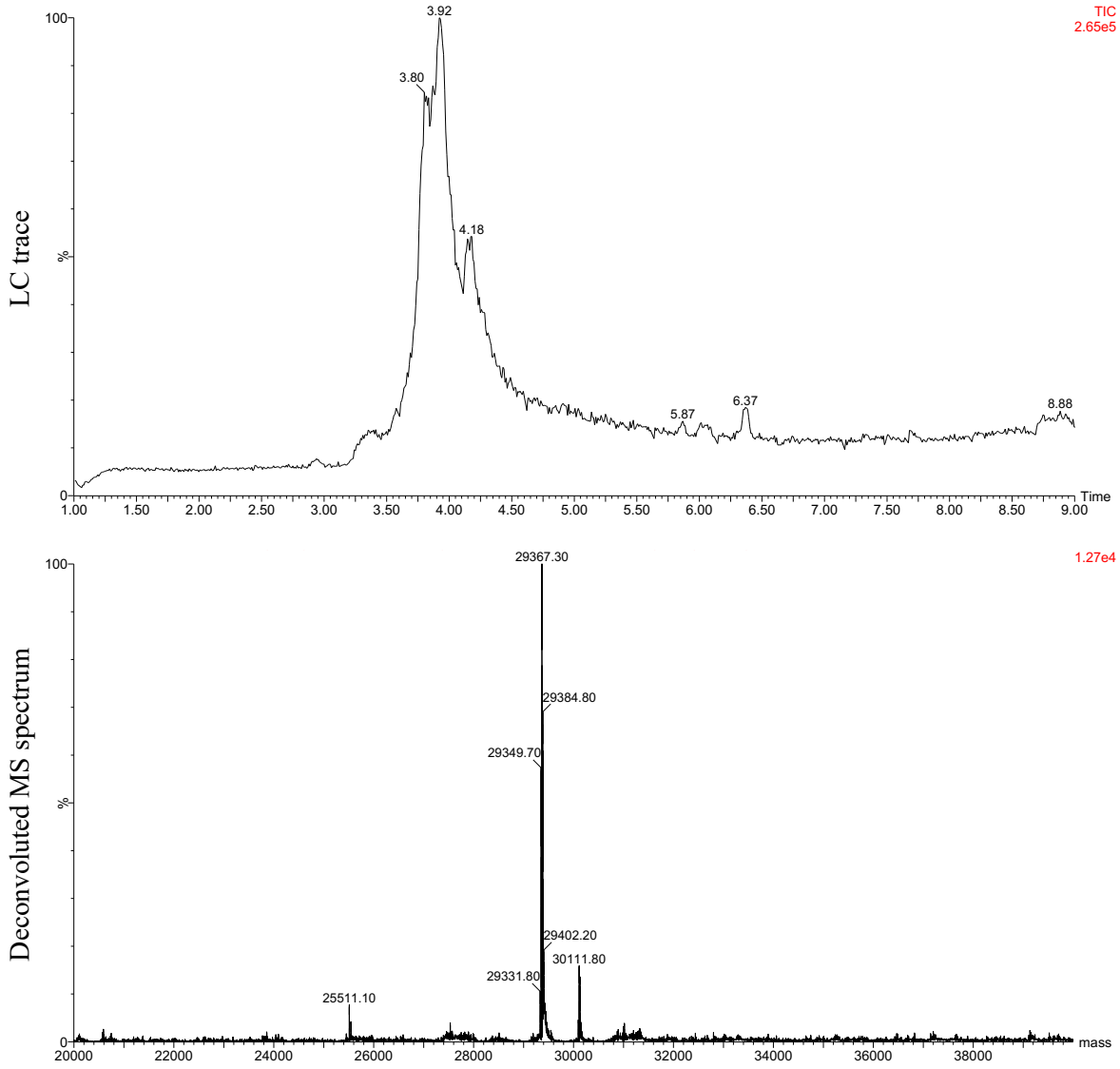

Supplementary Figure S24: HPLC-QTOF-MS traces of the tz-ADC 48h after activation with TCO **12,** showing release of MMAE from the tz-ADC. Incubation was performed in PBS at 37°C.

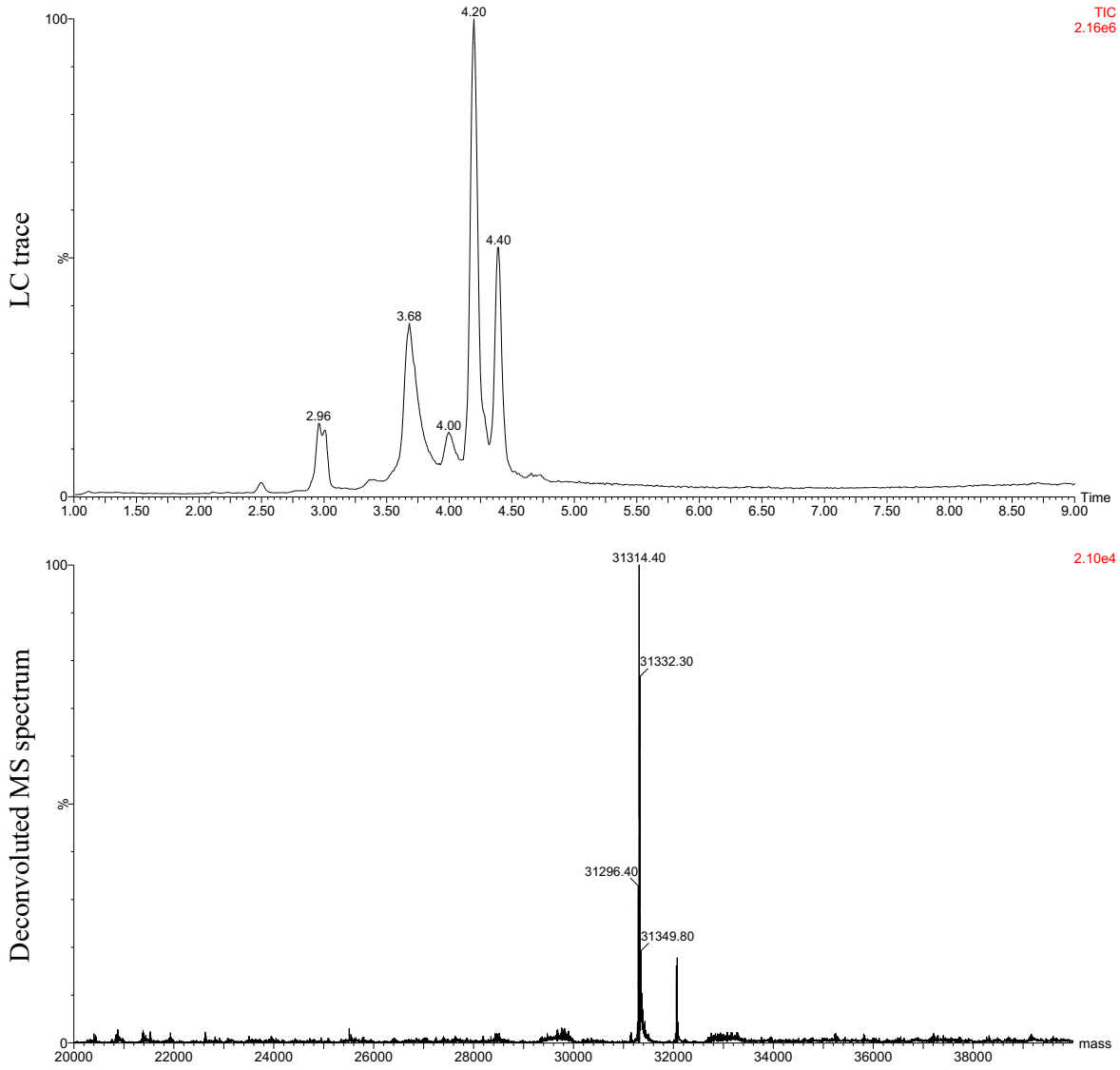

Supplementary Figure S25: HPLC-QTOF-MS traces of the tz-ADC 48h after activation with TCO **13,** showing release of MMAE from the tz-ADC. Incubation was performed in PBS at 37°C.

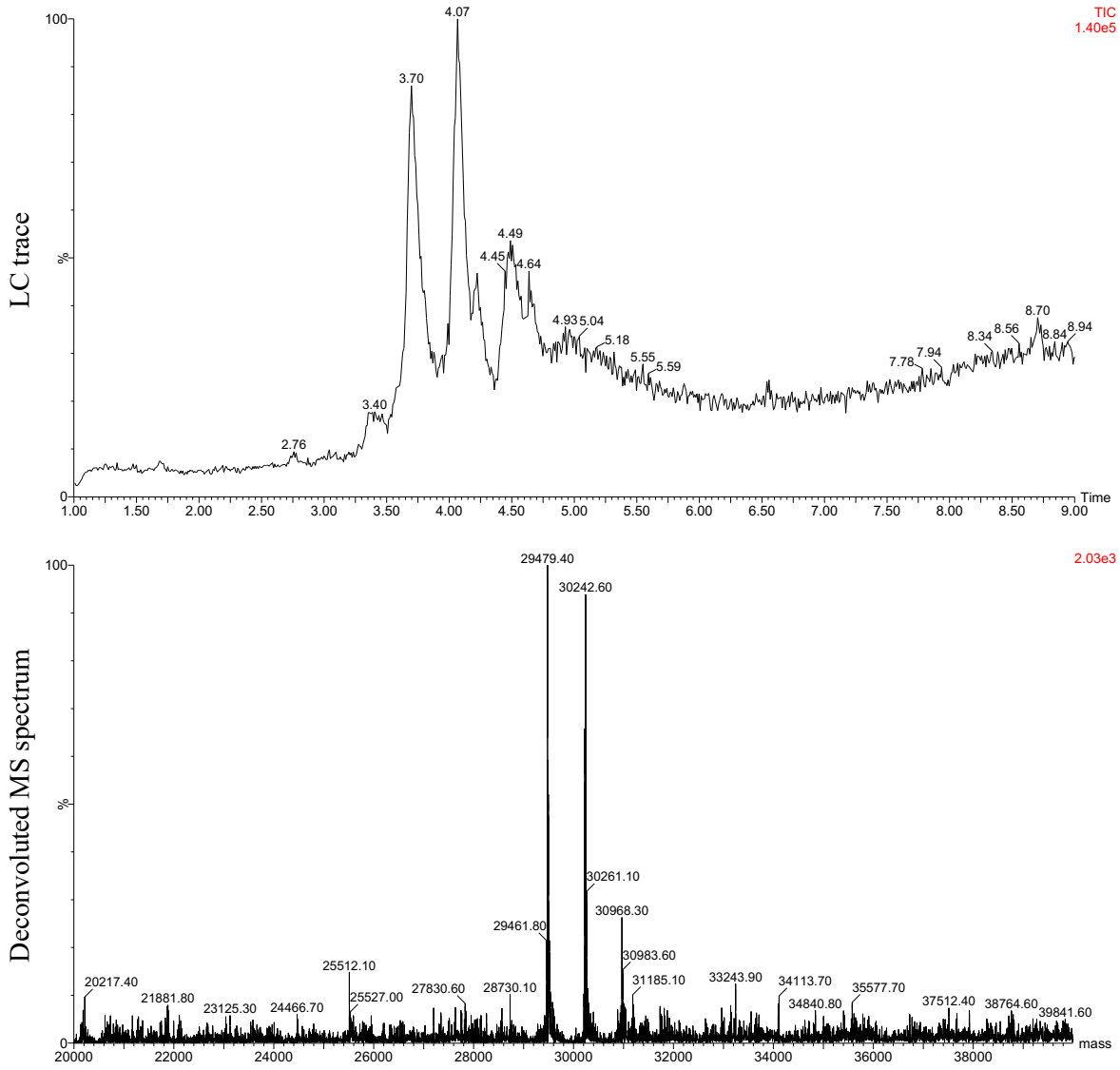

Supplementary Figure S26: HPLC-QTOF-MS traces of the tz-ADC 48h after activation with TCO **14,** showing release of MMAE from the tz-ADC. Incubation was performed in PBS at 37°C.

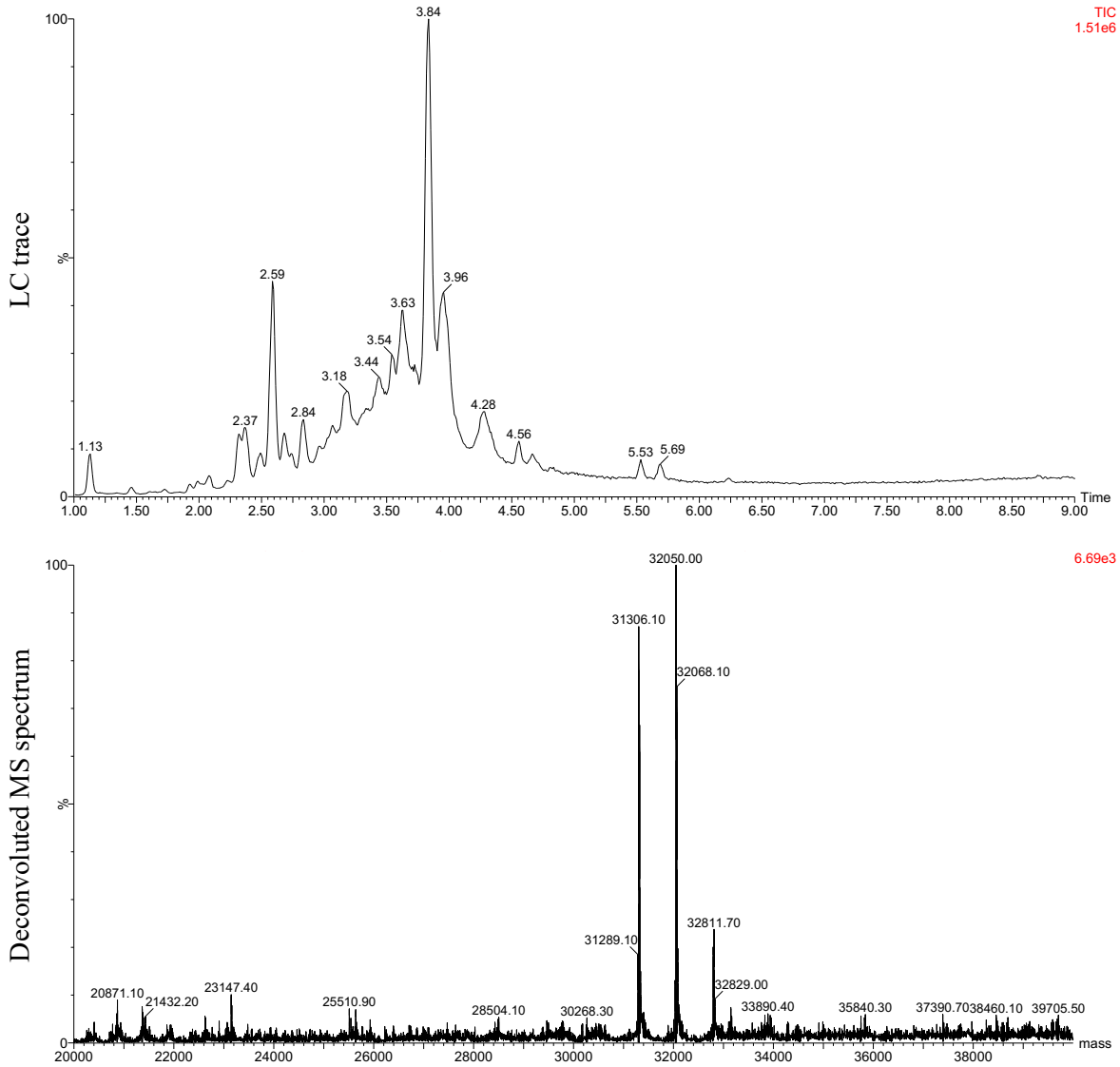

Supplementary Figure S27: HPLC-QTOF-MS traces of the tz-ADC 48h after activation with TCO **15,** showing release of MMAE from the tz-ADC. Incubation was performed in PBS at 37°C.

S3.6 Cytotoxicity assay

Supplementary Table S3: In vitro cytotoxicity assay: EC50 (half-maximal effective concentration) values in LS174T tumour cells.

	IC50 (nM):	+/-
tz-ADC + 15	0.6716	0.1412
MMAE	0.8457	0.23775
tz-ADC	67.57	23.775

S3.7 Radiolabelling 13 and 15

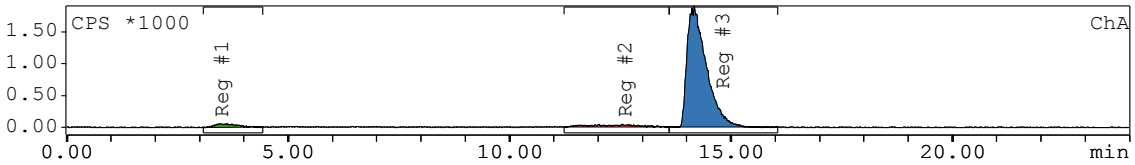

Supplementary Figure S28: HPLC γ-trace of axial-TCO-PEG-DOTA **13** after labeling.

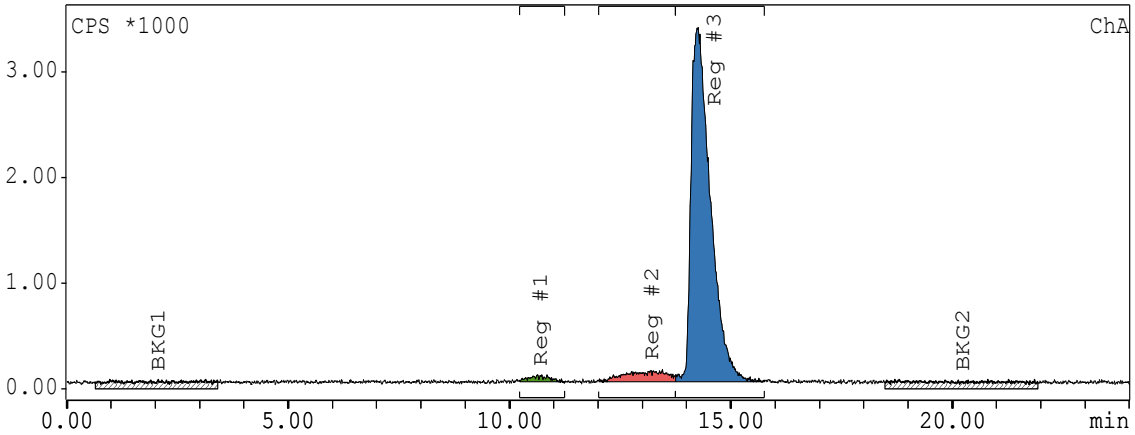

Supplementary Figure S29: HPLC γ-trace of s-TCO-PEG-DOTA **15** after labeling and purification.

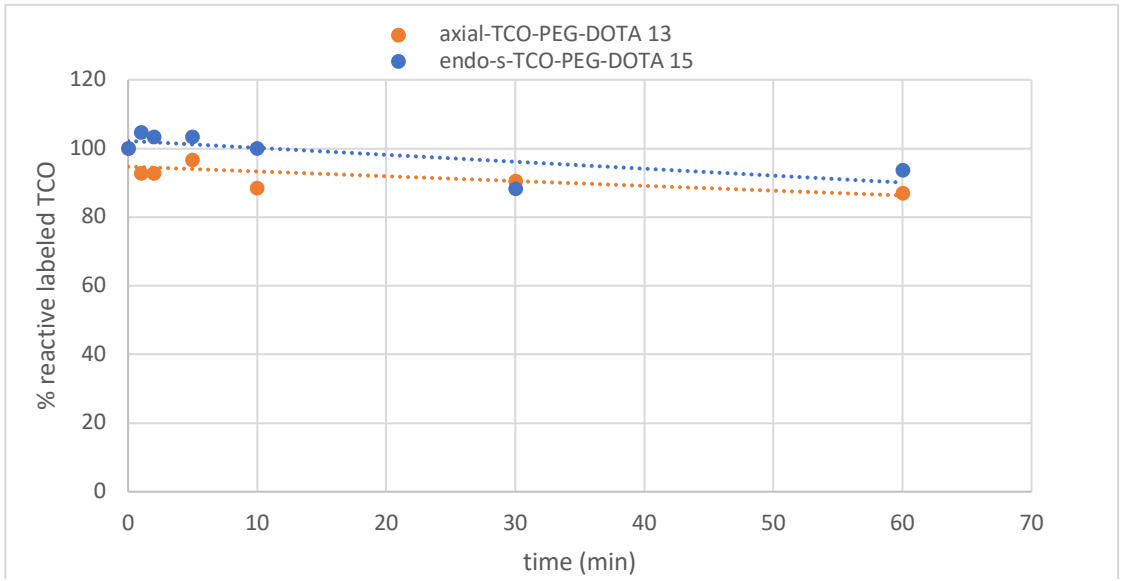

Supplementary Figure S30: Stability of ^{111}In-labeled axial-TCO-PEG-DOTA **13** and ^{111}In-labeled endo-s-TCO-PEG-DOTA **15**, investigated by incubating the labeled probe in PBS at 37°C and at various time points, reacting aliquots with a slight excess of **tz-ADC**. SDS-PAGE analysis was used to quantify the % ADC-reactive probe in time.

S3.8 Reaction kinetics between tetrazines and *trans*-cyclooctenes

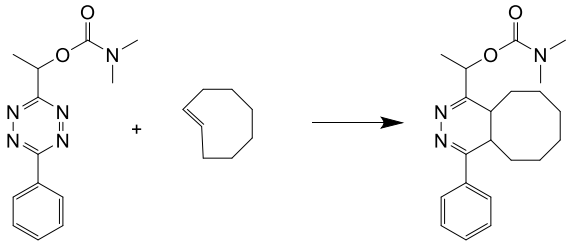

11 **12**

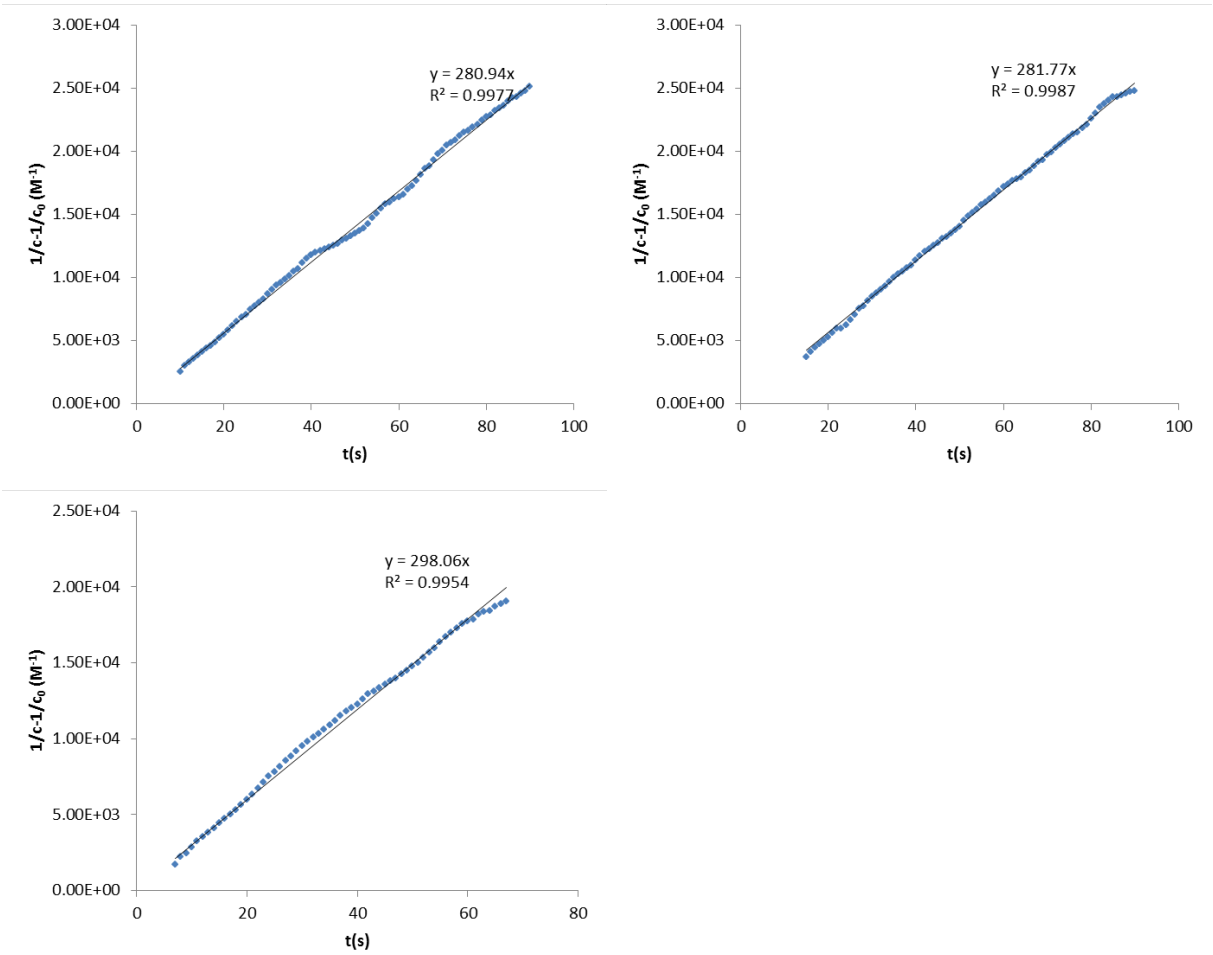

Supplementary Figure S31: Kinetic plots (N=3) of reaction of **11** with **12** in 25% acetonitrile/PBS at 20 °C, concentration of **11** and **12** is 0.167 mM, calculated $k_2 = 287 \pm 10\ M^{-1}\ s^{-1}$.

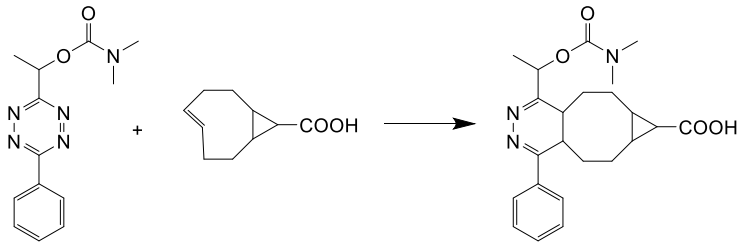

11 **14**

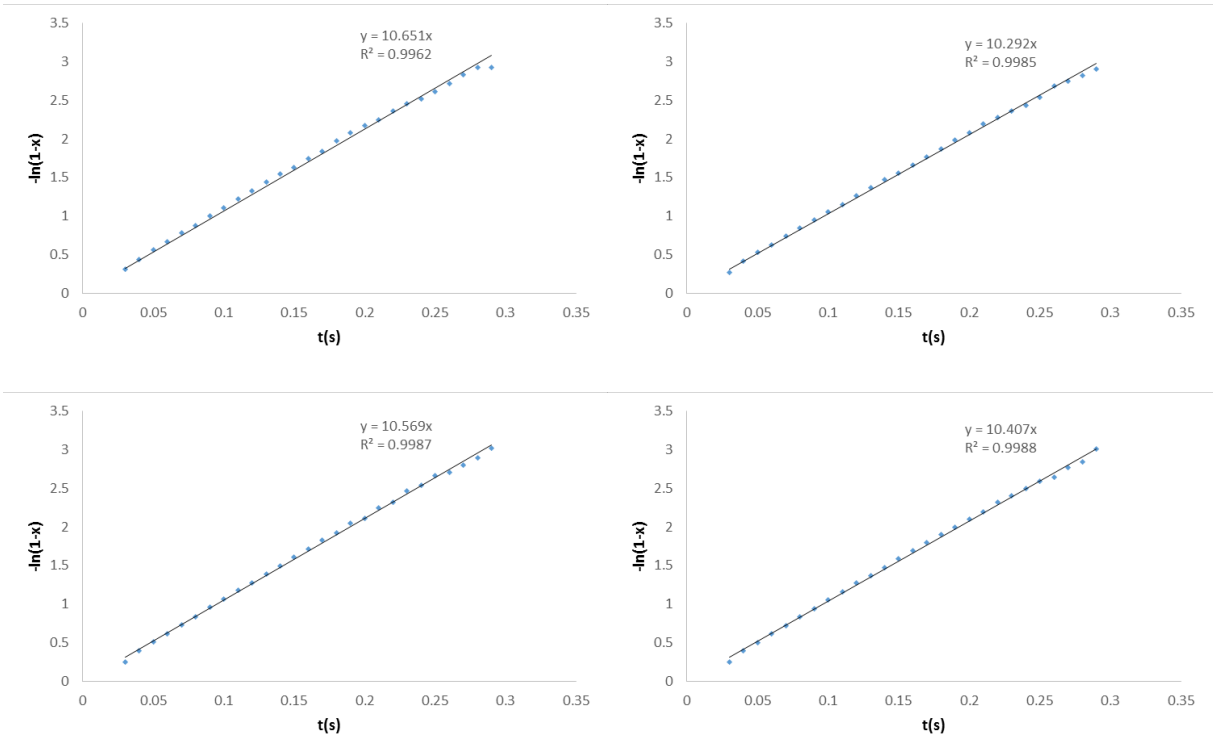

Supplementary Figure S32: Kinetic plots (N=4) of reaction of **11** with **14** in 25% acetonitrile/PBS at 20 °C, concentration of **11** is 0.050 mM and **14** is 0.439 mM, calculated $k_2 = 23.8*10^3 \pm 0.4*10^3$ M^{-1} s^{-1}.

S4 Spectra

S4.1 NMR spectral data, HPLC-PDA/MS and GC-MS chromatograms and mass data

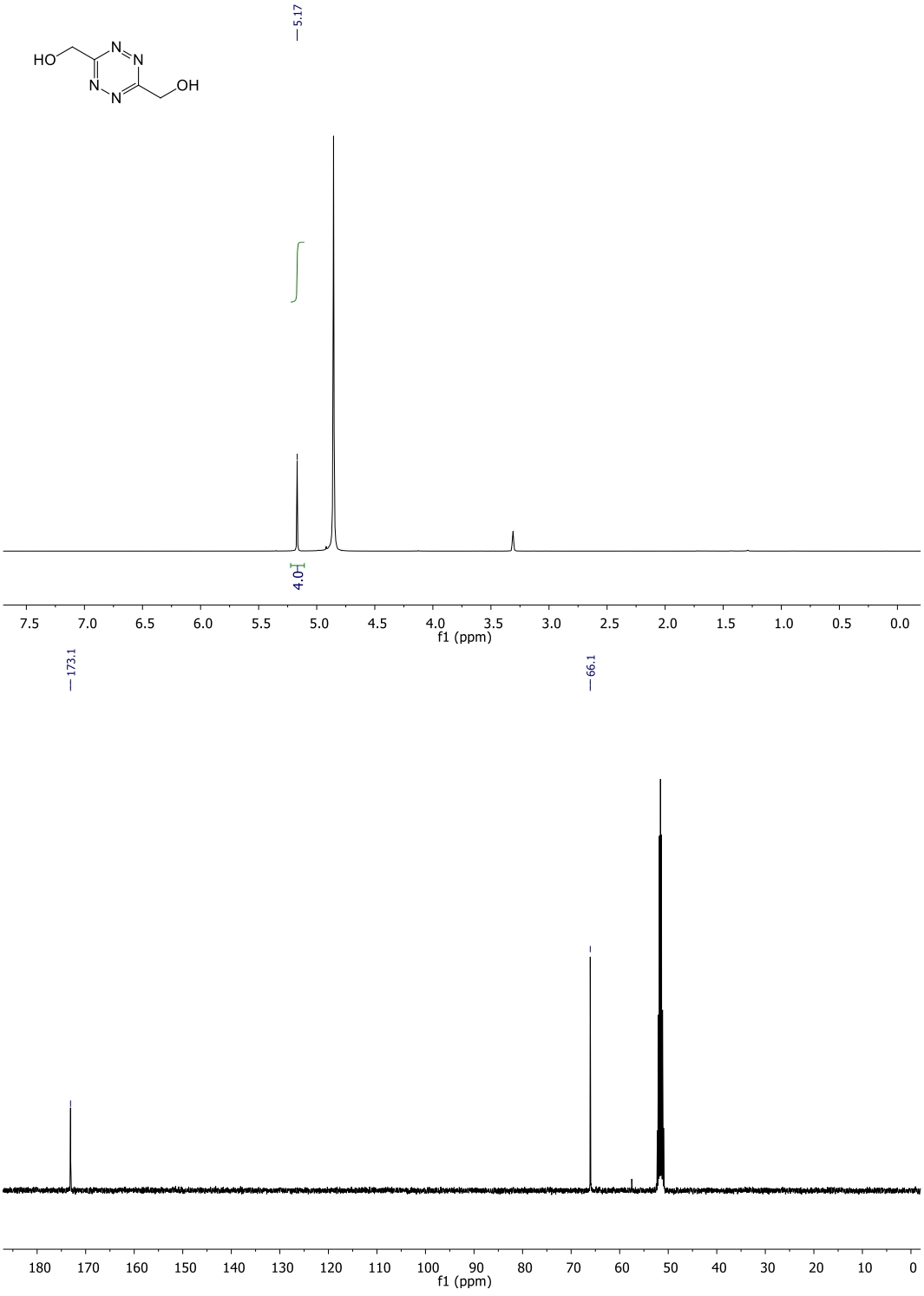

Supplementary Figure S33: ^{1}H- and ^{13}C-NMR spectra (MeOD) of (1,2,4,5-tetrazine-3,6-diyl)dimethanol (**S1**)

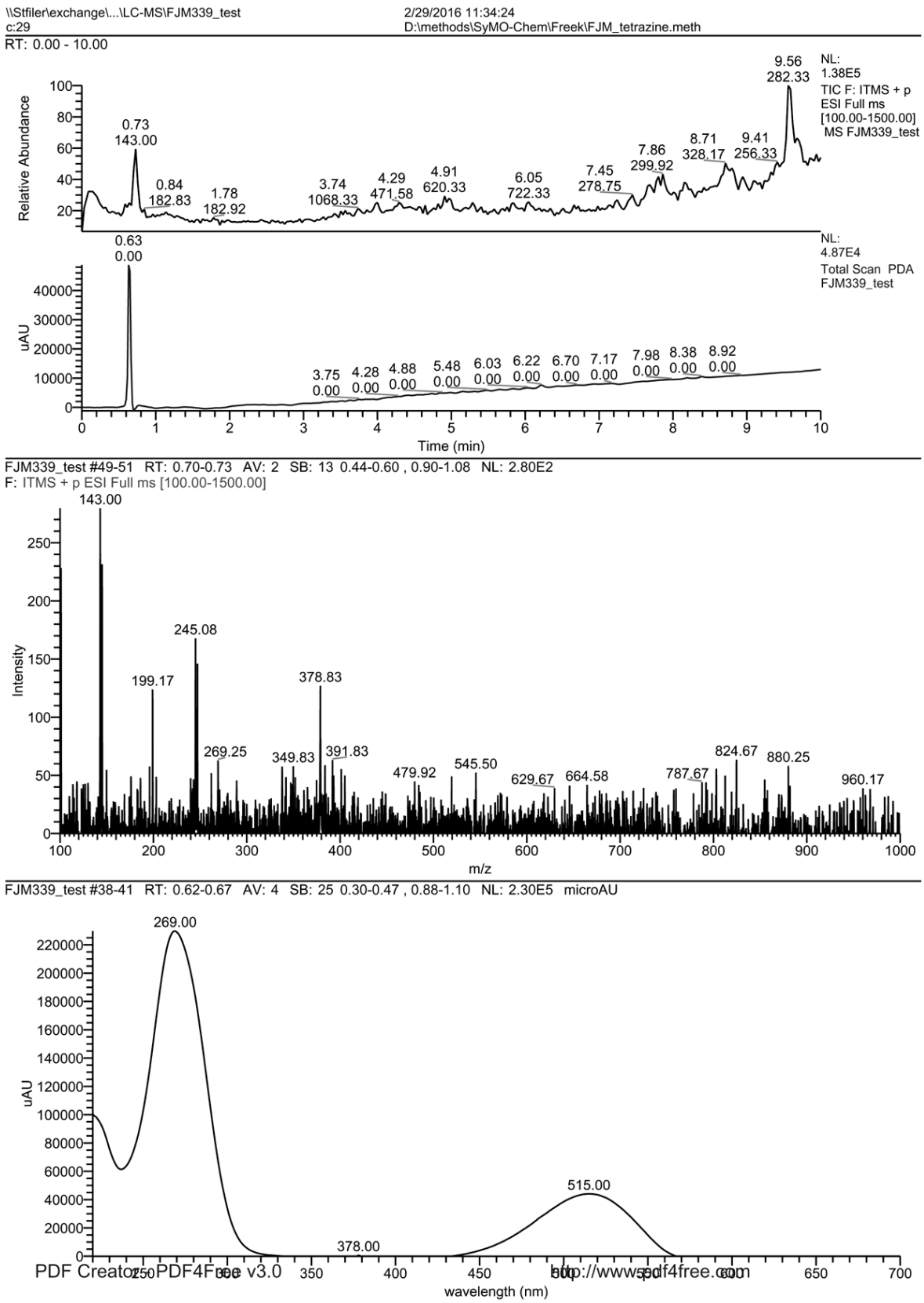

Supplementary Figure S34: HPLC-MS/PDA analysis of (1,2,4,5-tetrazine-3,6-diyl)dimethanol (**S1**)

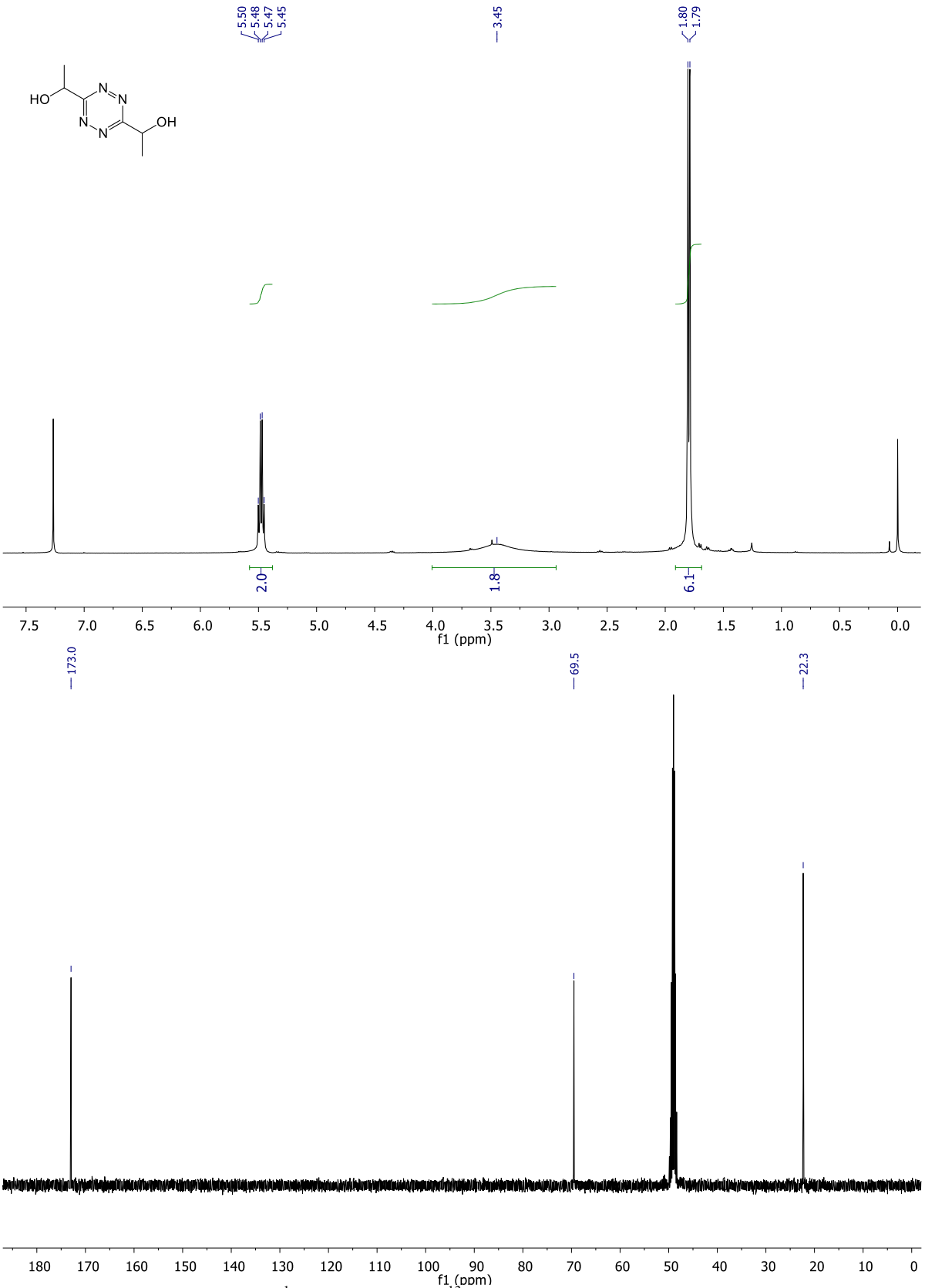

Supplementary Figure S35: ^{1}H- ($CDCl_3$) and ^{13}C-NMR (MeOD) spectra of 1,1'-(1,2,4,5-tetrazine-3,6-diyl)diethanol (**S2**)

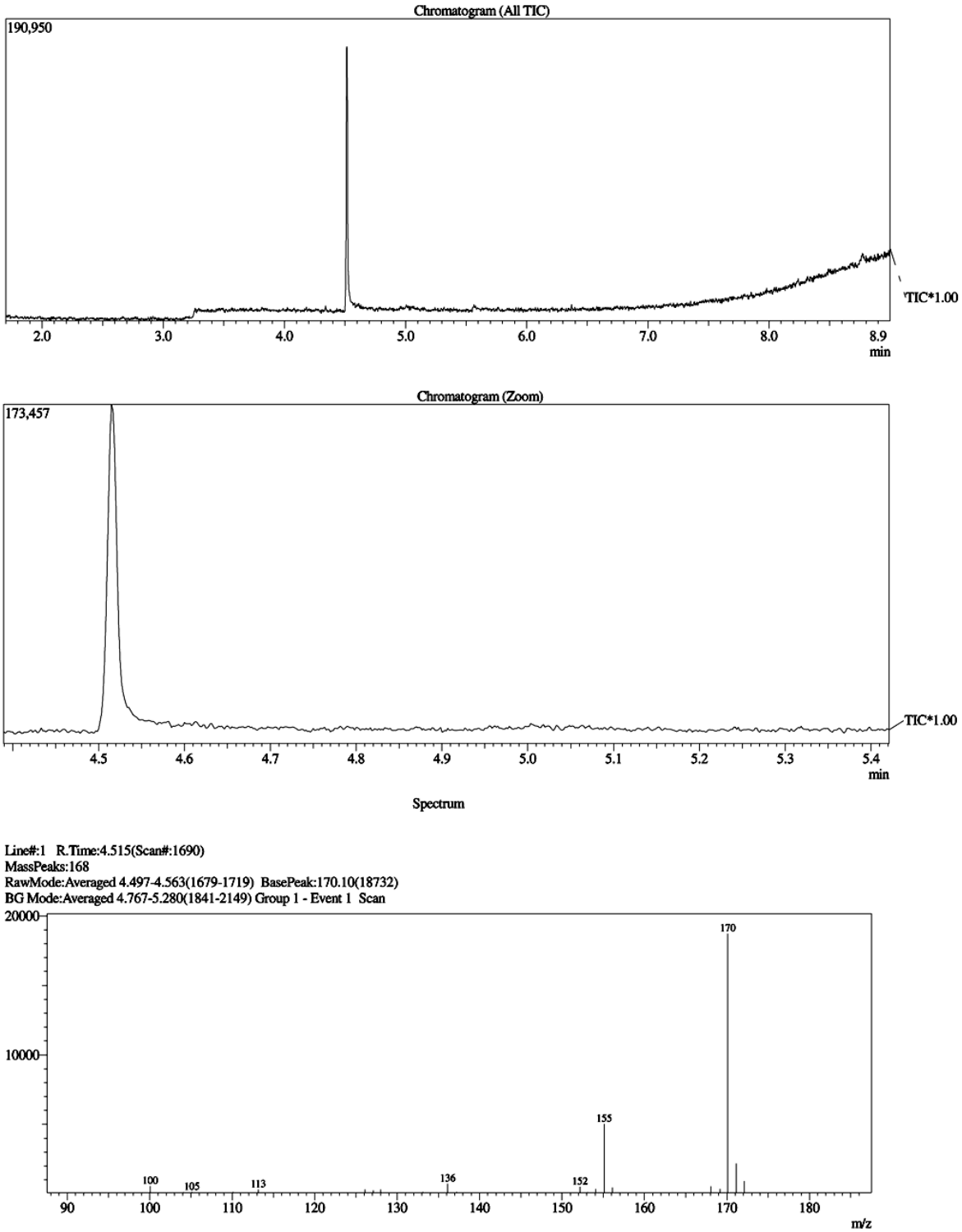

Supplementary Figure S36: GC-MS chromatogram of 1,1'-(1,2,4,5-tetrazine-3,6-diyl)diethanol (**S2**)

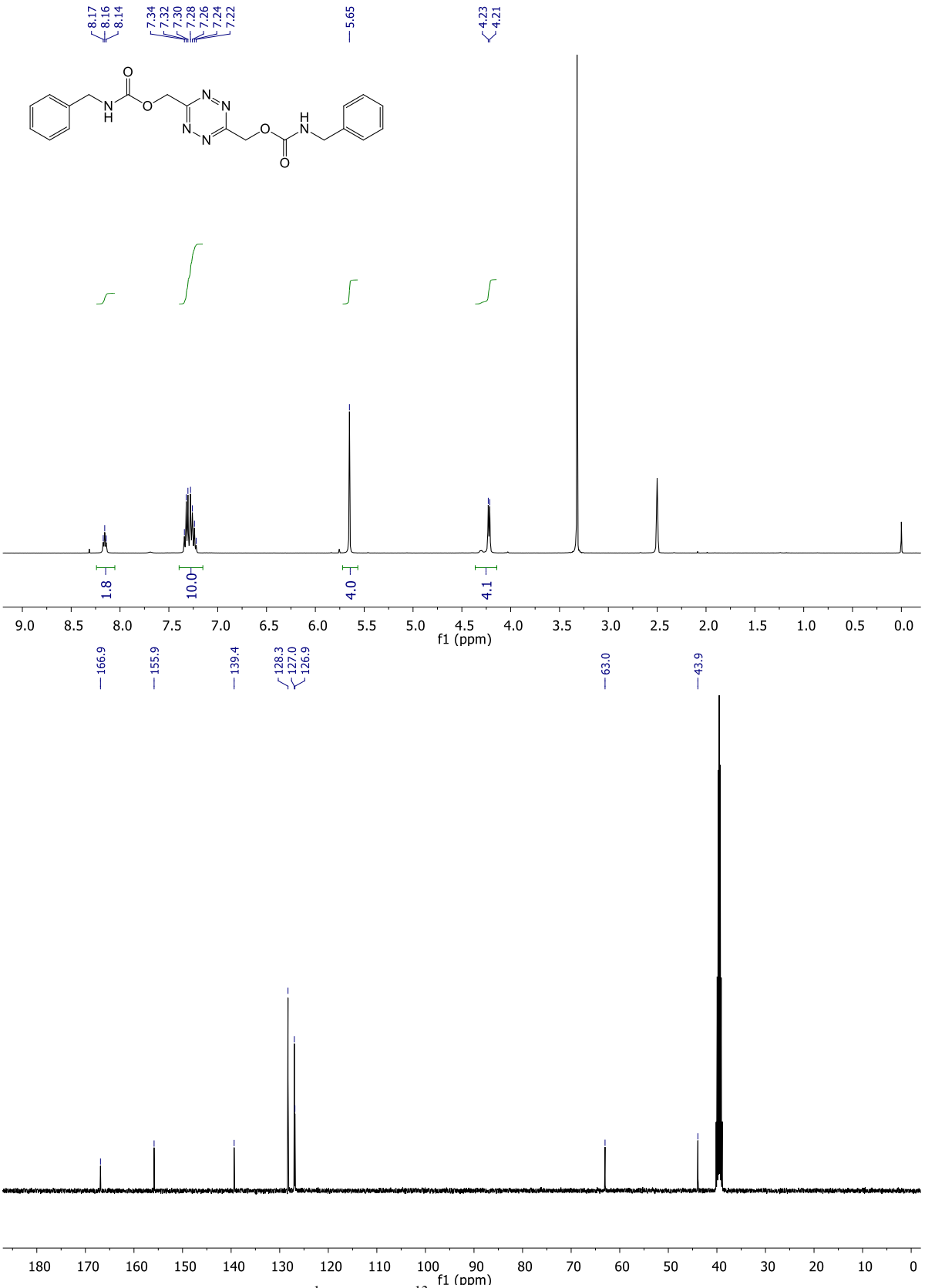

Supplementary Figure S37: ^{1}H- and ^{13}C-NMR spectra (d6-DMSO) of (1,2,4,5-tetrazine-3,6-diyl)bis(methylene) bis(benzylcarbamate) (**1**)

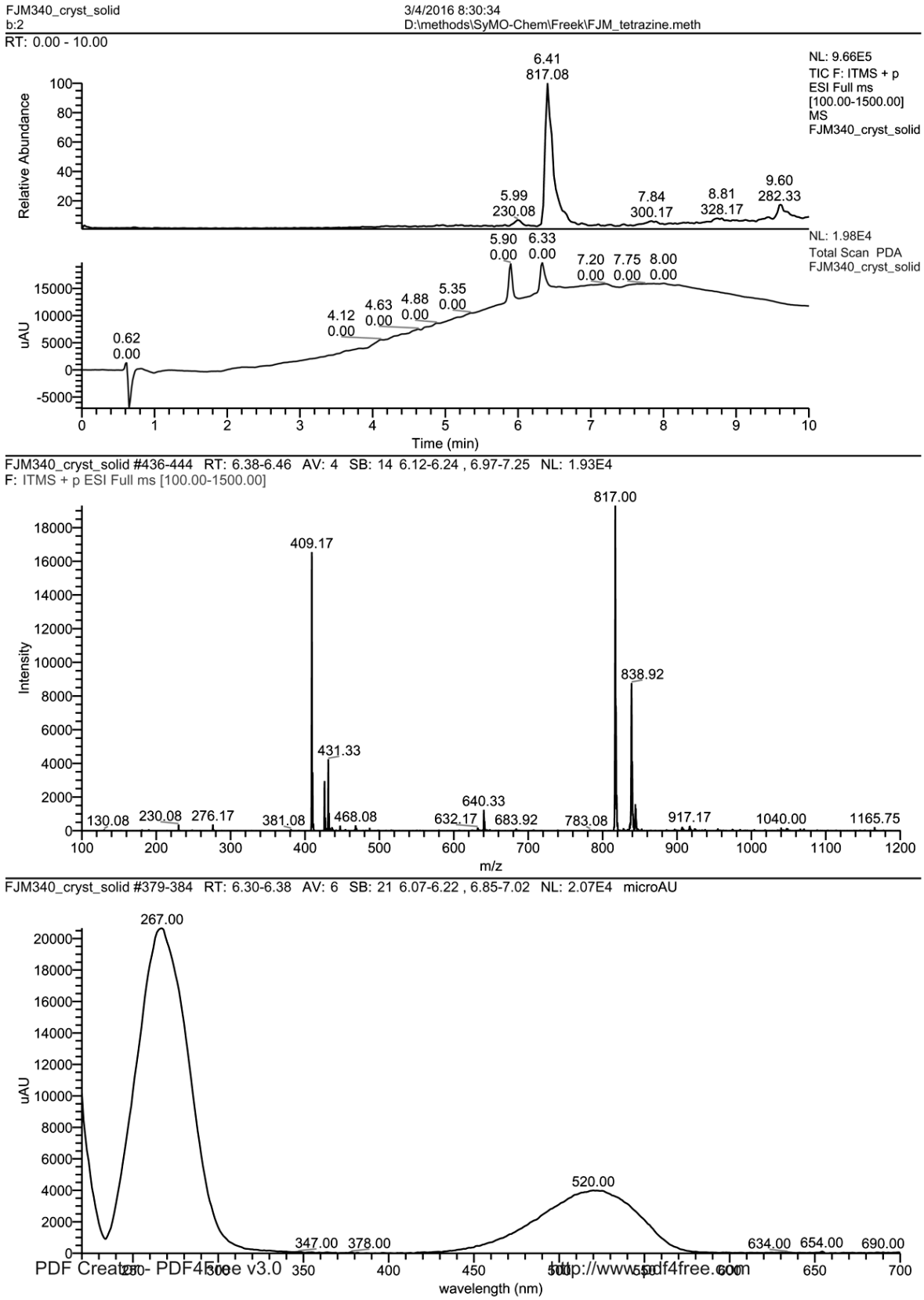

Supplementary Figure S38: HPLC-MS/PDA analysis of (1,2,4,5-tetrazine-3,6-diyl)bis(methylene) bis(benzylcarbamate) (**1**)

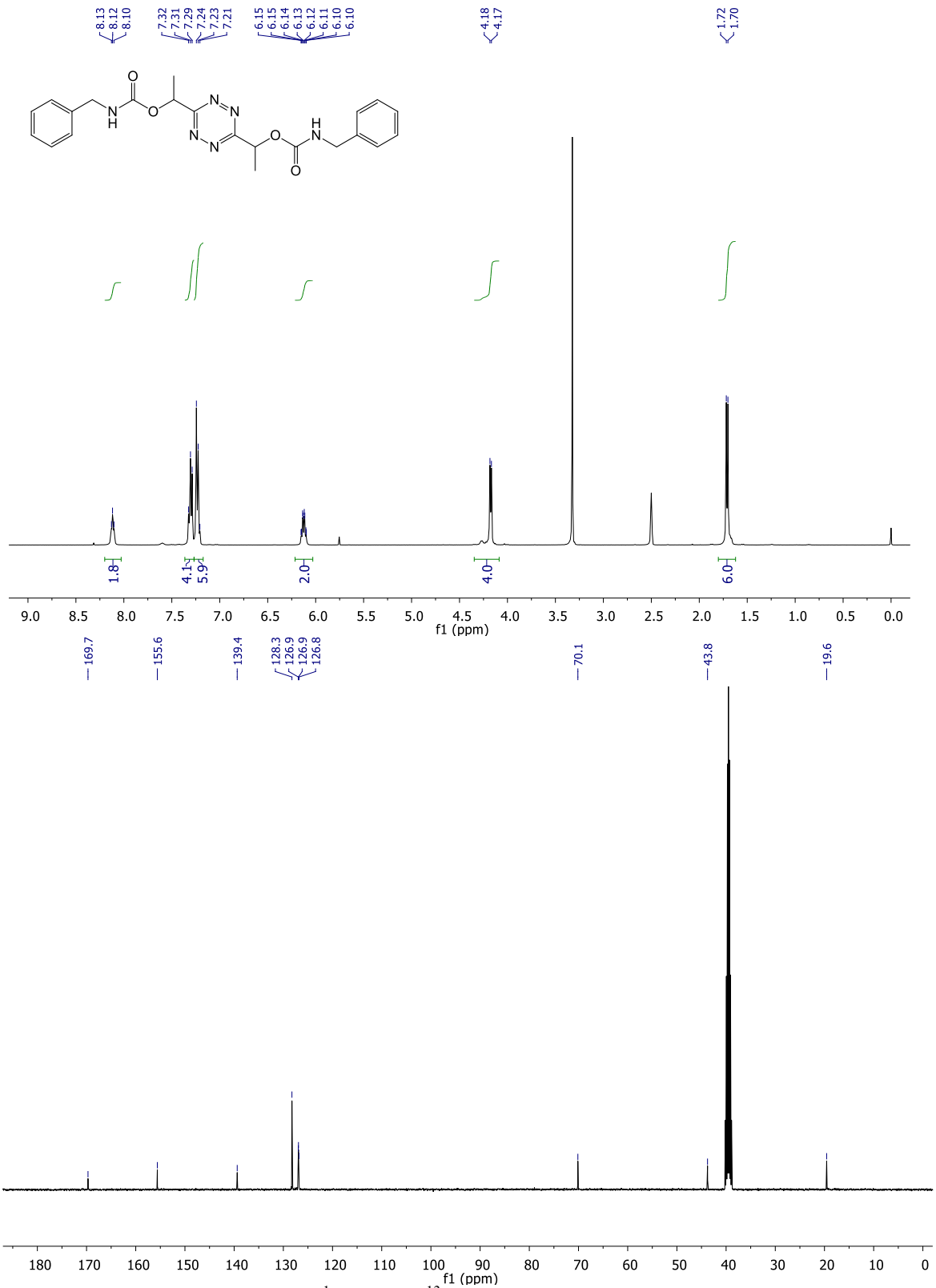

Supplementary Figure S39: ^{1}H- and ^{13}C-NMR spectra (d6-DMSO) of (1,2,4,5-Tetrazine-3,6-diyl)bis(ethane-1,1-diyl) bis(benzylcarbamate) (**2**)

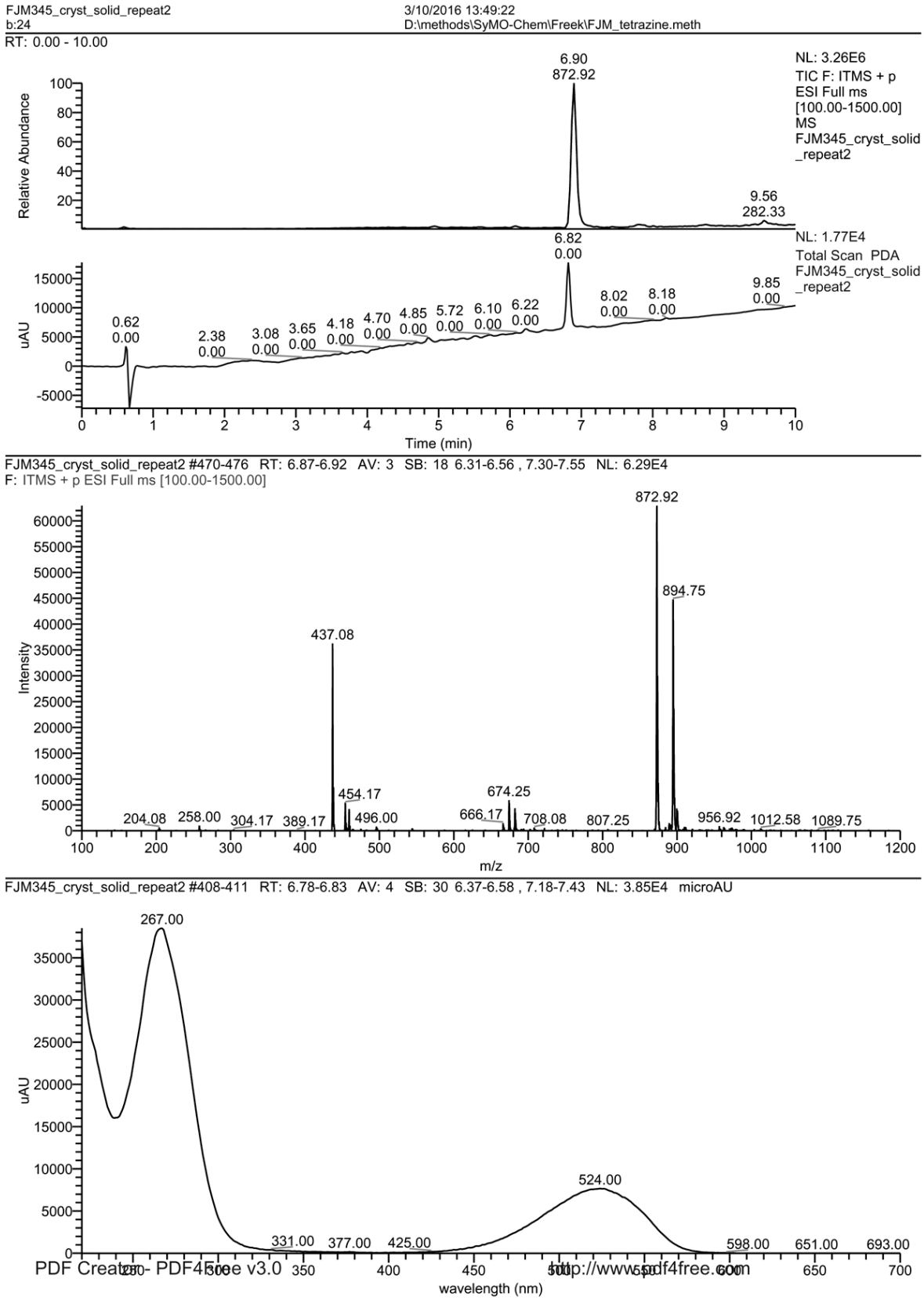

Supplementary Figure S40: HPLC-MS/PDA analysis of (1,2,4,5-Tetrazine-3,6-diyl)bis(ethane-1,1-diyl) bis(benzylcarbamate) (**2**)

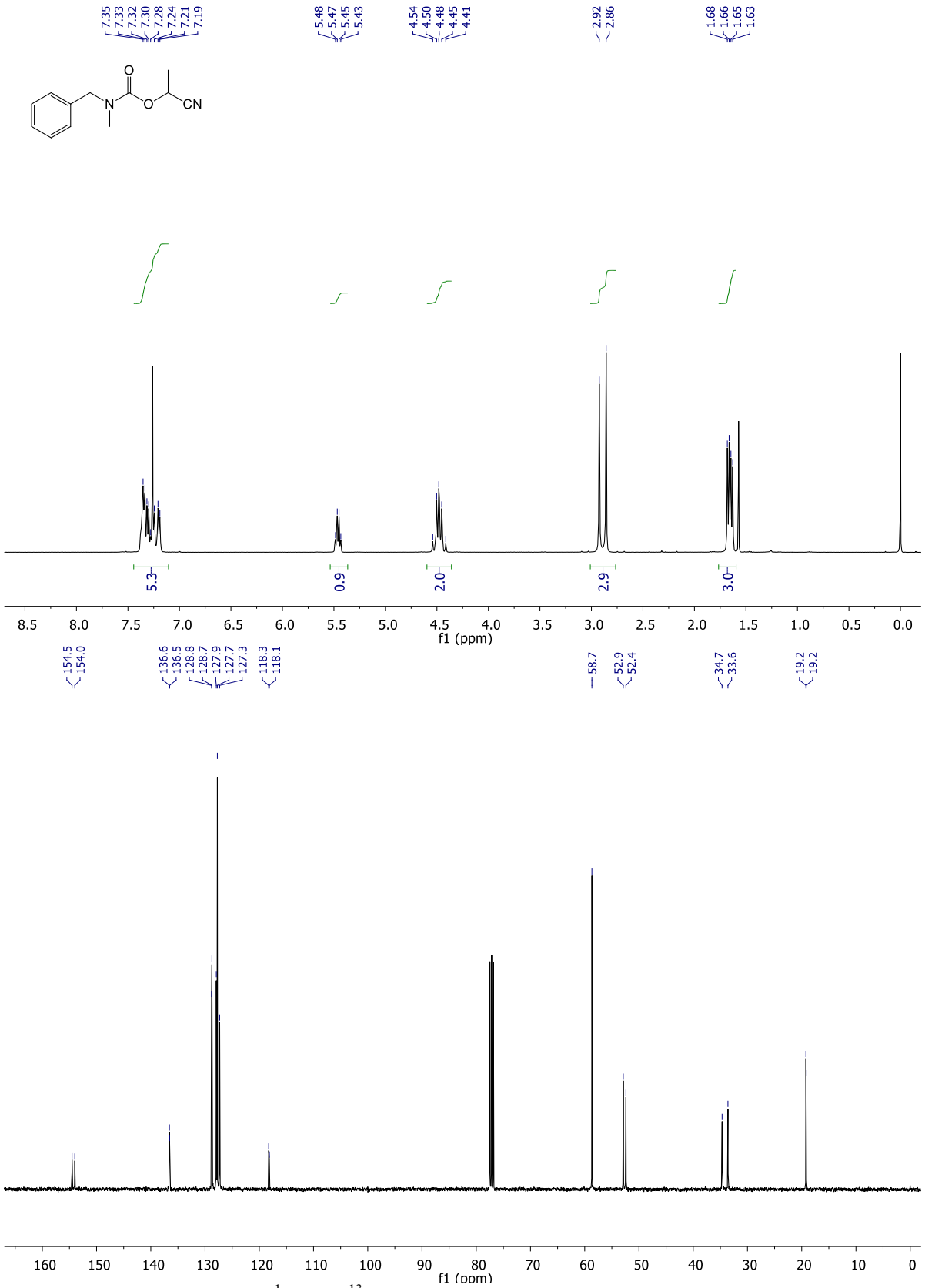

Supplementary Figure S41: ^{1}H- and ^{13}C-NMR spectra ($CDCl_3$) of 1-cyanoethyl benzyl(methyl)carbamate (**S3**)

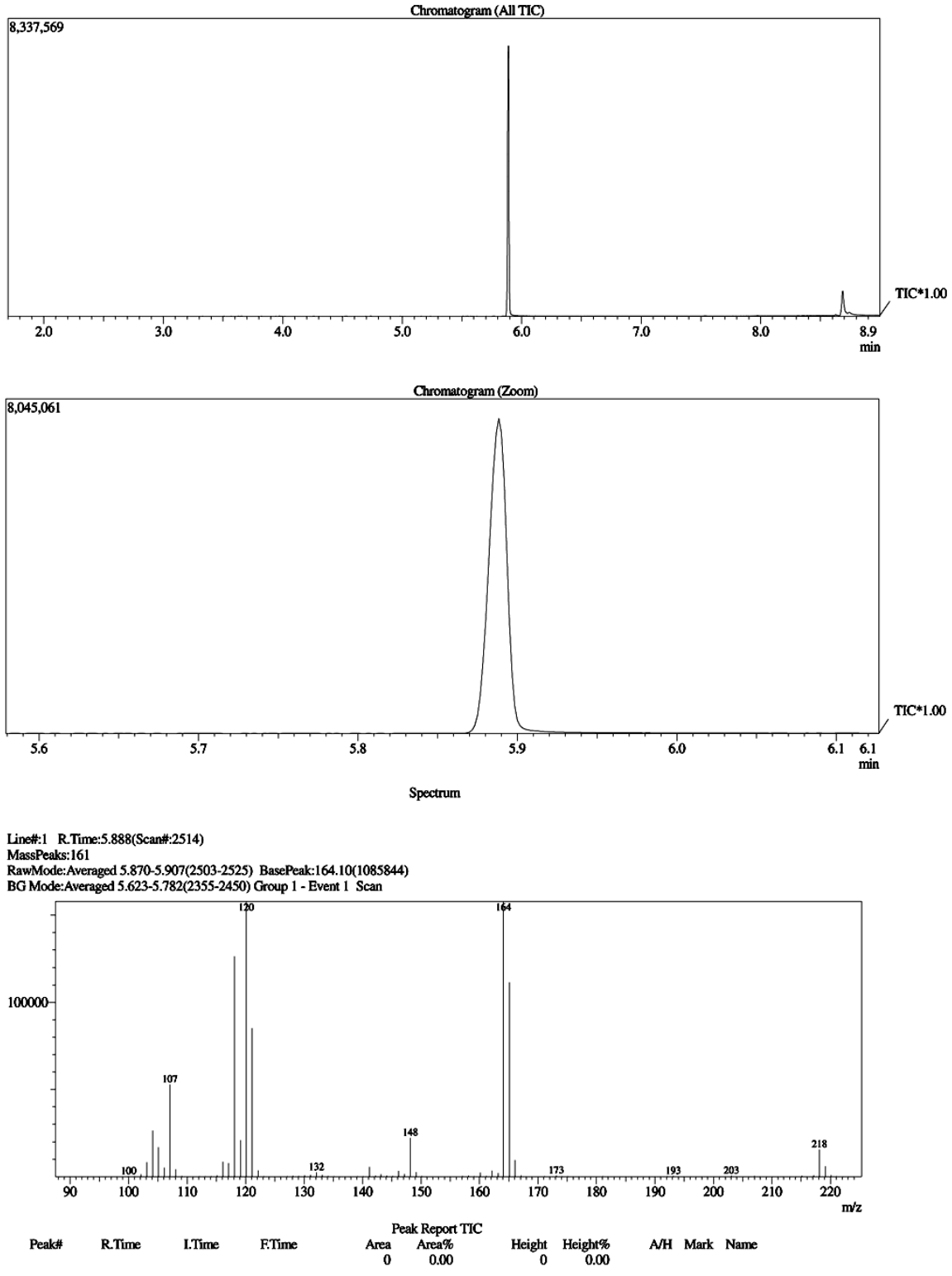

Supplementary Figure S42: GC-MS chromatogram of 1-cyanoethyl benzyl(methyl)carbamate (**S3**)

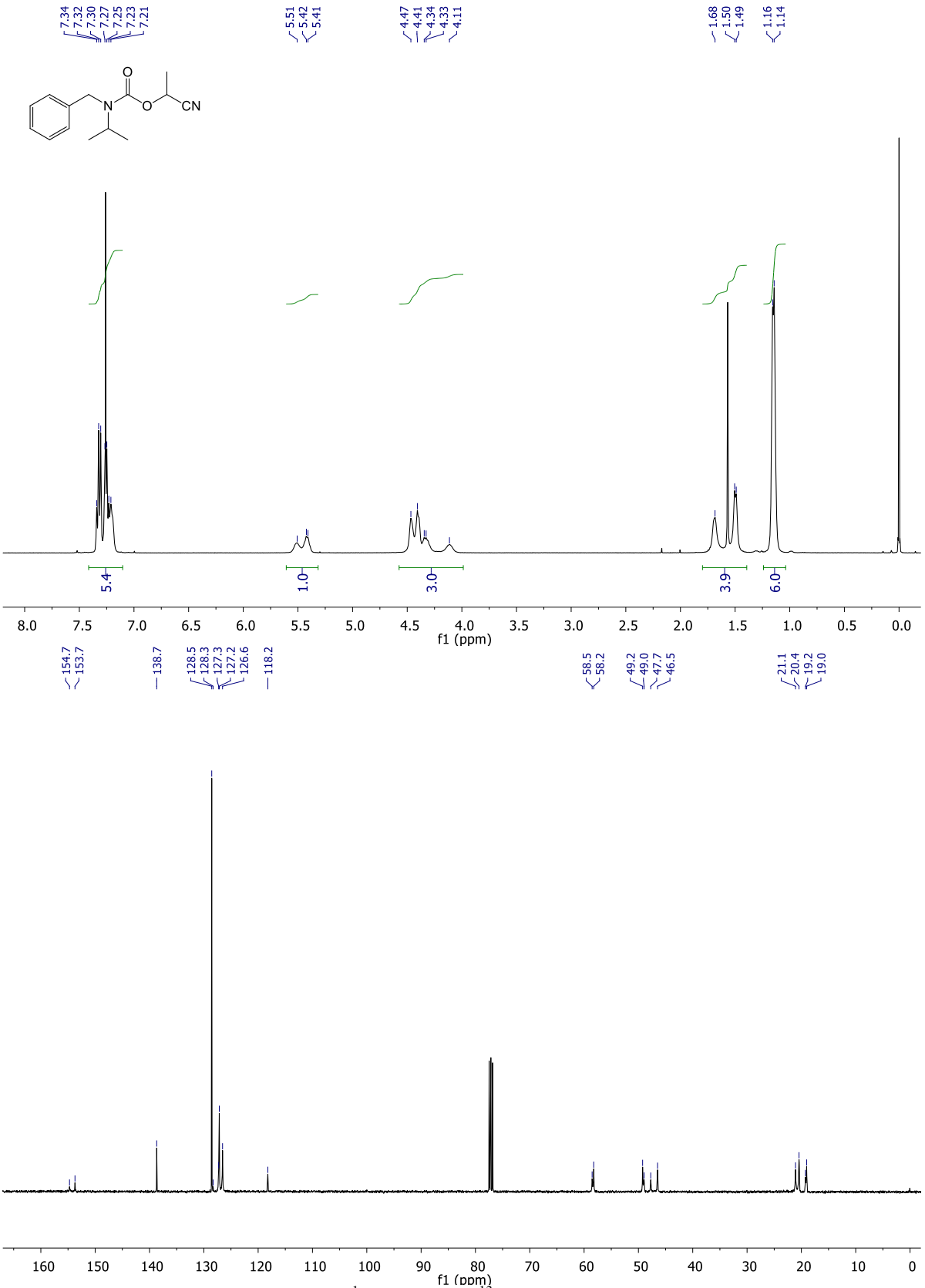

Supplementary Figure S43: ^{1}H- and ^{13}C-NMR spectra ($CDCl_3$) of 1-cyanoethyl benzyl(isopropyl)carbamate (**S4**)

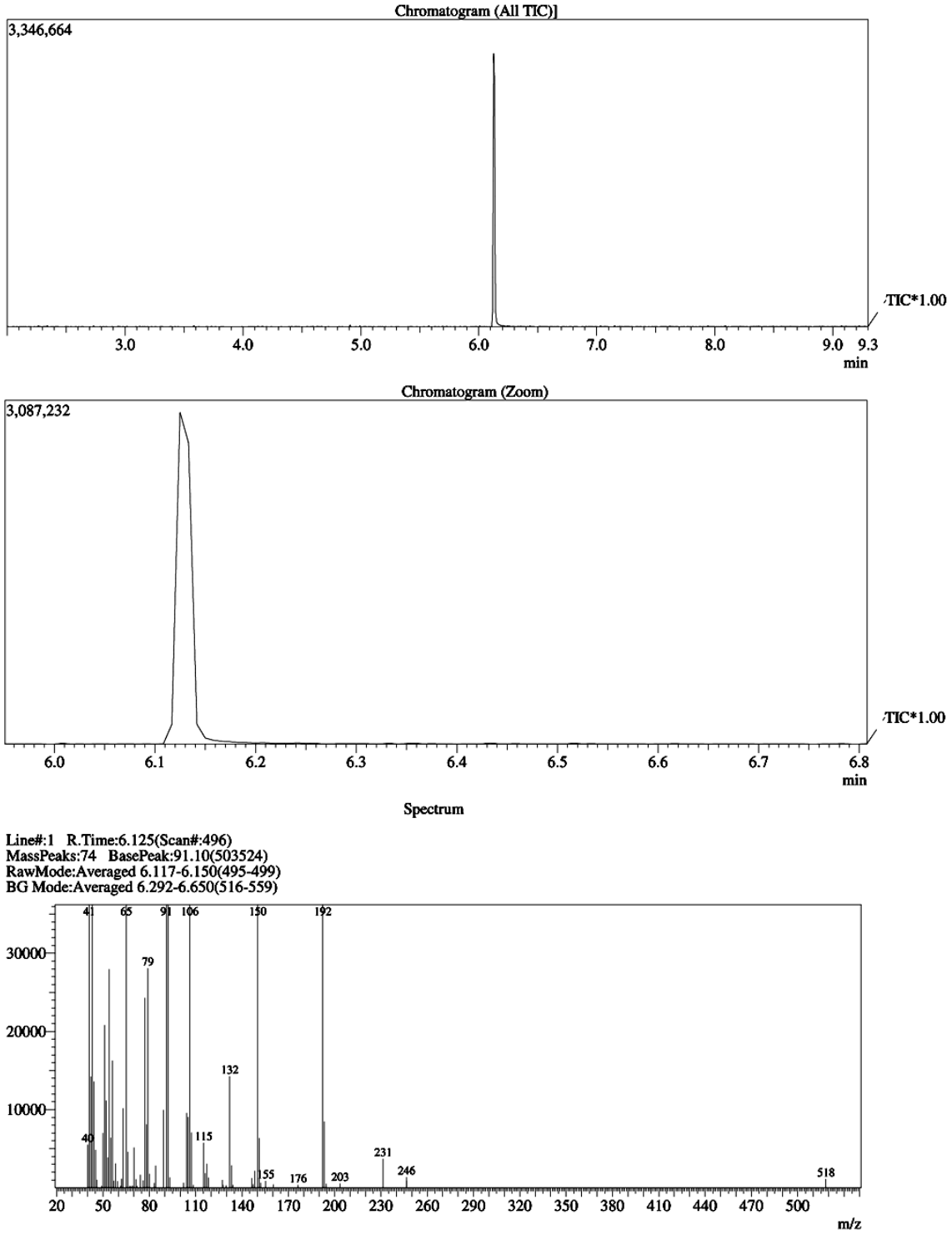

Supplementary Figure S44: GC-MS chromatogram of 1-cyanoethyl benzyl(isopropyl)carbamate (**S4**)

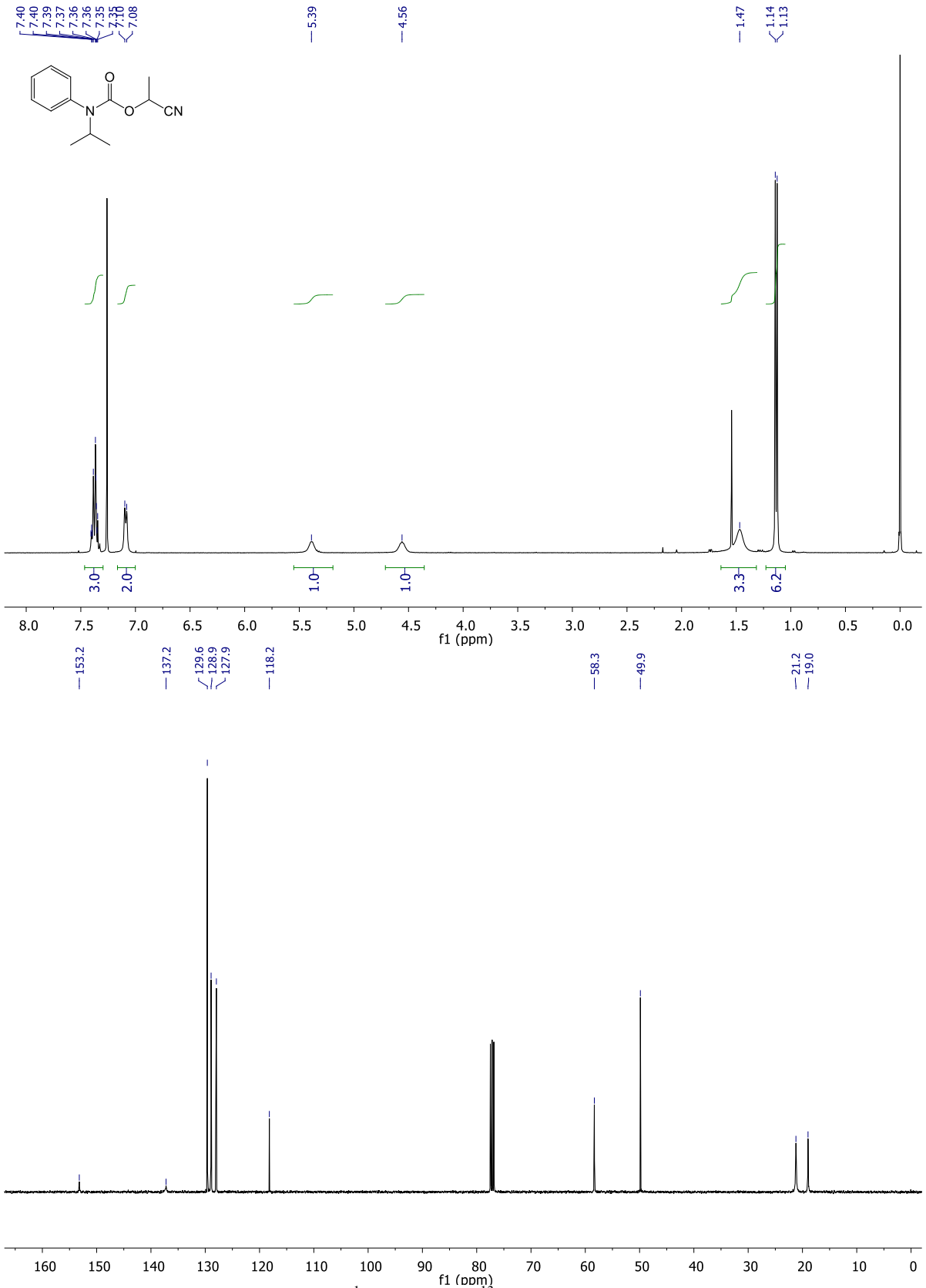

Supplementary Figure S45: ^{1}H- and ^{13}C-NMR spectra ($CDCl_3$) of 1-cyanoethyl isopropyl(phenyl)carbamate (**S5**)

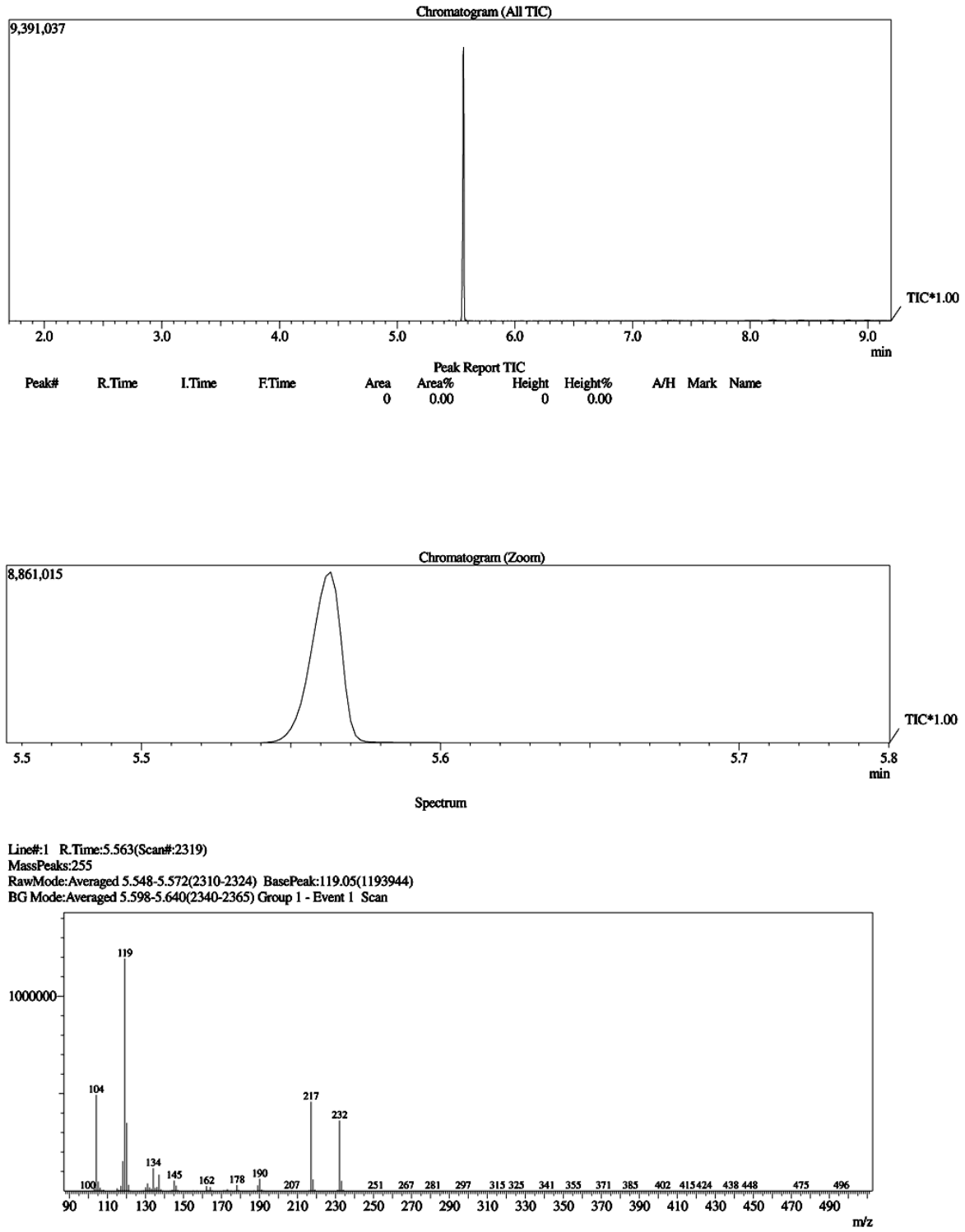

Supplementary Figure S46: GC-MS chromatogram of 1-cyanoethyl isopropyl(phenyl)carbamate (**S5**)

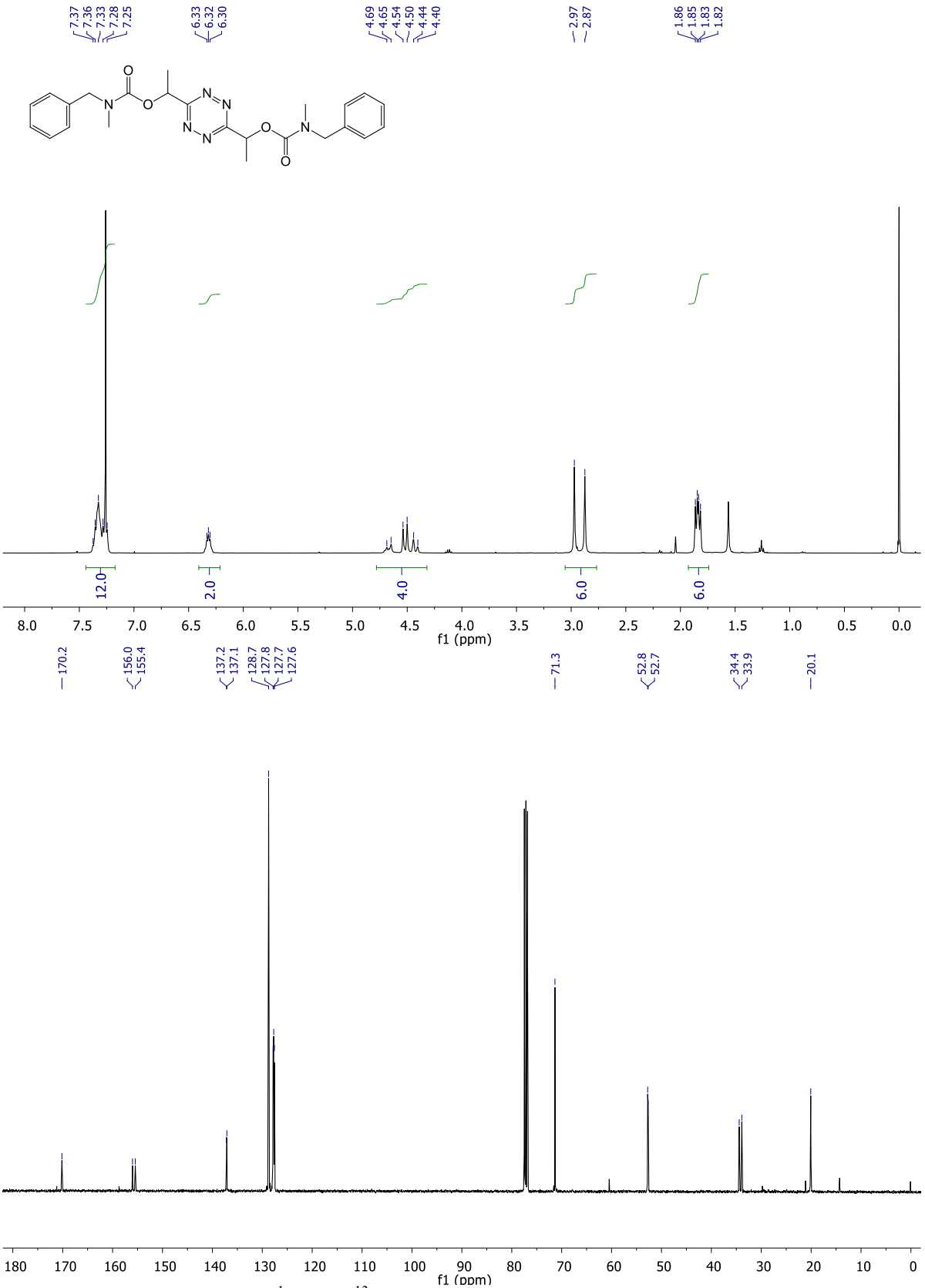

Supplementary Figure S47: ^{1}H- and ^{13}C-NMR spectra ($CDCl_3$) of (1,2,4,5-tetrazine-3,6-diyl)bis(ethane-1,1-diyl) bis(benzyl(methyl)carbamate) (**3**)

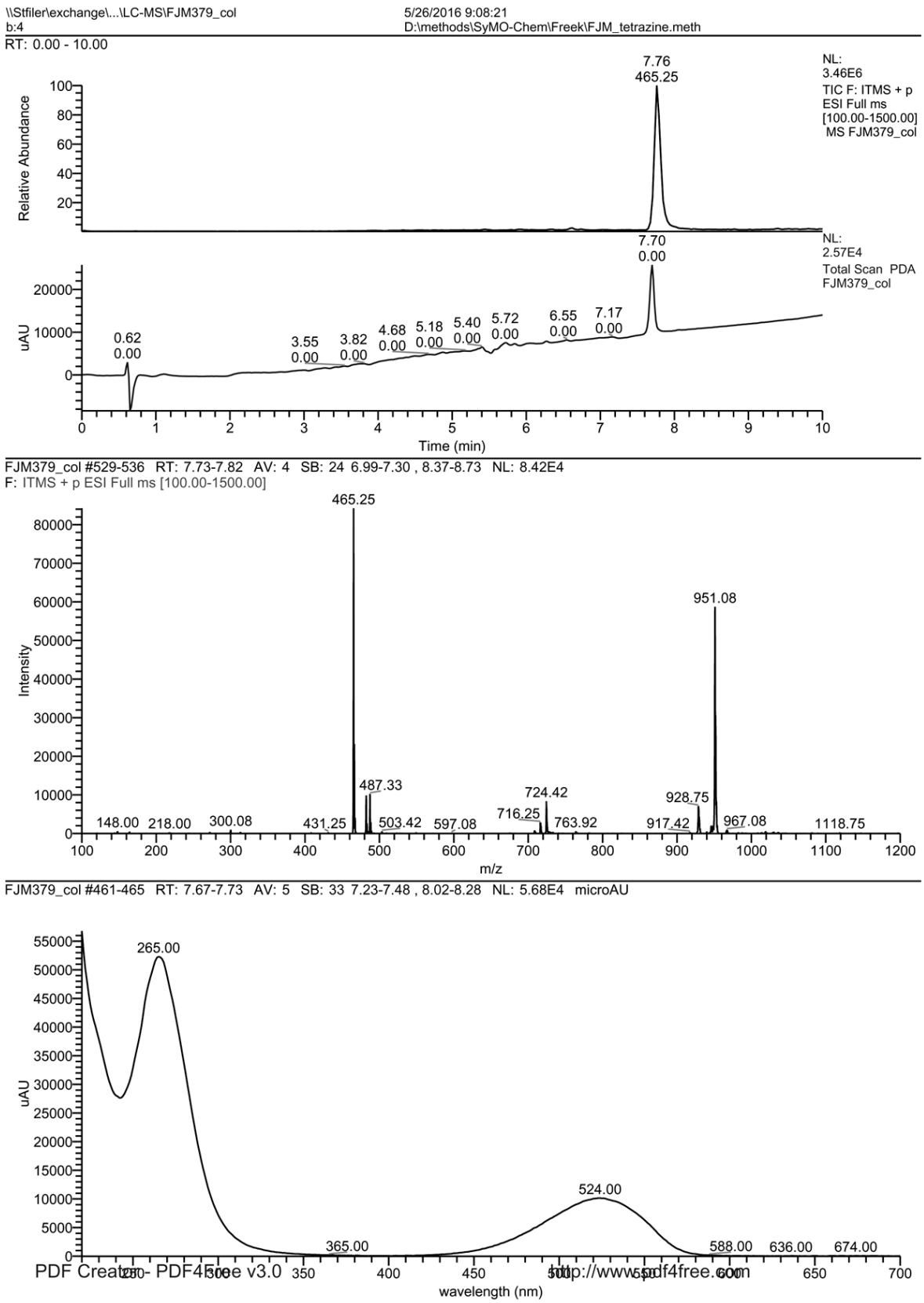

Supplementary Figure S48: HPLC-MS/PDA analysis of (1,2,4,5-tetrazine-3,6-diyl)bis(ethane-1,1-diyl) bis(benzyl(methyl)carbamate) (**3**)

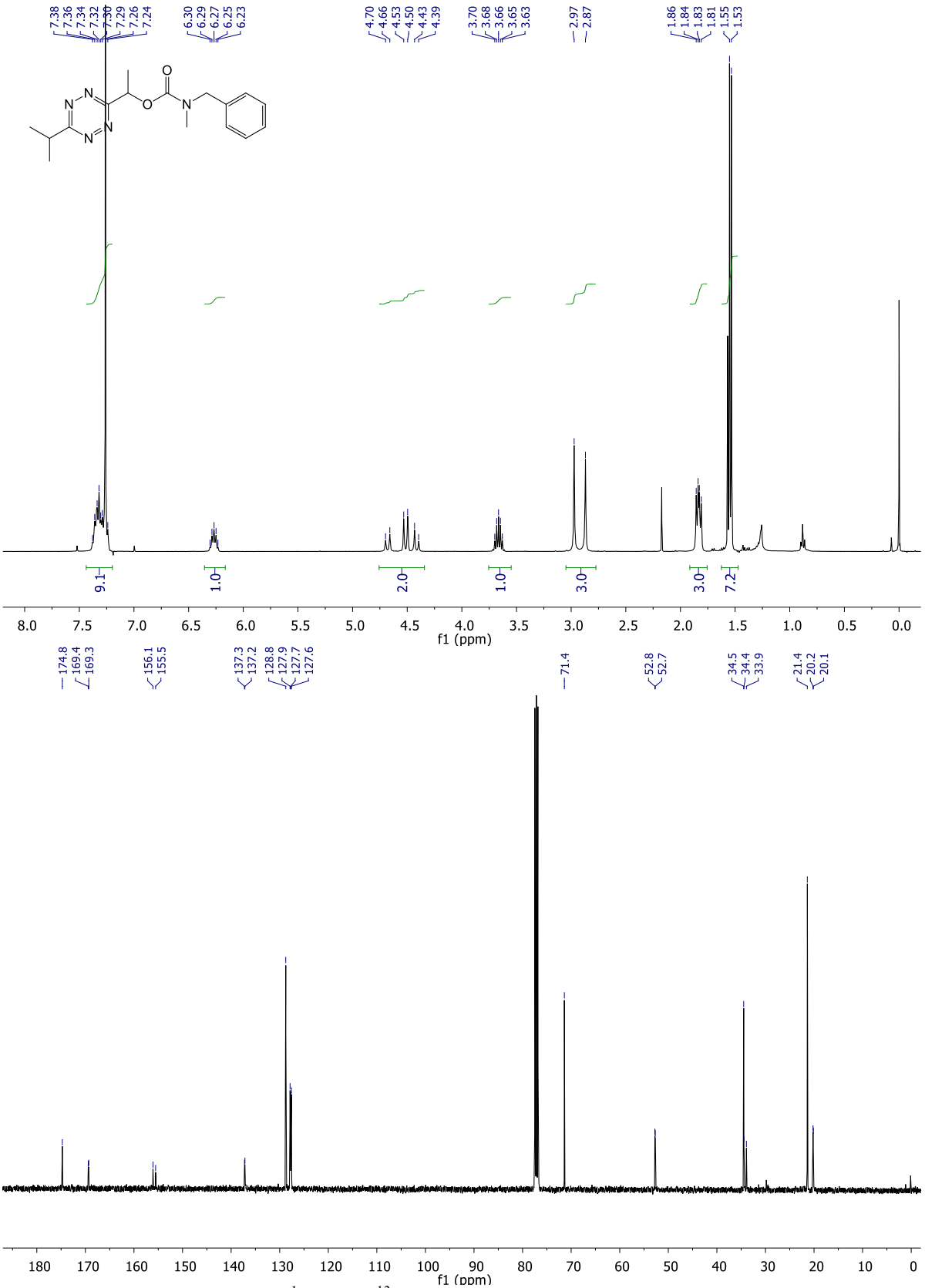

Supplementary Figure S49: ^{1}H- and ^{13}C-NMR spectra ($CDCl_3$) of 1-(6-isopropyl-1,2,4,5-tetrazin-3-yl)ethyl benzyl(methyl)carbamate (**5**)

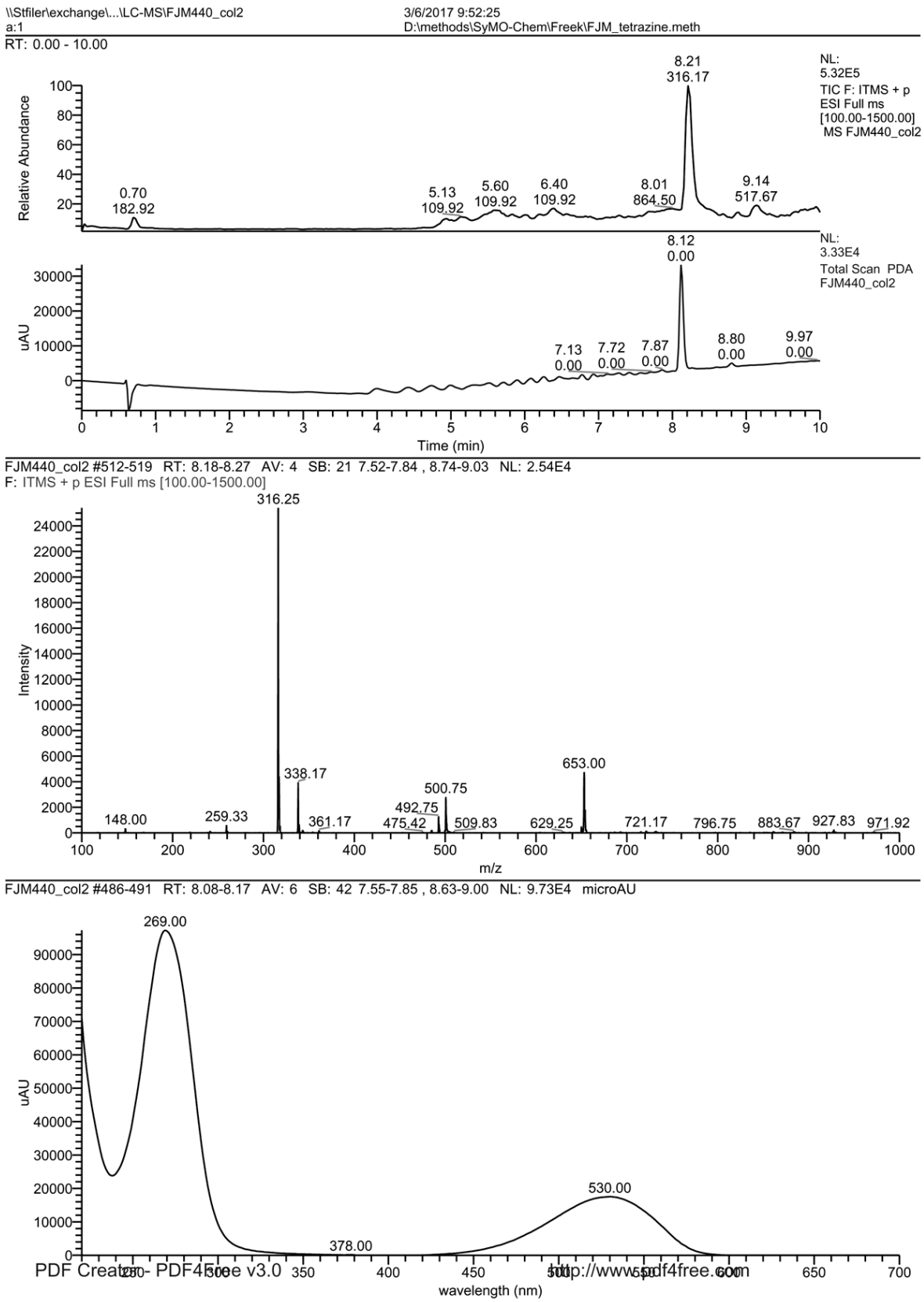

Supplementary Figure S50: HPLC-MS/PDA analysis of 1-(6-isopropyl-1,2,4,5-tetrazin-3-yl)ethyl benzyl(methyl)carbamate (**5**)

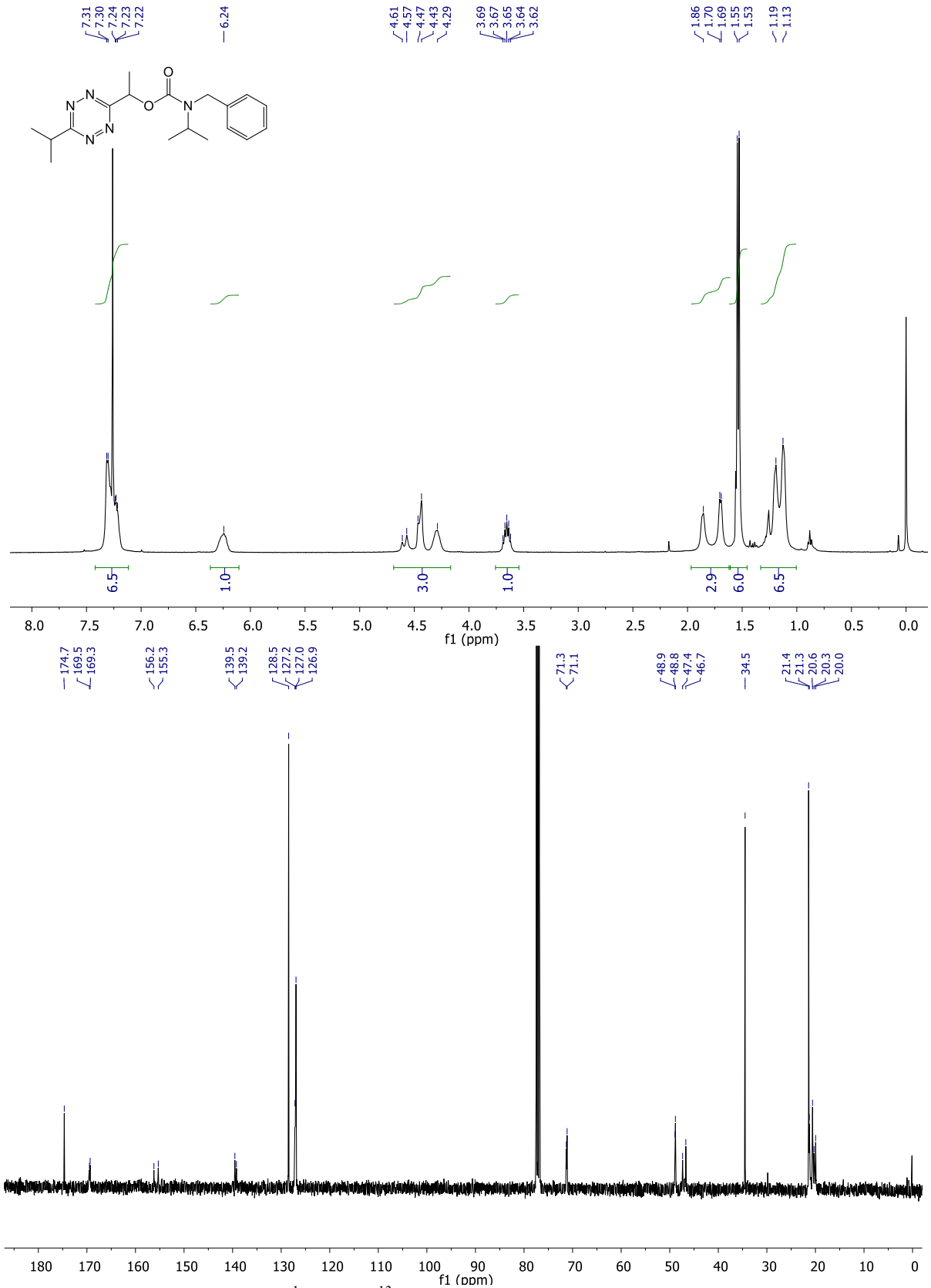

Supplementary Figure S51: ^{1}H- and ^{13}C-NMR spectra ($CDCl_3$) of 1-(6-isopropyl-1,2,4,5-tetrazin-3-yl)ethyl benzyl(isopropyl)carbamate (**6**)

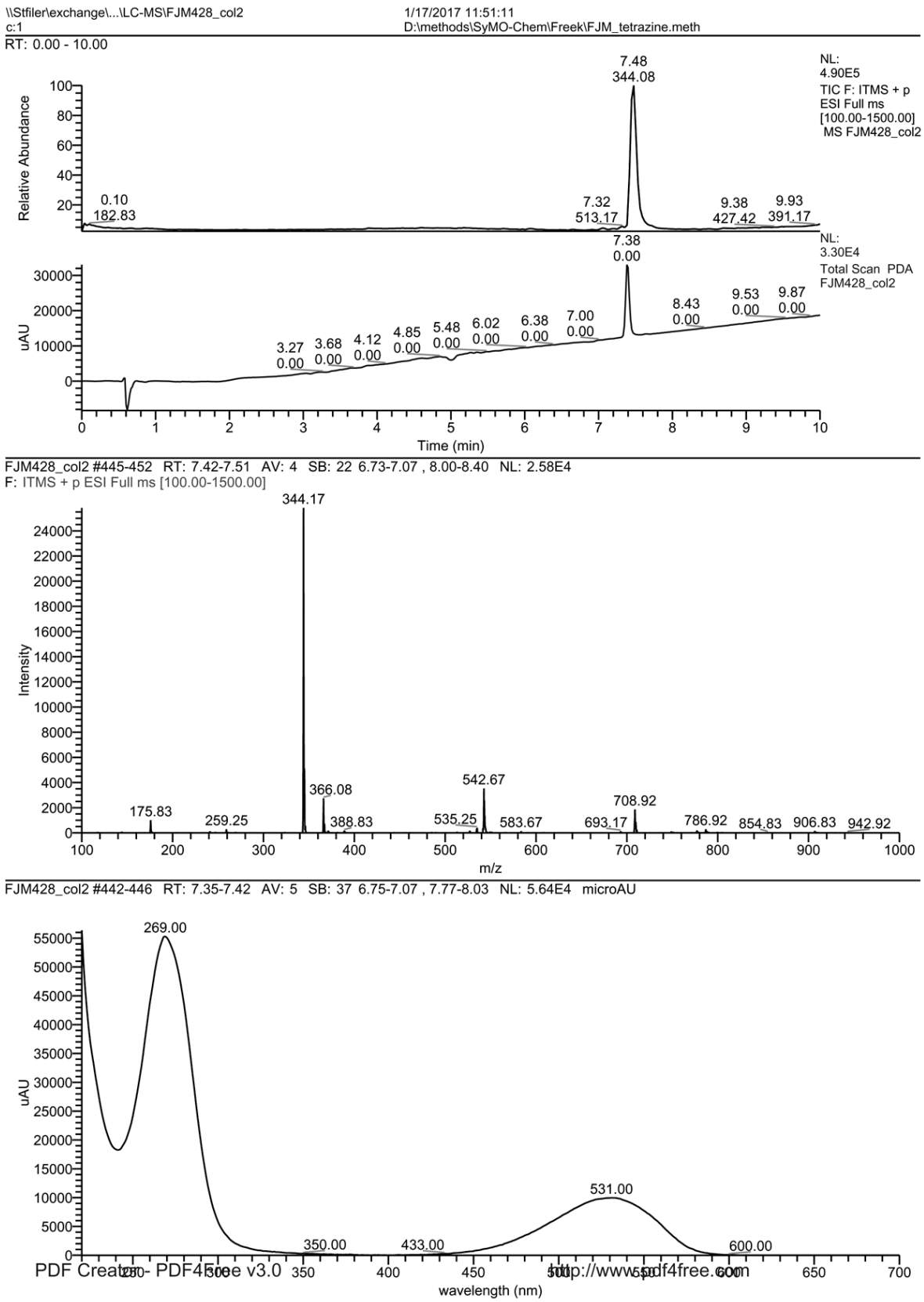

Supplementary Figure S52: HPLC-MS/PDA analysis of 1-(6-isopropyl-1,2,4,5-tetrazin-3-yl)ethyl benzyl(isopropyl)carbamate (**6**)

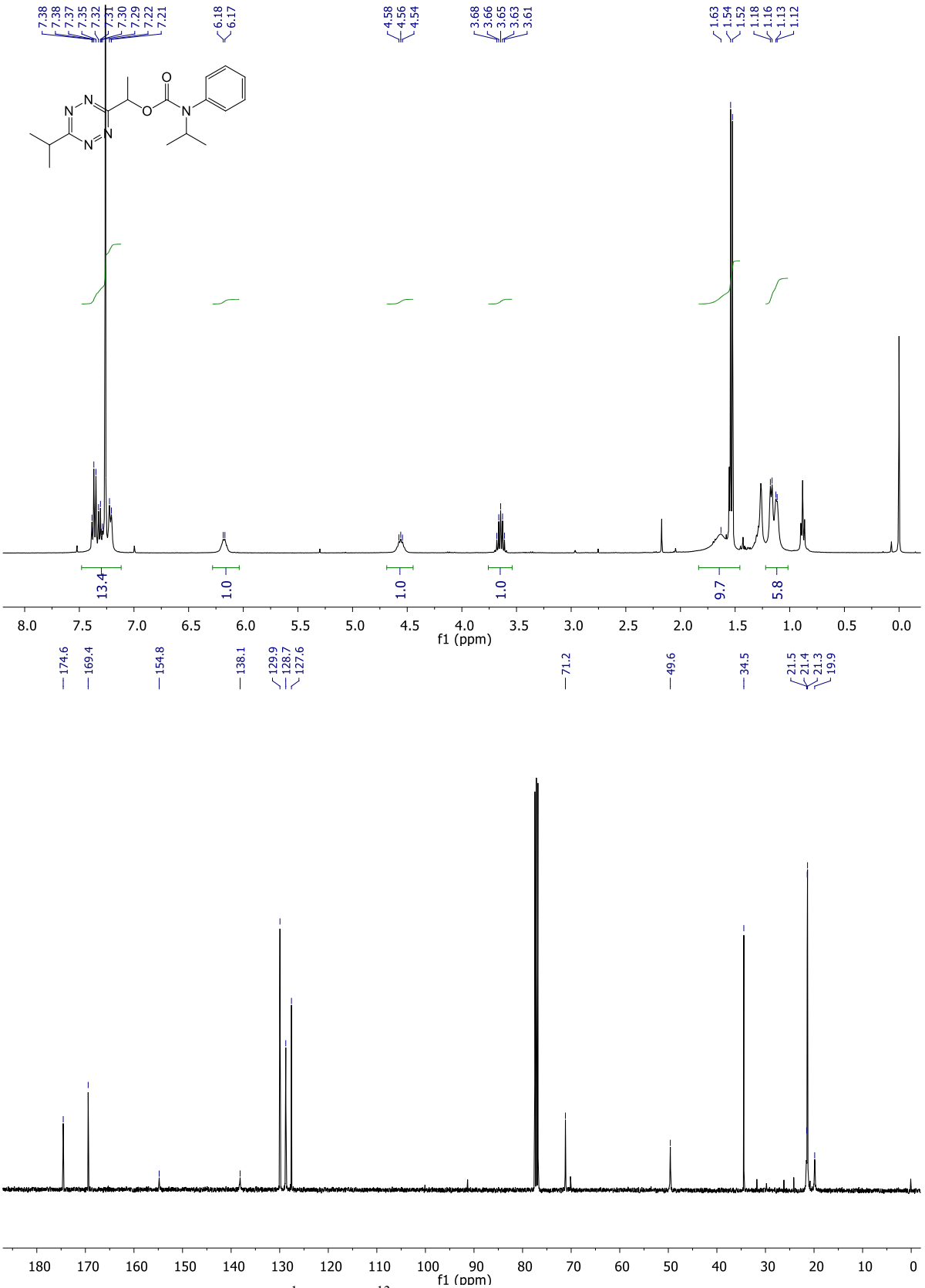

Supplementary Figure S53: ^{1}H- and ^{13}C-NMR spectra ($CDCl_3$) of 1-(6-isopropyl-1,2,4,5-tetrazin-3-yl)ethyl isopropyl(phenyl)carbamate (**8**)

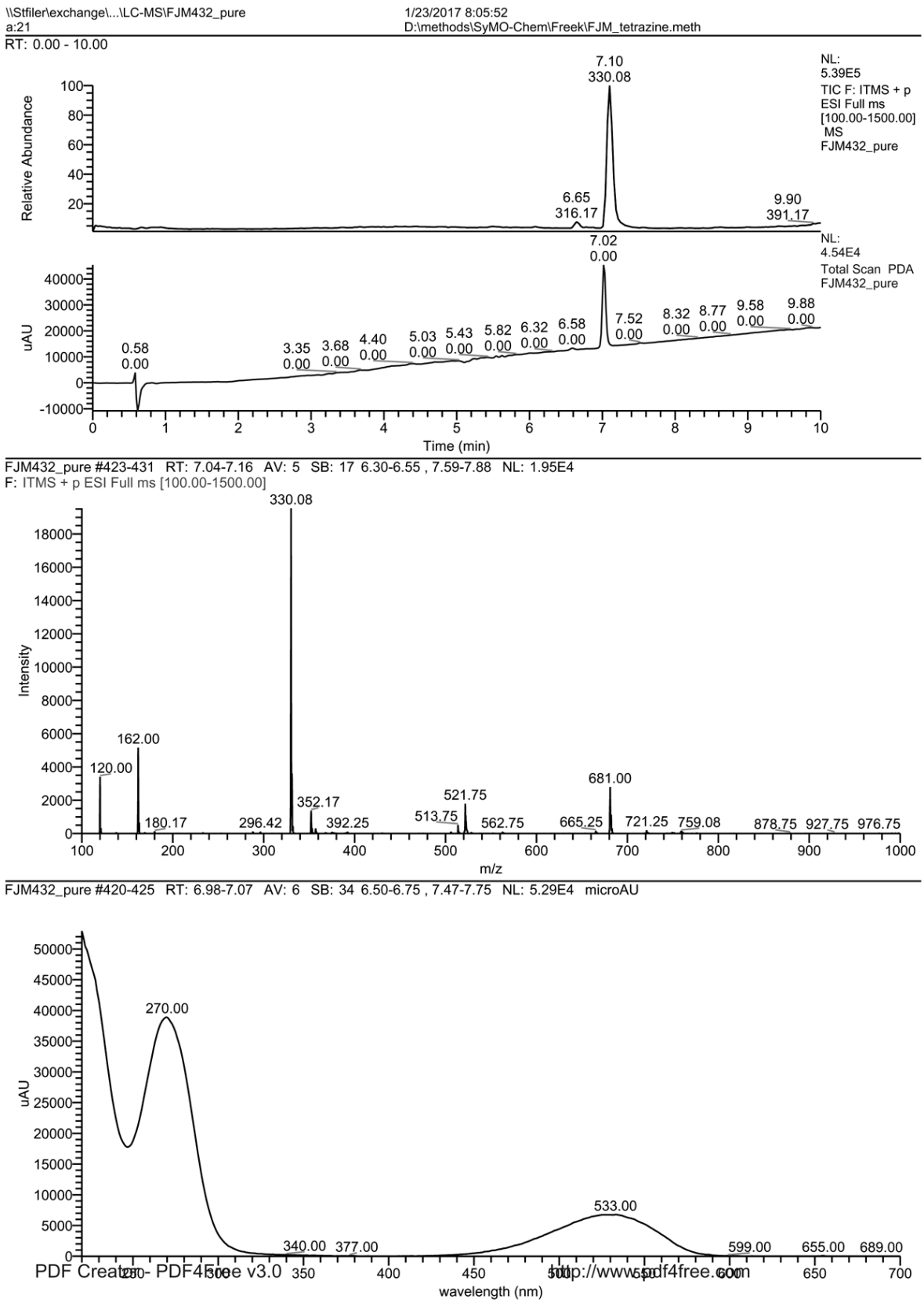

Supplementary Figure S54: HPLC-MS/PDA analysis of 1-(6-isopropyl-1,2,4,5-tetrazin-3-yl)ethyl isopropyl(phenyl)carbamate (**8**)

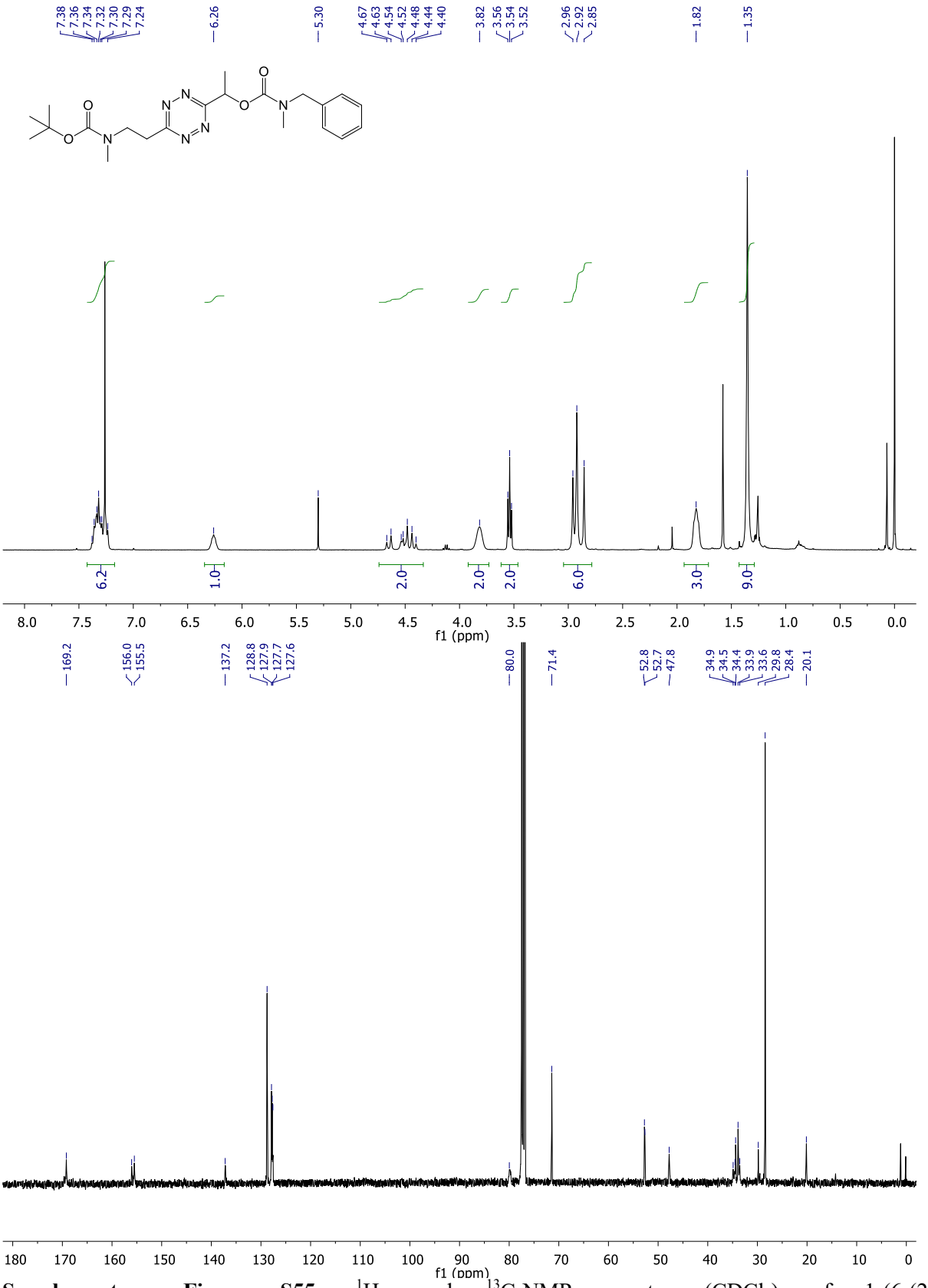

Supplementary Figure S55: ^{1}H- and ^{13}C-NMR spectra ($CDCl_3$) of 1-(6-(2-((*t*-butoxycarbonyl)(methyl)amino)ethyl)-1,2,4,5-tetrazin-3-yl)ethyl benzyl(methyl)carbamate (**9**)

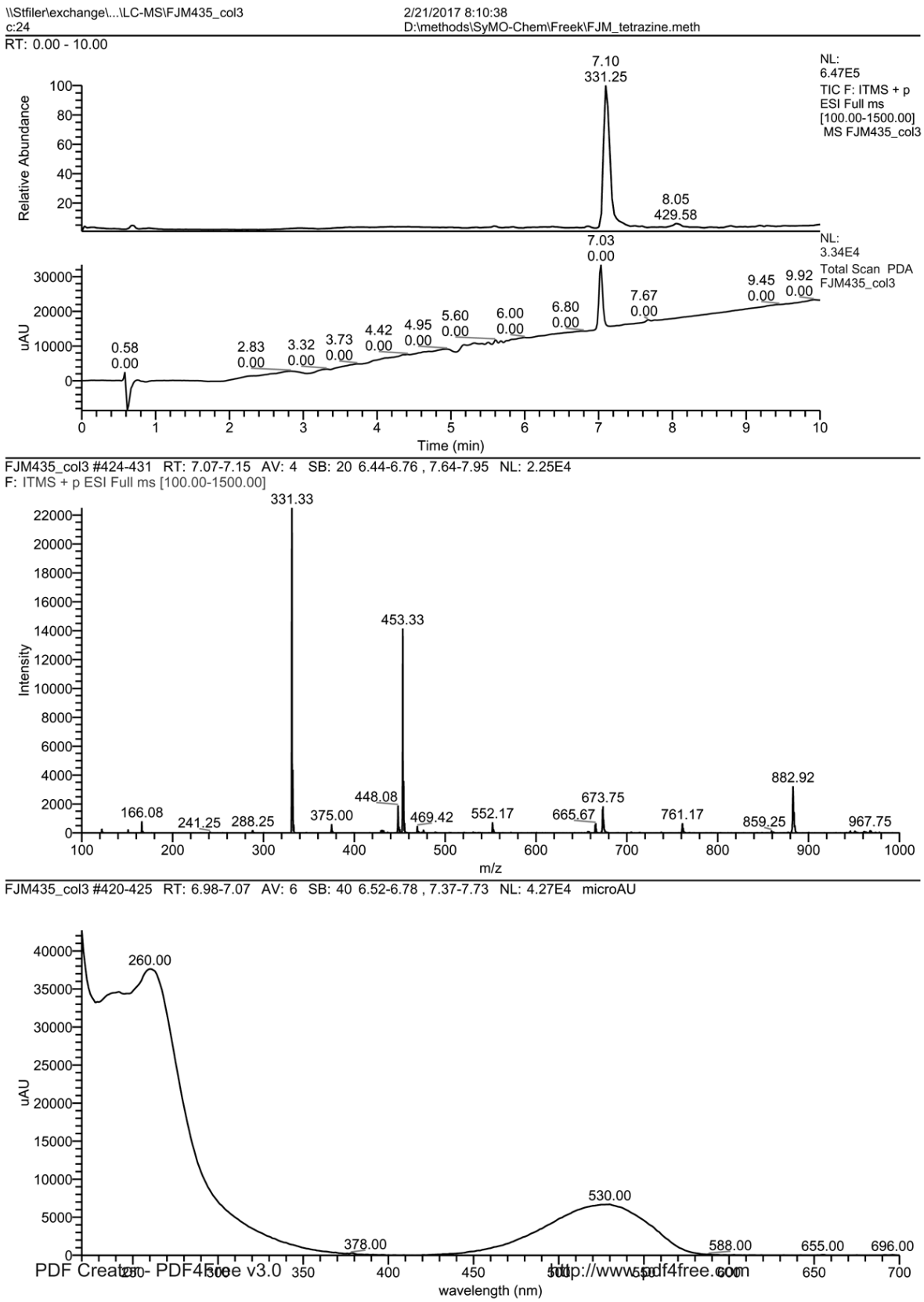

PDF Creator - PDF4Free v3.0 http://www.pdf4free.com

Supplementary Figure S56: HPLC-MS/PDA analysis of 1-(6-(2-((*t*-butoxycarbonyl)(methyl)amino)ethyl)-1,2,4,5-tetrazin-3-yl)ethyl benzyl(methyl)carbamate (**9**)

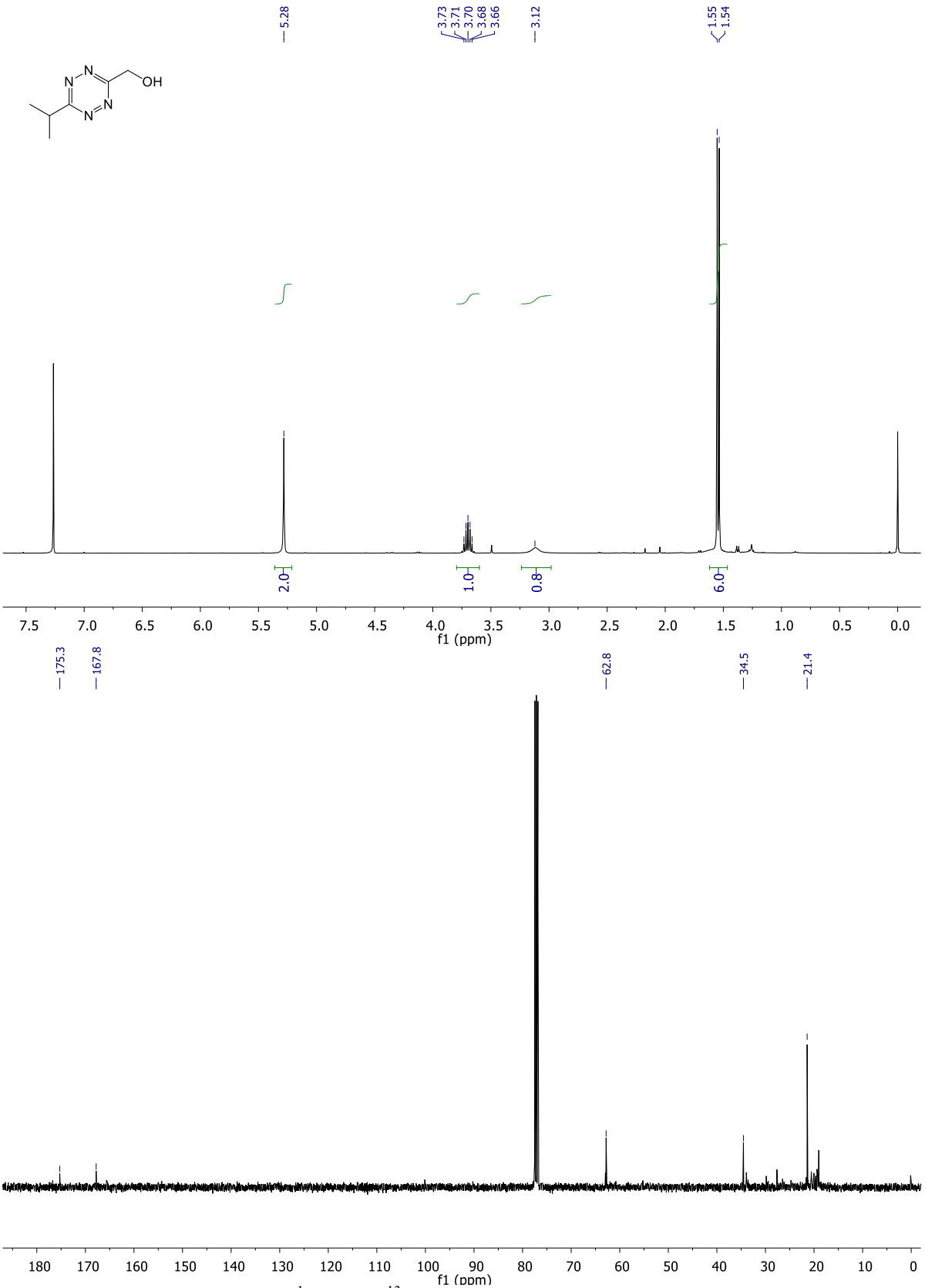

Supplementary Figure S57: ^{1}H- and ^{13}C-NMR spectra ($CDCl_3$) of (6-isopropyl-1,2,4,5-tetrazin-3-yl)methanol (**S6**)

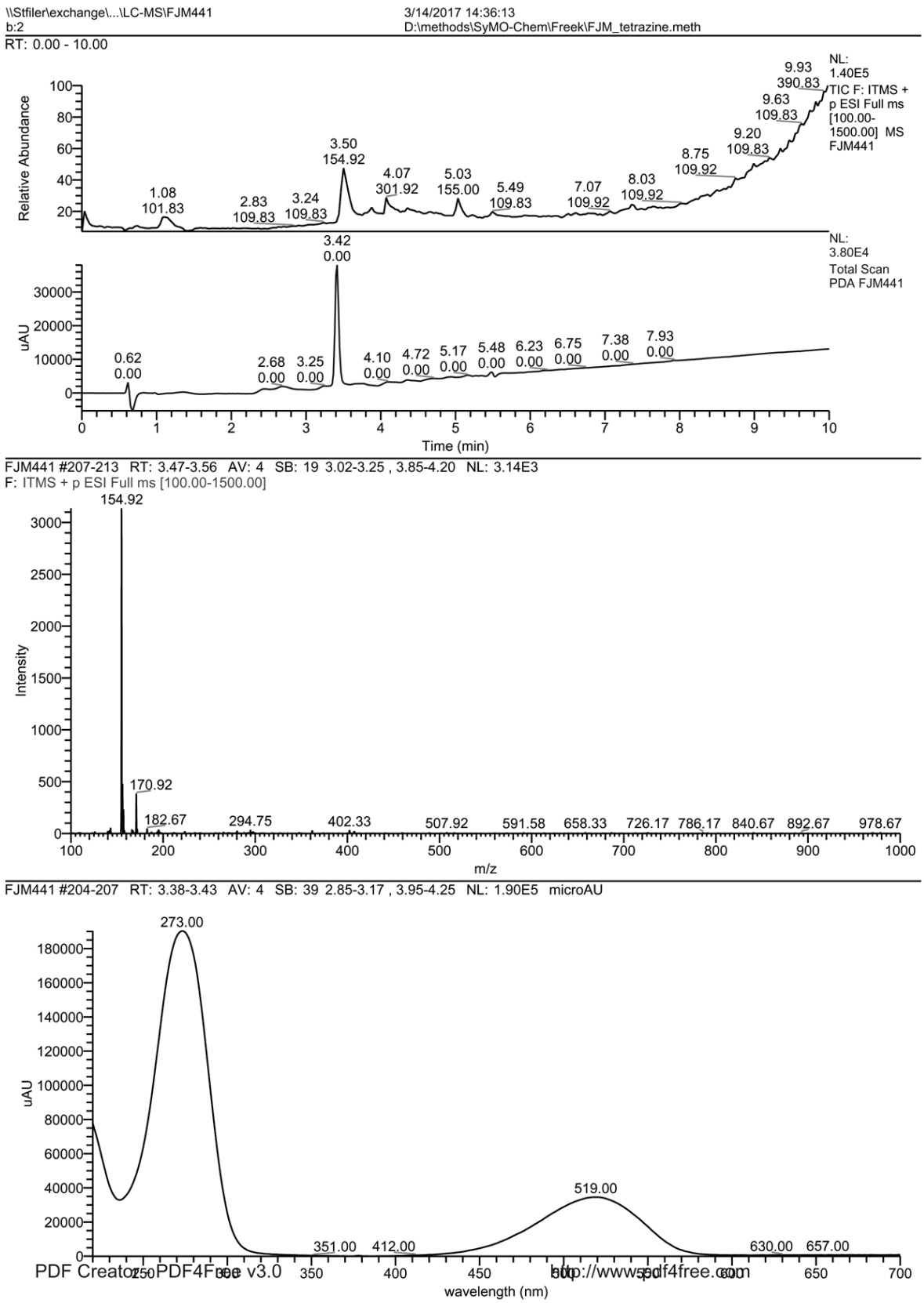

Supplementary Figure S58: HPLC-MS/PDA analysis of (6-isopropyl-1,2,4,5-tetrazin-3-yl)methanol (**S6**)

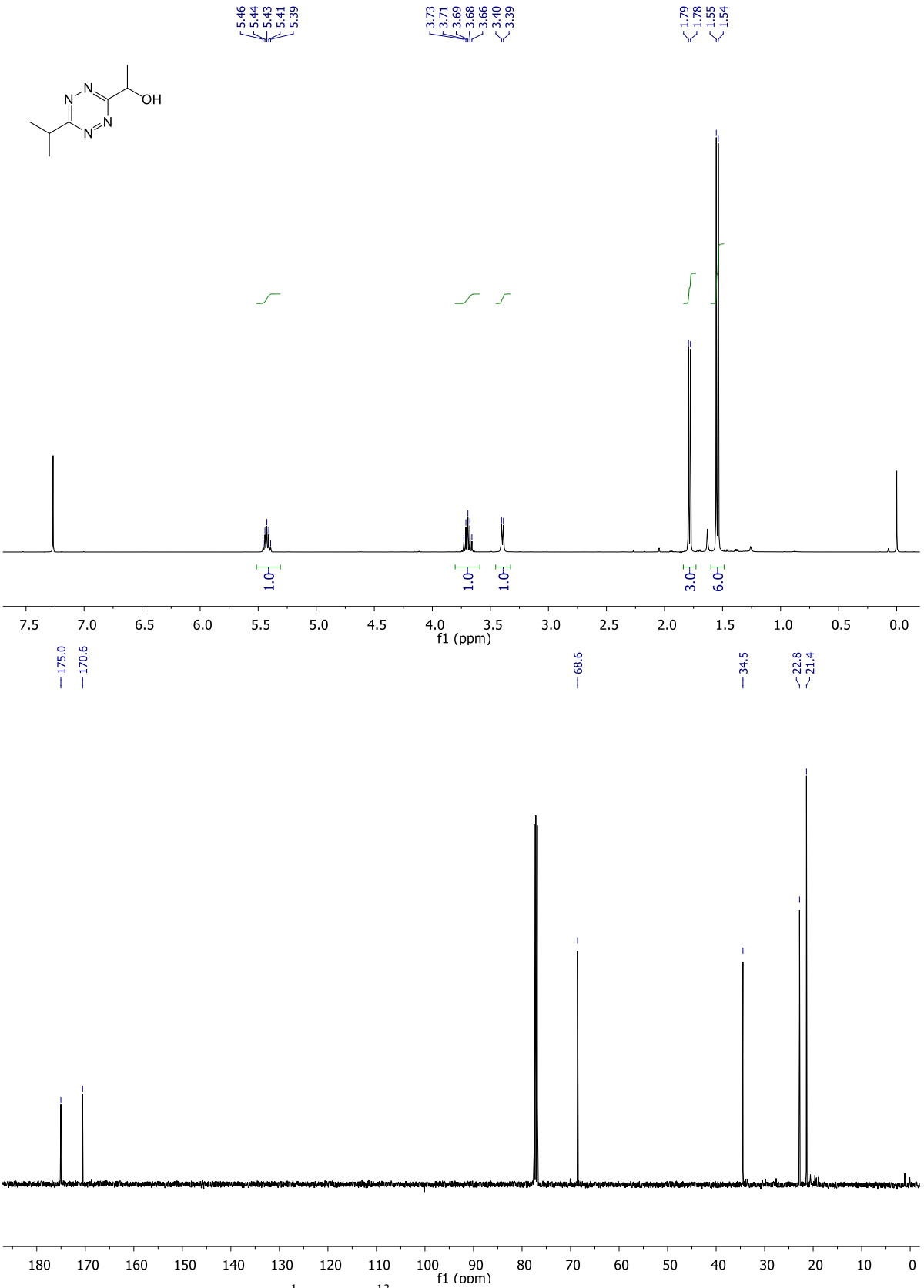

Supplementary Figure S59: ^{1}H- and ^{13}C-NMR spectra ($CDCl_3$) of 1-(6-isopropyl-1,2,4,5-tetrazin-3-yl)ethanol (**S7**)

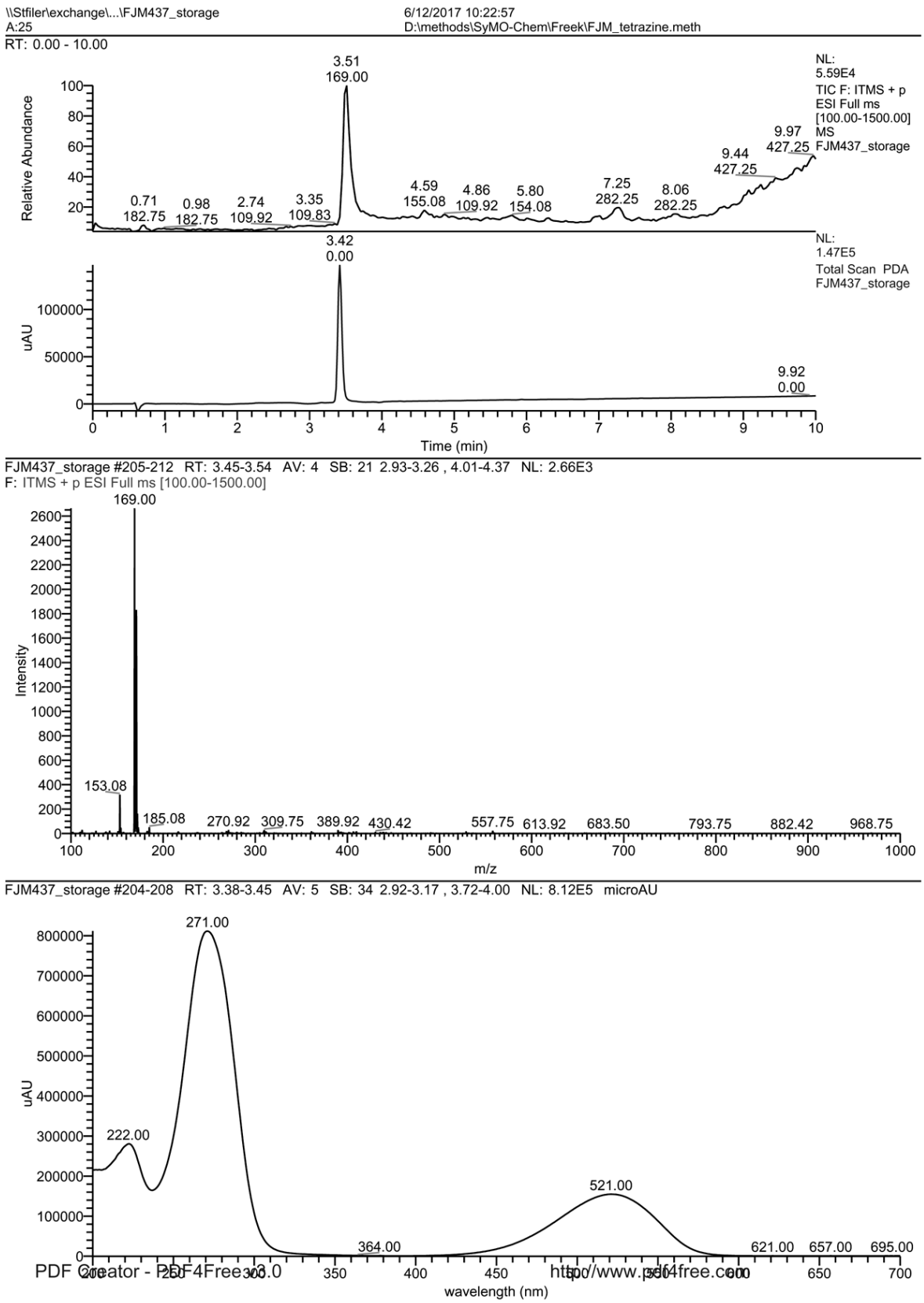

Supplementary Figure S60: HPLC-MS/PDA analysis of 1-(6-isopropyl-1,2,4,5-tetrazin-3-yl)ethanol (**S7**)

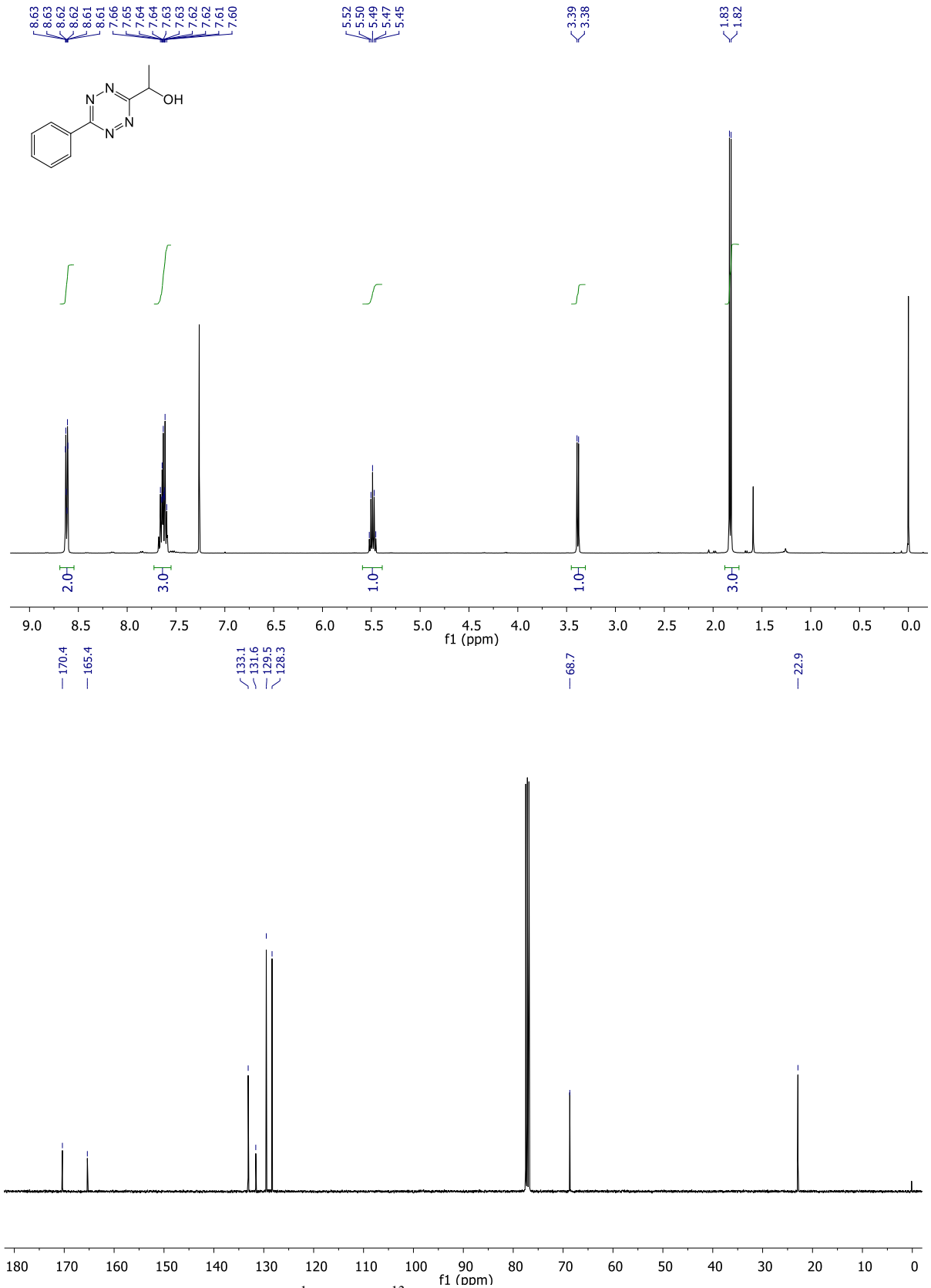

Supplementary Figure S61: ^{1}H- and ^{13}C-NMR spectra ($CDCl_3$) of 1-(6-phenyl-1,2,4,5-tetrazin-3-yl)ethanol (**S8**)

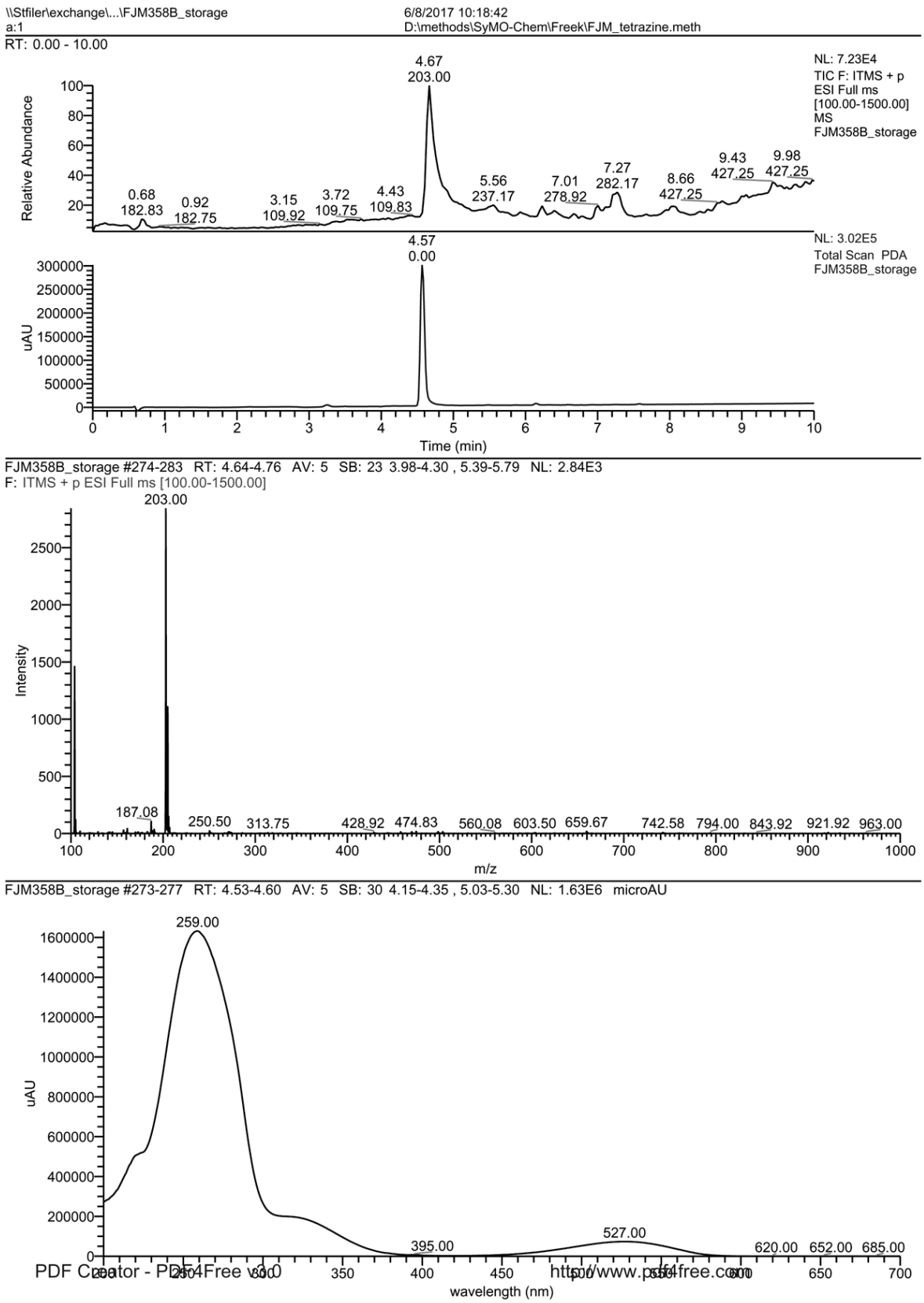

Supplementary Figure S62: HPLC-MS/PDA analysis of 1-(6-phenyl-1,2,4,5-tetrazin-3-yl)ethanol (**S8**)

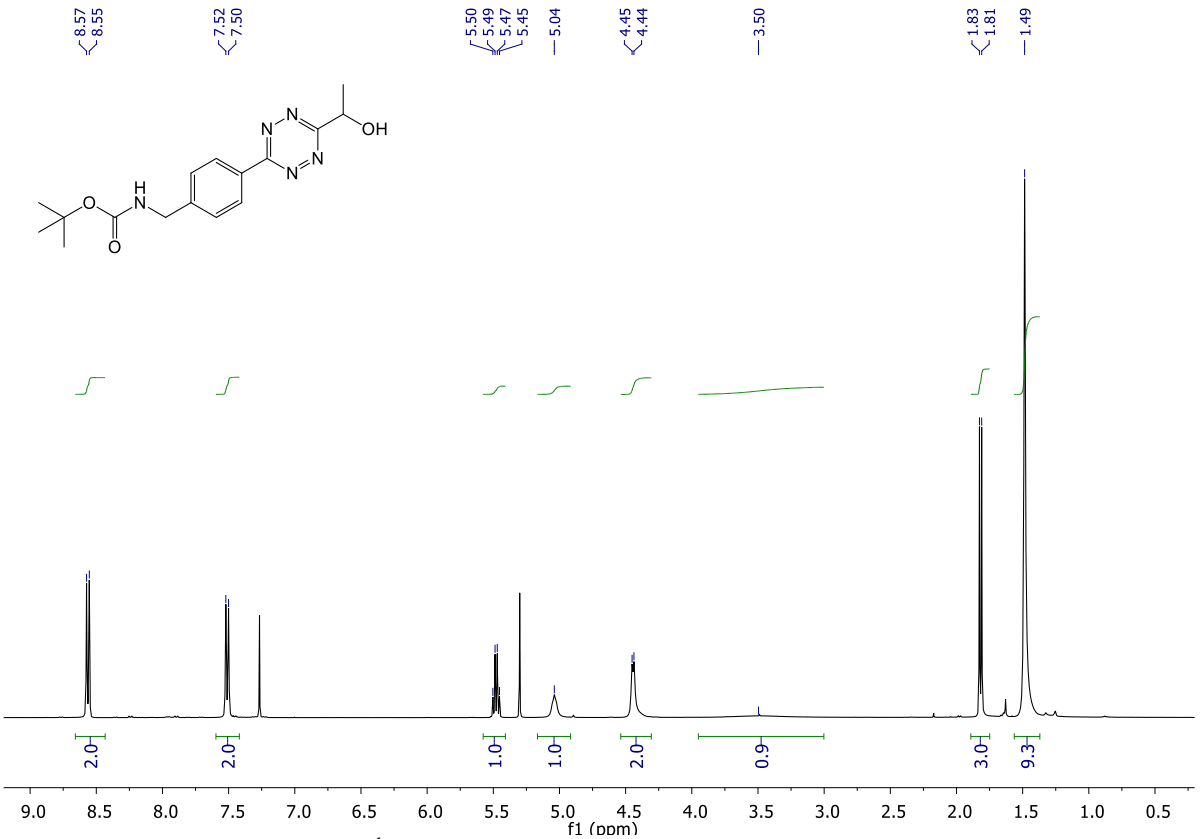

Supplementary Figure S63: ^{1}H-spectrum ($CDCl_3$) of *t*-butyl 4-(6-(1-hydroxyethyl)-1,2,4,5-tetrazin-3-yl)benzylcarbamate (**18**)

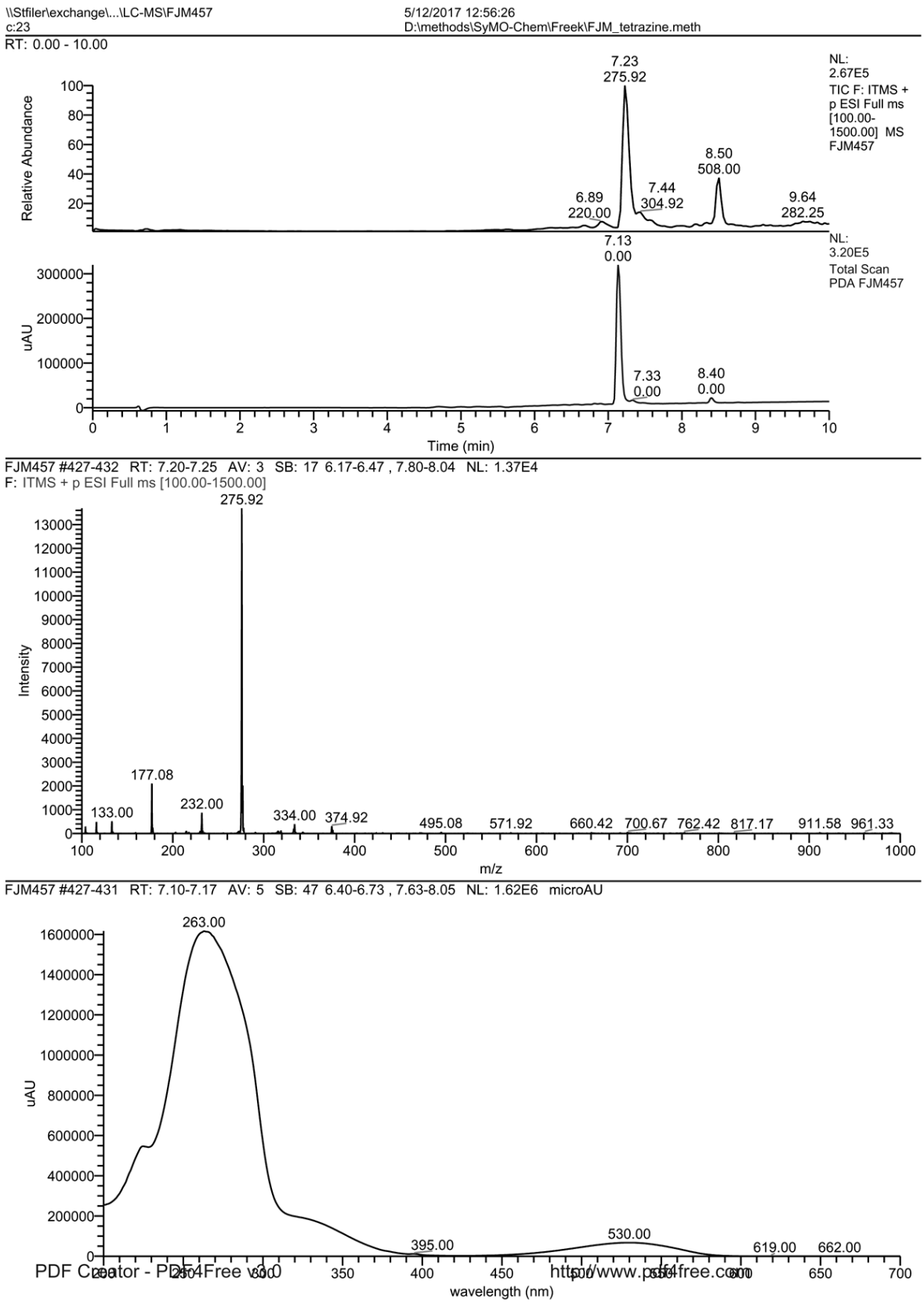

Supplementary Figure S64: HPLC-MS/PDA analysis of *t*-butyl 4-(6-(1-hydroxyethyl)-1,2,4,5-tetrazin-3-yl)benzylcarbamate (**18**)

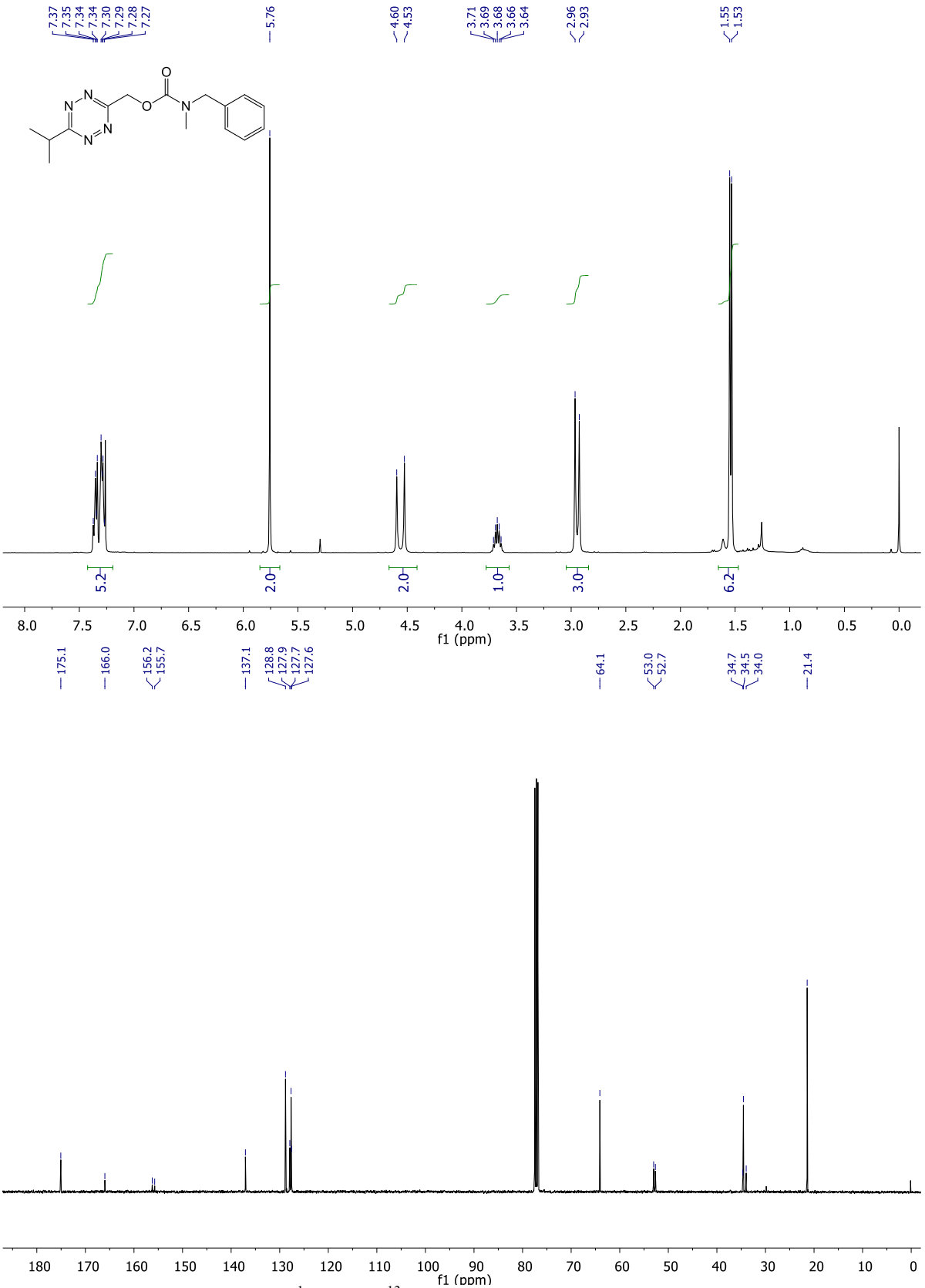

Supplementary Figure S65: ^{1}H- and ^{13}C-NMR spectra ($CDCl_3$) of (6-isopropyl-1,2,4,5-tetrazin-3-yl)methyl benzyl(methyl)carbamate (**4**)

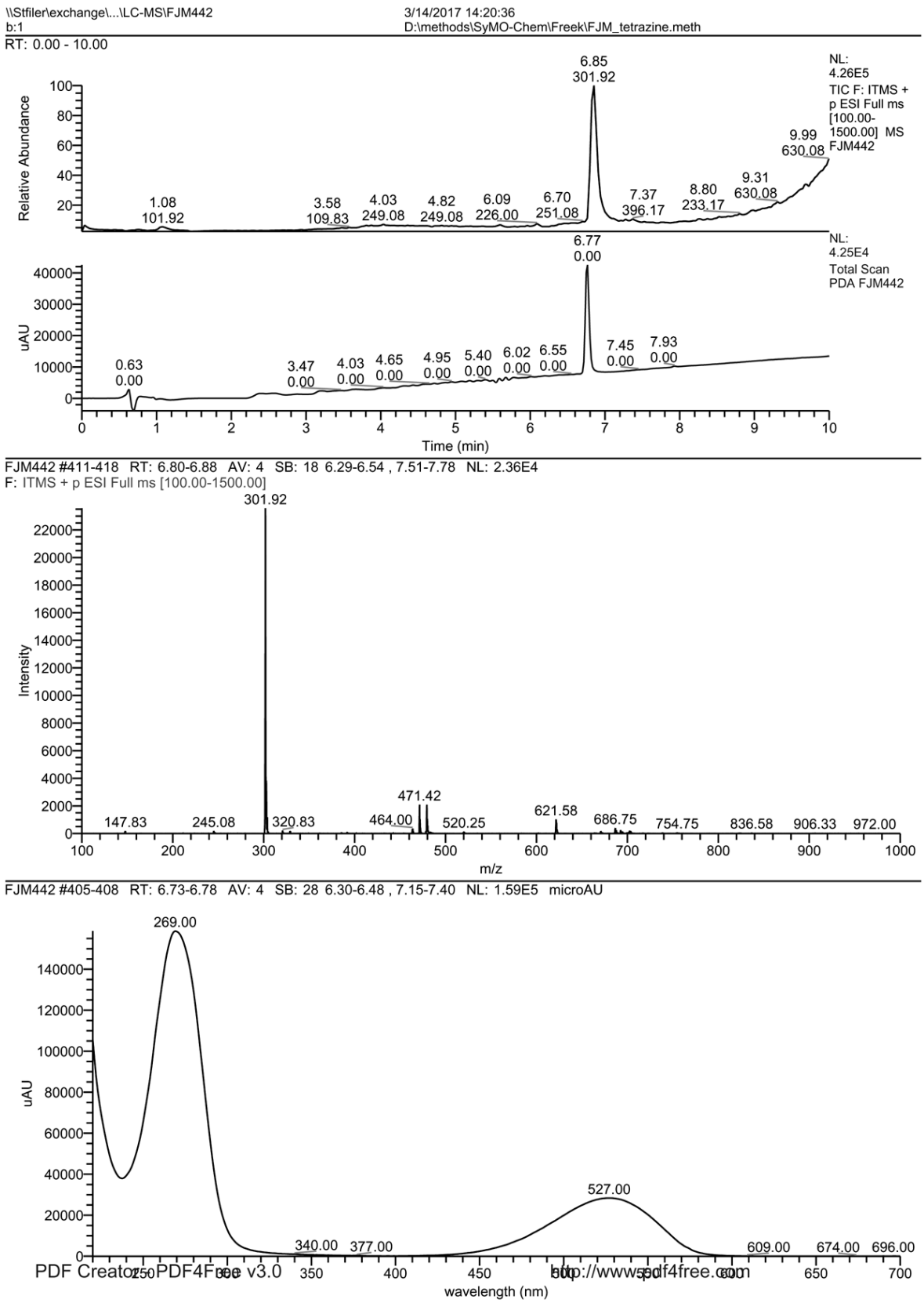

Supplementary Figure S66: HPLC-MS/PDA analysis of (6-isopropyl-1,2,4,5-tetrazin-3-yl)methyl benzyl(methyl)carbamate (**4**)

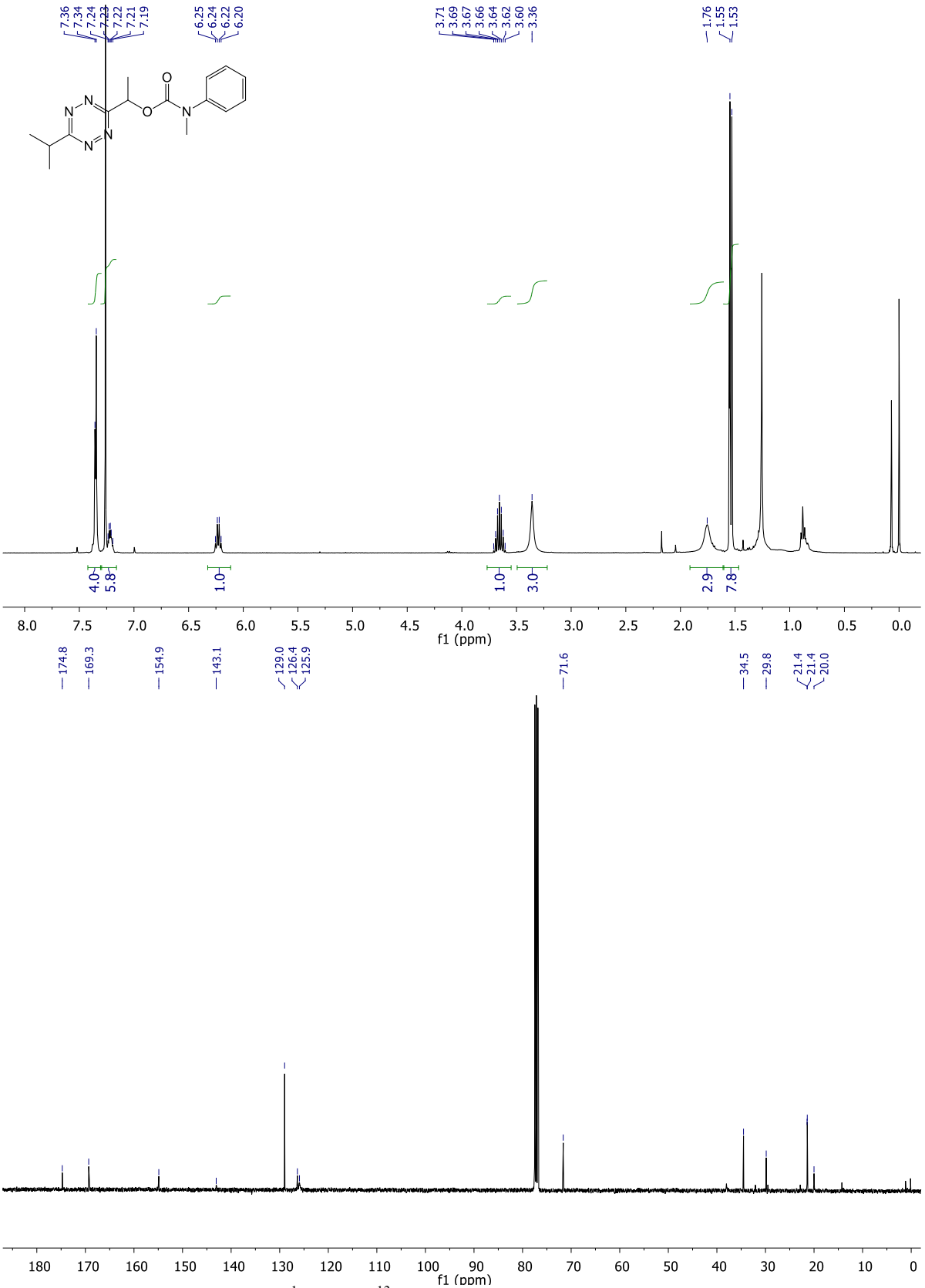

Supplementary Figure S67: ^{1}H- and ^{13}C-NMR spectra ($CDCl_3$) of 1-(6-isopropyl-1,2,4,5-tetrazin-3-yl)ethyl methyl(phenyl)carbamate (**7**)

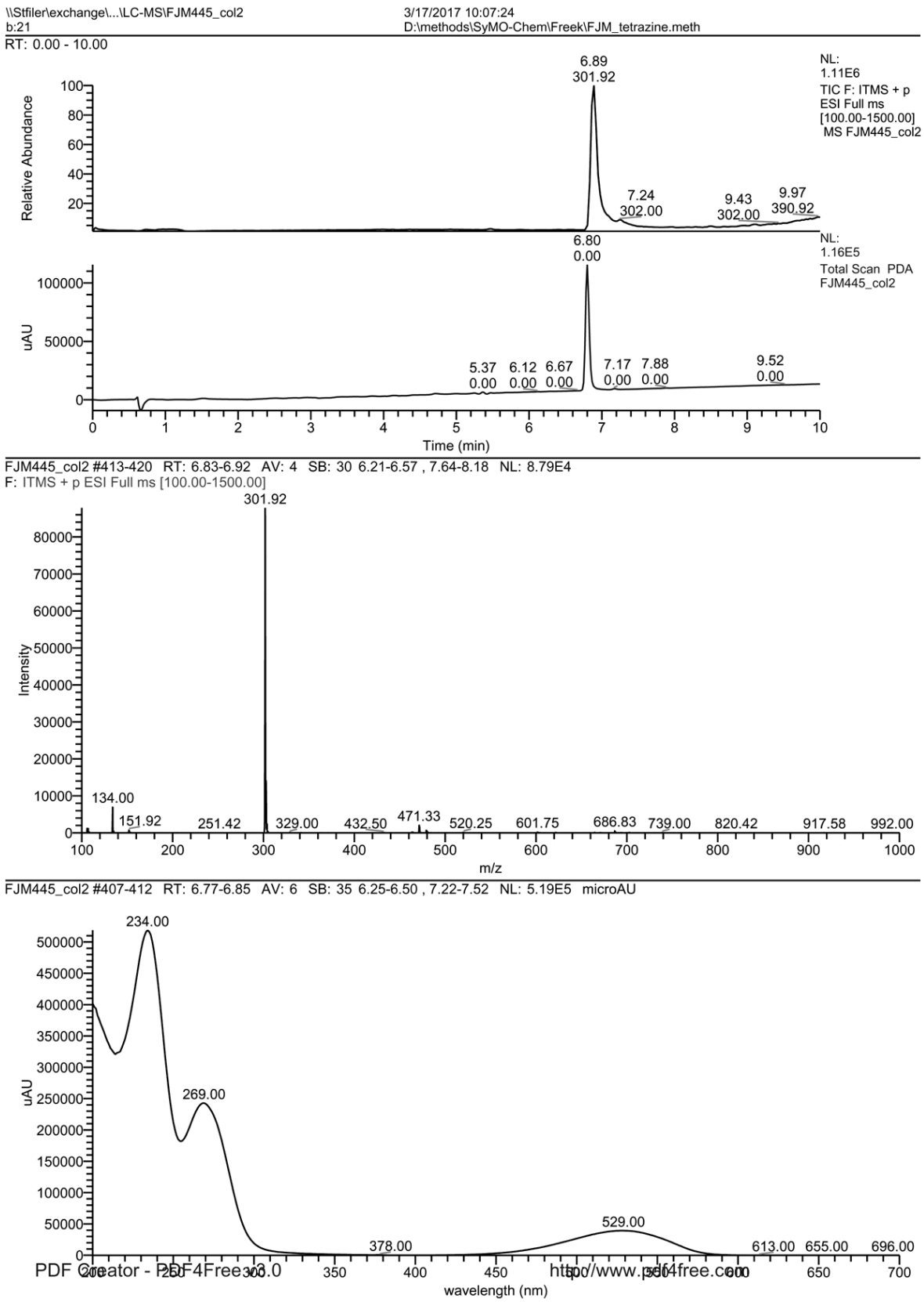

Supplementary Figure S68: HPLC-MS/PDA analysis of 1-(6-isopropyl-1,2,4,5-tetrazin-3-yl)ethyl methyl(phenyl)carbamate (**7**)

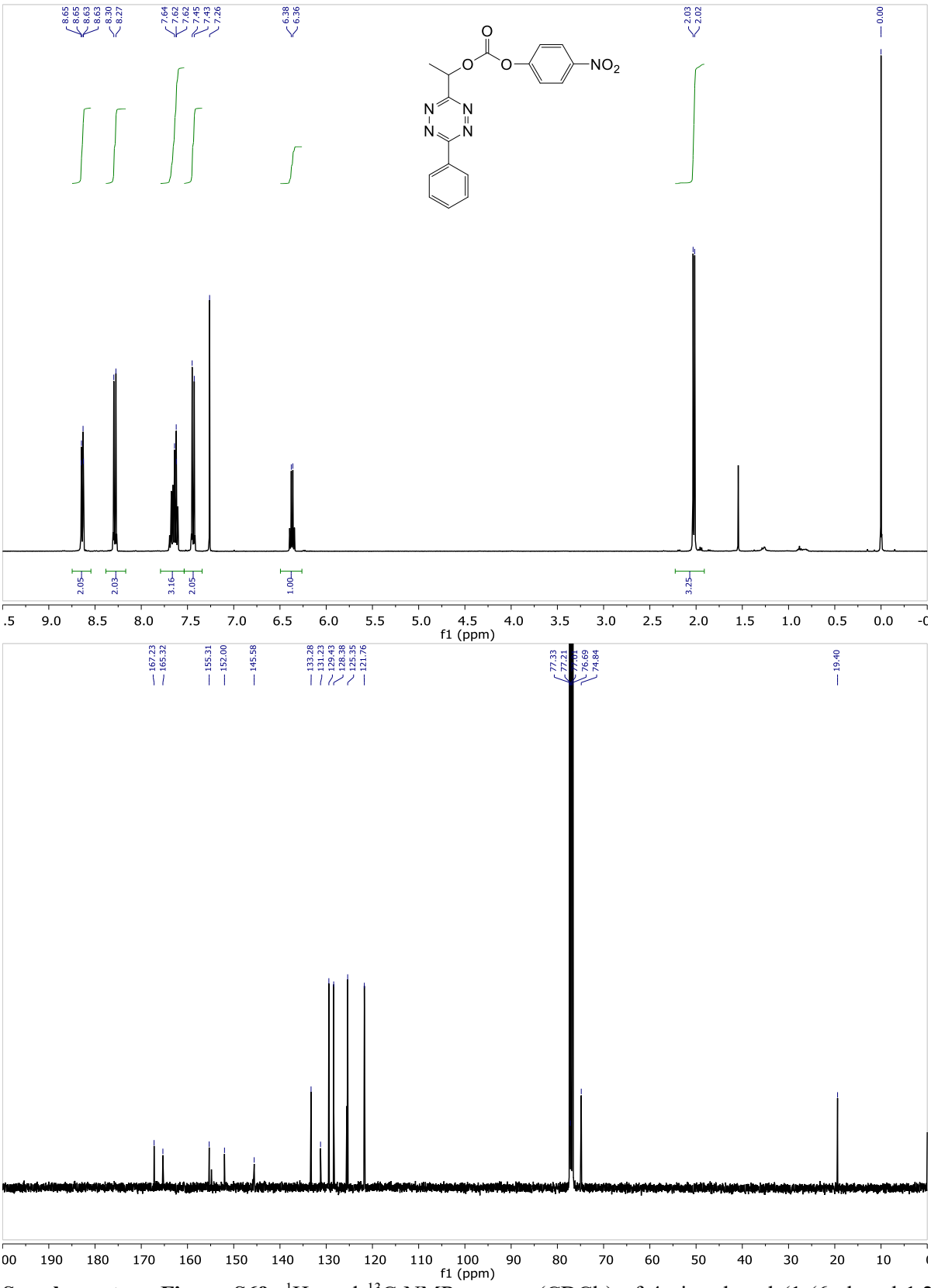

Supplementary Figure S69: ^{1}H- and ^{13}C-NMR spectra ($CDCl_3$) of 4-nitrophenyl (1-(6-phenyl-1,2,4,5-tetrazin-3-yl)ethyl) carbonate (**S9**)

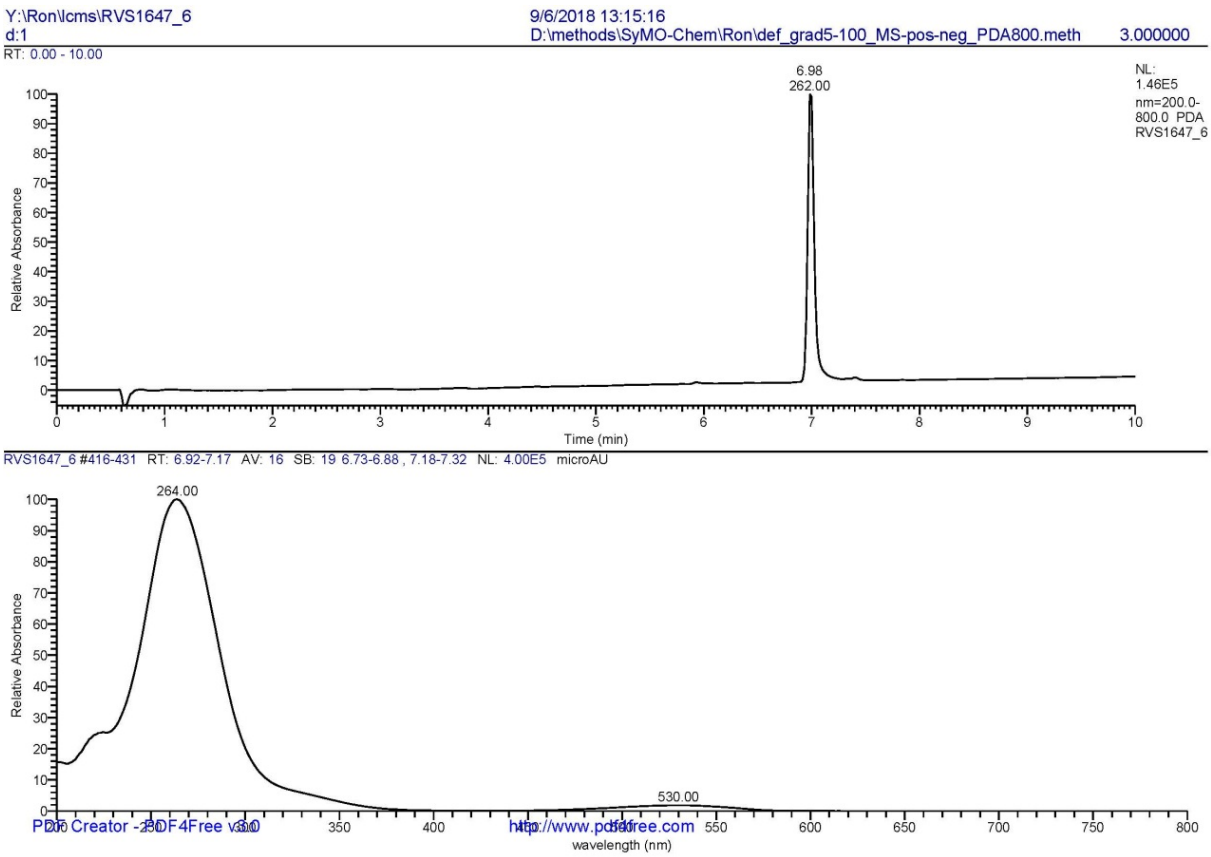

Supplementary Figure S70: HPLC-MS/PDA analysis of 4-nitrophenyl (1-(6-phenyl-1,2,4,5-tetrazin-3-yl)ethyl) carbonate (**S9**)

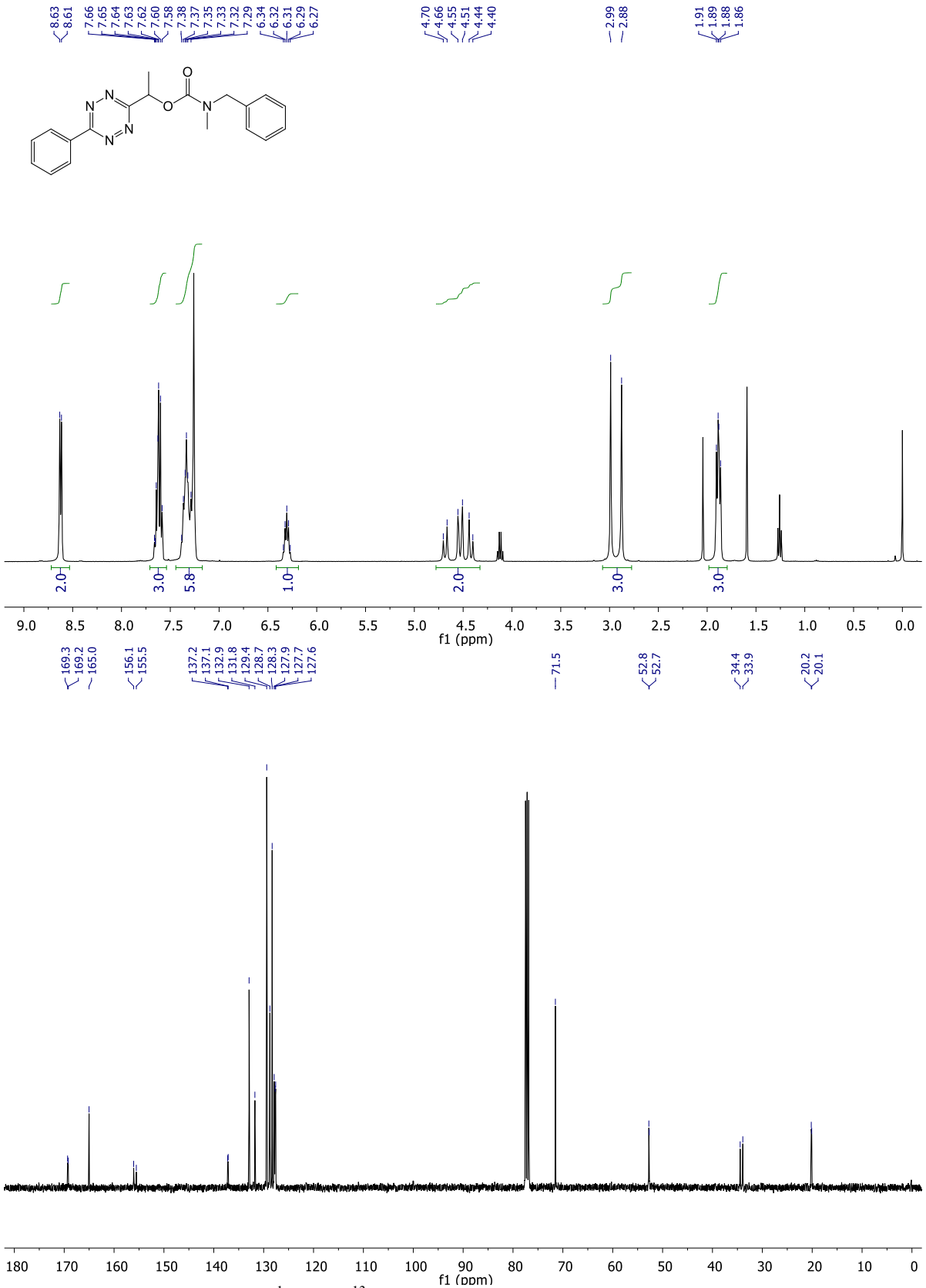

Supplementary Figure S71: ^{1}H- and ^{13}C-NMR spectra ($CDCl_3$) of 1-(6-phenyl-1,2,4,5-tetrazin-3-yl)ethyl benzyl(methyl)carbamate (**10**)

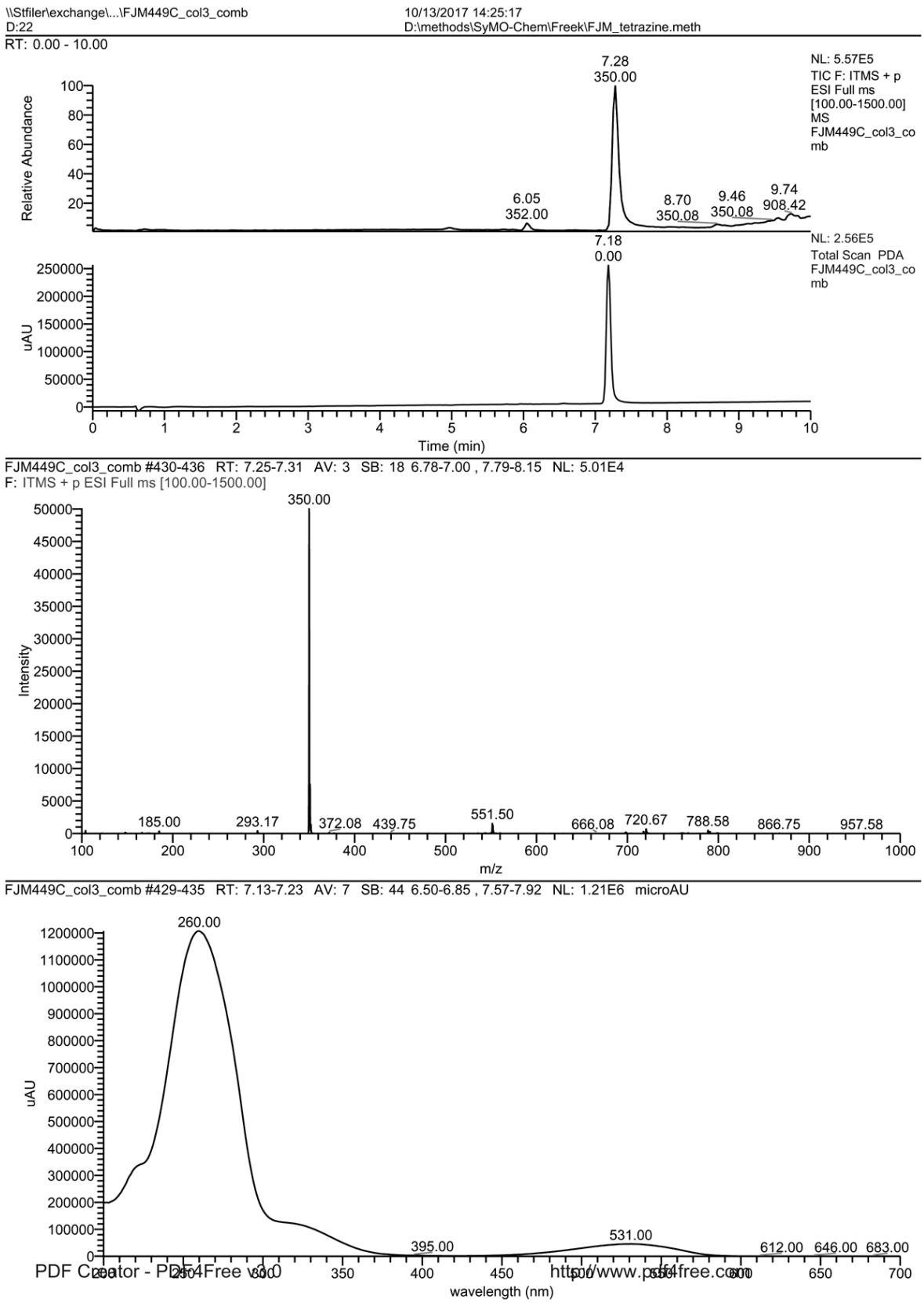

PDF Creator - PDF4Free v3.0 http://www.pdf4free.com

Supplementary Figure S72: HPLC-MS/PDA analysis of 1-(6-phenyl-1,2,4,5-tetrazin-3-yl)ethyl benzyl(methyl)carbamate (**10**)

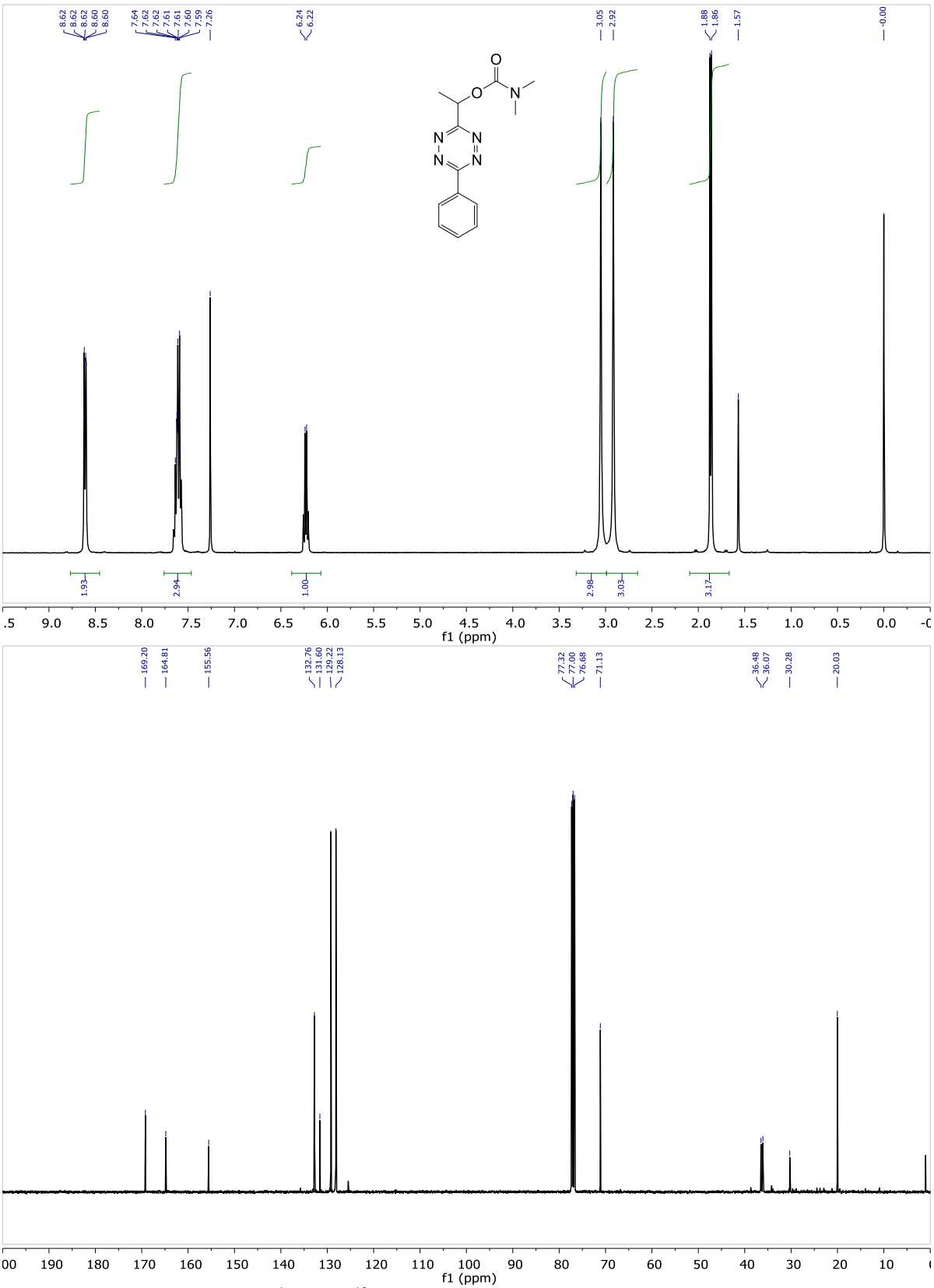

Supplementary Figure S73: ^{1}H- and ^{13}C-NMR spectra ($CDCl_3$) of 1-(6-phenyl-1,2,4,5-tetrazin-3-yl)ethyl dimethylcarbamate (**11**)

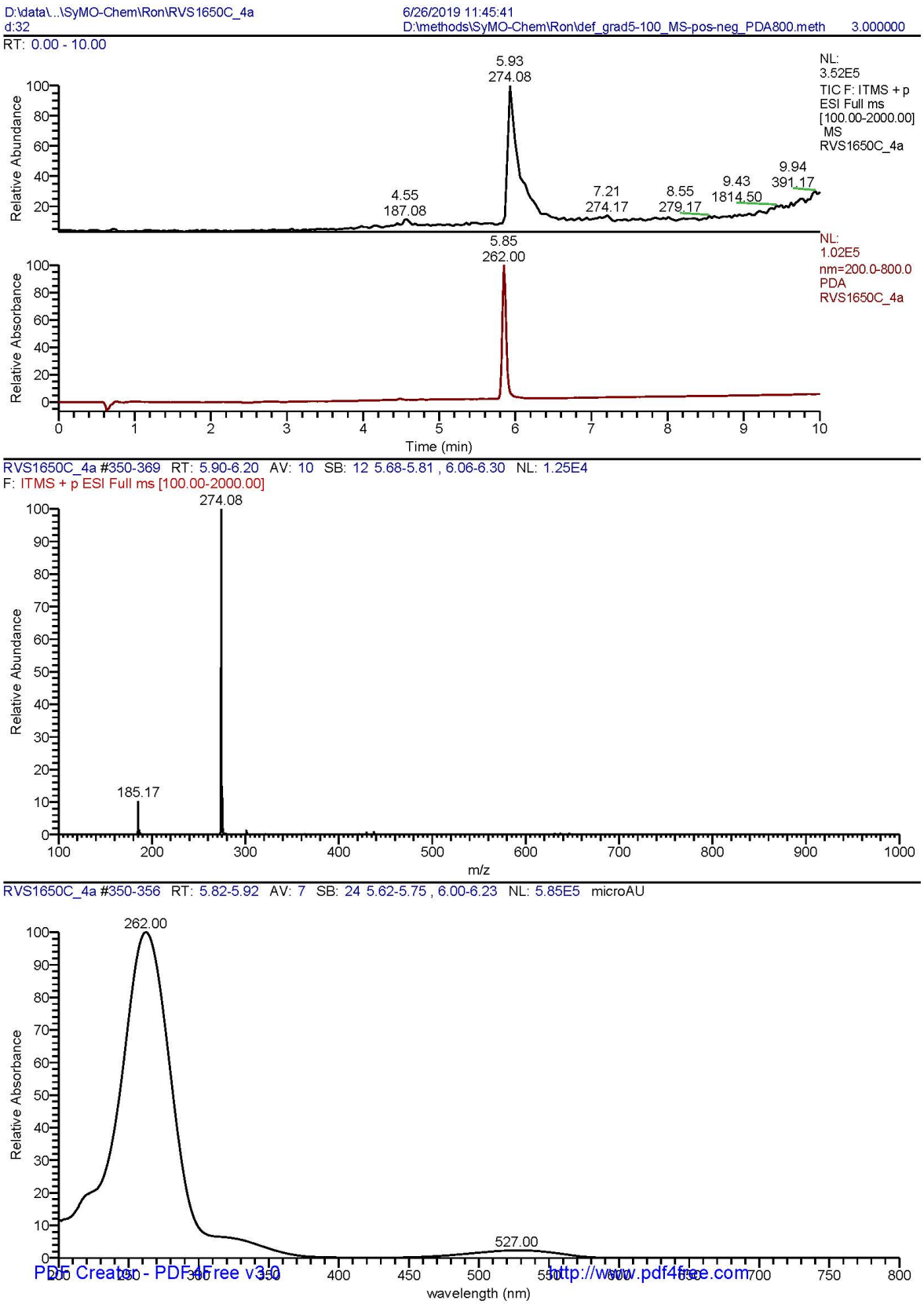

PDF Creator - PDF4Free v3.0 http://www.pdf4free.com

Supplementary Figure 74: HPLC-MS/PDA analysis of 1-(6-phenyl-1,2,4,5-tetrazin-3-yl)ethyl dimethylcarbamate (**11**)

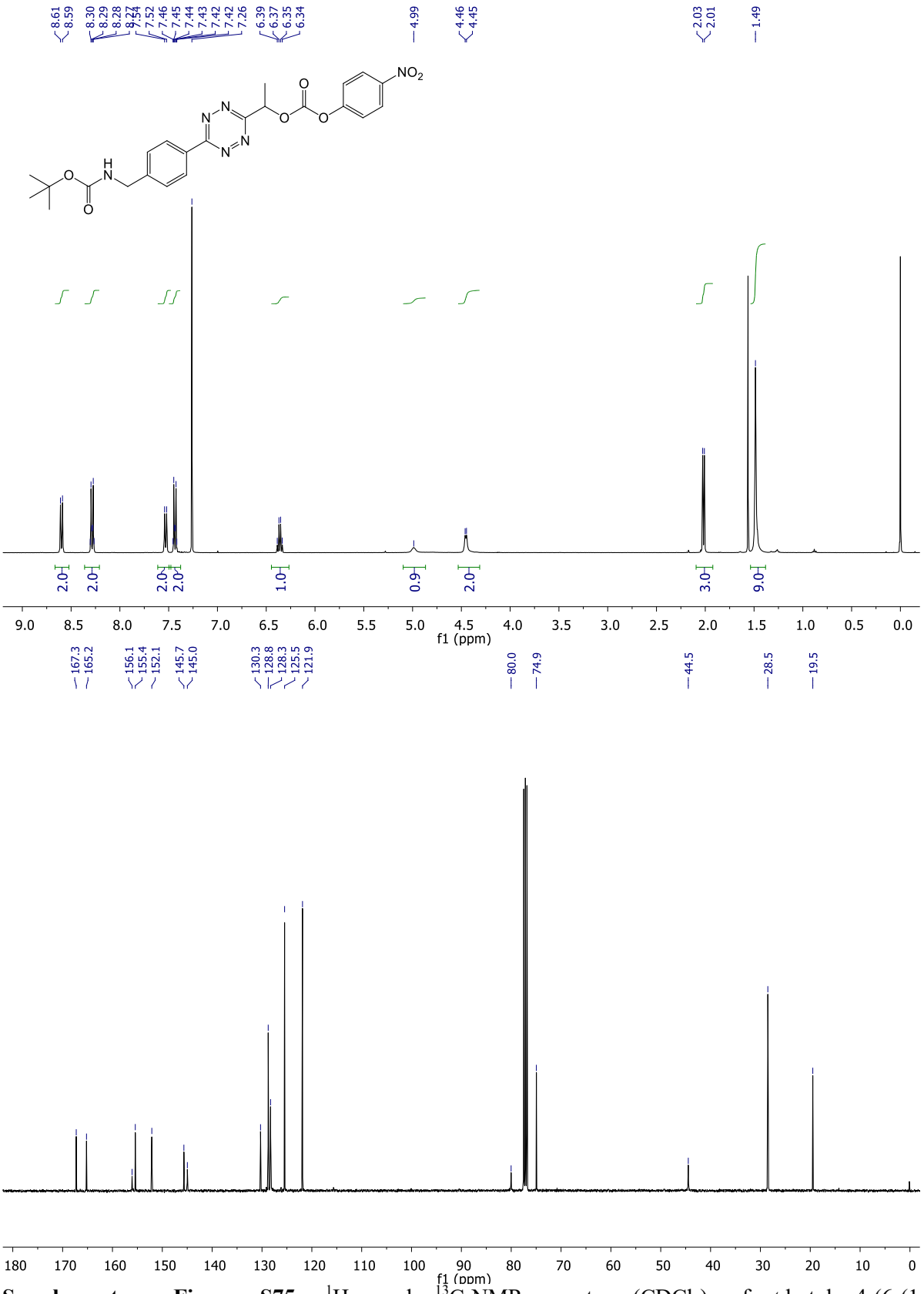

Supplementary Figure S75: ^{1}H- and ^{13}C-NMR spectra ($CDCl_3$) of *t*-butyl 4-(6-(1-(((4-nitrophenoxy)carbonyl)oxy)ethyl)-1,2,4,5-tetrazin-3-yl)benzylcarbamate (**19**)

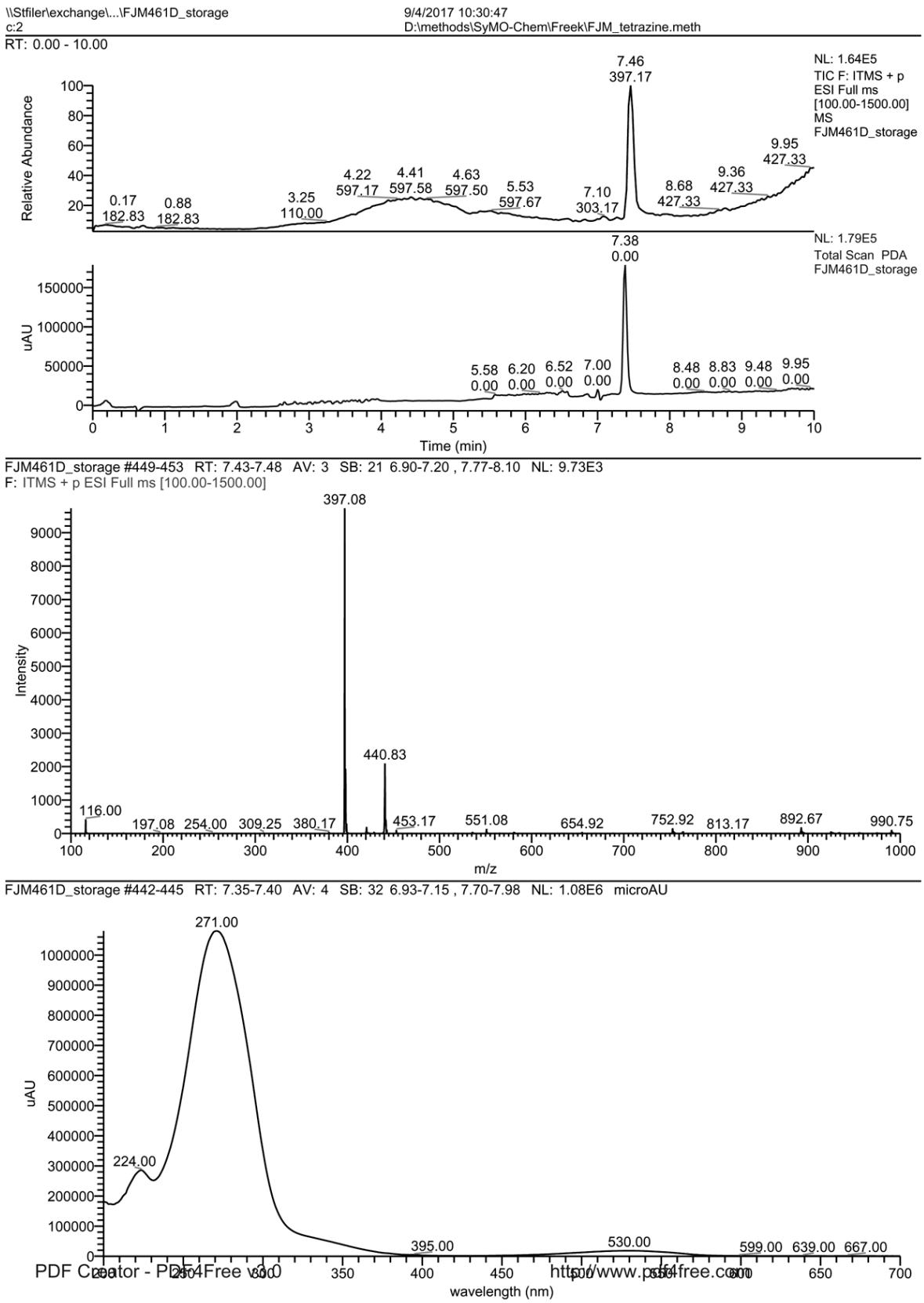

Supplementary Figure S76: HPLC-MS/PDA analysis of *t*-butyl 4-(6-(1-(((4-nitrophenoxy)carbonyl)oxy)ethyl)-1,2,4,5-tetrazin-3-yl)benzylcarbamate (**19**)

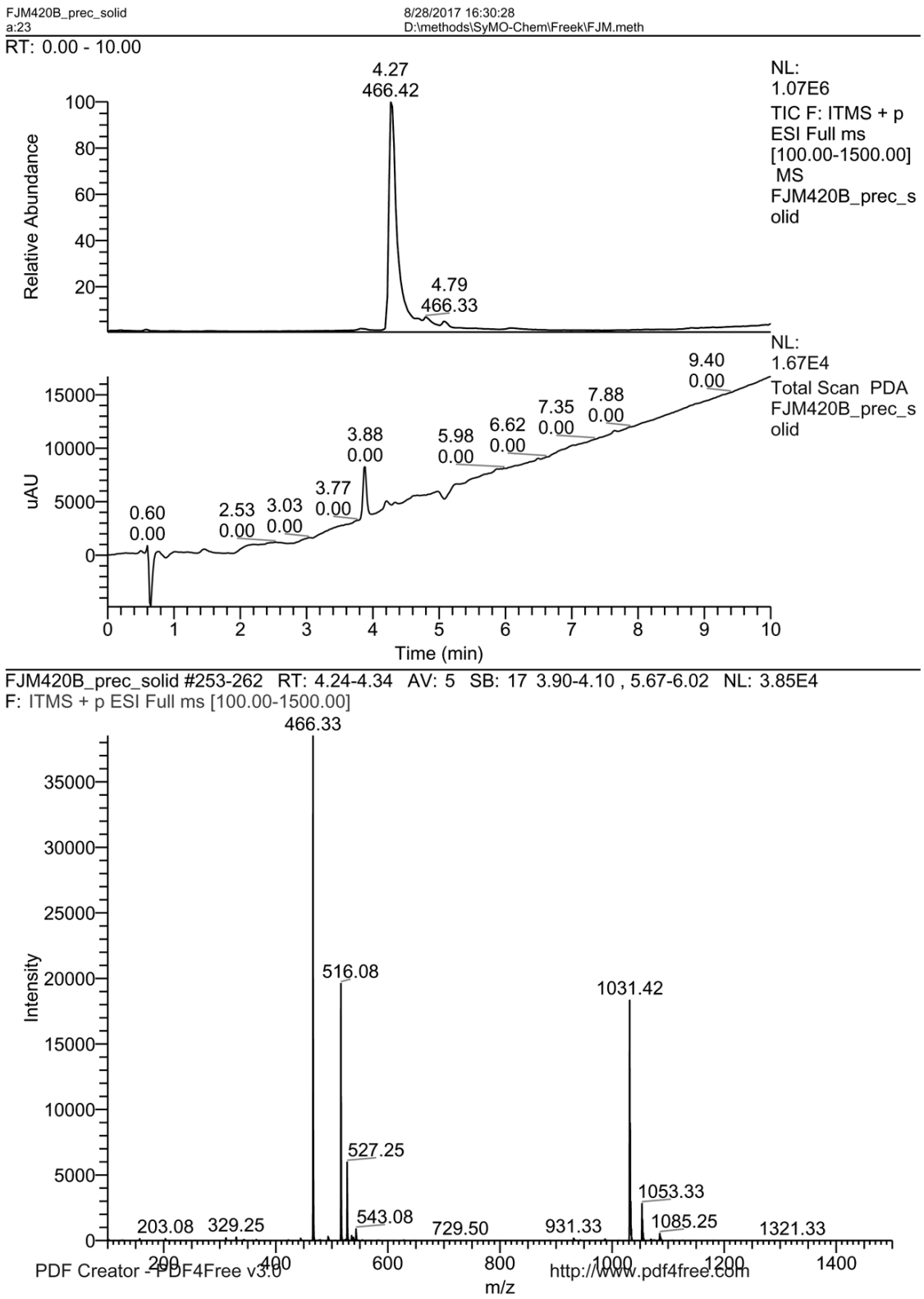

Supplementary Figure S77: HPLC-MS/PDA analysis of 2,2',2''-(10-(2,2-Dimethyl-4,42-dioxo-3,8,11,14,17,20,23,26,29,32,35,38-dodecaoxa-5,41-diazatritetracontan-43-yl)-1,4,7,10-tetraazacyclododecane-1,4,7-triyl)triacetic acid (**S11**)

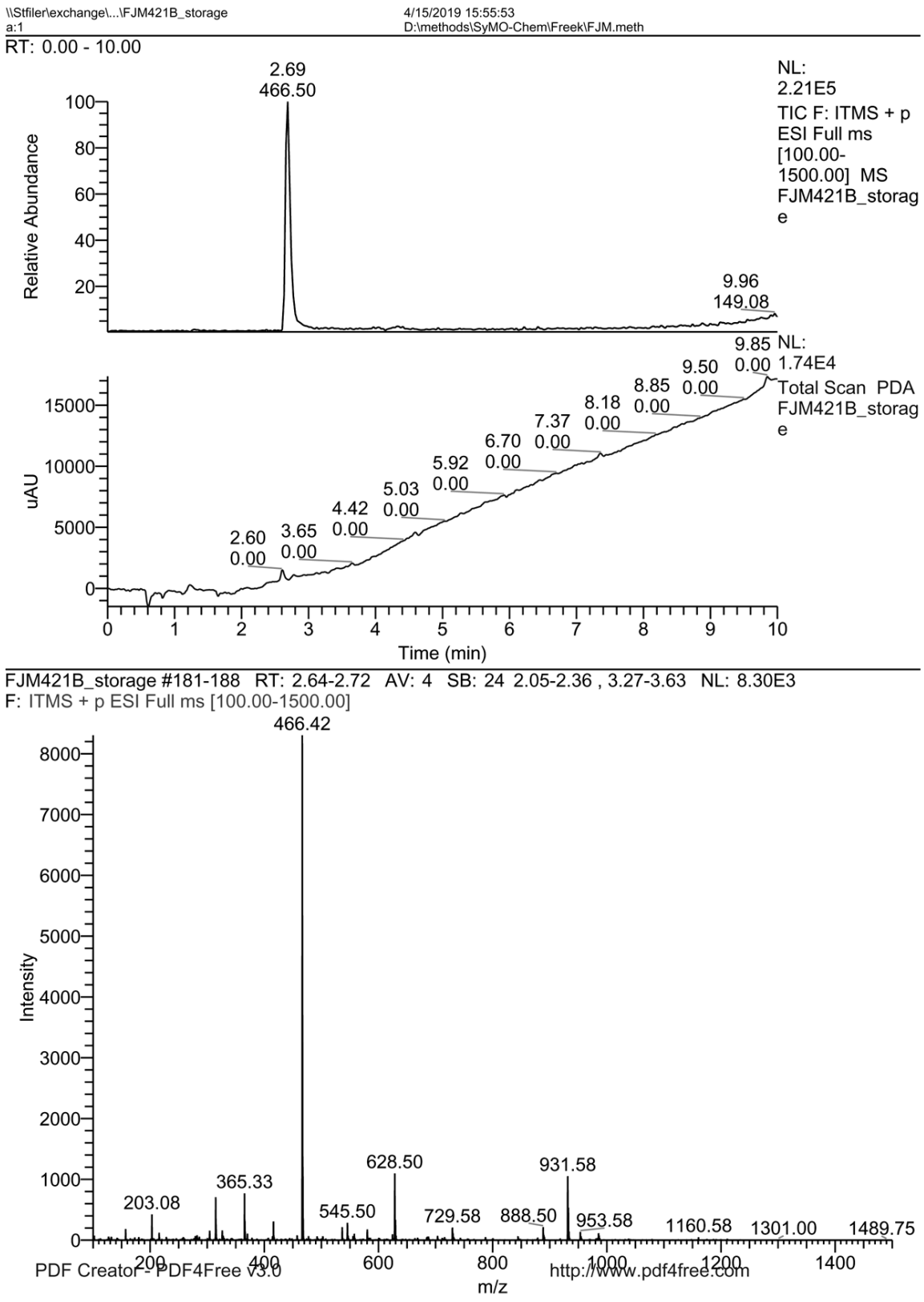

Supplementary Figure S78: HPLC-MS/PDA analysis of 2,2',2''-(10-(38-Amino-2-oxo-6,9,12,15,18,21,24,27,30,33,36-undecaoxa-3-azaoctatriacontyl)-1,4,7,10-tetraazacyclododecane-1,4,7-triyl)triacetic acid, TFA salt (**S12**)

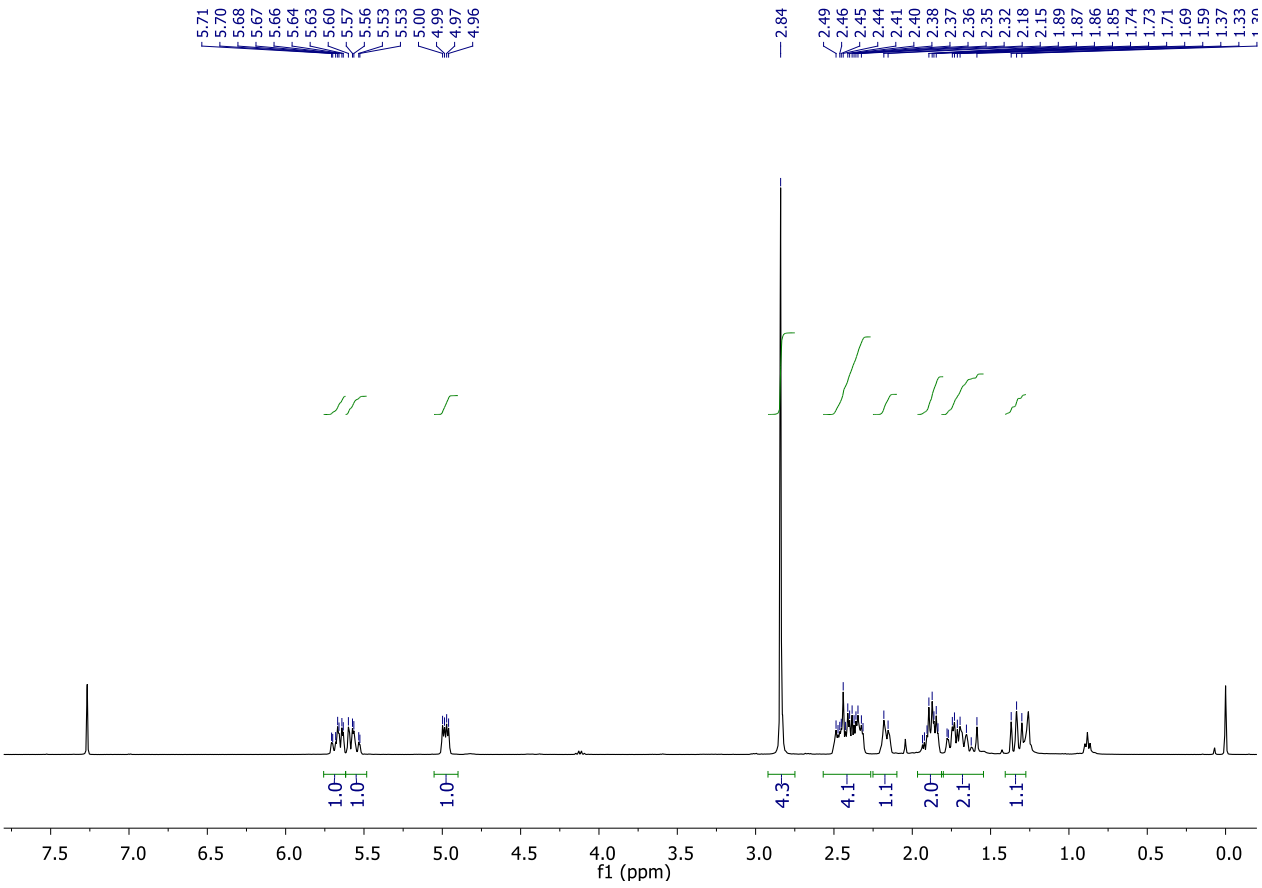

Supplementary Figure S79: ^{1}H-NMR spectrum ($CDCl_3$) of *rel*-(1*R*,4*E*,p*S*)-cyclooct-4-enyl 2,5-dioxopyrrolidin-1-yl carbonate (**S15**)

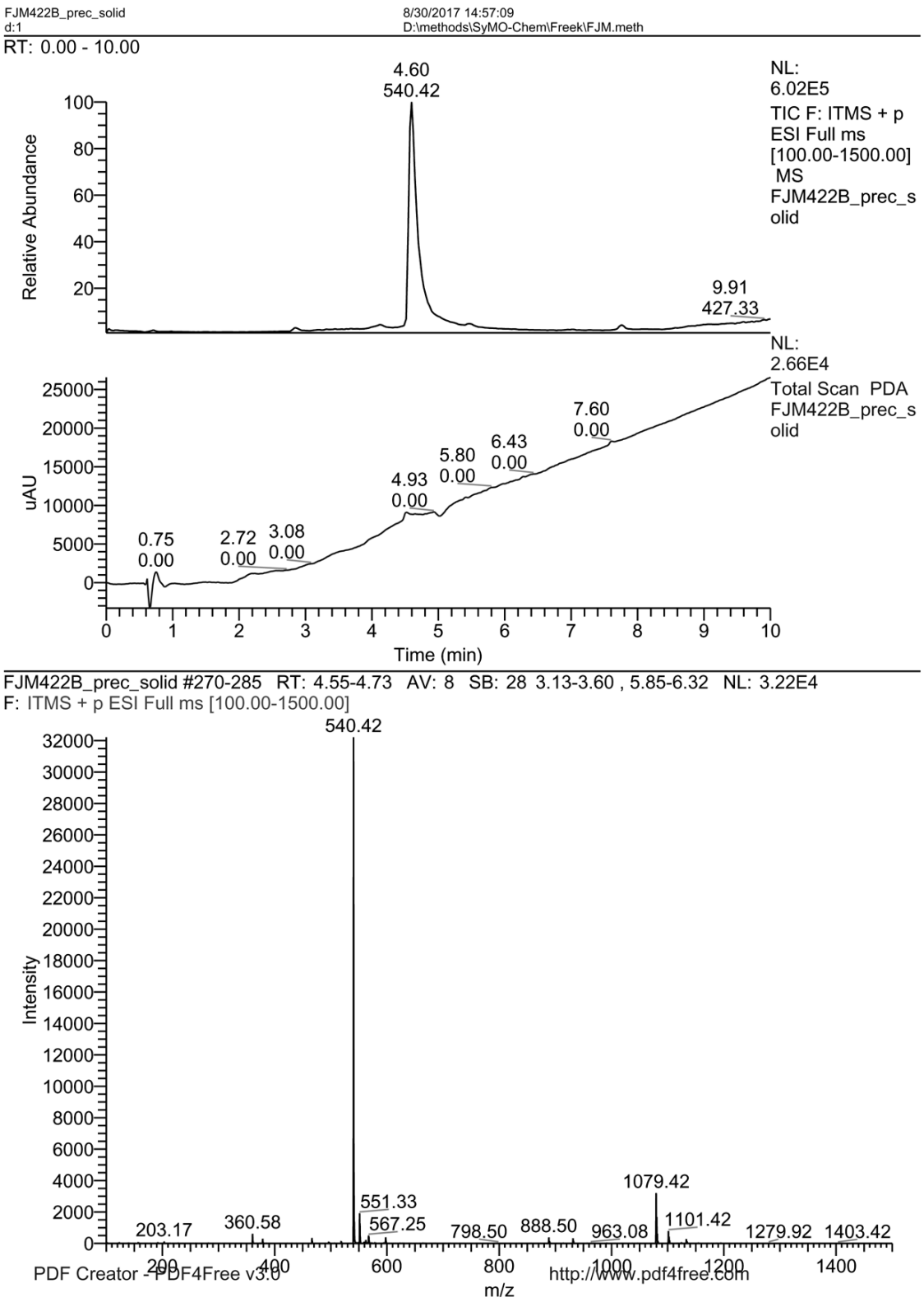

Supplementary Figure S80: HPLC-MS/PDA analysis of 2,2',2''-(10-(1-((1R,8S,9s,E)-bicyclo[6.1.0]non-4-en-9-yl)-1,39-dioxo-5,8,11,14,17,20,23,26,29,32,35-undecaoxa-2,38-diazatetracontan-40-yl)-1,4,7,10-tetraazacyclododecane-1,4,7-triyl)triacetic acid (**15**)

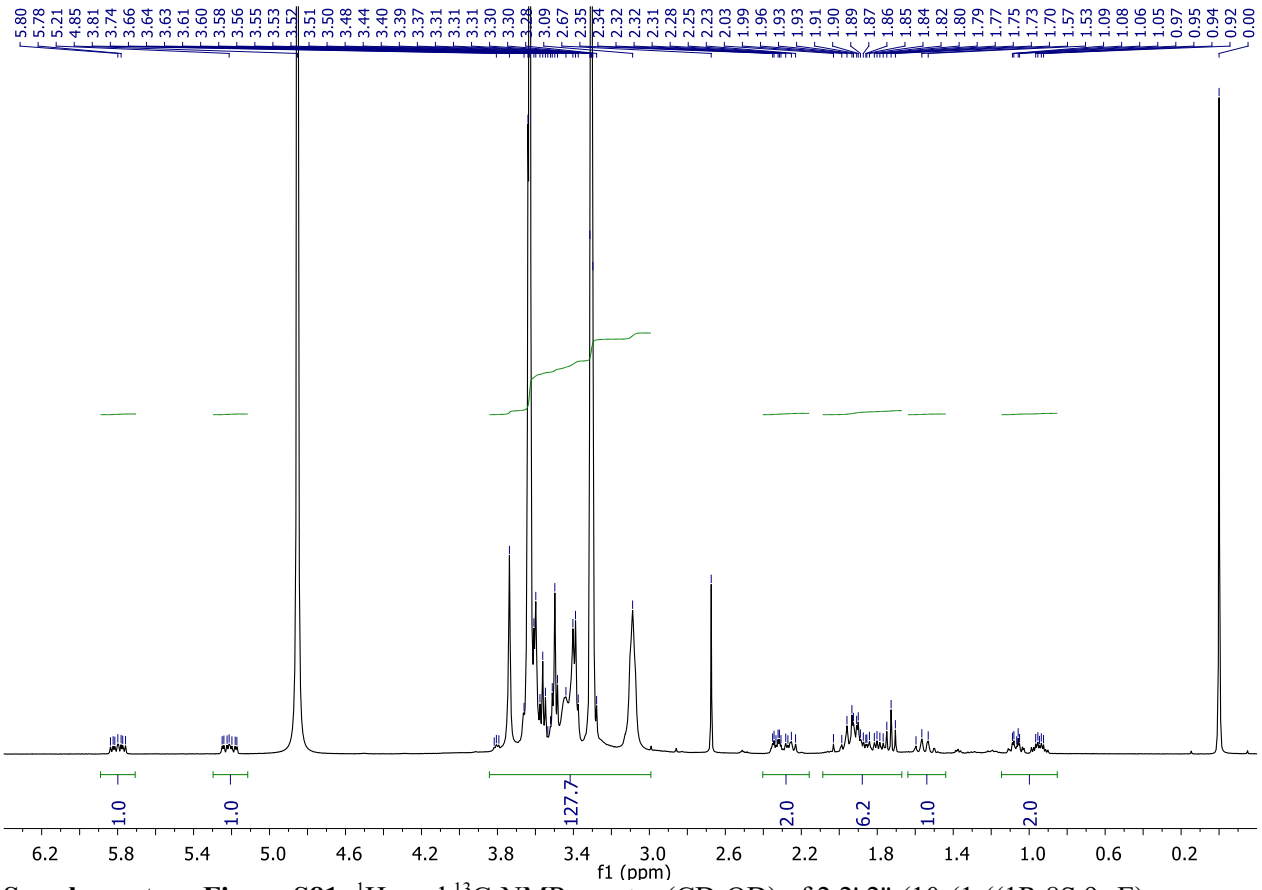

Supplementary Figure S81: ^{1}H- and ^{13}C-NMR spectra (CD_3OD) of 2,2',2''-(10-(1-((1R,8S,9s,E)-bicyclo[6.1.0]non-4-en-9-yl)-1,39-dioxo-5,8,11,14,17,20,23,26,29,32,35-undecaoxa-2,38-diazatetracontan-40-yl)-1,4,7,10-tetraazacyclododecane-1,4,7-triyl)triacetic acid (**15**)

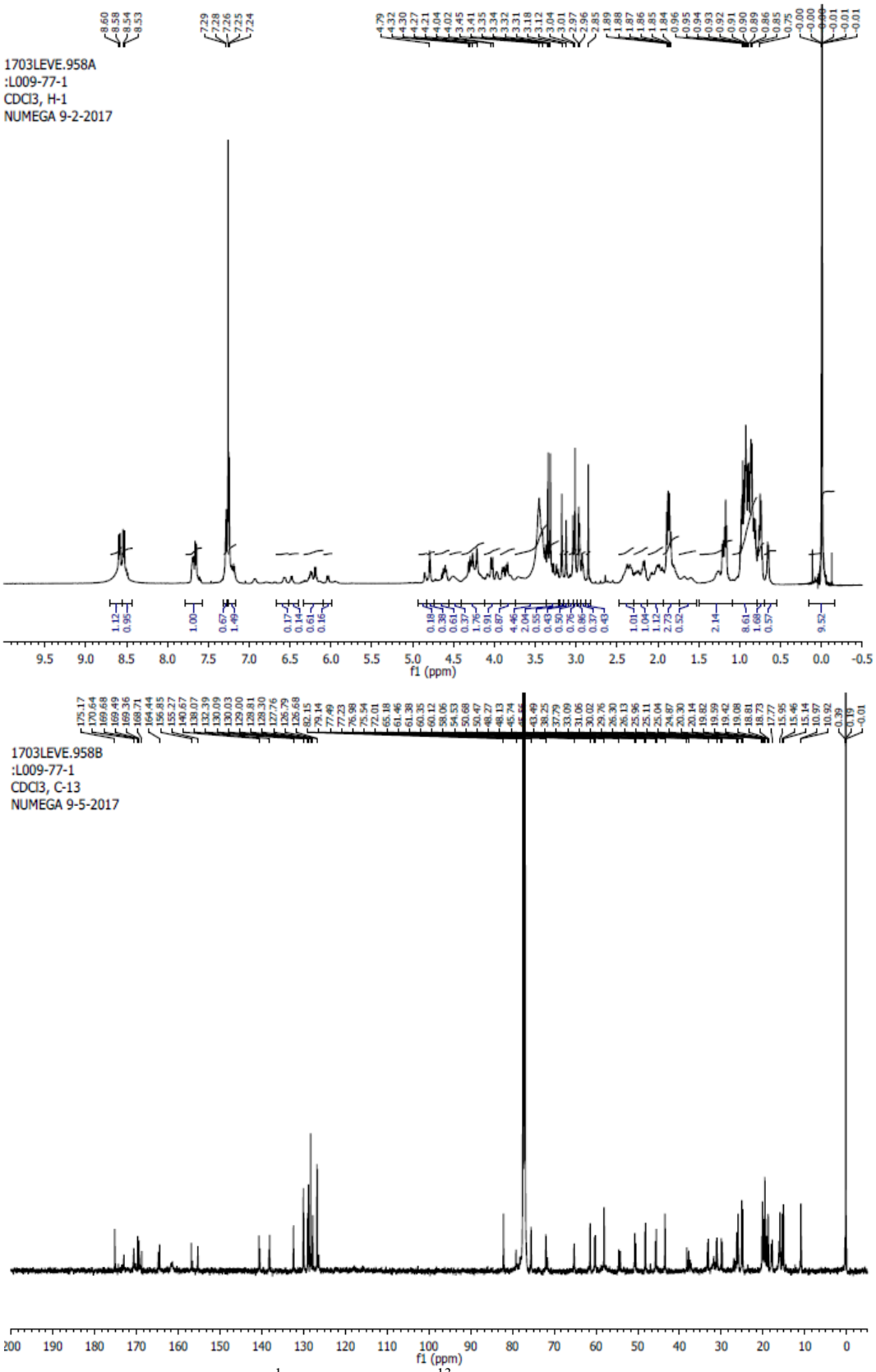

Supplementary Figure S82: (Top) ^{1}H and (bottom) ^{13}C spectra ($CDCl_3$) of compound **21**.

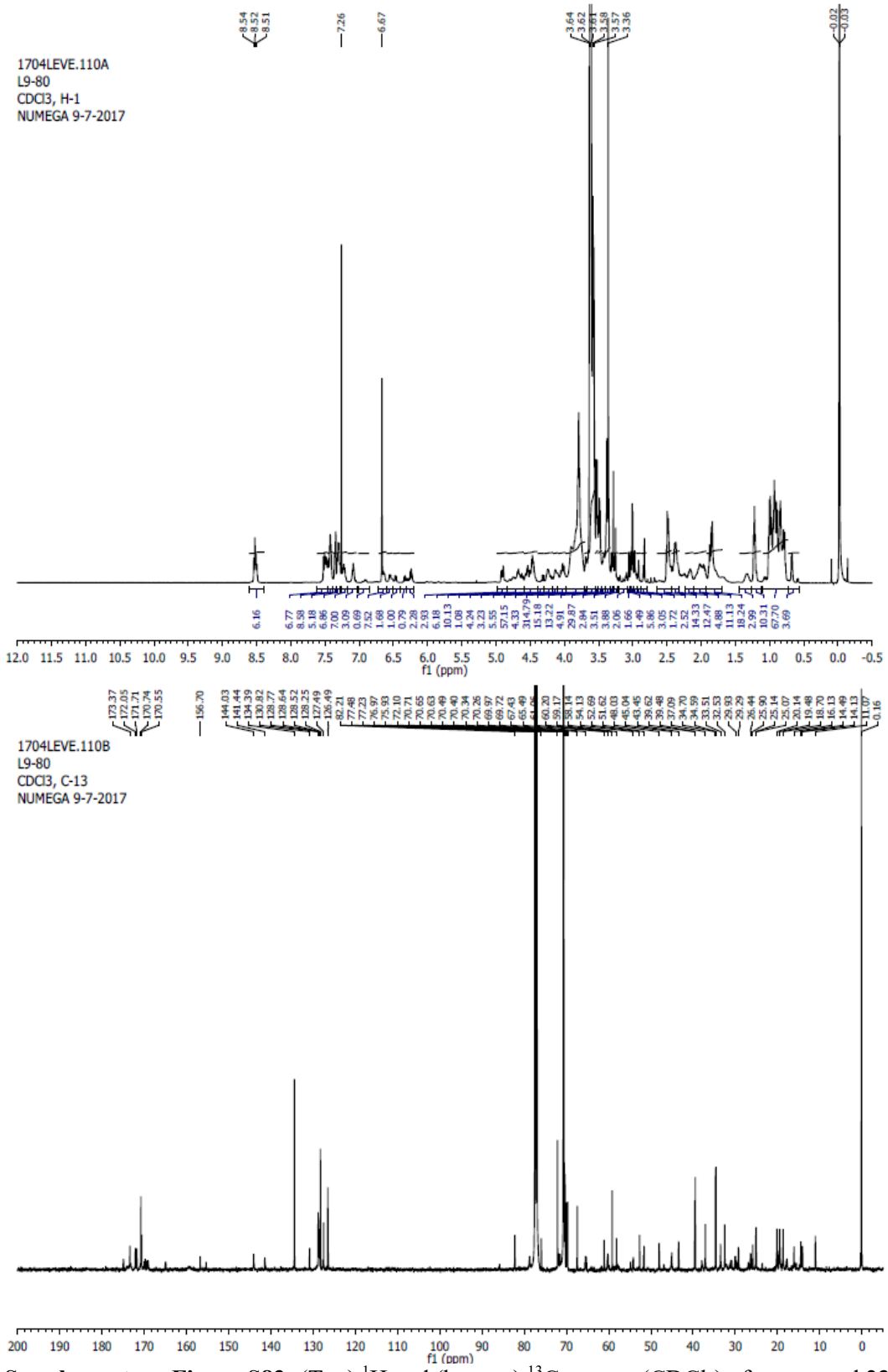

Supplementary Figure S83: (Top) ^{1}H and (bottom) ^{13}C spectra ($CDCl_3$) of compound **23**.

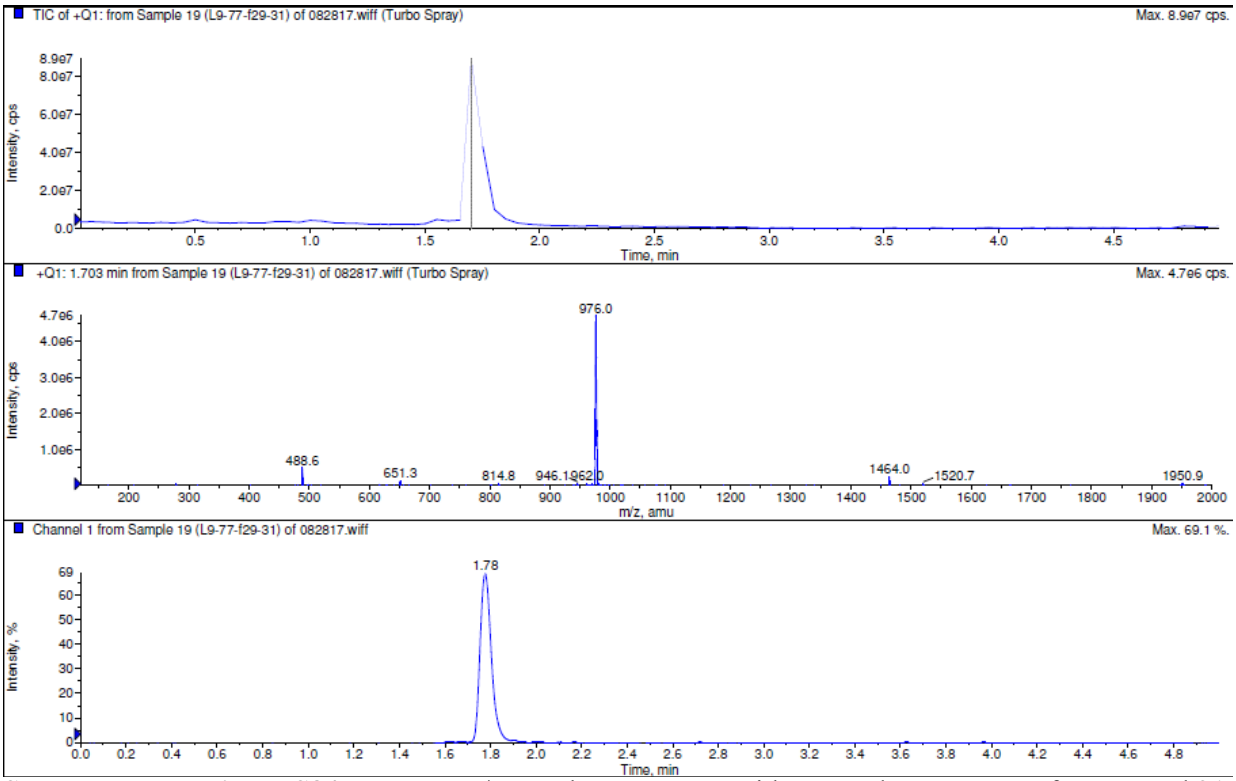

Supplementary Figure S84: HPLC-MS/PDA chromatogram with MS and UV spectra of compound **21**.

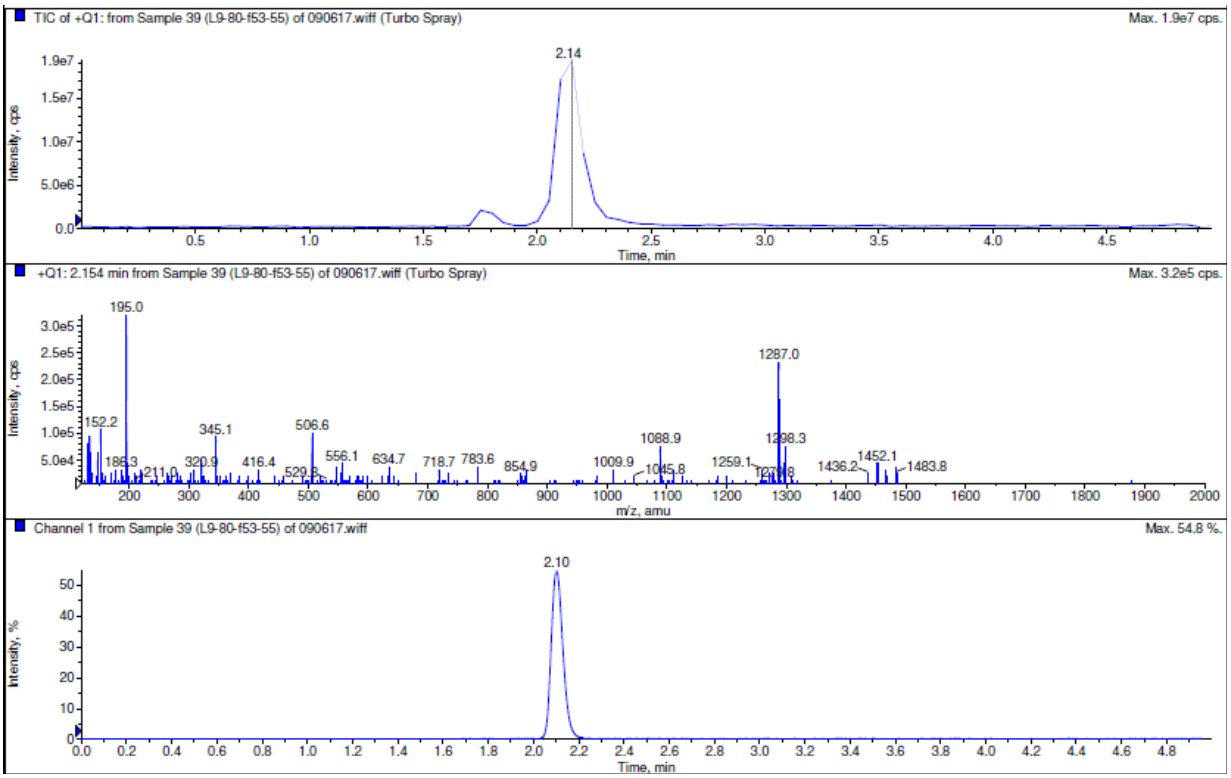

Supplementary Figure S85: HPLC-MS/PDA chromatogram with MS and UV spectra of compound **23**.

S5 Supplementary References

1. Eising, S., Lelivelt, F. & Bonger, K. M. Vinylboronic Acids as Fast Reacting, Synthetically Accessible, and Stable Bioorthogonal Reactants in the Carboni-Lindsey Reaction. *Angew. Chem. Int. Ed Engl.* **55**, 12243–12247 (2016).

2. Rossin, R., van Den Bosch, S. M., ten Hoeve, W., Carvelli, M., Versteegen, R. M. Lub, J., Robillard, M. Highly reactive trans-cyclooctene tags with improved stability for Diels-Alder chemistry in living systems. *Bioconjug. Chem.* **24,** 210–1217 (2013).

3. Shea, K. J. & Kim, J. S. Influence of strain on chemical reactivity. Relative reactivity of torsionally distorted double bonds in MCPBA epoxidations. *J. Am. Chem. Soc.* **114**, 3044–3051 (1992).

4. Velde, G. te *et al.* Chemistry with ADF. *J. Comput. Chem.* **22**, 931–967 (2001).

5. Becke, A. D. A new mixing of Hartree–Fock and local density-functional theories. *J. Chem. Phys.* **98**, 1372–1377 (1993).

6. Lee, C., Yang, W. & Parr, R. G. Development of the Colle-Salvetti correlation-energy formula into a functional of the electron density. *Phys. Rev. B* **37**, 785–789 (1988).

7. Vosko, S. H., Wilk, L. & Nusair, M. Accurate spin-dependent electron liquid correlation energies for local spin density calculations: a critical analysis. *Can. J. Phys.* **58**, 1200–1211 (1980).

8. Stephens, P. J., Devlin, F. J., Chabalowski, C. F. & Frisch, M. J. Ab Initio Calculation of Vibrational Absorption and Circular Dichroism Spectra Using Density Functional Force Fields. *J. Phys. Chem.* **98**, 11623–11627 (1994).

9. Klamt, A. Conductor-like Screening Model for Real Solvents: A New Approach to the Quantitative Calculation of Solvation Phenomena. *J. Phys. Chem.* **99**, 2224–2235 (1995).

10. Li, L. *et al.* Site-Specific Conjugation of Monodispersed DOTA-PEGn to a Thiolated Diabody Reveals the Effect of Increasing PEG Size on Kidney Clearance and Tumor Uptake with Improved 64-Copper PET Imaging. *Bioconjug. Chem.* **22**, 709–716 (2011).

11. Rossin, R. *et al.* Chemically triggered drug release from an antibody-drug conjugate leads to potent antitumour activity in mice. *Nat. Commun.* **9**, 1484 (2018).

12. Showell, G. A. *et al.* Tetrahydropyridyloxadiazoles: semi-rigid muscarinic ligands. *J. Med. Chem.* **34**, 1086–1094 (1991).

13. Anderson, J. R., Edwards, R. L. & Whalley, A. J. S. Metabolites of the higher fungi. Part 19. Serpenone, 3-methoxy-4-methyl-5-prop-1-enylfuran-2(5H)-one, a new γ-butyrolactone from the fungus Hypoxylon serpens(Barrons strain). *J. Chem. Soc. Perkin 1* 215–221 (1982) doi:10.1039/P19820000215.

14. Mier, W. *et al.* Conjugation of DOTA Using Isolated Phenolic Active Esters: The Labeling and Biodistribution of Albumin as Blood Pool Marker. *Bioconjug. Chem.* **16**, 237–240 (2005).

20191217_Click-to-Release from Tetrazine_SI.pdf (12.72 MiB) view on ChemRxiv • download file